Comptes Rendus
de l'Académie des sciences

1778-7025 (electronic)

Géoscience
Sciences de la Planète

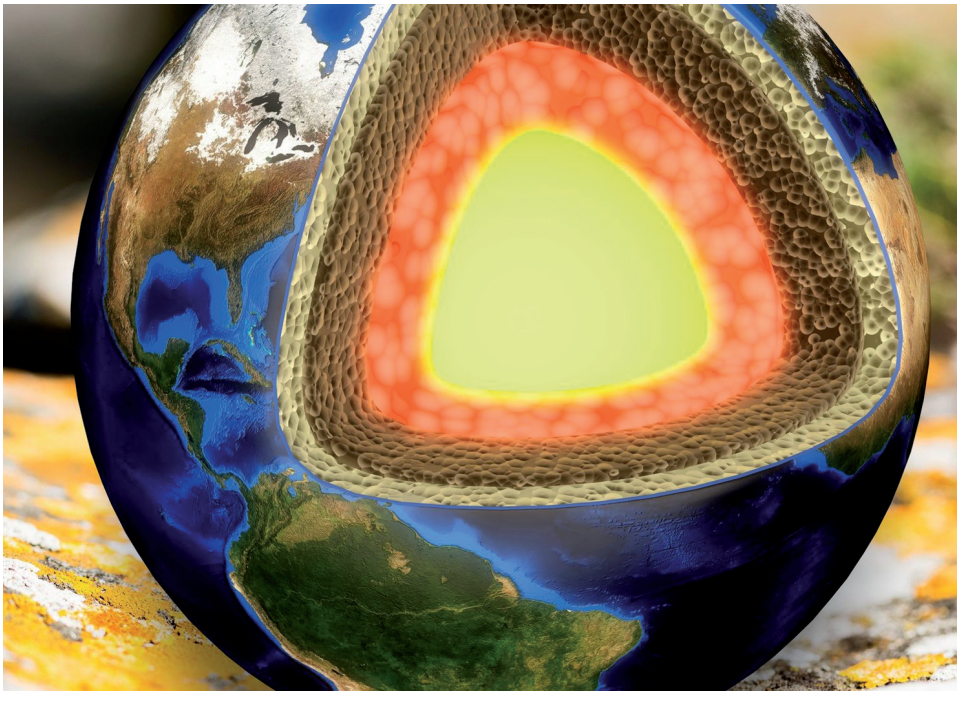

Volume 352, Special Issue 6-7, 2020

Special issue / *Numéro thématique*

Some aspects of current State of Knowledge on Triassic series on both sides of the Central Atlantic Margin / *Quelques aspects de l'état des connaissances des séries triasiques de part et d'autre de la Marge Atlantique*

Académie des sciences — Paris

INSTITUT DE FRANCE
Académie des sciences

CENTRE MERSENNE

Comptes Rendus

Géoscience

Objective of the journal

Comptes Rendus Géoscience is an internationally peer-reviewed electronic journal covering the full range of earth sciences and sustainable development. It publishes original research articles, review articles, historical perspectives, pedagogical texts, and conference proceedings of unlimited length, in English or French. *Comptes Rendus Géoscience* is published according to a virtuous policy of diamond open access, free of charge for authors (no publication fees) as well as for readers (immediate and permanent open access).

Editorial director: Étienne Ghys

Editors-in-chief: Éric Calais, Michel Campillo, François Chabaux, Ghislain de Marsily

Editorial Board: Jean-Claude André, Pierre Auger, Mustapha Besbes, Sylvie Bourquin, Yves Bréchet, Marie-Lise Chanin, Philippe Davy, Henri Décamps, Sylvie Derenne, Michel Faure, François Forget, Claude Jaupart, Jean Jouzel, Eric Karsenti, Amaëlle Landais, Sandra Lavorel, Yvon Le Maho, Mickaele Le Ravalec, Hervé Le Treut, Benoit Noetinger, Carole Petit, Valérie Plagnes, Pierre Ribstein, Didier Roux, Bruno Scaillet, Marie-Hélène Tusseau-Vuillemin, Élisabeth Vergès

Editorial secretary: Adenise Lopes

About the journal

All journal's information, including the text of published articles, which is fully open access, is available from the journal website at https://comptes-rendus.academie-sciences.fr/geoscience/.

Author enquiries

For enquiries relating to the submission of articles, please visit this journal's homepage at https://comptes-rendus.academie-sciences.fr/geoscience/.

Contact

Académie des sciences
23, quai de Conti, 75006 Paris, France
Tel: (+33) (0)1 44 41 43 72
CR-Geoscience@academie-sciences.fr

The articles in this journal are published under the license Creative Commons Attribution 4.0 International (CC-BY 4.0) https://creativecommons.org/licenses/by/4.0/deed.en

Comptes Rendus
Géoscience — Sciences de la Planète
2020, 352, nº 6-7

Contents / *Sommaire*

Sylvie Bourquin, Rachid Essamoud
Some aspects of current State of Knowledge on Triassic series on both sides of the Central Atlantic Margin 415-416

Abdelkrim Afenzar, Rachid Essamoud
Sedimentological and sequence stratigraphy analyses of the syn-rift Triassic series of the Mohammedia–Benslimane–ElGara–Berrechid basin (Moroccan Meseta) 417-441

Manuel García-Ávila, Ramon Mercedes-Martín, Manuel A. Juncal, José B. Diez
New palynological data in Muschelkalk facies of the Catalan Coastal Ranges (NE of the Iberian Peninsula) 443-454

Hind El Hachimi, Nasrrddine Youbi, José Madeira, Andrea Marzoli, João Mata, Hervé Bertrand, Mohamed Khalil Bensalah, Moulay Ahmed Boumehdi, Miguel Doblas, Fida Medina, Mohamed Ben Abbou, Línia Martins
Physical volcanology and emplacement mechanism of the Central Atlantic Magmatic Province (CAMP) lava flows from the Central High Atlas, Morocco 455-474

Manuel A. Juncal, José B. Diez, Raúl De la Horra, José F. Barrenechea, Violeta Borruel-Abadía, José López-Gómez
State of the art of Triassic palynostratigraphical knowledge of the Cantabrian Mountains (N Spain) 475-493

Bouziane Khalloufi, Nour-Eddine Jalil
Overview of the Late Triassic (Carnian) actinopterygian fauna from the Argana Basin (Morocco) 495-513

Uxue Villanueva-Amadoz, Marycruz Gerwert Navarro, Manuel A. Juncal, José B. Diez
Paleobotanical and palynological evidence for the age of the Matzitzi Formation, Mexico 515-538

Comptes Rendus
Géoscience — Sciences de la Planète
2020, 352, nº 6-7, p. 415-416
https://doi.org/10.5802/crgeos.37

Some aspects of current State of Knowledge on Triassic series on both sides of the Central Atlantic Margin / *Quelques aspects de l'état des connaissances des séries triasiques de part et d'autre de la Marge Atlantique*

Presentation of the special issue following the Second International Congress on the Permian and Triassic, Casablanca, Morocco, 2018 — Editorial

Some aspects of current State of Knowledge on Triassic series on both sides of the Central Atlantic Margin

Sylvie Bourquin[*, a] **and Rachid Essamoud**[b]

[a] Univ Rennes, CNRS, Géosciences Rennes - UMR 6118, F-35000, Rennes, France

[b] Dynamics of Sedimentary Basins & Geological Correlations Laboratory, Faculty of Sciences Ben M'Sik, Hassan II University of Casablanca. B.P. 7955, Sidi Othmane, Casablanca, Morocco

E-mails: sylvie.bourquin@univ-rennes1.fr (S. Bourquin), rachid.essamoud@univh2c.ma (R. Essamoud)

The Second International Congress on the Permian and Triassic, coinciding with the Eighth Meeting of the Moroccan Permian and Triassic Group, ICPT2-GMPT8, was held at the Ben M'sik Faculty of Sciences in Casablanca, from 25 to 27 April 2018. More than 60 international researchers participated in this congress: Morocco, Spain, Italy, France, Germany, England, Mexico.

The first two days were devoted to plenary lectures and oral communications grouped into 5 sessions. We were thus able to attend:

– 4 plenary lectures led by internationally renowned researchers: Sylvie BOURQUIN (Rennes, France) on "Late Permian to Middle Triassic sedimentation at the western peri-Tethyan domain: comparison between European and North African basins", Jonathan REDFERN (Manchester, England) on "Assessing the contribution of local versus regional drainage systems on the provenance of Upper Triassic fluvial deposits, Morocco", Jörg SCHNEIDER (Freiberg, Germany) on "Carboniferous, Permian and Triassic continental biota of Morocco—a state-of-the-art summary" and Nassreddine YOUBI (Marrakech, Morocco) on "The Permian and Triassic-Jurassic Large Igneous Provinces of Morocco: Current State of Knowledge and Future Research Directions",
– 30 oral communications distributed in 5 sessions: Palynology, paleoenvironments and paleoclimates (session 1), Paleontology, biostratigraphy and paleoenvironments (session 2), Sedimentary basins and geodynam-

* Corresponding author.

ics (session 3), Mineralization (session 4), Magmatism and geochronology (session 5),
– 20 posters.

A round table discussion was held at the end of the second day of the congress, during which debates took place on different aspects of this specific period of the Earth's history, in particular on paleoenvironmental, paleogeographic, paleoecological reconstructions, the Permian-Triassic transition in the terrestrial domain, paleoecological data or the importance of CAMP volcanism.

The third day was devoted to an excursion in the coastal Triassic basin of Berrechid-ElGara-Benslimane-Mohammedia, guided by Abdelkrim AFENZAR and Rachid ESSAMOUD, (Hassan II University of Casablanca) with the participation of 27 attendees.

This special issue gathers works carried out on the Triassic basins on both sides of the Atlantic margin, presented during this ICPT2-GMPT8 congress, addressing different geosciences themes:

– Afenzar A. & Essamoud R.—Sedimentological and sequence stratigraphy analyses of the syn-rift Triassic series of the Mohammedia-Benslimane-ElGara-Berrechid basin (Moroccan Meseta).
– García-Ávila M., Mercedes-Martín R., Juncal M. & Diez J.B.—New palynological data in Muschelkalk facies of the Catalan Coastal Ranges (NE of the Iberian Peninsula).
– El Hachimi H., Youbi N., Madeira J., Marzoli A., Mata J., Bertrand H., Bensalah M. K., Boumehdi M. A., Doblas M., Medina F., Ben Abbou M. & Martins L.—Physical volcanology and emplacement mechanism of the Central Atlantic Magmatic Province (CAMP) lava flows from the Central High Atlas, Morocco.
– Juncal M. A., Diez J. B., De la Horra R., Barrenechea J. F., Borruel-Abadía V. & López-Gómez J.—State of the Art of Triassic Palynostratigraphical Knowledge of the Cantabrian Mountains (N Spain).
– Khalloufi B. & Jalil N.-J.—Overview of the Late Triassic (Carnian) actinopterygian fauna from the Argana Basin (Morocco).
– Villanueva-Amadoz U., Gerwert Navarro M., Juncal M. A. & Diez J. B.—Paleobotanical and Palynological Evidence for the Age of the Matzitzi Formation, Mexico.

We would like to thank the editors of the Mersennes group for their editorial assistance for the preparation of these articles for Comptes Rendus Geoscience of the Académie des Sciences, the reviewers of these articles, as well as all the participants in the Casablanca Congress and especially those who allowed sharing their scientific advances in this thematic issue.

Sylvie Bourquin
Associated Editor
France
sylvie.bourquin@univ-rennes1.fr

Rachid Essamoud
President of GMPT, Invited Editor
Morocco
rachid.essamoud@univh2c.ma

Comptes Rendus
Géoscience — Sciences de la Planète
2020, 352, nº 6-7, p. 417-441
https://doi.org/10.5802/crgeos.36

Some aspects of current State of Knowledge on Triassic series on both sides of the Central Atlantic Margin / *Quelques aspects de l'état des connaissances des séries triasiques de part et d'autre de la Marge Atlantique*

Sedimentological and sequence stratigraphy analyses of the syn-rift Triassic series of the Mohammedia–Benslimane–ElGara–Berrechid basin (Moroccan Meseta)

Abdelkrim Afenzar[*, a] **and Rachid Essamoud**[a]

[a] Dynamics of Sedimentary Basins & Geological Correlations Laboratory, Faculty of Sciences Ben M'Sik, Hassan II University of Casablanca. B.P. 7955, Sidi Othmane, Casablanca, Morocco

E-mails: karim.afenzar@gmail.com (A. Afenzar), r.essamoud@gmail.com (R. Essamoud)

Abstract. Sedimentological analysis has shown that during the syn-rift phase (Upper Triassic) the Mohammedia–Benslimane–ElGara–Berrechid basin (MBEB) is characterized by detrital and evaporite sediment filling. A gradual decrease of palaeoslope over time led to the evolution of paleoenvironments of proximal alluvial fans system to braided rivers and then to an anastomosing system. These environments evolve finally to an alluvial plain associated with a coastal plain where playa lakes, mudflats and lagoons had developed.

We have identified fourteen genetic sequences which are included in four progradational-retrogradational minor cycles that are themselves grouped in one major cycle. These cycles are related to the variations of the base level. The dominance of the retrogradation phases giving an asymmetrical appearance to the cycles is related to the predominance of the base level rise. These variations are probably of allocyclic origin: tectonic and probably climatic, in relation with the Tethys and the Atlantic Ocean being opened.

Keywords. Sedimentology, Paleoenvironment, High resolution sequence stratigraphy, Rifting, Triassic.

Available online 14th December 2020

1. Introduction

The Moroccan Triassic basins are characterized by two sedimentary episodes (detrital and evaporitic). The deposition of the detrital episode started during (1) the Early Triassic in the Argana Valley, [e.g. Hofmann et al., 2000, Tourani et al., 2010]; (2) the Middle Triassic in the Central High Atlas [e.g. El Arabi et al., 2006] and in the Oujda mountains [e.g. Courel et al., 2003, Crasquin-Soleau et al., 1997,

* Corresponding author.

Oujidi and Elmi, 2000], and during (3) the Upper Triassic in the Middle Atlas basins [e.g. Baudelot et al., 1990, Lachkar et al., 2000] and in the Moroccan Atlantic margin (Essaouira basin, e.g. Hafid, 2000, Slimane and El Mostaïne, 1997; Doukkala basin, e.g. Hminna et al., 2013; Khémisset basin, e.g Et-Touhami, 1994, Taugourdeau-Lanz, 1978; Mohammedia–Benslimane–ElGara–Berrechid basin (MBEB), Afenzar, 2018).

The Moroccan salt series (evaporitic episode) are formed during the Upper Triassic as in the other Triassic continental basins, whether in the North of Gondwana (Algeria, e.g. Aït Salem et al., 1998, Bourquin et al., 2010, Courel et al., 2003; and Tunisia, e.g. Soto et al., 2017, Soussi and Ben Ismaïl, 2000, Soussi et al., 2001) or in Europe (Portugal, Alves et al., 2006, Ramos et al., 2017, Soto et al., 2017; Spain, e.g. Barrón et al., 2006, Bourrouilh et al., 1995, Ferrer et al., 2012, Gonzàlez de Aguilar, 2015, Ortí, 2004, Reolid et al., 2014, Roca et al., 2011; France, e.g. Bourquin and Guillocheau, 1993, 1996; Germany, e.g. Aigner and Bachmann, 1992, Kozur and Bachmann, 2008) or in Canada [Leleu et al., 2016, Miall and Balkwilla, 2019, Olsen, 1997, Wade et al., 1995, Welsink and Tankard, 2012].

In Morocco, existing data for the Triassic salt successions are scarce [e.g. Peretsman and Holser, 1988, Salvan, 1974]. In the Atlasic domain, the saliferous series is more reduced and is represented in outcrop by gypsum levels (Central High Atlas, e.g. Biron, 1982, Benaouiss et al., 1996, Courel et al., 2003, El Arabi, 2007, Baudon et al., 2012, Vergés et al., 2017; Argana Valley, e.g. Hofmann et al., 2000; Middle Atlas, e.g. Lorenz, 1976, Laville et al., 1995, Ouarhache et al., 2012). Towards the Mesetien domain and the Moroccan Atlantic margin domain, these successions become much more important. In all Triassic basins belonging to these two domains, the saliferous successions are similar. They are subdivided into two large parts recognized in borehole: (1) the lower part attributed to the Upper Triassic and (2) the upper part dated from the Lower Liassic, separated by the Central Atlantic Magmatic Province, i.e. CAMP basalt (Essaouira Basin, Echarfaoui et al., 002b, Hafid, 2000; Doukkala Basin, Echarfaoui et al., 002a, Salvan, 1984; Khémisset Basin, Et-Touhami, 1994, 1996, 1998, Salvan, 1982; MBEB Basin, Afenzar, 2018, Lyazidi, 2004, Salvan, 1984).

The MBEB Basin consists of a detrital and evaporitic sedimentary series of about 1500 m [Afenzar, 2018, BRPM, 1973]. This sedimentary series is subdivided into two main formations: a sandy-conglomeratic formation at the base (Formation A) and argillaceous-saliferous formation in the middle and top of the series (Formation B) [Afenzar, 2018, Afenzar and Essamoud, 2017] recovered by Triassic-Liassic basalts [Peretsman, 1985].

The aim of this study, from a detailed sedimentological analysis is (1) to reconstruct palaeoenvironment and (2) for the first time, to propose sequence stratigraphy analyses to constitute a basis of a stratigraphic correlation with other Triassic Atlantic basins. Moreover, the correlations in terms of sequence stratigraphy allow to constrain the spatial and temporal evolution of salt series and could guide the exploration and thus have an economic impact.

2. Geological setting

At the early Mesozoic, the Pangea continent was affected by an initial break-up associated with the early stages of the opening of the Central Atlantic Domain. During this phase, the Moroccan and North American Margins were subjected to an extensive tectonic regime that led to the opening of a set of rift basins [e.g. Courel et al., 2003, Hafid, 2000, Leleu et al., 2016, Le Roy and Piqué, 2001, Medina, 1995, Olsen, 1997, Piqué and Laville, 1995, Piqué et al., 1998]. The Moroccan basins are placed geographically in the central segment of Central Atlantic Domain and are laterally equivalent to the Nova Scotian basins [Hafid, 2000, Leleu et al., 2016]. The MBEB basin is a part of a Moroccan margin like the Khémisset, Doukkala, Essaouira, Souss and Tarfaya basins (Figure 1). Among these basins, the closest to MBEB Basin are Khémisset Basin in the north (separated by the Paleozoic basement of central Morocco) and Doukkala Basin in the south (separated by the Paleozoic of Casablanca block).

The MBEB basin is located in the North-West of the Moroccan coastal Meseta, about twenty kilometers northeast of Casablanca (Figure 2). The structure of this basin has been interpreted several times. The interpretations of El Wartiti et al. [1992] were based on the boundary with the Hercynian basement, which are unconformity contacts materialized by border faults controlling the

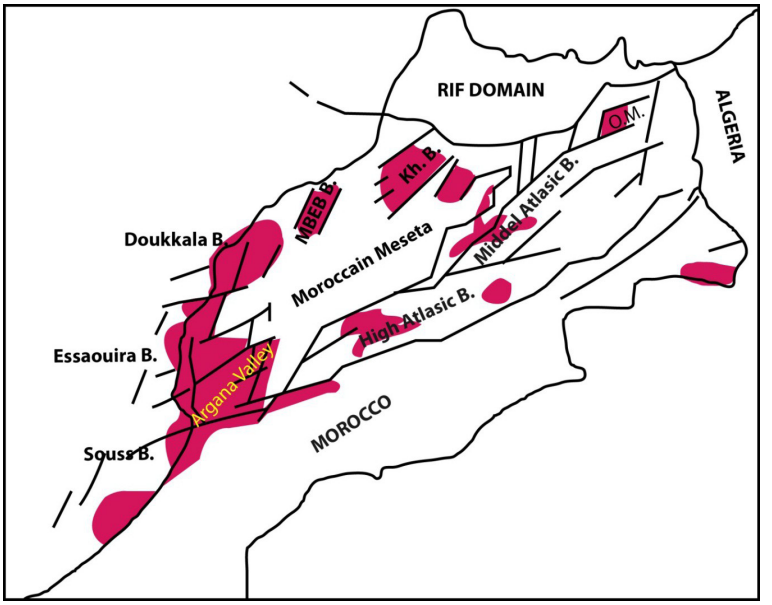

Figure 1. Paleogeographical location of Moroccan Triassic basins in the Late Norian (synthetic map based on Courel et al., 2003 and Leleu et al., 2016).

individualization of the basin and conditioning its filling.

Usually, this basin is presented as an immense shallow depression which seems to have originated from N–S to NE–SW half-graben structure [Afenzar, 2018, El Wartiti et al., 1992]. At the end of the Paleozoic and the early Mesozoic, this half-graben is developed and filled by an important detrital and evaporitic syn-rift sedimentary series; with a magmatic activity belonging to the CAMP [Manspeizer and Cousminer, 1988, Peretsman, 1985].

This basin was subjected to a NW–SE extension with a slight deformation component [El Wartiti et al., 1992]. The structure is controlled by a deep detachment, which is probably an ancient Hercynian weakness zone, and which plunges slightly towards the NNW. This is related to the opening of the proto-Atlantic domain [El Wartiti et al., 1992, Medina, 1994].

3. Lithostratigraphic framework

According to the old nomenclature, the lithostratigraphic series of the MBEB basin was subdivided into five main zones attributed to Permo-Triassic deposits [BRPM, 1973]: (1) Zone argileuse inférieure; (2) Zone salifère inférieure; (3) Zone basaltique; (4) Zone salifère supérieure; (5) Zone argileuse supérieure (Figure 3A).

According to the latest works, the sedimentary series in the MBEB basin is subdivided into two major series: Lower argillaceous-salt series attributed to Triassic and Upper argillaceous-salt series attributed to Liassic [Hssaida et al., 2012, Lyazidi, 2004]. The two parts are separated by a basaltic complex (Figure 3B).

This basalt was dated Late Triassic-Early Liassic (200 Ma) and belonged to the CAMP by several works based on radiometric dating data [Peretsman, 1985]. Subsequently the infra-basaltic series can be attributed to the Upper Triassic [Afenzar, 2018, El Wartiti et al., 1992, Lyazidi, 2004, Salvan, 1984].

In this study, we have subdivided this Upper Triassic part into two main formations: the sandy-conglomerate Formation (A) at the base of the series and the argillaceous-saliferous Formation (B), subdivided into two members, (1) Mudstone-siltstone Member and (2) Argillaceous-saliferous Member (Figure 3C).

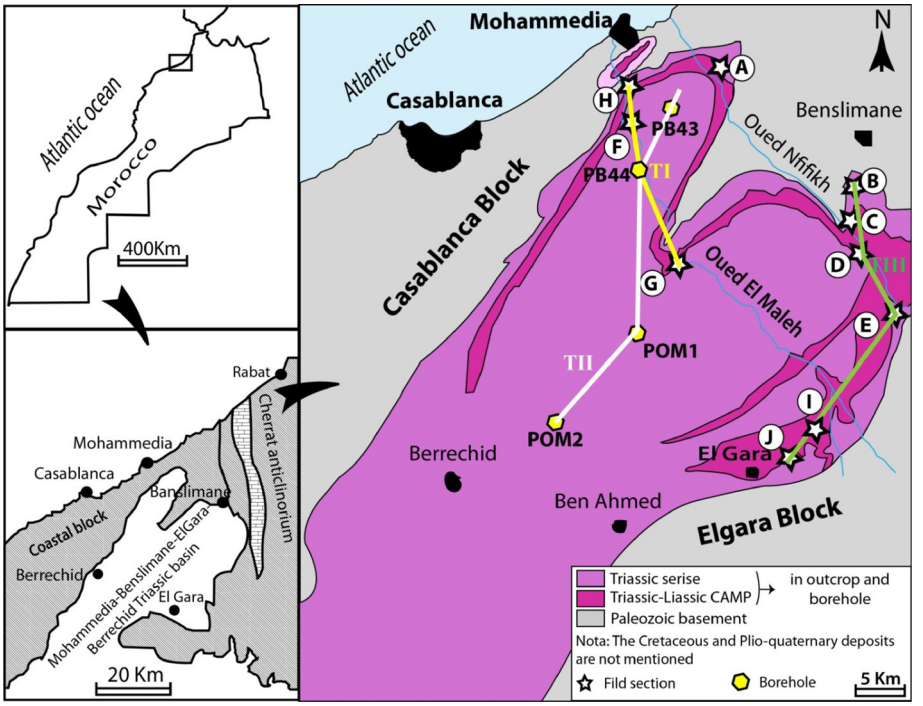

Figure 2. Geological map of the MBEB basin with the sections and boreholes analyzed as well as correlation transects in genetic stratigraphy (A: Chaâbat Al Hamra section, B: Chaâbat Lhmira, C: Assikriat section, D: Tlet Ziaida, E: Sidi Amour, F: Sidi Bouchaibe, G: Barrage Oued El Maleh, H: Sidi Bou Amar, I: Ouled Jhaich J: ElGara, TI, TII, TIII: correlation transects).

4. Method

This sedimentological study consists in a detailed analysis of the field sections (outcropping in the northeastern part of the basin) and drill cores of four boreholes (PB43 (712 m), PB44 (650 m), POM1 (1070 m) and POM2 (1350 m), Figure 2) for a better view of the sedimentary bodies and their spatial arrangements. This allows to characterize different facies and their associations as well as the architectural elements [Allen, 1983, Miall, 1985, 1996] which allow us to reconstruct the depositional environments and their evolutions over time and space.

In fact, the vertical and horizontal arrangement of these facies give birth to the characterized architectural elements according to several criteria determined by Allen [1983] and Miall [1985, 1996], which are: the nature of the upper and lower bounding surfaces, the external geometry, the scale, and the internal structures. The last step is the determination of paleoenvironment which is based on the nature and types of lithofacies already characterized and also on types of architectural elements.

The genetic stratigraphy applied in this study consists of a high-resolution correlation of all the field sections as well as the boreholes in the basin, which makes it possible to individualize isochronous markers separated by a few tens to hundreds of thousands years [e.g. Bourquin and Guillocheau, 1993, 1996].

After the characterization of sedimentary facies, deduction of depositional processes, identification of facies association and interpretation of depositional environments, and setting up a sedimentological model, the genetic unit are characterized and then stacking pattern showing the evolution over time of the depositional environment are established.

The second step consists in correlation of the genetic sequences according to three transects and based on reference levels which can serve as isochronous markers. For this objective four

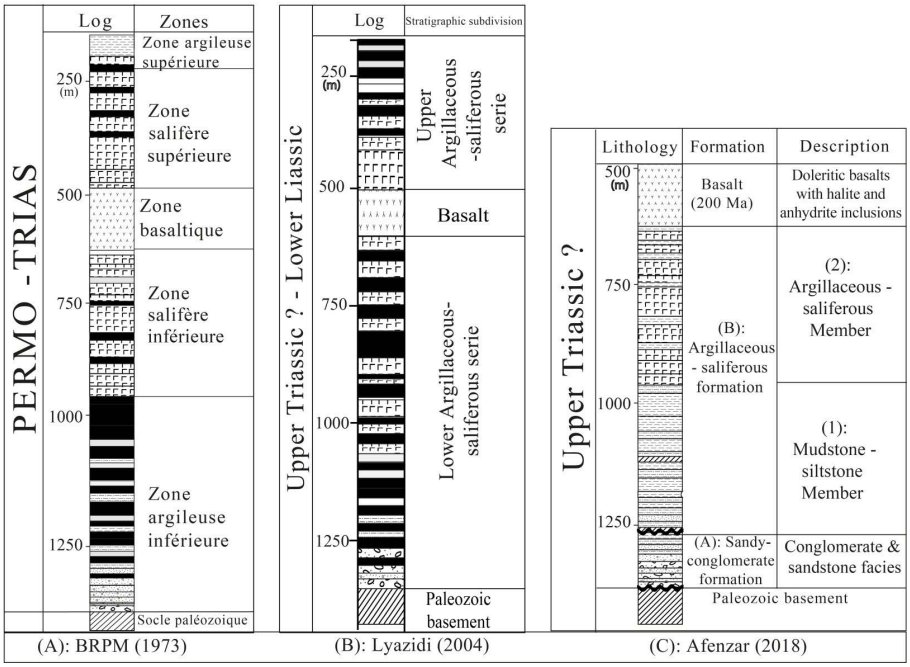

Figure 3. Lithostratigraphic subdivision of the detrital and evaporite infra-basaltic series of the Mohammedia–Benslimane–ElGara–Berrechid basin (A: BRPM, 1973; B: Lyazidi, 2004 C: Afenzar, 2018).

levels have been identified: (1) unconformity between the Hercynian basement and the first facies deposited in the basin; (2) contact between the siltstone-mudstone member and the basal part of the argillaceous-saliferous member; (3) contact between the top part of the argillaceous-saliferous member and the basal part of the member containing pure halitic facies; (4) the lower part of the basalt formation considered as the limit between the Upper Triassic and Lower Liassic [Peretsman, 1985]. A cartography of the genetic sequences was carried out below in order to obtain 2D and 3D geometries for a better interpretation of the evolution of these genetic units as well as the lateral passages of the facies.

5. Facies analysis

5.1. *Identification of lithofacies*

Fourteen facies were identified, described and interpreted in terms of depositional processes based on lithology, grain sizes and sedimentary structures [Miall, 1978, 1996] (Figures 4, 5 and 6, Table 1).

5.2. *Architectural elements*

In this study and according to architectural elements of [Miall, 1996, 2016] we used the abbreviation AE (Architectural Element) for the coding of these elements. This analysis made it possible to characterize six architectural elements (noted AE1 to AE6, Figures 5a, 5b, 5c and 5d) and two facies associations (AFP and AFE).

Architectural element AE1

This constitutes the basis of the series, it was determined in the Chaâbat El Hmira area on a vertical extent from 4 to 5 m. AE1 is formed mainly by facies association Fc1 and Fc2 corresponding to facies Gms and Gm of Miall [1978, 1996]. It is at the base of the series (in contact with the Paleozoic basement) and associated with the architectural elements AE2 and AE3 (Figure 5a). It is formed by gravity flow deposits, mainly pebbles and gravels poorly sorted, formed in the proximal areas of alluvial fans. According to all the criteria, this element corresponds to the element SG (Sediment Gravity Flow) of Miall [1985, 1996, 2016].

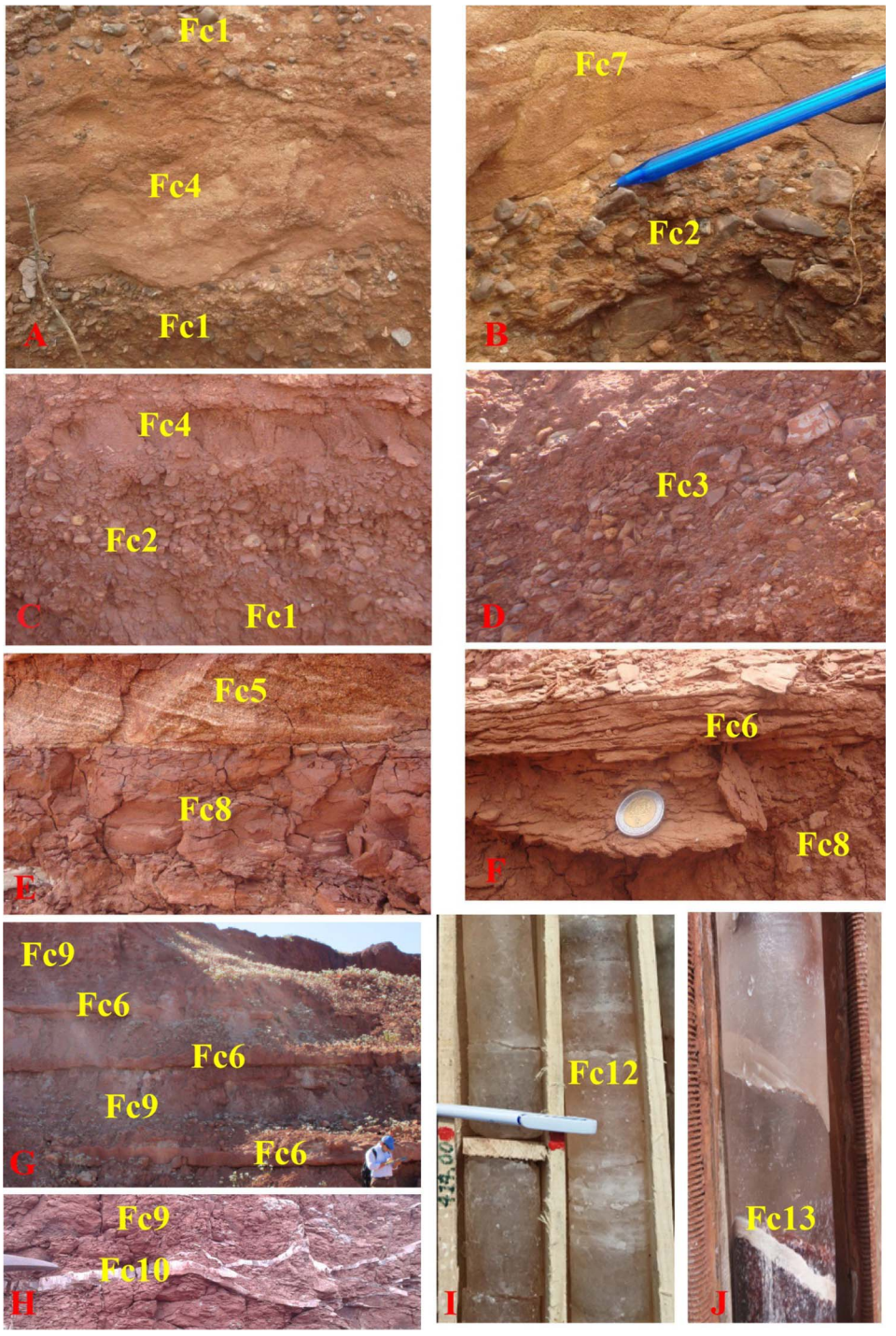

Figure 4. Illustration of the different facies identified in the basin. Description and interpretation in Table 1.

Architectural element AE2

AE2 (Figures 5a and 5b) is formed by lithofacies Fc2, Fc4, Fc5, Fc6 and Fc9. Regarding the internal structure, it is formed by poor matrix and imbricated pebbles facies (Fc2) showing channels lag and sieve deposits. In other cases, this element is formed by sandstone lithofacies characterized by horizontal planar bedding: upper flow regime (Fc6), and by some sandstone lithofacies showing the planar crossbeds (Fc5). Moreover, architectural element AE2 has fourth order basal boundary surfaces (4th: minor erosion) and over (5th: surface bounding generally flat to slightly concave-upward) [Miall, 1988]. These limits are sometimes erosive and slightly planar and in other cases erosive and concave to the top. Inside the element, and between the lithofacies, small boundaries can be identified. From these characteristics, we can say that AE2 resembles to the architectural element CH (Channels) of Miall [1985, 1996, 2016].

Architectural element AE3

It is formed mainly by assemblages of coarse lithofacies containing imbricated pebbles and gravels, showing horizontal stratification, sometimes planar crossbedding: Fc2 and Fc5 (Figure 5a). Sometimes minor lithofacies were identified between these major facies (Fc4 and Fc6). Most facies of this element are organized as tabular bodies of five to six meters thick. Also, it is formed from a 4% to 6% of fine to medium sandstones. AE3 corresponds to the architectural element GB (Gravel bars and bedforms). It is usually coarse deposits formed at gravels bars, these coarse deposits are sometimes intercalated by thin levels sandstones formed at low flows (speed decrease) [Massari, 1983, Miall, 1985, 1996, 2016].

Architectural element AE4

This architectural element (Figures 5b and 5c) is formed by medium to fine lithofacies assemblages: facies Fc5, Fc6 and Fc7 corresponding respectively to facies Sp, Sh and Sl of Miall [1978, 1996, 2016], but it is dominated by Fc7. The Fc6 and Fc7 facies are sometimes separated by a very fine facies: Fc8. Architectural element AE4 passes laterally into element OF. It is characterized by internal boundaries of second to third order, while its outer boundaries are fourth order. For this, AE4 has many similarities with the architectural element SB (Sand Bedform) of Miall [1985, 1996, 2016]. This architectural element characterizes in our case, crevasse channels and/or crevasse splays deposits.

Architectural element AE5

It is an assemblage of fine to very fine lithofacies. This element is presented as sandstone sheets with horizontal laminations from 40 to 80 cm thick: facies Fc6, it is intercalated with thin purplish siltstones and mudstones laminated: facies Fc8 and Fc9. This architectural element resembles to architectural element LS (sand laminated sheets) of Miall [1985] (Figure 5c). Lithofacies forming this architectural element have been interpreted as the product of flash floods [Miall, 1985, Rust, 1978, Sneh, 1983, Tunbridge, 1981, 1984]. The architectural characteristics of this element are well described by Tunbridge [1981] and Sneh [1983]. The sand sheets are deposited on flat surfaces slightly eroded, laterally, they can spread over hundreds of meters.

Architectural element AE6

Architectural element AE6 (Figures 5b and 5c) is considered as a major element in the basin, its thickness can reach forty meters. It is presented as large sheets (2 to 50 m thick), formed by purplish or red brick siltstones and mudstones, these siltstones and mudstones sometimes show a massive aspect with crude planar laminations indicating a quiet depositional setting. In other cases, they show horizontal laminations with very thin intercalations (5–15 cm) of fine sandstones. By these characteristics we can say that AE6 corresponds to the architectural element OF (Overbank fines) of Miall [1985, 1996, 2016].

According to Miall [1985, 1996], in most cases this element has a sheet geometrical form, reflecting its origin by vertical aggradation. In the vicinity of the active channels, these sheets are separated by crevasse splays. This architectural element may

Table 1. Description and interpretation of sedimentary facies of Triassic series of MBEB based on Miall (1978 and 1996), Bridge [2003] and Opluštil et al. [2005]

Facies code	Lithology and sedimentary structures	Depositional process	Interpretation
		Conglomeratic facies	
Fc1	Massive conglomerate (1 m to 4 m thick) with angular, disorganized and poorly sorted gravels. The matrix is formed by the fine sandstone. Without sedimentary structures (A, B Figure 4).	Gravity flows, Mass flow deposits	Equivalent to Gms of Miall [1996]. The absence of sedimentary structures and the existence of a mixture of fine and coarse materials suggest that this conglomerate is deposited by gravity flows: debris flow at proximal alluvial fans environment [Miall, 1978, 1985, 1996, Opluštil et al., 2005].
Fc2	Clast-supported stratified conglomerates with centimeter to decimeter-sized pebble-gravels, showing angular to sub-angular shapes and horizontal bedding imbrication (B & C, Figure 4).	Aggradational deposit	Equivalent to Gm of Miall [1996]. This facies (0.4 m to 2.5 m thick) has been deposited at median to distal alluvial fans or longitudinal bars in the braided rivers system. It can also be interpreted as sieve and/or lag deposits [Miall, 1978, 1985, 1996].
Fc3	Planar crossbeds conglomerate (0.5 m to 3 m thick). The matrix is formed mainly by clastic materials (clast-supported) which are very fine sandstones (D, Figure 4).	Progradational deposit	Equivalent to Gp of Miall [1996]: Deposit of longitudinal bar in a braided rivers system with shallow channels [Miall, 1978, 1985, 1996]. This facies present a similarity with conglomerate of the lower part of Bigoudine formation (T6) in the Argana valley [Hofmann et al., 2000].
		Sandstone facies	
Fc4	Massive coarse sandstone (1 m to 3 m thick) without any sedimentary structures. Sometimes it presents isolated large fragments (A & C, Figure 4).	Rapid deposits Gravity flow deposits	Equivalent to Sm of Miall [1996]. The presence of isolated large fragments is probably related to their falling along the slope [Sohn et al., 1997], associated with the deposition mechanism itself or a movement in a high load flow [Postma and Cruickshank, 1988]. According to [Einsele, 1992, Miall, 1985, 1996], these facies occur in alluvial fans environment.
Fc5	Fine to coarse sandstone (0.4 m to 2 m thick), showing the planar crossbeds (E, Figure 4).	Progradational deposit	Equivalent to Sp of Miall [1996]: Linguoid or transverse bars deposits (lower flow regime) [Bridge, 2003, Miall, 1985, 1996, Todd, 1996]. It is similar to some sandstone beds of the lower part of Oukaïmeden sandstone [Benaouiss et al., 1996].

(continued on next page)

Table 1. (continued)

Facies code	Lithology and sedimentary structures	Depositional process	Interpretation
Fc6	Fine to coarse sandstone (0.2 m to 1.5 m) characterized by horizontal laminations with parting or streaming lineation (F, Figure 4).	Plane-bed flow	Equivalent to Sh of Miall [1996]. This structure is generated by small longitudinal vortices affecting the entire turbulent boundary layer. It results from upper flow regime deposits [Miall, 1985, 1996].
Fc7	Fine sandstone (0.5 m to 2 m thick) characterized by low angle (<10°) planar cross beds.	Scour fills	Equivalent to Sl of Miall [1996]. It is a crevasse channel and/or a crevasse splay deposit often formed in the floodplain at anastomosed fluvial system.
		Fine facies	
Fc8	Massive to horizontal laminated siltstone. They have a reddish appearance with grey to greenish levels of mottling (E & F, Figure 4).	Overbank deposit	Equivalent to Fl of Miall [1996]. Vertical accretion deposit showing a laminar flow of very low energy. This facies is interpreted as a flood plain, overbank or playa deposits [Miall, 1985, 1996].
Fc9	Massive reddish mudstone (0.1 m to 6 m thick) showing mottling spots (C & H, Figure 4).	Overbank deposit	Equivalent to Fm of Miall [1996]. These mudstones can be deposited in (1) an alluvial plain of a braided system, (2) floodplain and playas, and sometimes in (3) distal alluvial fans [Mader, 1985]. These mudstones are interpreted as lacustrine or overbank deposit [Miall, 1996]. This facies and Fc8 sometimes have cyclicity similar to that described by Hofmann et al. [2000] in the Argana valley (T4, T5 and T7).
		Evaporite facies	
Fc10	Gypsum beds facies (0.1 m to 0.5 m). It is presented in the form of centimeter banks alternating with the siltstones and the mudstones facies (H, Figure 4).	Evaporation in a hot and humid environment	These facies are formed in relatively hot and humid environments by the precipitation of sulfated ions in supersaturated solutions subjected to intense evaporation [Warren, 2006, 2010].
Fc11	Fibrous gypsum (0.1 m to 0.2 m thick)	Diagenetic facies	Diagenetic origin [Afenzar and Essamoud, 2017, Afenzar, 2018, Et-Touhami, 1994, 1996].

(continued on next page)

Table 1. (continued)

Facies code	Lithology and sedimentary structures	Depositional process	Interpretation
Fc12	Milky clean halite deposited as decametric to metric beds rarely associated with very fine anhydrite laminae (I, Figure 4).	Evaporation in a hot and humid environment	The rhythmicity of this facies with the mudstone facies is probably due to the interventions of the slightly turbid continental waters which propagate on the surface of the brine [Afenzar, 2018, Et-Touhami, 1994, 1996, Sonnenfeld and Hodec, 1985]. The alternation of this halite with detrital and sulphate levels indicates that it is probably deposited in saline mudflats or evaporite flats.
Fc13	Phenoblastic halite with limpid crystals (J, Figure 4). (0.5 m to 0.5 m thick)	Diagenetic facies	Filling of dissolution cavities. Diagenetic origin [Afenzar, 2018, Et-Touhami, 1994, 1996].
Fc14	Millimeter to centimeter veins of fibrous halite.	Diagenetic facies	Filling of pre-existing fractures in the mudstone levels. It is presented as thin fibers elongated perpendicularly to the walls of mudstones. This halite is formed probably during diagenesis in the mudstone [Dumas, 1988, Et-Touhami, 1994, 1996, Hovorka, 1983].

fill abandoned channels, provided it has concave-up basal contact and ribbon to lenticular geometry of the channel itself [Ethridge et al., 1981, Miall, 1985].

Facies association of Playa (AFP)

It is a lithofacies combination of 5 to 6 m thick. It is formed by siltstone and mudstone lithofacies assemblage (*Fc8, Fc9*) and by fine sandstones sometimes showing horizontal flat beddings (lithofacies Sh). The facies association AFP presents a cyclicity of the sandstone, siltstone and mudstone facies; which shows that it is deposited in Playa Lake. The presence of sandstone deposits also shows that these playa lakes are shallow [Liu and Wang, 2001].

Evaporite facies association (AFE)

It is an association of mudstone (Fm) and evaporite facies (Fc10: beds gypsum, Fc11: fibrous gypsum, Fc12: milky halite, Fc13: phenoblastic halite, Fc14: fibrous halite). The thickness of the facies varies between 1 and 1.5 m for the siltstone, between 10 and 20 cm for the gypsum and between 10 cm and 2 m for the halite. These evaporite facies are often of primary and in other cases diagenetic origin. They are formed by the evaporation of saline waters in mudflats and lagoons in a hot and humid climate in relation to a "pellicular" sea that covered the basin in the Upper Triassic.

6. Paleoenvironment reconstruction

6.1. *Proximal alluvial fans system*

This fluvial model is characterized by massive conglomerate with angular, disorganized and poorly sorted gravels, and by massive coarse sandstone (two to three meters thick without any sedimentary structures). These lithofacies are associated in two architectural elements: AE1 (Sediment gravity flow SG) and AE2 (Channels CH). AE1 units are interbedded with channelized beds of AE2. By these architectural element characteristics (facies assemblage, geometry, bounding surfaces…), we can deduce that this depositional environment is similar to the model

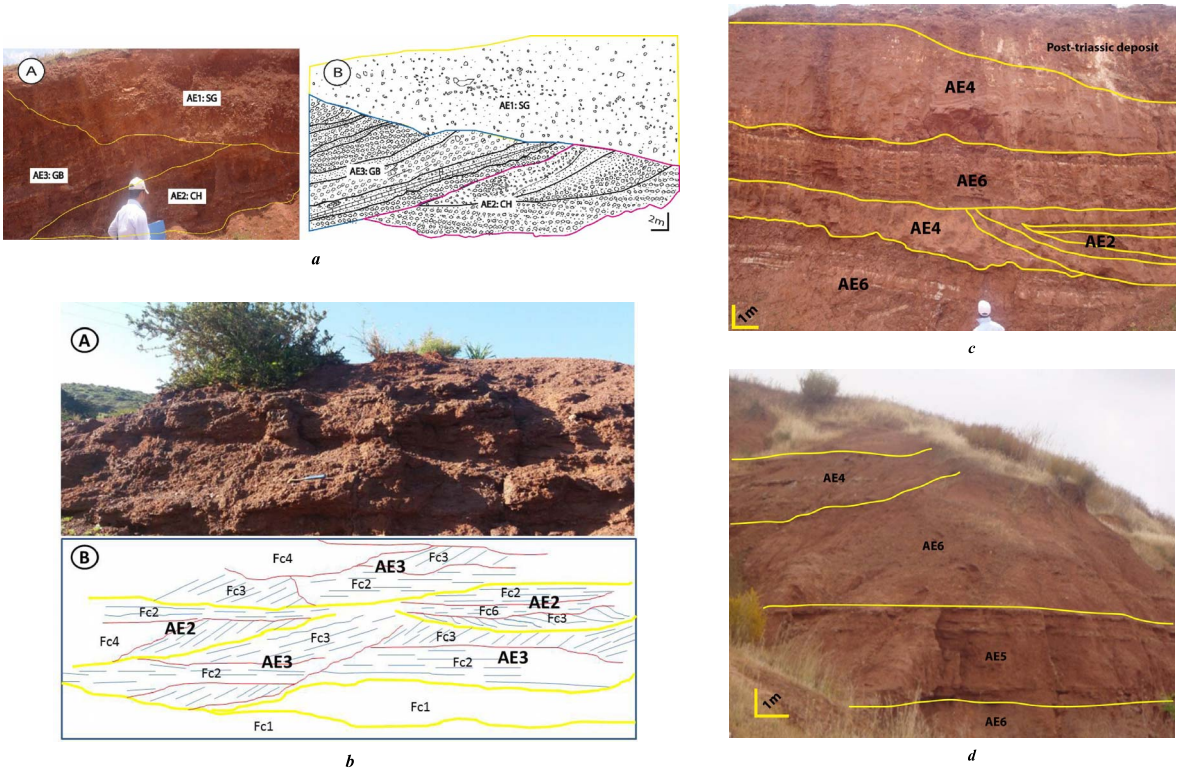

Figure 5. Architectural elements characterized in the basin (a: in Chaâbat Lhmira outcrop, b: in the Chaabat Al Hamra outcrop, c: in the top of Chaâbat Lhmira outcrop, d: in Assikriat outcrop).

No 1 of Miall [1985, 1996, 2016]. It is proximal alluvial fan with sediment gravity flows of gravelly rivers [Afenzar, 2018, Afenzar and Essamoud, 2017, Miall, 2016]. The frequency of debris flows depends strongly on source rock weathering characteristics, so that adjacent fans, the headwaters of which flow across contrasting bedrock units, may show quite different lithofacies assemblages [Hooke, 1967, Miall, 1996, 2016].

6.2. *Shallow channels of a braided rivers system*

The sediments characterizing this environment style are coarse to medium. It is a clast-supported stratified conglomerate with centimeter to decimeter-sized pebble-gravels, showing sub angular shapes and horizontal bedding imbrication (Fc2), and planar crossbeds conglomerate (Fc3). The medium to fine deposits are presented by massive coarse sandstone without any sedimentary structures (Fc4) and fine to coarse sandstone characterized by horizontal laminations with parting or streaming lineation (Fc6). The facies association of this style forms the architectural element AE2 (CH: channel) and AE3 (GB: gravel bars). In this environment, the architectural element AE3 is the most abundant. During the fluctuations stage, bar complexes become emergent, and are crossed by minor channels in which thin deposits of AE2 may form [Miall, 2016]. These fluvial style characteristics resemble to those of model No 2 of Miall [1985, 1996, 2016]. It is a proximal braided rivers system characterized by shallow channels and gravel bars.

6.3. *Floodplains in anastomosed rivers system*

This depositional environment is characterized essentially by fine to very fine deposits with a large thickness. In that case, these facies are organized into

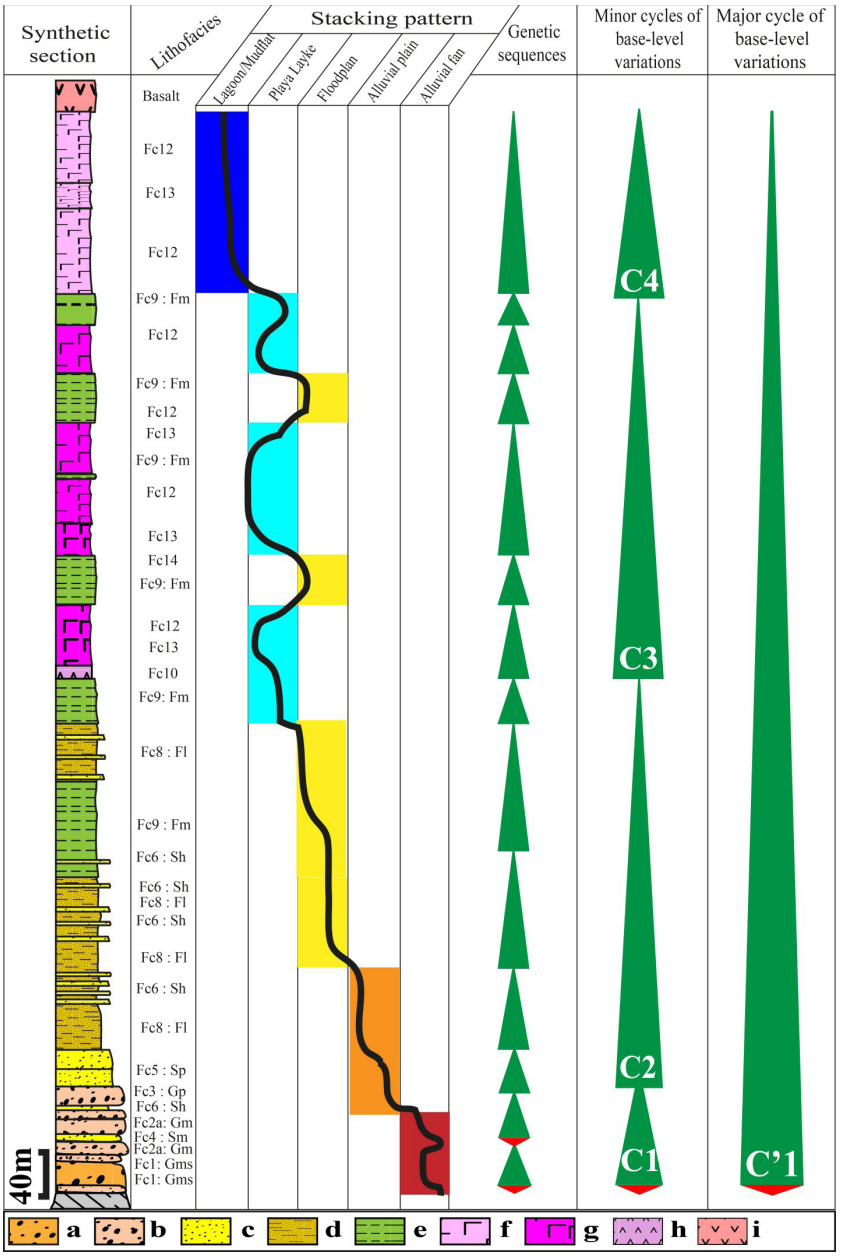

Figure 6. Synthetic sedimentary log of the basin with minor and major cycles of base-level variations. a and b: conglomerate; c: sandstone; d: siltstone; e: mudstone; f: pure halite; g: argillaceous halite; h: gypsum; i: basalt.

two architectural elements: AE4 (SB: Sand Bedforms) deposited in the crevasse splays, and architectural element AE6 (OF: Overbank Fine) formed in flood plains and abandoned channels. The element AE4 has a limited lateral extent and passes laterally into AE6. This type of fluvial style is much less studied and interpreted, unlike other types of depositional environment [Farrell, 1987, Kraus and Bown, 1988, Miall,

1985, 1996, 2016]. However, it is linked to an anastomosed environment characterized by low-energy floods with crevasse channels and crevasse splays.

6.4. *Coastal plains, playa lakes, mudflats and lagoons system*

This is a set of more distal deposit environments. They are characterized by deposits recorded in the middle and top part of the argillaceous-saliferous formation (B) and which is finally capped by Triassic-Liassic basalts. This system is characterized by massive to horizontal laminated siltstone, massive reddish mudstone showing mottling spots, gypsum beds facies alternating with the siltstones and the mudstones facies, fibrous gypsum, milky clean halite deposited as decametric to metric beds rarely associated with very fine anhydrite laminae and phenoblastic halite with limpid crystals.

This system probably corresponds to the large coastal plain downstream characterized by the development of playa lakes, mudflats and lagoons where the evaporite facies are formed by the evaporation of marine waters [Peretsman, 1985, Peretsman and Holser, 1988] under a hot and humid climate and in relation to a pellicular sea that covered the domain during the Upper Triassic time.

7. Genetic stratigraphy and correlation

7.1. *Identification of genetic sequences*

In the continental domain, as in our case, the identification of genetic sequences is complicated. A genetic sequence is usually represented by a period of erosion, by pass or stacked of fluvial deposits linked to the base level fall (i.e. progradation) and a period of aggradation accompanied the base level rise (i.e. retrogradation). The periods of base level fall correspond to a weak preservation of the facies whereas the period of aggradation corresponds to a significant sedimentary preservation [Bourquin et al., 1998, 2009, Hamon and Merzeraud, 2005, Homewood et al., 1992, Merzeraud, 1992].

Genetic sequence UG1

It is a genetic sequence in which an alluvial fan system evolves to a braided system with an alluvial plain. The period of base level fall (progradation) is characterized by a weak preservation of the thin conglomerate facies without sedimentary structure with coarse, angular and poorly sorted elements limited by erosion surfaces indicating the base level fall. The base level rise period (retrogradation) is characterized by the important preservation of alluvial fan facies and the development of conglomeratic facies (showing horizontal stratifications with imbricated and well-sorted pebbles-gravels) and sandstone facies showing horizontal planar bedding. These facies are organized into architectural elements: AE1, AE2 and AE3 formed in channels and bars in a braided river system.

Genetic sequence UG2

The base level fall period is characterized by the deposition of coarse massive sandstone facies without sedimentary structures. The base level rise is marked by well-organized facies with horizontal stratifications and other conglomerate facies showing planar cross-beds organized into architectural elements AE2 and AE3 deposited at the channels and bars in a braided fluvial system.

Genetic sequence UG3

This genetic sequence formed during the increase of the base level (retrogradation), is characterized by the development of distal fine facies forming the architectural element AE6 and deposited in the floodplain. The basal boundary of this sequence is marked sometimes by the passage of coarse facies formed at the bars in a braided system to fine facies of the floodplain.

Genetic sequence UG4

This sequence is characterized by its formation during the rise of the base level marked by the deposition of sandstone, siltstone and mudstone facies. These facies are associated in two architectural elements (AE2: CH and AE6: OF) formed in anastomosed channels with an immense floodplain. This period of base-level rise is also characterized by a decrease of grain-size, passing from channel sandstone facies to the siltstone-mudstone facies of the floodplain.

Genetic sequence UG5

UG5 is characterized by a period of base level rise associated with the development of sandstone

and mudstone facies organized into architectural elements AE4, AE5 and AE6 deposited in sand bars and crevasse splays at a floodplain related to an anastomosing fluvial system. The facies association is characterized by a gradual decrease of grain-size.

Genetic sequence UG6

This genetic sequence is formed during the base level rise period. It is represented by sandstone and siltstone-mudstone facies deposited in floodplains and probably in coastal plains characterized by architectural element AE6 and facies associations of playa (AFP).

Genetic sequence UG7

It is characterized by a period of base level rise, and formed by sandstone, siltstone, mudstone and evaporite facies. These facies form the association of Playa (AFP) and/or facies-association of evaporite (AFE) formed at playa lakes and at lagoons with an immense coastal plain.

Genetic sequences UG8 to UG14

The UG8 to UG14 genetic sequences are characterized by alternating siltstone, mudstone and evaporites facies (organized into architectural elements AE6, AFP and AFE) formed in a coastal plain associated with mud flats and lagoons. These genetic units have been identified mainly in boreholes at depths ranging from 500 m up to 1000 m. The maximum flooding surfaces of these sequences are between the mudstone facies and the evaporites facies.

7.2. *Genetic sequences correlations*

The genetic units are correlated from one section to the other (Figure 7) and from borehole to another (Figure 8). This correlation is based on the determination of reference levels. For this objective four limits have been identified:

- the first one is the unconformity between the Hercynian basement and the first facies deposited in the basin,
- the second reference level is the contact between the detrital facies and the first evaporites facies (gypsum) deposited in the basin and corresponds to the contact between the Mudstone-Siltstone Member and the basal part of the Argillaceous-Saliferous Member (Figure 3C),
- the third reference level concerns the contact between the upper part of the Argillaceous-saliferous Member and the basal part of pure halitic facies, located at the top of this Member,
- the fourth one is the beginning of the Basalt considered as the limit between the Upper Triassic and Lower Liassic [Peretsman, 1985].

For more precision, this correlation was carried out according to three transects: the first one (TI) N–S on Oued El Maleh river. The second transect (TII) N–S on the Oued Nfifikh and the last transect (TIII) N–S which links between the boreholes PB43, PB44, POM1 and POM2 (Figure 2). The stacking pattern of the genetic sequence allows the constitution of four minor cycles of base level variation (Figure 6).

The first cycle (C1) is characterized by conglomerate and sandstone deposits unconformably deposited on the Hercynian basement. The maximum flooding surface (MFS1) is marked by the passage of thin conglomerate facies without sedimentary structure with coarse, angular and poorly sorted elements limited by erosion surfaces to conglomerate facies, deposited in proximal alluvial fans and conglomerate and sandstone facies formed in a braided fluvial system with a progressive rise of base level (UG1 and UG2).

The second cycle (C2) (Figures 9, 10 and 11) has a remarkable base level increase. It is characterized by a vertical aggradation of the sandstone, siltstone and mudstone facies formed in an alluvial plain in braided system and/or in an anastomosing river system.

The third cycle (C3) (Figures 9, 10 and 11) was identified on the borehole (PB44). It is a retrogradational/aggradational cycle and is characterized by the appearance of the first evaporite facies. Its base is represented by gypsiferous mudstone and alternations of mudstone and bed gypsum. Then, there is a transition to alternations of halite (+/− closed lagoon) and mudstone formed in playa and mudflats.

The fourth and last cycle (C4) (Figure 11) is characterized by the rise of the base level, with the formation of pure halite facies, which shows a marine intervention stopped abruptly by basaltic effusions at the

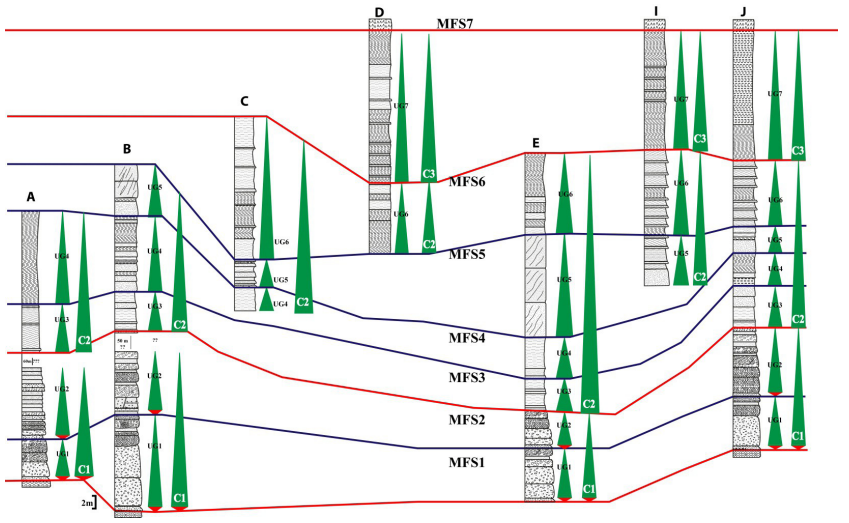

Figure 7. Correlation of genetic sequences based on the study of field sections on the Oued Nfifikh-ElGara axis (Transect II).

end of the Upper Triassic.

7.3. *Basin-wide genetic sequences cartography*

The identification of different orders of genetic sequence stacking and their correlation allow the cartography of their extent. The result is a paleogeographic reconstruction for each genetic sequence. This stratigraphic correlation makes it possible to study the distribution of facies in space within each sequence, and their evolution over time (Figures 9, 10 and 11).

At the base of MFS1, conglomerates have larger thicknesses in the center than at the ends for transect (TI) (Figure 9). For the transect (TII) (Figure 10), these conglomerates have significant thicknesses along the entire transect. At the north, some conglomeratic facies of the retrogradational part of the genetic sequence UG1 pass laterally to sandstone facies. The genetic sequence (UG1) of this cycle (C1) is formed in proximal deposition environments: alluvial fans, proximal braided system with remarkable variations of palaeoslope.

Between MFS1 and MFS2, an increase of base level leads to a change in the depositional environment to an alluvial plain characterized by sandstone and siltstone deposits. This rise of the base level is shown by well-developed braided channel facies and by a gradual decrease of grain size and then by the appearance of the well-sorted facies, with the disappearance of the angular elements and finally by the passage of the massive facies without sedimentary structure (Gms and Sm) at Planar cross-beds facies (Gp and Sp) then at Horizontal lamination facies (Gm and Sh) [Bourquin et al., 1998, 2009, Hamon and Merzeraud, 2005, Homewood et al., 1992, Merzeraud, 1992, Poli, 1997]. Lateral transition of facies is observed at the north of the transect (TI) (Figure 9) and the entire transect (TII) (Figure 10).

Between MFS2 and MFS4, we have noticed an appearance of evaporites facies that are concentrated in the middle of the transect (TI, Figure 9) and pass laterally to siltstone and mudstone at the same genetic sequence. For the transect (TIII, Figure 11), this interval (MFS2–MFS4) is characterized by a genetic sequence with purely saline facies. This passage of evaporites facies to mudstone facies is probably due either to the migration of deposition environment during the same time interval, or to the dissolution and erosion of these facies exposed in outcrop. The last cycle (C4) (Figures 10, 11) is characterized by a deposition of pure halite facies recovered by basalts, which shows the marine incursion before these basaltic effusions at the end of Triassic and early Jurassic.

These genetic sequences and progradational/retrogradational cycles show an evolution of the proximal fluvial environments (alluvial fans passing

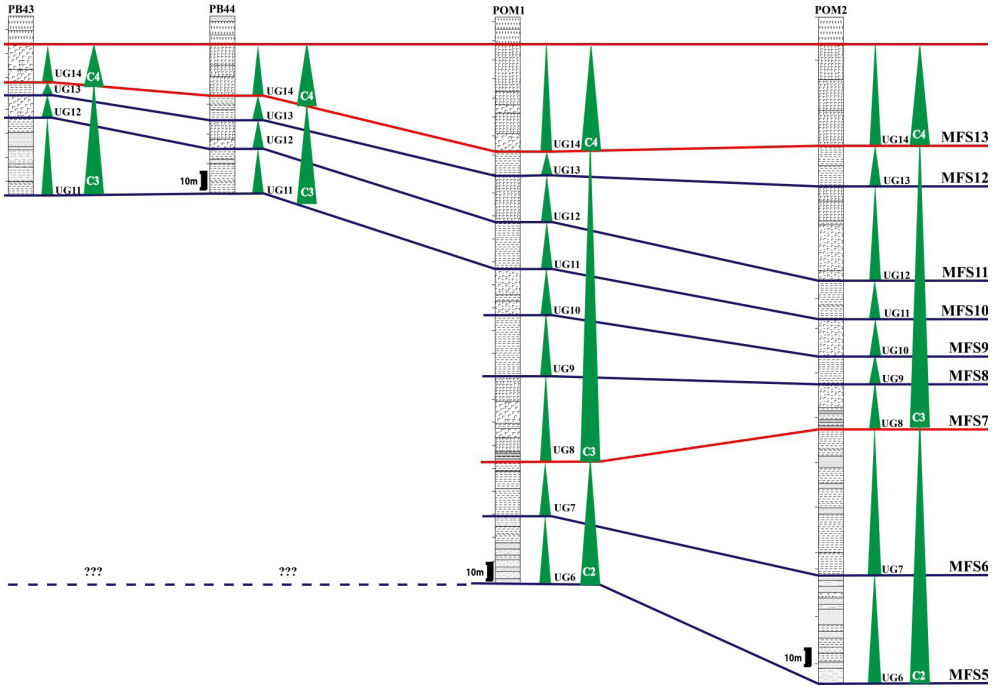

Figure 8. Correlation of genetic units based on the study of the central and northern boreholes of the basin (Transect III: N–S).

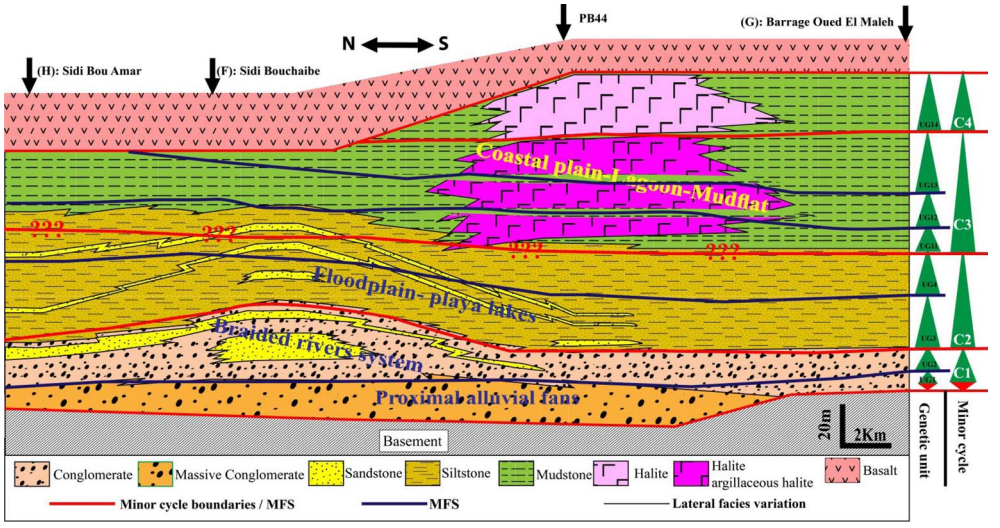

Figure 9. First transect (TI) N–S of correlation and cartography of genetic sequence and minor cycles of base-level variation.

laterally to braided system) at the base of the TI and TII (respectively Figures 9 and 10, orange and beige color) to a distal environments (anastomosed rivers and floodplains) in the middle of TI and TII and at the base of TIII (respectively Figures 9, 10 and 11, yellow and green color below MFS2), and then at a transition environment (coastal plain with lagoons and mudflats) at the top of the TI and TII and throughout

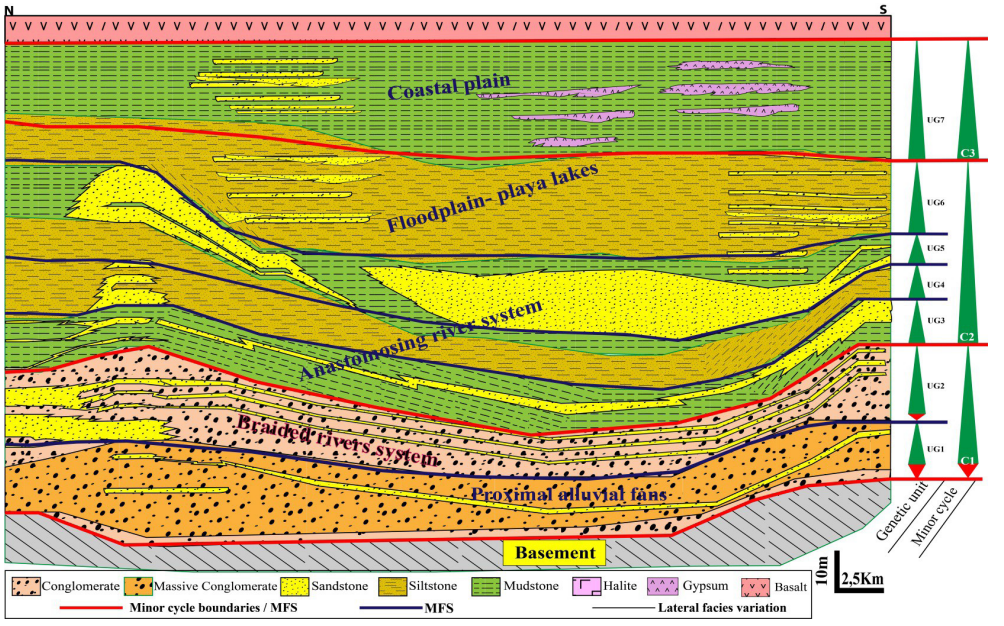

Figure 10. Second transect (TII) N–S of correlation and mapping of genetic sequence and minor cycles of base-level variation.

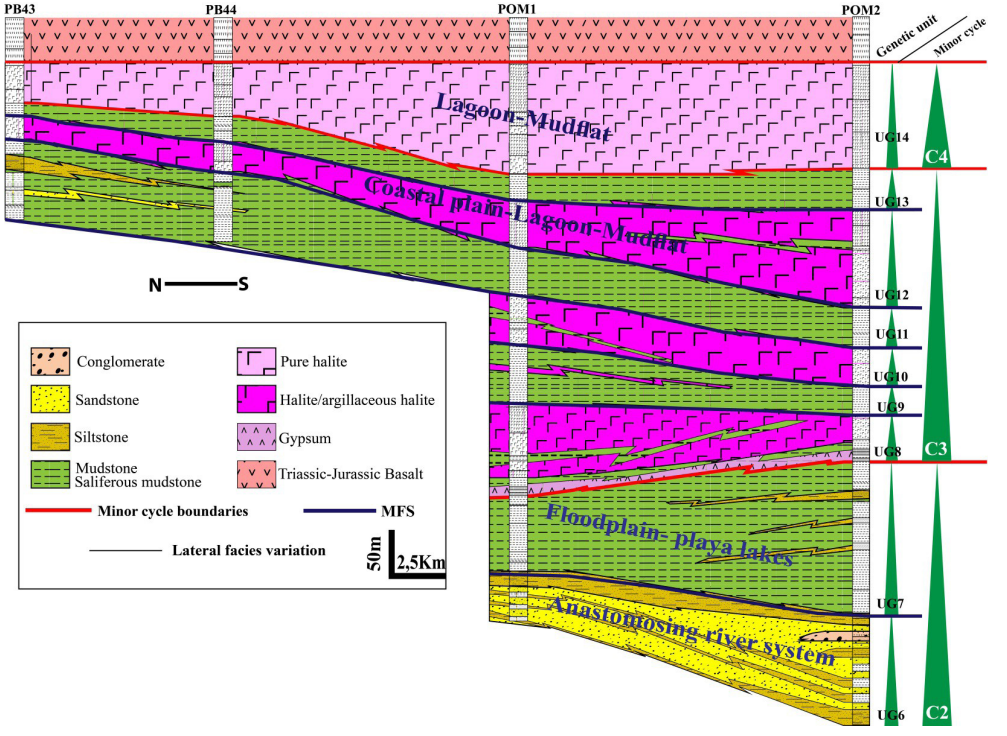

Figure 11. Third transect (TIII) N–S of correlation and mapping of genetic sequence and minor cycles of base-level variation.

the transect TIII (respectively Figures 9, 10 and 11, green and pink color).

8. Discussion

Paleoenvironmental evolution

Sedimentary analysis has shown that the studied basin is characterized by siliciclastic sedimentation at the beginning and then evaporitic at the end of the syn-rift sedimentary filling (Figure 6) [Afenzar, 2018]. First-cycle debris eroded from a mountainous source area are deposited at the edges of the basin in coarse alluvial fans, or transported to a coastal plain [Miall, 2016].

Based on the identified facies, and the characterized architectural elements and the alluvial styles, the depositional environments are evolved over time from:

- proximal alluvial fans system characterized by accumulation of gravity-flow sediments to a proximal braided system characterized by conglomeratic and sandstone bars;
- subsequently, the depositional environment has changed to an anastomosed system with a vast floodplain characterized by crevasse splays that pass laterally to overbank deposits (middle of the sedimentary series); these anastomosed systems occur in areas of active vertical aggradation, such as coastal systems during a time of rapidly rising base level;
- finally, these environments eventually evolve to a coastal plain where playa lakes, mudflats and lagoons have developed. In this phase, the syn-rift sedimentary series recorded a marine incursion at the Upper Triassic with saliferous sedimentation Afenzar [2018]. It is deduced from the presence of a thick saliferous series with a large lateral extension whose isotope ratios of sulfur and bromine contents indicate their marine origin [Peretsman, 1985, Peretsman and Holser, 1988]. These marine waters are probably of Tethyan origin and are also related to the opening of the Proto-Atlantic [Et-Touhami, 1994]. This marine incursion remains thin compared to the southwest European Triassic basins. In these cases, the well-developed marine domain is indicated by the presence of carbonates rich in marine species (e.g. Alpujarride carbonates in Betic Cordillera: Martin-Rojas et al., 2009). Leleu et al. [2016] specified that these marine ingressions from the Tethys domain are inferred from dolomite and marine fauna in Portugal and from thick salt deposits in Morocco and offshore Canada during the late Rhaetian.

Control factors

Detrital sedimentation in the MBEB basin can be interpreted as resulting from the filling of a ditch in the form of half-graben [El Wartiti and Fadli, 1985, El Wartiti et al., 1992], the replay of the Hercynian faults which caused the collapse of this ditch and the activation of erosion. According to Salvan [1984], distension and subsidence were localized in Meseta points (ex. MBEB basin), which led to the accumulation of salts deposits.

The MBEB basin is therefore an open continental zone, which has favored the registration of alluvial fans, high-energy fluvial systems, and then gradually filling up, we have moved to lakes, and to evaporites. It is a typical succession associated with geodynamic context of rift type.

In this basin, the silico-clastic sedimentation is the result of continental alteration, and therefore a good part of the budget of erosion will arrive in the basin. After the period of erosion (the ante-Triassic reliefs), the basin is an area of sedimentation. It is an extensive basin whose deposits are initially aggradational and then retrogradational.

The MBEB basin also recorded a budget of parameters (mainly tectonic, climate) that created accommodation and a parameter that fills this space: the sediment supply. The sediments are mostly red. This reflects the oxidizing conditions in which the sedimentation was carried out [Biron, 1982, Van Houten, 1973]. The evaporites indicate a relatively hot and humid climate that has favored their precipitation.

The palaeoenvironmental evolution was also controlled by the evolution of palaeoslope. The decrease of the latter is found in most Triassic rift basins belonging to the central Atlantic domain. Leleu and Hartley [2010] suggest that in the Fundy and Minas basins, the palaeoenvironmental transition is diachronous, such that it cannot be related to climatic controls of global or megaregional extent and the fining-upward profile can be explained by a decrease in source area relief by erosion within a hydrologically closed basin.

Paleogeography

The evaporitic deposits could correspond to a Late-Triassic transgression from the Tethys to the north and an epicontinental marine domain to the west [Beauchamp, 1988, Beauchamp et al., 1995, Oujidi et al., 2000]. A "pellicular" sea covered most of the Moroccan basins with intermediate facies, which was therefore a flat surface affected by localized subsidence (The MBEB basin is part of it) where the evaporitic thick layers accumulated. The marine character of the evaporites [Peretsman and Holser, 1988] denotes a first transgressive episode [Salvan, 1984] generalized throughout the Atlasic-Mesetien domain [Oujidi et al., 2000]. The detrital basins on either side of the future Atlantic Ocean are considered primarily purely continental, with the Newark Basin as a model [Smoot, 1991].

The idea of a secondary communication between the Tethyan marine domain and the proto-Atlantic via the basins of Khémisset, Roumani and MBEB, operating discontinuously is quite conceivable [Et-Touhami, 1994].

Relationship with Atlantic rifting

At the beginning of the Mesozoic, the northwestern part of the African continent was affected by an initial fracturing associated with the early stages of the opening of the central Atlantic (Atlantic rift).

Several authors consider that the opening of several Moroccan Triassic sedimentary basins (at least those in the southern edge of the Tethys) was initiated during this Triassic rifting. This opening was controlled by the reactivation of the preexisting weakness zones in the Paleozoic basement and inherited from the Hercynian orogeny [Courel et al., 2003, Hafid, 2000, Laville et al., 2004, Leleu et al., 2016, Le Roy and Piqué, 2001, Medina, 1994, Olsen, 1997, Piqué and Laville, 1995, Piqué et al., 1998].

The MBEB basin is part of the western province of Triassic deposits in Morocco, which correspond to all the basins of the Moroccan Atlantic margin (Doukkala, Argana, Essaouira…) in direct relation with the Atlantic rift [Beauchamp et al., 1985, Salvan, 1984, Van Houten, 1977]. The Triassic deposits are considered as syn-rift.

9. Conclusion

This sedimentological analysis carried out for the first time in this basin allowed the reconstruction of palaeoenvironments and thus the syn-rift sedimentary filling history during the Upper Triassic. During rifting, the MBEB Basin passed through three major phases of sedimentary filling. The first phase is purely continental. During this period, the first deposits arrived in the basin are of alluvial fan origin. Subsequently, the decrease in palaeoslope and the rise of the basal level resulted in paleoenvironmental changes (proximal fluvial system to a distal depositional environment). During the third phase, the syn-rift sedimentary series recorded a marine incursion at the Upper Triassic with saliferous sedimentation.

The correlation and cartography of the genetic sequences as well as the progradational/retrogradational cycles made it possible to obtain 2D/3D geometries of the basin according to the three correlation transects. This indicates a growth in the thickness of these sequences vertically (growth towards the top of the sandy-conglomeratic formation) and laterally (increase of the thickness of the genetic sequences while passing of borders to the center of the basin). These correlations also show lateral passages of the mudstone facies (NE-SE border) to the evaporite facies (basin center). The economic importance of these 2D/3D geometries lies in their orientation of the exploitation of pure halite facies whose thickness and quality increase towards the center of the basin.

From a paleogeographic point of view, the Mohammedia–Benslimane–ElGara–Berrechid Basin is part of the western Moroccan Triassic province, which corresponds to all the basins of the Moroccan Atlantic margin (Doukkala, Argana, Essaouira, Tarfaya) in relation to the rifting of Central Atlantic Domain. In this context, this study consists of a basic approach for all future studies concerning the stratigraphic correlations between this basin and the Triassic basins of the African Atlantic margin and Northeastern American margin.

Acknowledgments

We thank very much S. Leleu and S. Bourquin whose very stimulating reviews greatly enhanced the origi-

nal manuscript, and the Mohammedia rock salt company (SSM: Société de Sel de Mohammedia) through its general manager as well as the director of the salt mine for their help during the realization of this study.

References

Afenzar, A. (2018). *Sédimentologie de faci'es, paléoenvironnements et interpretation en termes de stratigraphie séquentielle haute résolution de la série syn-rift triasique du bassin de Mohammedia–Benslimane–ElGara–Berrechid (Meseta occidentale, Maroc)*. PhD thesis, Univ. Hassan II de Casablanca (Maroc).

Afenzar, A. and Essamoud, R. (2017). Sédimentologie de faciès des dépôts triasiques de la région d'Oued el Maleh et ElGara (Meseta, Maroc). *Intl J. Adv. Res.*, 5(5):1938–1949.

Aigner, T. and Bachmann, G. H. (1992). Sequence-stratigraphic framework of the German Triassic. *Sedim. Geol.*, 80:115–135.

Aït Salem, H., Bourquin, S., Courel, L., Fékirine, B., Hellal, C., Mami, L., and Téfiani, M. (1998). Triassic series on the Saharan platform in Algeria; Peritethyan onlaps and related structuration. In Crasquin-Soleau, S. and Barrier, E., editors, *Stratigraphy and Evolution of Peritethyan Platforms*, volume 5 of *Peri-Tethys Mémoir 3*, pages 177–191. Mém. Museum Natl. Hist. Nat., Paris.

Allen, J. R. L. (1983). Studies in fluviatile sedimentation: bars, bar-complexes and sandstone sheets (low-sinuosity braided streams) in the Brownstones (L. Devonian), Welsh Borders. *Sedim. Geol.*, 33:237–293.

Alves, T. M., Moita, C., Sandnes, F., Cunha, T., Monteiro, J. H., and Pinheiro, L. M. (2006). Mesozoic-Cenozoic evolution of North Atlantic continental-slope basins: The Peniche Basins, western Iberian margin. *AAPG Bull.*, 90(1):31–60.

Barrón, E., Gómez, J. J., Goy, A., and Pieren, A. P. (2006). The Triassic–Jurassic boundary in Asturias (northern Spain): Palynological characterisation and facies. *Rev. Palaeobot. Palynol.*, 138(3–4):187–208.

Baudelot, S., Charrière, A., Ouarhache, D., and Sabaoui, A. (1990). Données palynologiques nouvelles concernant l'Ordovicien et le Trias-Lias du Moyen Atlas. *Géol. Méditerr.*, 17:263–277.

Baudon, C., Redfern, J., and Driessche, J. V. D. (2012). Permo-Triassic structural evolution of the Argana valley impact of the Atlantic rifting in the High Atlas, Morocco. *J. Afr. Earth Sci.*, 65:91–104.

Beauchamp, J. (1988). Triassic sedimentation and rifting in the High Atlas (Morocco). In Manspeizer, W., editor, *Triassic-Jurassic Rifting: Continental Breakup and the Origin of the Atlantic Ocean and Passive Margins*, Developments in Geotectonics 22, pages 477–497. Elsevier, New York.

Beauchamp, J., Benaouiss, N., and Courel, L. (1995). Où était donc le domaine marin dans le Maroc africain au Trias supérieur. *C. R. Acad. Sci. Paris, Ser. IIa*, 221:1033–1040.

Beauchamp, J., Ferrandini, J., and Ferrandini, M. (1985). La série mésozoïque du haut atlas de marrakech. Field trip guide IGCP183, october1985, 42 p.

Benaouiss, N., Courel, L., and Beauchamp, J. (1996). Rift-controlled fluvial/tidal transitional series in the Oukaimeden Sandstones, High Atlas of Marrakesh (Morocco). *Sedim. Geol.*, 107:21–36.

Biron, P. E. (1982). Le Permo-Trias de la région de l'Ourika (Haut-Atlas de Marrakech, Maroc): lithostratigraphie, sédimentologie, tectonique et minéralisations. Stratigraphy. Université Scientifique et Médicale de Grenoble.

Bourquin, S., Bourges, P., and Rigollet, C. (1998). High-resolution sequence stratigraphy of an alluvial fan-fan delta environment: stratigraphic and geodynamic implications – an example from the Keuper Chaunoy Sandstones, Paris Basin. *Sedim. Geol.*, 121:207–237.

Bourquin, S., Eschard, R., and Hamouche, B. (2010). High-resolution sequence stratigraphy of Upper Triassic succession (Carnian–Rhaetian) of the Zarzaitine outcrops (Algeria): A model of fluvio-lacustrine deposits. *J. Afr. Earth Sci.*, 58:365–386.

Bourquin, S. and Guillocheau, F. (1993). Géométrie des séquences de dépôt du Keuper (Ladinien à Rhétien) du Bassin de Paris: implications géodynamiques. *C. R. Acad. Sci. Paris, Ser. II*, 317:1341–1348.

Bourquin, S. and Guillocheau, F. (1996). Keuper stratigraphic cycles in the Paris basin and comparison with cycles in other peritethyan basins (German basin and Bresse-Jura basin). *Sedim. Geol.*, 105(3–4):159–182.

Bourquin, S., Guillocheau, F., and Péron, S. (2009).

Braided river within an arid alluvial plain (example from the early Triassic, western German Basin): criteria of recognition and expression of stratigraphic cycles. *Sedimentology*, 56:2235–2264.

Bourrouilh, R., Richter, J. P., and Zolnai, G. (1995). The North Pyrenean Aquitaine basin, France: Evolution and hydrocarbons. *AAPG Bull.*, 79:831–853. 491P.

Bridge, J. S. (2003). *Rivers and Floodplains: Forms, Processes, and Sedimentary Records*. Blackwell, Oxford.

BRPM (1973). Rapports inédits de fin de sondages concernant les recherches de sels potassiques dans le bassin salifère de berrechid–elgara. Bureau de Recherches et de Participations Minières (BRPM), Maroc.

Courel, L., Ait Salem, H., Benaouiss, N., Et-Touhami, M., Fekirine, B., Oujidi, M., Soussi, M., and Tourani, A. (2003). Mid-Triassic to Early Liassic clastic/evaporitic deposits over the Maghreb platform. *Palaeogeogr. Palaeoclimatol. Palaeoecol.*, 196:157–176.

Crasquin-Soleau, S., Rakus, M., Oujidi, M., Courel, L., Et-Touhami, M., and Benaouiss, N. (1997). Découverte d'une faune d'ostracodes dans le Trias des monts d'Oujda (Maroc); relations paléogéographiques entre les plates-formes nord et sud de la Téthys. *C. R. Acad. Sci. Paris, Ser. IIa*, 324:111–118.

Dumas, D. (1988). *Le Paléogène salifère du bassin de Valence (Sud-Est de la France): géométrie et sédimentologie des dépôts, synthèse de bassin*. PhD thesis, Université Claude Bernard, Lyon.

Echarfaoui, H., Hafid, M., and Aït Salem, A. (2002a). Structure sismique du socle paléozoïque du bassin des Doukkala, Môle côtier, Maroc occidental. Indication en faveur de l'existence d'une phase éovarisque. *C. R. Geosci.*, 334:13–20.

Echarfaoui, H., Hafid, M., Aït Salem, A., and Aït Fora, A. (2002b). Analyse sismo-stratigraphique du bassin d'Abda (Maroc occidental), exemple de structures inverses pendant le *rifting* atlantique. *C. R. Geosci.*, 334:371–377.

Einsele, G. (1992). *Sedimentary Basins: Evolution, Facies and Sediment Budgets*. Springer, New York, NY.

El Arabi, E., Bienvenido Diez, J., Broutin, J., and Essamoud, R. (2006). Première caractérisation palynologique du Trias moyen dans le Haut Atlas; implications pour l'initiation du *rifting* téthysien au Maroc. *C. R. Geosci.*, 338:641–649.

El Arabi, E. H. (2007). La série permienne et triasique du rift haut-atlasique: nouvelles datations; évolution tectono-sédimentaire. Thèse d'Etat, Faculté des sciences Aïn Chok. Université Hassan II de Casablanca, Maroc, page 225.

El Wartiti, M. and Fadli, D. (1985). Relations socle-couverture au cours du Trias dans la zone de BenSlimane-ElGara (Maroc nord mesetien). *Bull. Sci. Terre, Rabat*, 1:54–66.

El Wartiti, M., Medina, F., and Fadli, D. (1992). Effects of the Central Atlantic early *rifting* in the northern border of the Berrechid–ElGara basin (Morocco). *Gaia*, 4:31–38.

Et-Touhami, M. (1994). Le Trias évaporitique du bassin de Khémisset (Maroc central). *Notes Mem. Serv. Geol. Maroc, Rabat*, 373:211.

Et-Touhami, M. (1996). L'origine des accumulations salifères du Trias marocain : apport de la géochimie du brome du sel du bassin de Khémisset (Maroc Central). *C. R. Acad. Sci. Paris, Ser. IIa*, 323:591–598.

Et-Touhami, M. (1998). Le Trias salifère marocain: typologie des cristaux de l'halite et faciès halitiques. *Afr. Geosci. Rev.*, 5(1–2):107–115.

Ethridge, F. G., Jackson, T. J., and Youngberg, A. D. (1981). Flood-basin sequence of a fine-grained meander belt subsystem: the coal-bearing Lower Wasatch and Upper Fort Union Formations, southern Powder River Basin, Wyoming. In Ethridge, F. G. and Flores, R. M., editors, *Recent and Ancient Nonmarine Depositional Environments, Models for Exploration*, volume 31 of *Special Publication*, pages 191–209. SEPM Society for Sedimentary Geology.

Farrell, K. M. (1987). Sedimentology and facies architecture of overbank deposits of the Mississippi River, False River region, Louisiana. In Ethridge, F. G., Flores, R. M., and Harvey, M. D., editors, *Recent Developments in Fluvial Sedimentology*, volume 39 of *Special Publications*, pages 111–120. SEPM Society for Sedimentary Geology.

Ferrer, O., Jackson, M. P. A., Roca, E., and Rubinat, M. (2012). Evolution of salt structures during extension and inversion of the Offshore Parentis Basin (Eastern Bay of Biscay). In Alsop, G. I., Archer, S. G., Hartley, A. J., Grant, N. T., and Hodgkinson, R., editors, *Salt Tectonics, Sediments and Prospectivity*, volume 363 of *Special Publications*, pages 361–379. Geological Society of London.

Gonzàlez de Aguilar, J. P. (2015). *Salt tectonics in in-*

verted continental margins: Seismic interpretation in the Cantabrian Margin. PhD thesis, Granada: Universidad de Granada.

Hafid, M. (2000). Triassic-Liassic extensional systems and their Tertiary inversion, Essaouira Basin (Morocco). *Mar. Petrol. Geol.*, 17:409–429.

Hamon, Y. and Merzeraud, F. (2005). Nouvelles données sur le Trias de Sologne (Chémery, Sud-Ouest du bassin de Paris) : stratigraphie et environnements de dépôts. *Géol. France*, 176:3–22.

Hminna, A., Voigt, S., Klein, H., Saber, H., Schneider, J. W., and Hmich, D. (2013). First occurrence of tetrapod footprints from the continental Triassic of the Sidi Said Maachou area (Western Meseta *Morocco*). *J. Afr. Earth Sci.*, 80:1–7.

Hofmann, A., Tourani, A., and Gaupp, R. (2000). Cyclicity of Triassic to Lower Jurassic continental red beds of the Argana Valley, Morocco; implications for palaeoclimate and basin evolution. *Palaeogeogr. Palaeoclimatol. Palaeoecol.*, 161:229–266.

Homewood, P. W., Guillocheau, F., Eschard, R., and Cross, T. A. (1992). Corrélation hautre definition et stratigraphie génétique: une demarche intégrée. *Bull. Centres Rech. Explor. Prod. Elf Aquitaine*, 16:357–381.

Hooke, R. L. (1967). Processes on arid-region alluvial fans. *Geology*, 75:438–460.

Hovorka, S. D. (1983). Sedimentary structures and diagenetic modifications in halite and anhydnte, Palo Duro Basin. In *Geology and Geohydrology of the Palo Duro Basin, Texas Panhandle*, Geological Circular 83-4, pages 49–57. Bureau Economic Geology, Austin.

Hssaida, T., Zahour, G., Oulmach, F., Youssfi, Z., Chahaldi, S., and Habid, A. (2012). Nouvelles datations des argilites post-basaltiques du bassin de l'Oued Mellah (Meseta occidentale, Maroc). *Notes Mem. Serv. Geol. Maroc*, 575:131–137.

Kozur, H. W. and Bachmann, G. H. (2008). Updated correlation of the Germanic Triassic series within the Tethyan scale and assigned numeric ages. *Beri. Geologischen Bundesanstalt*, 76:53–58.

Kraus, M. J. and Bown, T. M. (1988). Pedofacies analysis; a new approach to reconstructing ancient fluvial sequences. *Geol. Soc. Am. Spec. Paper*, 216:143–152.

Lachkar, G., Ouarhache, D., and Charrière, A. (2000). Nouvelles données palynologiques sur les formations sédimentaires associées aux basaltes triasiques du Moyen Atlas et de la Haute Moulouya (Maroc). *Revue Micropal.*, 43(4):281–299.

Laville, E., Charroud, A., Fedan, B., Charroud, M., and Piqué, A. (1995). Inversion négative et *rifting* atlasique ; l'exemple du bassin triasique de Kerrouchèn (Maroc). *Bull. Soc. Geol. France*, 166:364–374.

Laville, E., Piqué, A., Amrhar, M., and Charroud, M. (2004). A restatement of the Mesozoic Atlasic Rifting (Morocco). *J. Afr. Earth Sci.*, 38:145–153.

Le Roy, P. and Piqué, A. (2001). Triassic-Liassic Western Moroccan synrift basins in relation to the Central Atlantic opening. *Mar. Geol.*, 172:359–381.

Leleu, S. and Hartley, A. J. (2010). Controls on the stratigraphic development of the Triassic Fundy Basin, Nova Scotia: implications for the tectonostratigraphic evolution of Triassic Atlantic rift basins. *Geol. Soc. Lond. J.*, 167:437–454.

Leleu, S., Hartley, A. J., Oosterhout, C. V., Kennan, L., Ruckwied, K., and Gerdes, K. (2016). Structural, stratigraphic and sedimentological characterization of a wide rift system: The Triassic rift system of the central Atlantic Domain. *Earth-Sci. Rev.*, 158:89–124.

Liu, Z. and Wang, C. (2001). Facies analysis and depositional systems of Cenozoic sediments in the Hoh Xil basin, northern Tibet. *Sedim. Geol.*, 140:251–270.

Lorenz, J. C. (1976). Triassic sediments and basin structure of the Kerrouchen basin, Central Morocco. *J. Sedim. Petrol.*, 46(4):897–905.

Lyazidi, A. (2004). *Evolution géodynamique du bassin triasique de Berrechid–ElGara–Benslimane (Meseta Nord Occidentale, Maroc)*. PhD thesis, Université Mohammed V-Agdal Rabat, Maroc.

Mader, D. (1985). Braidplain, floodplain and playa lake, alluvial-fan, aeolian and palaeosol facies composing a diversified lithogenetical sequence in the permian and Triassic of South Devon (England). In Mader, D., editor, *Aspects of Fluvial Sedimentation in the Lower Triassic Buntsandstein of Europe*, Lecture Notes in Earth Sciences, pages 15–64. Springer, Berlin/Heidelberg/New York/Tokyo.

Manspeizer, W. and Cousminer, H. L. (1988). Late Triassic–early Jurassic synrift basins of the U.S. Atlantic margin. In Sheridan, R. E. and Grow, J. A., editors, *The Atlantic Continental Margin. Geol. N. Am.*, volume I-2, pages 197–216. U.S. Geol. Soc.

Am., Boulder.

Martin-Rojas, I., Somma, R., Delgado, F., Estevez, A., Iannace, A., Perrone, V., and Zamparelli, V. (2009). Triassic continental rifting of Pangaea: direct evidence from Alpujarride carbonates, Betic Cordillera, SE Spain. *J. Geol. Soc. Lond.*, 16:447–458.

Massari, F. (1983). Tabular cross-bedding in Messinian fluvial channel conglomerates, southern Alps. In Collinson, J. D. and Lewin, J., editors, *Modern and Ancient Fluvial Systems*, volume 6 of *Special Publications of the international association of sedimentologists*, pages 287–300. John Wiley & Sons.

Medina, F. (1994). Evolution structurale du haut atlas occidental et des régions voisines du trias à l'actuel, dans le cadre de l'ouverture de l'atlantique central et de la collision afrique-europe. State Thesis, University Mohammed V, Rabat, Morocco.

Medina, F. (1995). Syn- and post-rift evolution of the El Jadida-Agadir basin (Morocco) : constraints for the rifting model of the central Atlantic. *Can. J. Earth. Sci.*, 32:1273–1291.

Merzeraud, G. (1992). *Géométrie et signification géodynamique des séquences de dépôts en domaine continental et marin restreint: exemple du Lias inférieur du Sud-Ouest du bassin de Paris*. PhD thesis, Université de Strasbourg.

Miall, A. D. (1978). Lithofacies types and vertical profile models in braided river deposits: a summary. *Can. Soc. Petrol. Geol. Mem.*, 5:597–604.

Miall, A. D. (1985). Architectural-element analysis: a new method of facies analysis applied to fluvial deposits. *Earth-Sci. Rev.*, 22:261–308.

Miall, A. D. (1988). Architectural elements and bounding surfaces in fluvial deposits: anatomy of the Kayenta Formation (Lower Jurassic) Southwest Colorado. *Sediment. Geol.*, 55:233–262.

Miall, A. D. (1996). *The Geology of Fluvial Deposits, Sedimentary Facies, Basin Analysis and Petroleum Geology*. Springer-Verlag, Germany, 4th edition.

Miall, A. D. (2016). Facies analysis. In *Stratigraphy: A Modern Synthesis*. Springer, Cham.

Miall, A. D. and Balkwilla, H. (2019). The Atlantic margin basins of North America. In Miall, A. D., editor, *The Sedimentary Basins of the United States and Canada*. Elsevier, Amsterdam, 2nd edition.

Olsen, P. E. (1997). Stratigraphic record of the Early Mesozoic breakup of Pangea in the Laurasia–Gondwana rift system. *Annu. Rev. Earth Planet. Sci.*, 2:337–401.

Opluštil, S., Martínek, K., and Tasàryovà, Z. (2005). Facies and architectural analysis of fluvial deposits of the Nýřany Member and the Týnec Formation (Westphalian D-Barruelian) in the Kladno-Rakovník and Pilsen basins. *Bull. Geosci.*, 80(1):45–66.

Ortí, F. (2004). Cordilleras Ibérica y Costero-Catalana. El rift Mesozoico Ibérico: 5.3.1.4 Últimas etapas de actividad del rifting. Sedimentos asociados. In Vera, J. A., editor, *Geología de España*, pages 492–495. Sociedad Geológica de España e Instituto Geológico y Minero de España, Madrid.

Ouarhache, D., Charrière, A., Chalot-Prat, F., and El Wartiti, M. (2012). Chronologie et modalités du *rifting* triasico-liasique à la marge sud-ouest de la Téthys alpine (Moyen Atlas et Haute Moulouya, Maroc) ; corrélations avec le *rifting* atlantique : simultanéité et diachronisme. *Bull. Soc. Geol. France*, 183(3):233–249.

Oujidi, M., Courel, L., Benaouiss, N., El Mostaine, M., El Youssi, M., Et Touhami, M., Ouarhache, D., Sabraoui, A., and Tourani, A. I. (2000). Triassic series of Morocco: stratigraphy, paleogeography and structuring of the Southwestern Peri-Tethyan platform. An overview. In Crasquin-Soleau, S. and Barbier, E., editors, *Peri-Tethys Memoir: 5. New Data on Peri-Tethyan Sedimentary Basins*, volume 182, pages 11–22. Mem. Mus. Natl. Hist. Nat., Paris.

Oujidi, M. and Elmi, S. (2000). Evolution de l'architecture des Monts d'Oujda (Maroc oriental) pendant le Trias et au début du Jurassique. *Bull. Soc. Geol. France*, 171:169–179.

Peretsman, C. G. (1985). A geochemical and petrographic analysis of early mesozoic evaporites from morocco: implications for the history of the north atlantic. Ms. Thesis, University of Oregon.

Peretsman, C. G. and Holser, T. W. (1988). Geochemistry of Moroccan evaporites in the setting of the North Atlantic rift. *J. Afr. Earth Sci.*, 7(2):375–383.

Piqué, A. and Laville, E. (1995). L'Ouverture initiale de l'Atlantique central. *Bull. Soc. Geol. France*, 166(6):725–738.

Piqué, A., Le Roy, P., and Amrhar, M. (1998). Transtensive synsedimentary tectonics associated with ocean opening; the Essaouira-Agadir segment of the Moroccan Atlantic margin. *J. Geological Soc. Lond.*, 155:913–928.

Poli, E. (1997). *Stratigraphie séquentielle haute-*

résolution, modèles de dépôt et géométrie 2D-3D des séquences triasiques de la marge téthysienne ardéchoise. PhD thesis, Université de Bourgogne-Centre des Sciences de la Terre.

Postma, G. and Cruickshank, C. (1988). Sedimentology of a late Weichselian to Holocene terraced fan delta, Varangerfjord, northern Norway. In Nemec, W. and Steel, R. J., editors, *Fan Deltas: Sedimentology and Tectonic Settings*. Blackie, London.

Ramos, A., Fernàndez, O., Muñoz, J. A., and Terrinha, P. (2017). Impact of basin structure and evaporite distribution on salt tectonics in the Algarve Basin, Southwest Iberian margin. *Mar. Petrol. Geol.*, 88:961–984.

Reolid, M., Pérez-Valera, F., Benton, M. J., and Reolid, J. (2014). Marine flooding event in continental Triassic facies identified by a nothosaur and placodont bonebed (South Iberian Paleomargin). *Facies*, 60:277–293.

Roca, E., Muñoz, J. A., Ferrer, O., and Ellouz, N. (2011). The role of the Bay of Biscay Mesozoic extensional structure in the configuration of the Pyrenean orogeny: Constraints from the MARCONI deep seismic reflection survey. *Tectonics*, 30. (TC2001).

Rust, B. R. (1978). Depositional models for braided alluvium. In Miall, A. D., editor, *Fluvial Sedimentology*, volume 5 of *Memoir*, pages 605–625. Canadian Society of Petroleum Geologists.

Salvan, H. M. (1974). Les séries salifères du Trias marocain; caractères généraux et possibilités d'interprétation. Service de la Carte géologique du Maroc. Rabat-Chellah. *Bull. Soc. Geol. France*, 7(6).

Salvan, H. M. (1982). Les évaporites triasiques du Maroc : Caractères généraux-répartition-interprétation. *Colloque Permo-Trias marocain Fac. Sci. Marrakech*, 1:73–84.

Salvan, H. M. (1984). Les formations évaporitiques du Trias marocain. Problèmes stratigraphiques, paléogéographiques et paléoclimatiques. Quelques réflexions. *Rev. Geogr. Phys. Geol. Dyn., Paris*, 25:187–203.

Slimane, A. and El Mostaïne, M. (1997). Observations biostratigraphiques au niveau des formations rouges de la séquence synrift dans les bassin des doukkala et essaouira. *Première Réunion du Groupe Marocain du Permien et du Trias*, page 54.

Smoot, J. P. (1991). Sedimentary facies and depositional environments of early Mesozoic Newark Supergroup basins, eastern North America. *Palaeogeogr, Palaeoclimatol. Palaeoecol.*, 84:369–423.

Sneh, A. (1983). Desert stream sequences in the Sinai Peninsula. *J. Sediment. Petrol*, 53:1271–1280.

Sohn, Y. K., Kim, S. B., Hwang, I. G., Bahk, J. J., Choe, M. Y., and Chough, S. K. (1997). Characteristics and depositional processes of large-scale gravelly Gilbert-type foresets in the Miocene Doumsan fan delta, Pohang Basin, SE Korea. *J. Sedim. Res.*, 67(1):130–141.

Sonnenfeld, P. and Hodec, P. P. (1985). Origin of clay films in rock salt. *Sediment. Geol.*, 44(1–2):113–120.

Soto, J. I., Flinch, J. F., and Tari, G. (2017). Permotriassic basins and tectonics in Europe, North Africa and the Atlantic margins: a synthesis. In Soto, J. I., Flinch, J. F., and Tari, G., editors, *Permo-Triassic Salt Provinces of Europe, North Africa and the Atlantic Margins: Tectonics and Hydrocarbon Potential*, pages 3–41. Elsevier, Amsterdam.

Soussi, M. and Ben Ismaïl, M. H. (2000). Platform collapse and pelagic seamount facies: Jurassic development of central Tunisia. *Sedim. Geol.*, 133:93–113.

Soussi, M., Cirilli, S., and Abbes, C. (2001). Nouvelles données palynologiques sur la formation Rhéouis: Conséquences sur les corrélations et la paléogéographie de la Tunisie au Trias supérieur. *Notes du Service Géologique Tunisie*, 67:87–105.

Taugourdeau-Lanz, J. (1978). Pollens des niveaux sédimentaires associés aux basaltes du Trias sur la bordure septentrionale du Maroc Central: Précisions stratigraphiques. *Notes Mem. Serv. Geol. Maroc*, 40(275):135–146.

Todd, S. P. (1996). Process deduction from fluvial sedimentary structures. In Carling, P. A. and Dawson, M. R., editors, *Advances in Fluvial Dynamics and Stratigraphy*, pages 299–350. Wiley, Chichester.

Tourani, A., Benaouiss, N., Gand, G., Bourquin, S., Jalil, N. E., Broutin, J., Battail, B., Germain, D., Khaldoune, F., Sebban, S., Steyer, J. B., and Vacant, R. (2010). Evidence of an Early Triassic age (Olenakian) in Argana Basin (High Atlas, Morocco) based on new chirotherioid traces. *C. R. Palevol*, 9:201–208.

Tunbridge, I. P. (1981). Sandy high-energy flood sedimentation some criteria for recognition, with an example from the Devonian of S.W. England. *Sediment Geol.*, 28:79–96.

Tunbridge, I. P. (1984). Facies model for a sandy

ephemeral stream and clay playa complex, the Middle Devonian Trentishoe Formation of North Devon. *U.K. Sedimentology*, 31:697–715.

Van Houten, F. B. (1973). Origin of red beds: a review - 1961–1972. *Ann. Rev. Earth Planet. Sci.*, 1:39–61.

Van Houten, F. B. (1977). Triassic-Liassic deposits of Morocco and eastern North America: comparison. *AAPG Bull.*, 61(1):79–99.

Vergés, J., Moragas, M., Martín-Martín, J. D., Saura, E., Casciello, E., Razin, P., Grelaud, C., Malaval, M., Joussiame, R., Messager, G., Sharp, I., and Hunt, D. W. (2017). Chapter 26: Salt Tectonics in the Atlas Mountains of Morocco. In Soto, J. I., Flinch, J. F., and Tari, G., editors, *Permo-triassic Salt Provinces of Europe, North Africa and the Atlantic Margins*, pages 563–576. Elsevier, Amsterdam, the Netherlands.

Wade, J. A., MacLean, B. C., and Williams, G. L. (1995). Mesozoic and Cenozoic stratigraphy, eastern Scotian Shelf: New interpretations. *Can. J. Earth Sci.*, 32:1462–1473.

Warren, J. K. (2006). *Evaporites: Sediments, Resources and Hydrocarbons*. Springer, Berlin.

Warren, J. K. (2010). Evaporites through time: Tectonic, climatic and eustatic controls in marine and nonmarine deposits. *Earth-Sci. Rev.*, 98:217–268.

Welsink, H. and Tankard, A. (2012). Extensional tectonics and stratigraphy of the Mesozoic Jeanne d'Arc basin, Grand Banks of Newfoundland A2 - Roberts, D. G. In Bally, A. W., editor, *Regional Geology and Tectonics: Phanerozoic Rift Systems and Sedimentary Basins*, pages 336–381. Elsevier, Boston.

Comptes Rendus
Géoscience — Sciences de la Planète
2020, 352, nº 6-7, p. 443-454
https://doi.org/10.5802/crgeos.8

Some aspects of current State of Knowledge on Triassic series on both sides of the Central Atlantic Margin / *Quelques aspects de l'état des connaissances des séries triasiques de part et d'autre de la Marge Atlantique*

New palynological data in Muschelkalk facies of the Catalan Coastal Ranges (NE of the Iberian Peninsula)

Manuel García-Ávila [*, a], **Ramon Mercedes-Martín** [b], **Manuel A. Juncal** [a] **and José B. Diez** [a]

[a] Departamento de Xeociencias Mariñas e Ordenación do Territorio, Universidade de Vigo. E-36310, Vigo, Spain

[b] SZALAI Grup S.L. 07314 Caimari, Mallorca, Spain

E-mails: manugarcia@uvigo.es (M. García-Ávila), info@ramonmercedes.com (R. Mercedes-Martín), majuncales@uvigo.es (M. A. Juncal), jbdiez@uvigo.es (J. B. Diez)

Abstract. The Middle Triassic (Ladinian) deposits of the Catalan Basin (Spain) are essentially represented by extensive marine carbonate platforms developed in a rift tectonic setting. During the Ladinian, a regional sea-level drop led to a significant paleogeographic reorganisation of the depocentres of eastern Iberia producing a relevant shift in the distribution of the sedimentary environments. To better calibrate the age of the correlative conformity and the associated depositional facies, a new palynological study was carried out in two localities in Tarragona province (Spain). The palynological assemblages suggest a Longobardian–Cordevolian age (Middle–Late Triassic transition) for the materials deposited below and above the correlative conformity. This study allows a refined biostratigraphic and sedimentary correlation between the carbonate sediments in the Catalan Basin and those in the Iberian Ranges and adjacent basins of the Tethys region.

Keywords. Longobardian, Ladinian, Triassic, Palynostratigraphy, Spain.

1. Introduction

The evolution of Iberia during the Upper Permian and Mesozoic can be divided into three rift cycles and post-rift stages. The rift cycle corresponding to the Late Permian–Triassic, mainly affected the eastern part of the Iberian plate giving rise to basins that were filled with sediments attributed to the Germanic facies during the late Permian and Triassic times [Ramos et al., 1996, Salas and Casas, 1993, Salas et al., 2001].

In Iberia, the Triassic stratigraphic record can be subdivided into the three parts, from the base to the top: Buntsandstein facies (continental clastic sediments and red beds), Muschelkalk facies (marine carbonates, evaporites and red beds) and Keuper facies (tidal and sabkha deposits) [Calvet et al., 1990, Virgili et al., 1983].

In the Triassic Catalan basin, the Muschelkalk facies (Anisian to Ladinian) is constituted by two marine carbonate sequences with an interstrat-

* Corresponding author.

ified evaporite-siliciclastic unit. The second carbonate sequence was recently subdivided into two Transgressive–Regressive sequences corresponding to two fault-block, microbial-dominated carbonate ramps separated by a marked correlative conformity formed in association with a regional sea-level fall [Mercedes-Martín et al., 2013, 014a]. Ammonites, bivalves and palynomorphs have been previously used to constrain the age of these platforms particularly in open marine, deep ramp settings where these organisms are better preserved in organic-rich sediments [Calvet et al., 1990]. However, refined biostratigraphic surveys are needed to: (i) shed light on the age of the correlative conformity which leads to a significant paleogeographic reorganisation of the depocentres of eastern Iberia [Mercedes-Martín et al., 014b], and (ii) identify the Ladinian–Carnian transition in marine sediments. Palynological assemblages can help to temporally constrain the age of these carbonate-shale sequences since palynomorphs are easily well-preserved in organic-rich facies and their remains are abundant in the study area.

1.1. *Background*

There are previous palynological studies that analyse different assemblages in the Catalan Coastal Ranges. Following the chronostratigraphic order, we have the following data.

For the Lower Muschelkalk facies, in Figaró-Montmany area (Barcelona), Solé de Porta et al. [1987] studied a palynological assemblage which was dated as middle Anisian. This assemblage contains *Alisporites grauvogeli*, cf. *Latosaccus latus*, *Microcachryidites doubingeri*, *Microcachryidites fastidioides*, *Platysaccus reticutatus*, *Striatoabieites aytugii*, *Sulcatisporites* cf. *reticulatus*, *Triadispora aurea*, *Triadispora crassa*, *Triadispora falcata*, *Triadispora plicata*, *Voltziaceaesporites heteromorpha*, *Alisporites* sp., *Aratrisporites* sp., *Cyclotriletes* sp., *Punctatisporites* sp., *Sulcatisporites* sp., *Triadispora* sp., and unidentified bisaccates.

For the Lower Muschelkalk–Middle Muschelkalk Calvet and Marzo [1994] suggested an Upper Anisian age, using a palynological assemblage identified in El Figaro (Barcelona): *Alisporites grauvogeli*, *Lunatisporites acutus*, *Microcachryidites doubingeri*, *Praecirculina granifer*, *Striatoabieites aytugii*, *Stellatopollenites thiergartii* (= *Hexasaccites muelleri*), *Cycadopites* sp., *Cyclotriletes* sp., and *Triadispora* sp.

In the base of the Middle Muschelkalk Solé de Porta et al. [1987] studied an outcrop in La Riba (Tarragona). This outcrop consists of dark shales, dating by this author as Upper Anisian according to the following palynological assemblage: *Alisporites grauvogeli*, *Cyclotriletes* cf. *granulatus*, *Cyclotriletes* cf. *oligogranifer*, *Cyclotriletes triassicus*, *Kuglerina meieri*, *Lunatisporites acutus*, *Microcachryidites doubingeri*, *Microcachryidites fastidioides*, *Praecirculina granifer*, *Striatoabieites aytugii*, *Stellatopollenites thiergartii* (= *Hexasaccites muelleri*), *Triadispora aurea*, *Triadispora crassa*, *Triadispora falcata*, *Triadispora plicata*, *Triadispora staplinii*, *Triadispora suspecta*, *Alisporites* sp., *Cycadopites* sp., *Cyclotriletes* sp., *Lunatisporites* sp., *Punctatisporites* sp., *Sulcatisporites* sp., and *Triadispora* sp.

Also, Diez [2000] analysed the base of the Middle Muschelkalk in the outcrop of "El Figaro", characterised by an organic-rich interval. This palynological assemblage is constituted by the following species: *Alisporites* cf. *grauvogeli*, *Heliosaccus dimorphus*, *Lunatisporites* cf. *acutus*, *Ovalipollis* cf. *ovalis*, *Parasaccites* cf. *korbeensis*, *Punctatisporites fungosus*, *Triadispora epigona*, *Triadispora falcata*, *Triadispora staplinii*, *Verrucosisporites remyanus*, cf. *Alisporites*, *Alisporites* sp., *Aratrisporites* sp., *Calamospora* sp., cf. *Illinites*, *Microreticulatisporites* sp., and *Platysaccus* sp. Despite the high palynological diversity, this assemblage did not provide detailed chronostratigraphic information.

The palynological content of the Middle Muschelkalk of the Catalan Basin was studied by Visscher [1967] in Pradell (Tarragona) giving an assemblage of poor chronostratigraphic value: *Alisporites grauvogeli*, *Angustisulcites klausii*, *Voltziaceaesporites heteromorpha*, and *Triadispora* sp.

Subsequently, Calvet and Marzo [1994] studied the upper part of the Middle Muschelkalk succession in La Riba (Tarragona) suggesting a Ladinian age on the basis of the following assemblage: *Duplicisporites granulatus*, *Duplicisporites scurrilis* (= *Paracirculina scurrilis*), *Ovalipollis ovalis*, *Praecirculina granifer*, *Staurosaccites quadrifidus*, and *Triadispora* sp.

Finally, for the Upper Muschelkalk, Solé de Porta et al. [1987] studied the microflora of Capafons Unit, in Capafons (Tarragona) which raised a Ladinian microflora constituted by the speciments:

Camerosporites secatus, *Duplicisporites granulatus*, *Duplicisporites scurrilis* (= *Paracirculina scurrilis*), *Microcachryidites doubingeri*, *Microcachryidites fastidioides*, *Ovalipollis ovalis*, *Praecirculina granifer*, *Rimaesporites potonei*, *Striatoabieites aytugii*, *Triadispora aurea*, *Triadispora crassa*, *Triadispora falcata*, *Triadispora plicata*, *Triadispora suspecta*, *Platysaccus* sp., *Triadispora* sp., and *Verrucosisporites* sp. Also, Calvet and Marzo [1994] studied two palynological assemblages from Rojals and Rasquera Units. The Rojals Unit was recognised at the top of Rojals Unit from la Riera de Sant Jaume (Barcelona) and contains *Camerosporites secatus*, *Duplicisporites scurrilis* (= *Paracirculina scurrilis*), *Ovalipollis cultus*, *Ovalipollis ovalis*, *Praecirculina granifer*, *Triadispora crassa*, *Alisporites* sp., *Calamospora* sp., and *Triadispora* sp. The Rasquera Unit was recognised from marly sediments sampled in Rasquera (Tarragona) yielding *Camerosporites secatus*, *Praecirculina granifer*, *Ovalipollis ovalis*, *Staurosaccites quadrifidus*, *Triadispora crassa*, *Platysaccus* sp., and *Triadispora* sp. An Upper Ladinian age was suggested for both units [Calvet and Marzo, 1994].

Unfortunately, the mentioned previous studies other than that the work of Diez [2000], lack accurate representation of the listed palynomorphs, so a critical motivation of our work was to study similar stratigraphic units in the Catalan Basin to obtain new appropriated data. This study aims at characterising new palynological assemblage from two outcrops located in the surroundings of Falset and Rasquera (Tarragona, Spain), contributing to better constrain the age of the Upper Muschelkalk facies of the Catalan Basin.

2. Geological setting

The study area is located in the Catalan Coastal Ranges, which developed by inversion of the Mesozoic rifts during the Palaeogene [Salas et al., 2001]. The Triassic materials of the Catalan Coastal Ranges are widely distributed in an area about 300 km long and 200 km wide showing a NE-SW orientation. During the Triassic, the basin opened towards the SE into the Neotethys Sea, with shallow depocentres located towards the western and northern parts of the Spanish Meseta [Calvet et al., 1990].

During the Permian to Middle Triassic times, Iberia experienced the development of graben systems that were closely related to the rapid propagation of the northern Europe-Greenland Sea rift to the south and the propagation of the Neotethys Sea to the west. The late Permian and Mesozoic evolution of Iberia can be divided into four major rift cycles and post-rift stages [Ramos et al., 1996, Salas and Casas, 1993, Salas et al., 2001]. The first of these cycles (late Permian-Triassic rift cycle of Salas and Casas [1993]) broadly affected the eastern part of the Iberian plate (including the Triassic Catalan Basin). This cycle was divided into several syn-rift and post-rift phases [Vargas et al., 2009] providing evidence that the Triassic of Iberia was marked by generalised pulses of rapid syn-rift subsidence which influenced the deposition of extensive carbonate ramps [Mercedes-Martín et al., 2013, 014a, Tucker et al., 1993].

These Triassic graben systems were filled with sediments attributed to Germanic facies during the late Permian and Triassic allowing a tripartite facies subdivision of such deposits. The lower part is made up of continental Buntsandstein siliciclastics and red beds, the middle part is composed of marine Muschelkalk limestones, evaporites and red beds, and the upper part consisting of tidal, sabkha and evaporite deposits of the Keuper facies [Virgili et al., 1983].

In the Catalan Basin, the Muschelkalk facies (Anisian to Ladinian, Middle Triassic) consist of two marine carbonate units separated by a siliciclastic-evaporite unit. The second carbonate unit (Upper Muschelkalk) records paleogeographical thickness variations between the shallowest carbonate deposits, located in the Gaià domain, and the deeper carbonate-shale deposits, located in the Baix Ebre-Priorat domain [Calvet et al., 1987, Calvet and Tucker, 1988] (Figure 1). The outcrops studied in this work belongs to the Baix Ebre-Priorat domain.

The Ladinian sedimentary record of the Triassic Catalan Basin has been recently divided into two transgressive–regressive (T-R) sequences by [Mercedes-Martín et al., 014a]. The two T-R sequences represent examples of carbonate ramps, with low-gradient depositional angles and clearly recognised lateral relationships of facies belts. The depositional model for the T-R Sequence 1 corresponds to a microbial-dominated fault-block carbonate ramp. The T-R Sequence 1 (early Ladinian)

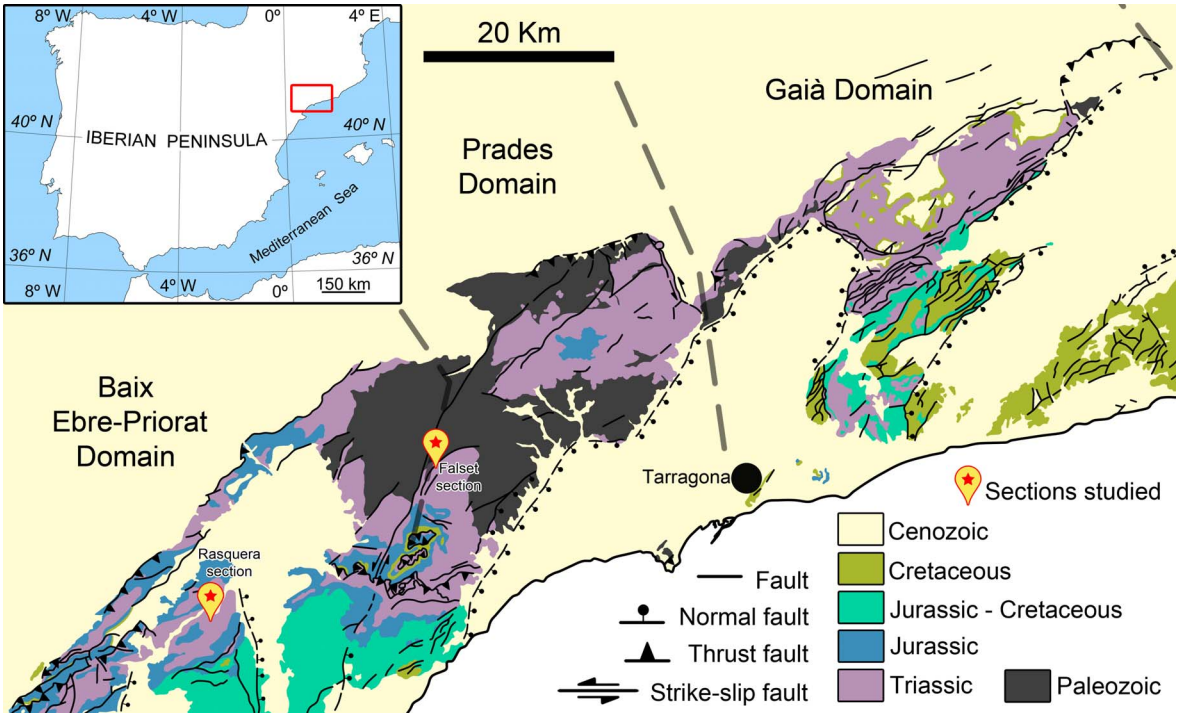

Figure 1. Geographical and geological location of the study area.

contains widespread microbial carbonate deposits: stromatolites in the inner ramp (up to 10 m thick) and thrombolytic biostromes and mounds in the middle ramp (up to 70 m thick). However, the T-R Sequence 2 (late Ladinian) is made up of oolitic stromatolites in the inner ramp, and internal shoals and sheltered lagoons in the middle-outer ramp [Mercedes-Martín et al., 2013, 014a,b].

Both T-R sequences are bounded by a prominent correlative conformity associated with incised-valley erosional features and collapse breccia fillings. The correlative conformity was interpreted as formed by a significant sea-level drop of at least 50 m [Mercedes-Martín et al., 2013, 014a]. The deep-water expression of such surface is the correlative conformity, which was recognised in the Rasquera section (Figure 2).

2.1. *Stratigraphy of the Baix Ebre-Priorat domain*

From a lithostratigraphic perspective, the Upper Muschelkalk is constituted by different units in the Baix Ebre-Priorat domain (Figure 2). Calvet et al. [1987] and Calvet and Tucker [1988] recognised five units, which from base to top are: (1) the Rojals Unit, (2) the Benifallet Unit, (3) the Rasquera Unit, (4) the Tivissa Unit, and (5) the Capafons Unit. Collectively, the sedimentary sections studied in this work (Falset and Rasquera, Figures 2, 3) contain the lithological units 1 to 4 which have been placed in the stratigraphic sequence framework provided by Mercedes-Martín et al. [2013].

Rojals Unit. It is made up to 14 m thick carbonate succession sharply lying on top of the Middle Muschelkalk siliciclastic-evaporitic deposits. Rojals Unit is composed of several alternating facies: grey massive bioturbated mudstone; grey laminated mudstone-wackestone with mud-cracks and evaporitic moulds; grey wackestone with ripple lamination; white oolitic grainstone showing ripple, herringbone, planar, and wavy laminations; planar to domal stromatolites with occasional flat-pebble intraclasts and bivalve fragments [Calvet et al., 1987]. The Rojals Unit represents the Transgressive Systems Tract of the T-R sequence 1 of [Mercedes-Martín et al., 2013] dated as early Ladinian. This unit is outcropping in Rasquera section (Figures 2, 3).

Benifallet Unit. It is composed by up to 20 m of a

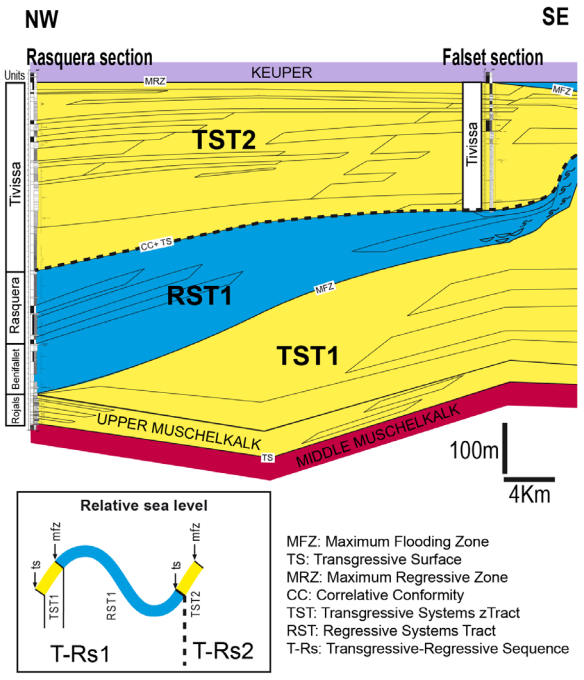

Figure 2. Depositional profile and sequence stratigraphic interpretation of the Upper Muschelkalk rocks in the Catalan Basin (Baix Ebre-Priorat domain). Note the location of the studied sections (Rasquera and Falset) and the lithological units of Calvet et al. [1987]. The black dotted line represents the correlative conformity (see text for more details).

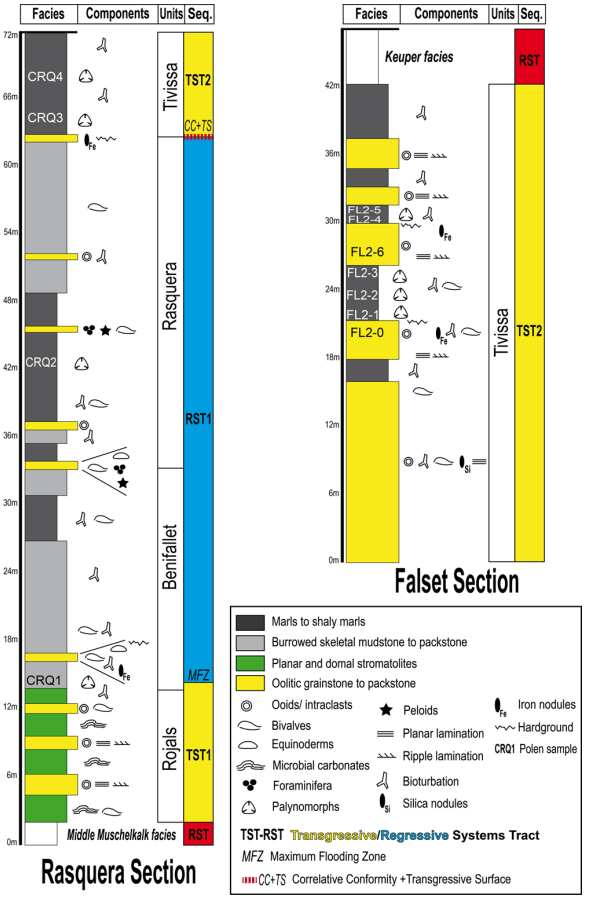

Figure 3. Stratigraphic sections studied (Rasquera and Falset) displaying the main lithological, sequence stratigraphical, and paleontologic characteristics (modified from Mercedes-Martín et al. [014a]).

carbonate succession sharply lying on top of the Rojals Unit. Benifallet Unit is constituted by an array of facies: grey to greenish skeletal mudstone to wackestone with echinoid and bivalve allochems; massive to bioturbated mudstone to wackestone with occasional ripple and herringbone lamination; marly to shaley dolostones with evidence of bioturbation and bivalve fauna. A change from the Rojals Unit (shallow water stromatolitic facies) to Benifallet Unit (deeper water burrowed mudstone to wackestone) was identified as the Maximum Flooding Zone of the T-R sequence 1. Thus, Benifallet Unit was interpreted to be the lower portion of the Regressive Systems Tract of the T-R sequence 1 of Mercedes-Martín et al. [2013], and it was dated as early Ladinian. This unit is outcropping in Rasquera section (Figures 2, 3).

Rasquera Unit. It is made up of at least 40 m of a carbonate-marly succession sharply lying on top of the Benifallet Unit. Rasquera Unit is characterised by a wide range of lithofacies including alternation of grey skeletal mudstone-wackestone (with bivalves as *Daonella*, brachiopods, peloids, foraminifera and ostracods) with dark marls/shales forming nodular and continuous beds; grey bioturbated mudstone-wackestone with bivalves arranged in massive to nodular layers; wackestone-packstone with echinoids, foraminifera, peloids, and brachiopods organised in massive beds exhibiting cross-bedded laminations. Rasquera Unit was interpreted to be the upper portion of the Regressive Systems Tract of the T-R sequence 1 of Mercedes-Martín et al. [2013],

and it was dated as late Ladinian on the basis of ammonoids (*Prothachyceras steinmann*, *P. hispanicum*, *Hungarites pradoi*) and conodonts (*Metapolygnathus mungoensis*, *Pseudofurnishius murcianus*) [Calvet et al., 1987, Calvet and Tucker, 1988]. However, a early Ladinian age was determined by Mercedes-Martín et al. [2013] by the stratigraphic relationships and lateral facies distributions. This unit is outcropping in Rasquera section (Figures 2, 3).

Tivissa Unit. It is composed of at least 42 m-thick of a coarse-grained carbonate succession alternating with shale/marl-rich intervals. The base of this unit is characterised by an iron-rich hardground containing abundant ammonite fauna. This unit is made up of the following facies: bioturbated marlstone-shale; marlstone with thin-bedded bioturbated limestones; thick-bedded and massive mudstone and wackestone; bioclastic packstone-grainstone with ooids, echinoids, peloids and molluscs with evidence of ripple and planar laminations, and silica o iron nodules. This unit is interpreted as the Transgressive Systems Tract of the T-R sequence 2 [Mercedes-Martín et al., 2013] which is bounded by a composite stratigraphic surface (correlative conformity and transgressive surface). The Tivissa Unit was dated as late Ladinian by ammonite fauna (*Hungarites pradoi*, *Protrachyceras hispanicum*, *P. ibericum*, *P. batalleri*, and *P. vilanovae*), and conodonts (*Metapolygnathus mungoensis*, *Pseudofurnishius murcianus*) [Calvet and Tucker, 1988, Calvet et al., 1987]. This unit is cropping out both in Rasquera and Falset sections (Figures 2, 3).

3. Materials and methods

In this paper, we have studied two stratigraphic sections close to Falset and Rasquera, in the province of Tarragona (Spain).

In the Rasquera Section (40° 59′ 41.40″ N, 0° 34′ 6.12″ E) four samples were collected in marly levels. Sample CRQ-1 and CRQ-2 were collected below the correlative conformity (see Figure 3), while samples CRQ-3 and CRQ-4 were collected above. In the Falset section (41° 9′ 2.66″ N, 0° 51′ 35.30″ E) five samples were sampled (FL2-1 to FL2-5) above the correlative conformity. All the samples contained palynomorphs. Due to the positive results of the marly levels, two new complementary samples were subsequently collected in the Falset section (FL2-0 and FL2-6) in limestone levels. Both samples were negative in both marine and continental palynomorphs.

Palynological samples were processed using HCl-HF-HCl attack techniques as described by Wood et al. [1996] in the palynological Laboratory of Geosciences Department at the University of Vigo. A dispersing agent was added to facilitate filtering and sieving at 10 μm. The palynological slides were studied under a Leica DM 2000 LED, and the photomicrographs were taken with a Leica ICC50 W camera using ×1000 magnification.

The slides are stored in the palynological Laboratory of Geosciences Department at the University of Vigo.

4. Results

Two palynological assemblages were considered (Supplementary Table 1), and a synthetic assemblage is shown in Figure 4. The isolated and complete assemblages of each section are shown in the Supplementary data.

The samples CRQ-1 to CRQ-4 in the Rasquera section contain: *Aratrisporites granulatus* (Klaus 1960) Playford and Dettmann 1965, *Calamospora tener* (Leschik) Mädler 1964, *Camerosporites secatus* Leschik 1956, *Duplicisporites granulatus* (Leschik) Scheuring 1970, *Ellipsovelatisporites rugosus* Scheuring 1970, *Lunatisporites noviaulensis* (Leschik 1956) de Jersey 1979, *Microcachryidites doubingeri* Klaus 1964, *Microcachryidites fastidioides* Klaus 1964, *Ovalipollis cultus* Scheuring 1970, *Ovalipollis ovalis* (Krutzsch 1955) Scheuring 1970, *Ovalipollis pseudoalatus* (Thiergart) Schuurman 1976, *Palaeospongisporis europaeus* Schulz 1965, *Paracirculina tenebrosa* Scheuring 1970, *Patinasporites densus* Leschik 1955, *Platysaccus papilionis* Potonié and Klaus 1954, *Praecirculina granifer* (Leschik) Klaus 1960, *Striatoabieites aytugii* (Visscher) Scheuring 1970, *Triadispora crassa* Klaus 1964, *Triadispora epigona* Klaus 1964, *Triadispora falcata* Klaus 1964, *Triadispora plicata* Klaus 1964, *Triadispora staplinii* (Jansonius) Klaus 1964, *Triadispora suspecta* Scheuring 1970, *Chordasporites* sp., *Concavisporites* sp., *Deltoidospora* sp., *Maculatasporites* sp., *Microcachryidites* sp., *Paracirculina* sp., *Retusotriletes* sp., *Triadispora* sp., *Verrucosisporites* sp., *Cymatiosphaera* sp., *Tasmanites* sp., and foraminiferal test lining.

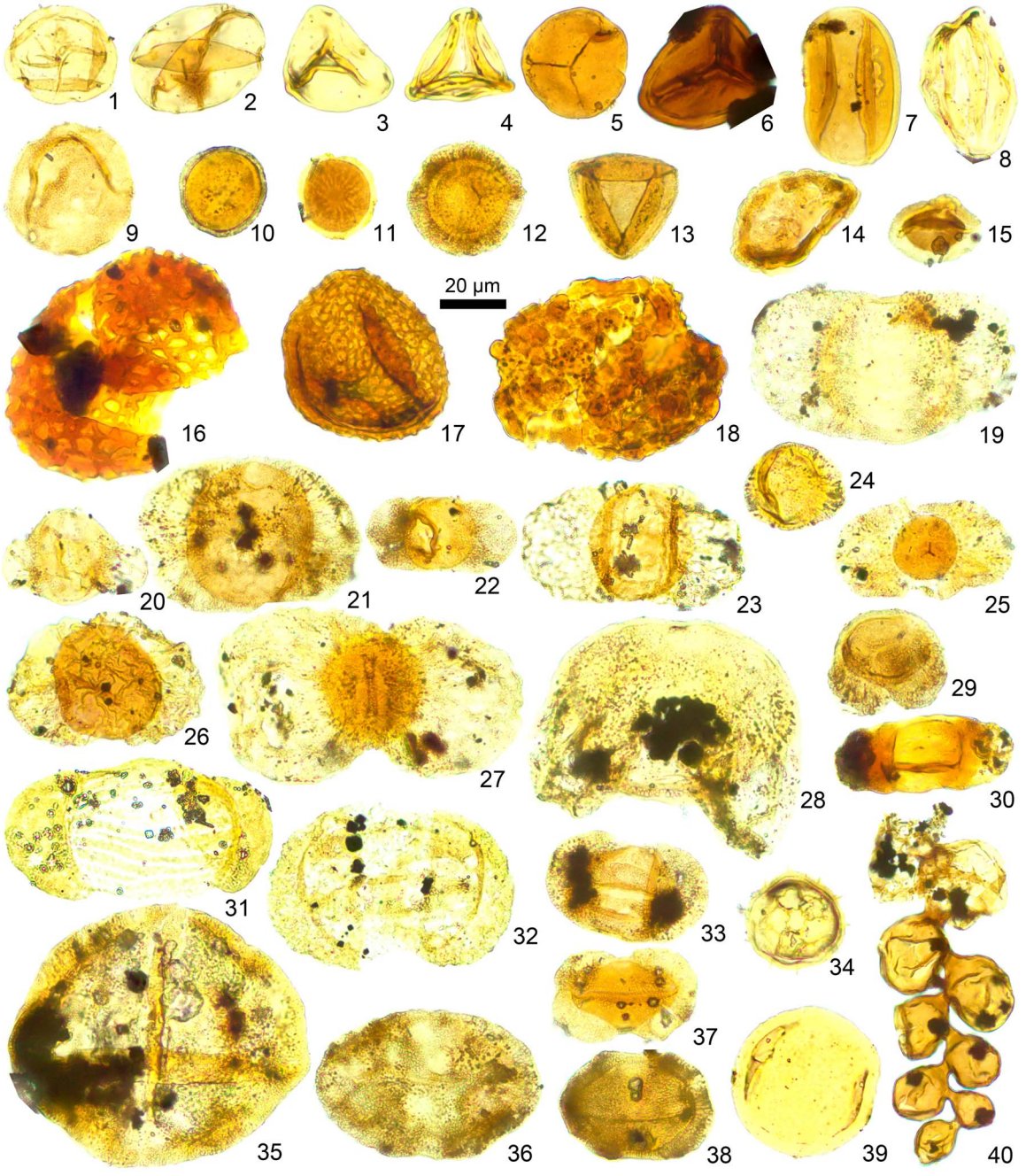

Figure 4. Synthesis of the palynomorphs found in the Falset and Rasquera sections. (1) *Calamospora* sp., (2) *Calamospora tener*, (3) *Deltoidospora* sp., (4) *Concavisporites* sp., (5) *Retusotriletes* sp., (6) *Camarozonosporites laevigatus*, (7) *Chasmatosporites* sp., (8) *Ephedripites* sp., (9) *Praecirculina granifer*, (10) *Paracirculina scurrilis*, (11) *Paracirculina tenebrosa*, (12) *Patinasporites densus*, (13) *Duplicisporites granulatus*, (14) *Camerosporites secatus*, (15) *Aratrisporites granulatus*, (16) *Palaeospongisporis europaeus*, (17) *Maculatasporites* sp., (18) *Verrucosisporites* sp., (19) *Alisporites* sp., (20) *Triadispora falcata*, (21) *Triadispora plicata*, (22) *Triadispora crassa*, (23) *Triadispora staplinii*, (24) *Triadispora epigona*, (25) *Triadispora suspecta*, (26) *Ellipsovelatisporites rugosus*, (27) *Platysaccus papilionis*, (28) *Microcachryidites fastidioides*, (29) *Microcachryidites doubingeri*, (30) *Chordasporites* sp., (31) *Striatoabieites aytugii*, (32) *Lunatisporites noviaulensis*, (33) *Lunatisporites acutus*, (34) *Cymatiosphaera* sp., (35) *Staurosaccites quadrifidus*, (36) *Ovalipollis pseudoalatus*, (37) *Ovalipollis cultus*, (38) *Ovalipollis ovalis*, (39) *Tasmanites* sp., (40) foraminiferal test lining.

The samples FL2-1 to FL2-5 in the Falset section contain: *Aratrisporites granulatus* (Klaus 1960) Playford and Dettmann 1965, *Calamospora tener* (Leschik) Mädler 1964, *Camarozonosporites laevigatus* Schulz 1967, *Camerosporites secatus* Leschik 1956, *Duplicisporites granulatus* (Leschik) Scheuring 1970, *Lunatisporites acutus* Leschik 1956, *Microcachryidites doubingeri* Klaus 1964, *Microcachryidites fastidioides* Klaus 1964, *Ovalipollis cultus* Scheuring 1970, *Ovalipollis pseudoalatus* (Thiergart) Schuurman 1976, *Paracirculina scurrilis* Scheuring 1970, *Paracirculina tenebrosa* Scheuring 1970, *Patinasporites densus* (Leschik) Scheuring 1970, *Platysaccus papilionis* Potonié and Klaus 1954, *Praecirculina granifer* (Leschik) Klaus 1960, *Staurosaccites quadrifidus* Dolvy 1976, *Striatoabieites aytugii* (Visscher) Scheuring 1970, *Triadispora crassa* Klaus 1964, *Triadispora epigona* Klaus 1964, *Triadispora falcata* Klaus 1964, *Triadispora suspecta* Scheuring 1970, *Alisporites* sp., *Calamospora* sp., *Chasmatosporites* sp., *Concavisporites* sp., *Ephedripites* sp., *Maculatasporites* sp., *Microcachryidites* sp., *Retusotriletes* sp., *Triadispora* sp. and *Verrucosisporites* sp. We also identified *Tasmanites* sp. and foraminiferal test lining.

5. Discussion

5.1. *Age assessment*

The First Appearance Datum (FAD) of *Camerosporites secatus* is documented in the early Fassanian (early Ladinian) of alpine Domaine of Europe [Roghi, 1995, Stockar et al., 2012, Van Der Eem, 1983, Visscher and Brugman, 1981], and the FAD of *Duplicisporites granulatus* raises a middle Fassanian age in central and northwestern Europe [Kürschner and Herngreen, 2010]. By the other hand, the bisaccate pollen grains like *Lunatisporites noviaulensis*, *Microcachryidites doubingeri*, and *Microcachryidites fastidioides* are characteristic of the Early-Middle Triassic and rarely appear in early Carnian assemblages (e.g. Doubinger and Bühmann, 1981, in Germany; Doubinger and Adloff, 1983, in the Mediterranean area; Orłowska-Zwolińska, 1983, 1985, in Poland; Eshet, 1990, in Israel; Kürschner and Herngreen, 2010 in central and northwestern Europe). The Last Appearance Datum (LAD) of *Protodiploxypinus fastidioides* (= *Microcachryidites fastidioides*) is reported in the middle Longobardian of central and northwestern Europe [Kürschner and Herngreen, 2010].

Van Der Eem [1983] in Wester Dolomites (Italy), Scheuring [1970] in Solothurner Jura (Switzerland) and Kürschner and Herngreen [2010] in Central and northwestern of Europe placed the first appearance of *Patinasporites densus* to the base of the early Carnian. Cirili [2010] in the revision of the Upper Triassic materials in Central and Northwestern of Europe suggested for this taxon a Carnian–early Norian age. Scheuring [1970] in Solothurner Jura (Switzerland) linked the presence of *Ellipsovelatisporites rugosus* to Gipskeuper, with an late Ladinian–early Norian age.

The two assemblages correspond to the intervals between *Camerosporites secatus–Enzonalasporites vigens*/*Enzonalasporites vigens – Patinasporites densus* phases [Van Der Eem, 1983], the *Heliosaccus dimorphus*/*Porcellispora longdonensis* Zones of Orłowska-Zwolińska [1983, 1985, 1988] amended by Herngreen [2005], zones GTr 11 and 12 in the palynostratigraphical subdivision of the Germanic Basin [Heunisch, 1999], and the *Heliosaccus dimorphus*/*Camerosporites secatus* zones [Kürschner and Herngreen, 2010].

The palynological assemblages studied in the Upper Muschelkalk of the Catalan Coastal Ranges are comparable with other assemblages recognised in the middle-upper part of Royuela Formation in Torrecilla and Arroyo de San Roman (Guadalajara, Spain; Ramos 1979), the Upper Muschelkalk of Alcalá de la Selva and Barranco del Contador, Cañete Formation (Teruel, Spain; Arche et al. 1995), the Upper Muschelkalk of Pantano de la Tranquera (Zaragoza, Spain. García-Royo et al. 1989), and the assemblage SC-2 of Juncal et al. [2018] in the Paris Basin.

Thus, the palynomorph assemblages identified from Falset and Rasquera sections raise a Longobardian–Cordevolian age.

This palynological dating is consistent with the age provided by ammonite fauna and conodonts from Rasquera and Falset Units [Calvet and Tucker, 1988, Calvet et al., 1987] and is coherent with previous biostratigraphical and sedimentological correlations between the Muschelkalk of the Catalan Basin and the Iberian Ranges [Diez et al., 2014].

5.2. *Paleoenvironmental and paleoecological remarks*

The lithostratigraphical data suggest deposition in the middle to outer carbonate ramp environments with a predominant increase in water depth towards Rasquera section, where marls and shaly marls are more abundant [Mercedes-Martín et al., 2013, 014b]. Despite the marine character of the sediments, the overall palynological assemblage found in marly levels, present a clear dominance of continental palynomorphs. Notwithstanding, although scarce, some samples show the presence of authochtonous marine prasinophytes (*Tasmanites* and *Cymatiosphaera*), and foraminiferal test linings indicating that mixing of marine and continental associations occurred at least in the more proximal parts of the basin.

Moreover, as mentioned previously, the absence of palynomorphs in the sampled coarse-grained carbonate intervals could be due to deposition of these sediments in moderate to high energy and oxygenated environments which can encourage the rapid disintegration of the organic remains. The limited tissue preservation of the studied carbonates can also be attributed to the pervasive post-depositional dolomitisation that these rocks have suffered [Tucker and Marshall, 2004]. Consequently, the taphonomic bias produced should be kept in mind when carrying out the approximate hinterland and coastal floral reconstruction. This same bias makes it impossible to make percentage variation graphs of palynomorphs to try to discern the paleoclimatic evolution of the study area.

The composition of the microfloras of the Falset and Rasquera assemblages reflects a flora dominated by xerophytic species whose pollen grains were transported by wind and water currents to the deposition zone. The presence of *Triadispora* spp. indicates an influx of hinterland elements also with saline mudflats [Brugman et al., 1994, Roghi et al., 2010]. In addition, the occurrence of *Duplicisporites*, *Camerosporites*, *Paracirculina* and *Praecirculina* (Circumpolles group) could represent a xerophytic coastal vegetation [Roghi et al., 2010] due to their Cheirolepidiaceae affinity [Roghi, 2004, Scheuring, 1970, 1978, Visscher et al., 1994, Zavialova and Roghi, 2005]. Although the Cheirolepidiaceae could live in a wide variety of habitats, the presence of this group in the Falset and Rasquera assemblages could indicate a drier and/or saline influence [Kustatscher et al., 2018].

Although scarcer, the occurrence of spores could indicate the presence of hygrophytic vegetation. In addition, coastal, swamp and freshwater environments could have sourced different lycophytes (*Aratrisporites*) to marine settings. Small and larger ferns (e.g. *Verrucosisporites*, *Deltoidospora* and *Concavisporites*) are typically associated to more humid environments in the hinterland, while bryophytes (*Maculatasporites*), and horsetail specimens (*Calamospora*) could have been sourced from wetter areas and along a small river.

Based on the probable parent plant affinities of the palynological record (see Supplementary data) in combination with sedimentological data, we can propose an approximate paleoenvironmental reconstruction of the study area (Figure 5).

6. Conclusions

The palynological assemblages recognised from Rasquera and Falset Sections give a Longobardian–Cordevolian age.

Our data are in agreement with the marine previous biostratigraphycal data published, providing the most complete and recent figuration of the palynomorphs of the Catalan Basin. This refined calibration helps to constrain the age of the Upper Muschelkalk sediments themselves, and the overlying Keuper facies (Ladinian–Carnian) in the Catalan Coastal Ranges and the stratigraphical correlation whit the Iberian Ranges, and adjacent basins of the Tethys region.

Although taphonomic bias is important, the composition of the recovered oryctocoenosis makes it possible to sketch the composition of the continental flora in the source sedimentary area. However, the decrease in preservation due to the increase in the proportion of carbonates indicates that the bias makes impossible, as in most cases, the statistical use of the data in the deduction of paleoclimatic evolution.

Acknowledgements

The authors are grateful to the anonymous reviewers for helpful and constructive suggestions, and the

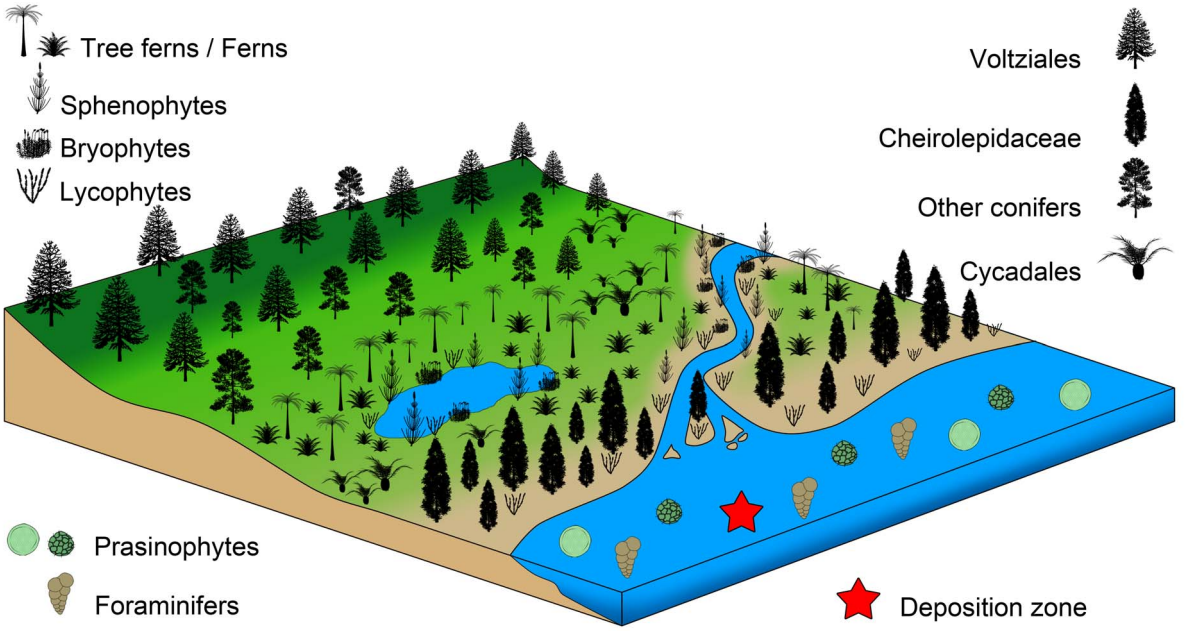

Figure 5. Paleoenvironmental reconstruction based on palynomorphs assemblages.

editor Dr. Sylvie Bourquin for her valuable recommendations. This work was supported by projects CGL2014-52699P (Spanish Ministry of Economy) and GRC 2015/020 (Xunta de Galicia) and a Percy Sladen Memorial Fund Grant of the Linnean Society of London (RM-M).

Supplementary data

Supporting information for this article is available on the journal's website under https://doi.org/10.5802/crgeos.8 or from the author.

References

Arche, A., López-Gómez, J., Herranz, P., Márquez-Aliaga, A., and Solé de Porta, N. (1995). The Permian and Triassic sediments of the Teruel area, SE Iberian Ranges, Spain. *Sci. Geol. Bull.*, 48(1–3):101–117.

Brugman, W. A., Van Bergen, P. R., and Kerp, J. H. E. (1994). A quantitative approach to Triassic palynology: the Lettenkeuper of the Germanic Basin as an example. In Traverse, A., editor, *Sedimentation of Organic Particles*, pages 409–429. Cambridge University Press.

Calvet, F., March, M., and Pedrosa, A. (1987). Estratigrafía, sedimentología y diagénesis del Muschelkalk superior de los Catalánides. *Cuad. Geol. Ibérica*, 11:171–198.

Calvet, F. and Marzo, M. (1994). *El Triásico de las Cordilleras Costero-Catalanas. Estratigrafía, Sedimentología y Análisis Secuencial.* Gráficas Cuenca, S.A., Cuenca, Spain.

Calvet, F. and Tucker, M. E. (1988). Outer ramp cycles in the Upper Muschelkalk of the Catalan Basin, northeast Spain. *Sediment. Geol.*, 57:185–198.

Calvet, F., Tucker, M. E., and Henton, J. M. (1990). Middle Triassic carbonate ramp systems in the Catalan Basin, Northeast Spain: facies, systems tracts, sequences and controls. *Carbonate Platforms, Facies, Seq. Evol.*, 9:79–108.

Cirili, S. (2010). Upper Triassic-lowermost Jurassic palynology and palynostratigraphy: a review. In Lucas, S. G., editor, *Triassic Timescale*, Special Publications 334, pages 285–314. Geological Society of London, London, United Kingdom.

Diez, J. B. (2000). *Geología y Palaeobotánica de la*

Facies Buntsandstein en la Rama Aragonesa de la Cordillera Ibérica. Implicaciones bioestratigráficas en el Peritethys Occidental. PhD thesis, Universidad de Zaragoza (Spain)/Université Paris VI (France).

Diez, J. B., Arche, A., Broutin, J., Bourquin, S., De la Horra, R., Ferrer, J., García-Gil, S., and López-Gómez, J. (2014). Palynostratigraphic Data for the Buntsandstein and Muschelkalk Facies from the Iberian Ranges (Spain). In Rocha, R., Pais, J., Kullberg, J. C., and Finney, S., editors, *Strati 2013*. Springer, Switzerland.

Doubinger, J. and Adloff, M. C. (1983). Triassic palynomorphs of the mediterranean area. Centre de Sédimentologie et Géochimie de la Surface, Strasbourg, France (unpublished).

Doubinger, J. and Bühmann, D. (1981). Röt bei Borken und bei Schlüchtern (Hessen, Deutschland): Palynologie und Tonmineralogie. *Z. Dtsch. Geologischen Ges.*, 132(1):421–449.

Eshet, Y. (1990). The palynostratigraphy of the Permian Triassic boundary in Israel: two approaches to biostratigraphy. *Israel J. Earth Sci.*, 39:1–15.

García-Royo, J. F., Arche, A., and Doubinger, J. (1989). Palinomorfos del Triásico de la región Nuevalos-Cubel (provincia de Zaragoza). *Rev. Espa nola de Micropaleontología*, 21(1):125–137.

Herngreen, G. F. W. (2005). Triassic sporomorphs of nw europe: taxonomy, morphology and ranges of marker species with remarks on botanical relationship and ecology and comparison with ranges in the alpine triassic. Kenniscentrum Biogeology (UU/TNO)—TNO report, NITG 04–176-C, Ned Inst Toegepaste Geowet TNO, Utrecht.

Heunisch, C. (1999). Die Bedeutung der Palynologie für Biostratigraphie und Fazies in der Germanischen Trias. In Hauschke, N. and Wilde, V., editors, *Trias, Eine ganz andere Welt, Mitteleuropa im frühen Erdmittelalter*, pages 207–220. Pfeil Verlag, München.

Juncal, M., Bourquin, S., Beccaletto, L., and Diez, J. B. (2018). New sedimentological and palynological data from the Permian and Triassic series of the Sancerre-Couy core, Paris Basin, France. *Geobios*, 51(6):517–535.

Kürschner, W. M. and Herngreen, G. F. W. (2010). Triassic palynology of central and northwestern Europe: a review of palynofloral diversity patterns and biostratigraphic subdivisions. In Lucas, S. G., editor, *Triassic Timescale*, Special Publications 334, pages 263–283. Geological Society of London, London, United Kingdom.

Kustatscher, E., Ash, S., Karasev, E., Pott, C., Vajda, V., Yu, J., and McLoughlin, S. (2018). Flora of the Late Triassic. In Tanner, L. H., editor, *The Late Triassic World*, Topics in Geobiology 46, pages 545–622. Springer, Cham.

Mercedes-Martín, R., Arenas, C., and Salas, R. (2014a). Diversity and factors controlling widespread occurrence of syn-rift Ladinian microbialites in the western Tethys (Triassic Catalan Basin, NE Spain). *Sediment. Geol.*, 313:68–90.

Mercedes-Martín, R., Salas, R., and Arenas, C. (2013). Facies heterogeneity and depositional models of a Ladinian (Middle Triassic) microbial-dominated carbonate ramp system (Catalan Coastal Ranges, NE Spain). *Mar. Pet. Geol.*, 46:107–128.

Mercedes-Martín, R., Salas, R., and Arenas, C. (2014b). Microbial-dominated carbonate platforms during the Ladinian rifting: sequence stratigraphy and evolution of accommodation in a fault-controlled setting (Catalan Coastal Ranges, NE Spain). *Basin Res.*, 26:269–296.

Orłowska-Zwolińska, T. (1983). Palynostratigraphy of the upper part of Triassic Epicontinental sediments in Poland. *Prace Instytutu Geologicznego*, 104:1–89.

Orłowska-Zwolińska, T. (1985). Palynological zones of the Polish epicontinental Triassic. *Bull. Pol. Acad. Sci. Math., Earth Sci.*, 33(3–4):107–117.

Orłowska-Zwolińska, T. (1988). Palynostratigraphy of Triassic deposits in the vicinity of Brzeg (SE part of the Fore-Sudetic Monocline). *Kwart. Geologiczny*, 32(2):349–366.

Ramos, A. (1979). *Estratigrafía y paleogeografía del Pérmico y Triásico al oeste de Molina de Aragón*. PhD thesis, Universidad Complutense, Madrid (Spain).

Ramos, A., Sopeña, A., Sánchez-Moya, A., and Muñoz, A. (1996). Subsidence analysis, maturity modelling and hydrocarbon generation of the Alpine sedimentary sequence in the NW of the Iberian Ranges (Central Spain). *Cuad. Geol. Ibérica*, 21:23–53.

Roghi, G. (1995). *Analisi palinologica del Trias medio del Sudalpino*. PhD thesis, Univ. Padova.

Roghi, G. (2004). Palynological investigations in the Carnian of the Cave del Predil area (Julian Alps, NE Italy). *Rev. Palaeobot. Palynol.*, 132:1–35.

Roghi, G., Gianolla, P., Minarelli, L., Pilati, C., and

Preto, N. (2010). Palynological correlation of Carnian humid pulses throughout western Tethys. *Palaeogeogr. Palaeoclimatol. Palaeoecol.*, 290:89–106.

Salas, R. and Casas, A. (1993). Mesozoic extensional tecton- ics, stratigraphy and cristalevolution turing the Alpine cycle of the eastern Iberian basin. *Tectonophysics*, 228:33–55.

Salas, R., Guimera, J., Mas, R., Martin-Closas, C., Melendez, A., and Alonso, A. (2001). Evolution of the Mesozoic Iberian Rift System and its Cainozoic inversion (Iberian chain). In Ziegler, P. A., Cavazza, W., Robertson, A. H. F., and Crasquin-Soleau, S., editors, *Peri-Tethys Memoir 6: Peri-Tethyan Rift/Wrench Basins and Passive Margins*, Mem. Mus. Hist. Natl. 186, pages 145–185. ISBN: 2-85653-528-3.

Scheuring, B. W. (1970). Palynologische und palynostratigraphische Utersuchungen des Keupers im Bölchentunnel (Solothurner Jura). *Schweiz. Paläontol. Abh.*, 88:1–187.

Scheuring, B. W. (1978). Mikrofloren aus den Meridelkalken des Mte. San Giorgio (Kanton Tessin). In *Schweizerische Paläontologische Abhandlungen*, volume 100.

Solé de Porta, N., Calvet, F., and Torrentó, L. (1987). Análisis palinológico del Triásico de los Catalánides (NE España). *Cuadernos Geología Ibérica*, 11:237–254.

Stockar, R., Baumgartner, P. O., and Condon, D. (2012). Integrated Ladinian biochronostratigraphy and geochrononology of Monte San Giorgio (Southern Alps, Switzerland). *Swiss. J. Geosci.*, 105:85–108.

Tucker, M. and Marshall, J. (2004). Diagenesis and geochemistry of Upper Muschelkalk (Triassic) buildups and associated facies in Catalonia (NE Spain): a paper dedicated to Francesc Calvet. *Geol. Acta*, 2(4):257–269.

Tucker, M. E., Calvet, F., and Hunt, D. (1993). Sequence stratigraphy of carbonate ramps: systems tracts, models and application to de Muschelkalk carbonate platforms of eastern Spain. *Spec. Publ. Int. Assoc. Sediment.*, 18:397–415.

Van Der Eem, J. G. L. A. (1983). Aspects of Middle and Late Triassic Palynology: 6. Palynological investigations in the Ladinian and Lower Karnian of the Western Dolomites, Italy. *Rev. Palaeobot. Palynol.*, 39:189–300.

Vargas, H., Gaspar-Escribano, J. M., López-Gómez, J., Van Wees, J. D., Cloetingh, S., de La Horra, R., and Arche, A. (2009). A comparison of the Iberian and Ebro Basins during the Permian and Triassic, eastern Spain: a quantitative subsidence modelling approach. *Tectonophysics*, 474:160–183.

Virgili, C., Sopena, A., Arche, A., Ramos, A., and Hernando, S. (1983). Some observations on the Triassic of the Iberian Peninsula. *NeueBeitr. Biostratigr. Tethys-Trias, Schriftenr. Erdwiss. Komrn.*, 5:287–294.

Visscher, H. (1967). Permian and Triassic palynology and the concept of "Tethys twist". *Palaeogeogr. Palaeoclimatol. Palaeoecol.*, 3:151–166.

Visscher, H. and Brugman, W. A. (1981). Ranges of selected palynomorphs in the Alpine Triassic of Europe. *Rev. Palaeobot. Palynol.*, 34:115–128.

Visscher, H., Van Route, M., Brugman, W. A., and Poort, R. J. (1994). Rejection of a Carnian (Late Triassic) "pluvial event" in Europe. *Rev. Palaeobot. Palynol.*, 83:217–226.

Wood, D. G., Gabriel, A. M., and Lawson, J. C. (1996). Palynological techniques – processing and microscopy. In Jansonius, J. and McGregor, D. C., editors, *Palynology: Principles and Applications*, volume 1, pages 29–50. AASP Foundation, Dallas, Texas, USA.

Zavialova, N. E. and Roghi, G. (2005). Exine morphology and ultrastructure of *Duplicisporites* from the Triassic of Italy. *Grana*, 44:337–342.

Comptes Rendus
Géoscience — Sciences de la Planète
2020, 352, nº 6-7, p. 455-473
https://doi.org/10.5802/crgeos.7

Some aspects of current State of Knowledge on Triassic series on both sides of the Central Atlantic Margin / *Quelques aspects de l'état des connaissances des séries triasiques de part et d'autre de la Marge Atlantique*

Physical volcanology and emplacement mechanism of the Central Atlantic Magmatic Province (CAMP) lava flows from the Central High Atlas, Morocco

Hind El Hachimi[*, a], Nasrrddine Youbi[b, c], José Madeira[c, d], Andrea Marzoli[e], João Mata[c, d], Hervé Bertrand[f], Mohamed Khalil Bensalah[b, c], Moulay Ahmed Boumehdi[b, c], Miguel Doblas[g], Fida Medina[h], Mohamed Ben Abbou[i] and Línia Martins[c, d]

[a] Geology Department, Faculty of Sciences, Chouaïb Doukkali University, 24000, El Jadida, Morocco

[b] Geology Department, Faculty of Sciences-Semlalia, Cadi Ayyad University, Prince Moulay Abdellah Boulevard, P.O. Box 2390, Marrakech, Morocco

[c] Instituto Dom Luiz (IDL), Faculdade de Ciências, Universidade de Lisboa, Campo Grande, 1749-016, Lisboa, Portugal

[d] Departamento de Geologia, Faculdade de Ciências, Universidade de Lisboa, 1749-016 Lisboa, Portugal

[e] Dipartimento di Geoscienze, Università di Padova, Italy

[f] Université de Lyon, Laboratoire de Géologie de Lyon, Ecole Normale Supérieure de Lyon, Université Lyon 1, CNRS UMR 5276, Lyon, France

[g] Instituto de Geociencias (CSIC-UCM), c/ Doctor Severo Ochoa 7, Ciudad Universitaria, 28040, Madrid, Spain

[h] Moroccan Association of Geosciences, Oued Dra Street, 28, Rabat, Morocco

[i] Geology Department, Faculty of Sciences Dhar Al Mahraz, Sidi Mohammed Ben Abdellah University, Fès, Morocco

E-mails: elhachimi.h@ucd.ac.ma (H. El Hachimi), youbi@uca.ac.ma (N. Youbi), jmadeira@fc.ul.pt (J. Madeira), andrea.marzoli@unipd.it (A. Marzoli), jmata@fc.ul.pt (J. Mata), herve.bertrand@ens-lyon.fr (H. Bertrand), bensalah@uca.ac.ma (M. K. Bensalah), boumehdi@uca.ac.ma (M. A. Boumehdi), m.doblas@igeo.ucm-csic.es (M. Doblas), f_medina@geoscimar.org (F. Medina), benabbou@hotmail.com (M. Ben Abbou), liniamartins@gmail.com (L. Martins)

Abstract. The best preserved and most complete lava flow sequences of the Central Atlantic Magmatic Province (CAMP) in Morocco are exposed in the Central High Atlas and can reach up to 300 m in thickness. Four distinct formations, emplaced in subaerial environments, are classically recognized: the

[*] Corresponding author.

Lower, Intermediate, Upper and Recurrent formations. These formations are separated by paleosoils and sedimentary sequences (mudstones, siltstones, sandstones, limestones), that are in general less than two meter-thick and may exceptionally reach a thickness of 80 m, representing minor periods of volcanic quiescence. CAMP lava flows of the Central High Atlas can be grouped into two main categories: subaerial compound pahoehoe flows and simple flows. The former type is exclusively confined to the Lower and Intermediate Formations, while simple flows occur in the Upper and Recurrent Formations. The dominance of compound flows in the two lowermost units of the CAMP suggests a slow emplacement during successive sustained eruptive episodes. Instead the thick single flows characterizing the Upper and Recurrent units indicate higher effusive rates. Basaltic pillow lavas (always of short lateral extent: 10 to 100 m), showing radial jointing and vitreous rinds, identical to those found in the Western Meseta, are occasionally associated with hyaloclastites in the base of the Intermediate Formation, immediately above clastic sediments, or in the Upper Formation. The occurrence of pillow lavas does not imply a generalized subaqueous environment at the time of the lava emission. Instead, they represent subaerial flows that entered small lakes occupying depressions on the volcanic topography of the Lower and Intermediate Formations. The short lateral extent of the pillow lavas and their constant stratigraphic position, the existence of lava flows with unequivocal subaerial characteristics associated to sediments containing fossilized wood, clearly indicate onshore emplacement.

Keywords. Large igneous province (LIP), Central Atlantic Magmatic Province (CAMP), Pahoehoe flows, Simple flows, High Atlas, Morocco.

1. Introduction

The Central Atlantic Magmatic Province (CAMP) is one of the largest continental flood basalt (CFB) provinces on Earth [Marzoli et al., 1999] (Figure 1a, b). This Large Igneous Province (LIP) extends for more than 7500 km from north to south. It may have covered over 10 million km^2, with a total volume of magma exceeding 3 million km^3 [Marzoli et al., 2018]. The CAMP was emplaced during the early stages of breakup of the Pangean supercontinent that led to the opening of the Central Atlantic Ocean. Pangean intracontinental rifting began in the Late Permian–Early Triassic [El Arabi et al., 2006, Medina, 1995, 2000, Ruellan, 1985, Youbi et al., 2003] and progressed northwards, following the direction of the late Palaeozoic Alleghenian–Hercynian orogenic belt. The oldest identified magnetic anomalies on conjugate margins from the Central Atlantic (ECMA in North America and S1 in Morocco) were initially dated as Middle Jurassic [Klitgord and Schouten, 1987], but later reconstructions of the opening of the Central Atlantic Ocean (e.g. Sahabi et al. 2004) suggest that the age of the earliest oceanic crust is Sinemurian (196.5 to 189.6 Ma). The peak activity of the CAMP straddled the Triassic–Jurassic boundary, at ca. 201 Ma [Blackburn et al., 2013, Davies et al., 2017, Marzoli et al., 1999], and probably lasted less than 1 million years, while the late activity reached the Sinemurian [Marzoli et al., 2018].

CAMP magmatism is represented by extrusive rocks (mostly lava flows and very minor pyroclastics) and remnants of intrusive (layered intrusions, sill complexes and dike structures) (Figure 1b) that occurred in once-contiguous parts of north-western Africa, south-western Europe, North and South America (e.g., De Min et al. 2003, Hames et al. 2003, Knight et al. 2004, McHone and Puffer 2003, Martins et al. 2008, Marzoli et al. 2004, 2019, Tegner et al. 2019, Verati et al. 2007, Youbi et al. 2003). Lava flow sequences are thicker in Morocco and North America (total thickness up to about 300 m and 500 m, respectively; Kontak [2008], Marzoli et al. [2019], Merle et al. [2014]) than in Portugal, and South America (up to 130–170 m, Bertrand et al. [2014], Martins et al. [2008], Merle et al. [2011]). In Algeria, only 10–15 m are preserved in the western Saharan Atlas [Meddah et al., 2017]. Most CAMP rocks are low-Ti tholeiitic Continental Flood Basalts (CFBs), whereas high-Ti CFBs are restricted to a narrow zone in the southern margin of the West African Craton (Liberia, Sierra Leone) and north-eastern South America (Surinam, French Guyana and northern Brazil; e.g., Callegaro et al. [2017], Deckart et al. [2005], Merle et al. [2011]).

In Morocco, CAMP lava flows can be found in all structural domains (Figure 1c) north of the South Atlas Fault. In the Anti-Atlas, the CAMP is represented by intrusions such as the Foum Zguid dike and the Draa sills (e.g., Salvan 1984, Van Houten 1977). The volcanic pile overlies a Late Triassic clastic and evaporitic sedimentary sequence. The total thickness of the Moroccan CAMP lava flow piles ranges normally from 100 to 300 m. However, it may be as thin as

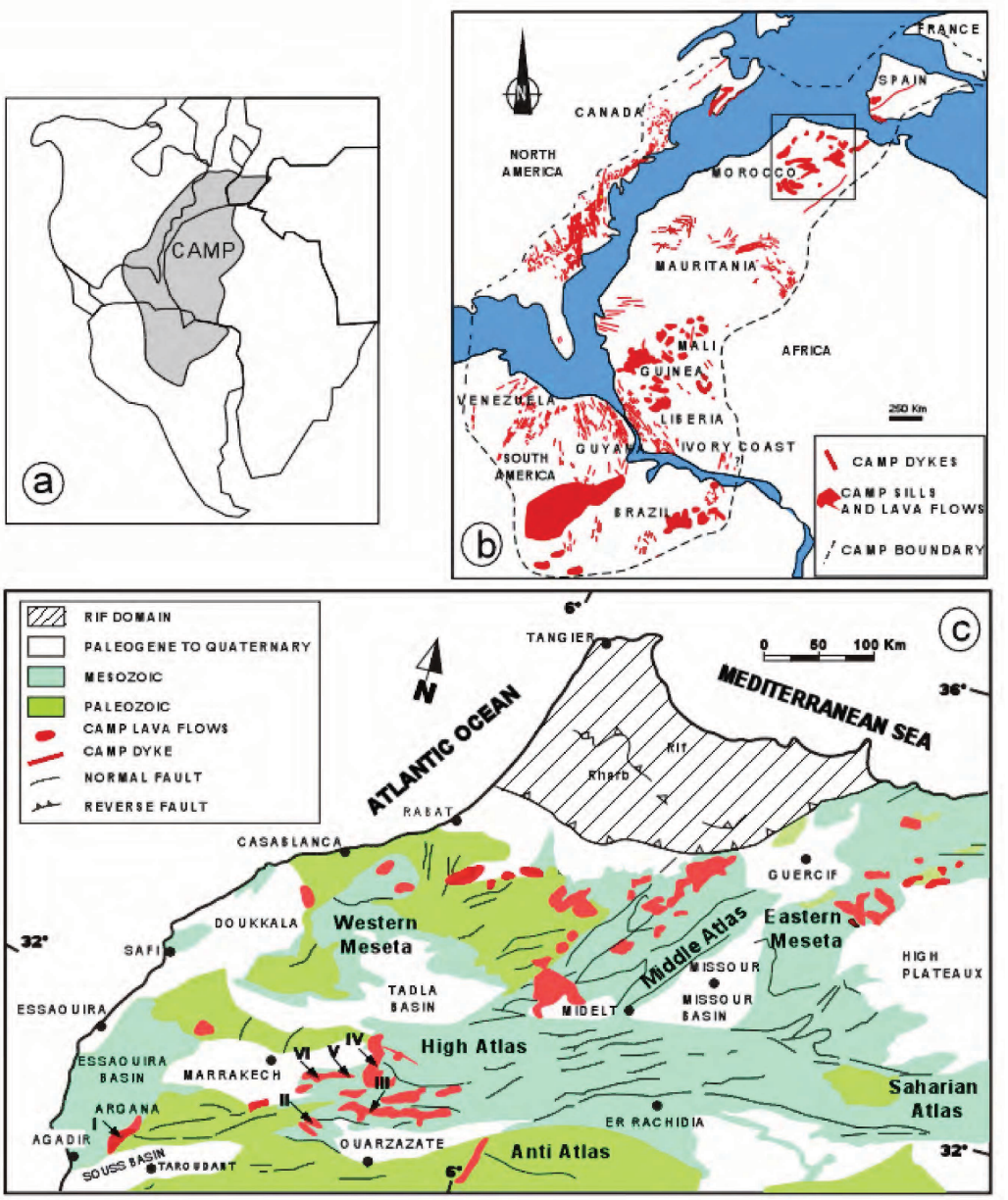

Figure 1. (a) Reconstruction of the Pangea supercontinent at time of CAMP emplacement and schematic extent of the CAMP. (b) Distribution of CAMP lava flows, sills and dikes. The dashed line shows the estimated global surface area of the CAMP. (c) Simplified geological map of the northern part of Morocco showing the distribution of CAMP products and the location of the studied sections: I – Argana (Latitude: 30° 43′ 21″ N; Longitude: 9° 14′ 03″ W); II – Tiourjdal (Latitude: 31° 07′ 74″ N; Longitude: 7° 22′ 70″ W); III – Telouet (Latitude: 31° 15′ 83″ N; Longitude: 7° 17′ 29″ W); IV – Oued Lahr (Latitude: 31° 36′ 45″ N; Longitude: 7° 22′ 53″ W); V – Jbel Imzar (Latitude: 31° 35′ 48″ N; Longitude: 7° 25′ 46″ W); VI – Ait Ourir (Latitude: 31° 32′ 50″ N; Longitude: 7° 40′ 20″ W).

8 m, or even absent on uplifted and eroded inter-basin blocks on the interior of the Moroccan Meseta. The difference in thickness from one area to another (from 8 to ca 300 m) can be explained either by dif-

ferential subsidence of a pre-volcanic basement during the emplacement of the lava flows (syn-rift series), or by the emplacement of the flows on an irregular paleotopography related to horst and graben structures. The most-studied area is the Central High Atlas, where the CAMP is best preserved and the most complete basaltic lava piles are exposed. Although the CAMP volcanism is mainly subaerial, subaquatic volcanic products also occur locally in relation with the presence of lakes of probable tectonic origin [El Ghilani et al., 2017].

The main objectives of this paper are: (i) to describe the stratigraphy, morphology and internal structures of the CAMP basalt lava flows of the Triassic–Jurassic basins of Morocco, (ii) to define lava flow emplacement mechanisms, and (iii) to discuss implications on the evolution of the CAMP and other Large Igneous Provinces.

2. Terminology and methodology

Based on their surface morphology and internal structure, basaltic lava flows have been subdivided into pillow, pahoehoe, and aa flows (e.g., Macdonald 1953, 1967, White et al. 2009). Pahoehoe flows are characterised by a smooth, billowy or ropy surface and exhibit a typical three-tiered structure [Aubele et al., 1988], comprising: (i) a basal lava crust; (ii) a lava core; and (iii) an upper lava crust. Aa flows are characterized by angular, spinose clinkers at both the flow top and bottom and tend to be usually thicker when compared to pahoehoe flows. A wide range of intermediate flow types occur between these two end-member types such as rubbly pahoehoe, slab pahoehoe, and toothpaste pahoehoe [Keszthelyi and Thordarson, 2000, Keszthelyi, 2002, Macdonald, 1953, 1967, Rowland and Walker, 1987] . These transitional lavas show some of the characteristics of both aa and pahoehoe lavas. For example, the rubbly pahoehoe has been suggested for a lava type that has a flow top composed of broken pieces of smaller pahoehoe lobes rather than spinose aa clinker [Keszthelyi and Thordarson, 2000].

According to Self et al. [1997, 1998] and Thordarson and Self [1998] the products of an effusive eruption can be subdivided into three hierarchic levels, *flow lobe*, *lava flow*, and *lava flow field*, respectively:

(i) a *flow lobe* is an individual unit of lava enclosed in a chilled crust, varying in length from decimetres to several kilometres and up to 60 m in thickness [Wilmoth and Walker, 1993]. Lobes can be classified in two types: S-type ("spongy") lobes and P-type lobes ("pipe amygdale-bearing") Wilmoth and Walker [1993]. S-type lobes lack pipe vesicles and are vesicular throughout their thickness. P-type lobes are characterized by pipe vesicles and display a typical internal structure with a vesicular base and top, and a relatively vesicle poor core;

(ii) a *lava flow* is a regional subunit formed during a continuous effusive event (during a single eruption), which may consist of several flow lobes. If a lava flow consists of a single flow lobe it is referred to as a *simple lava flow* [Walker, 1971] and if the lobe has a sheet-like or tabular geometry it is classified as a *sheet lobe*; conversely, the term *compound lava flow* [Walker, 1971] describes a lava flow composed of multiple lobes and toes;

(iii) a *lava flow field* is a complex body that may consist of several lava flows and is usually identified on the basis of mineralogy and chemistry (or of stratigraphic criteria) as the product of a single eruption.

We also use the terminology of Fisher [1961, 1966] to describe volcaniclastic (e.g., peperite, hyaloclastite) and epiclastic deposits (e.g., mudstone, siltstone, sandstone, limestone) that has been used by other authors for the description of primary volcaniclastic rocks (e.g., Manville et al. 2009, White and Houghton 2006). Fisher's pioneering classification [Fisher, 1961, 1966] subdivided volcaniclastic rocks into pyroclastic, hyaloclastic, autoclastic and epiclastic classes based on the particle forming processes. Pyroclastic fragments (produced by explosive fragmentation), hyaloclastic (quench fragmentation), and autoclastic (mechanical self-fragmentation) can be applied to both individual grains and their deposits [Fisher and Schmincke, 1984]. Epiclastic is restricted to fragments derived from weathering and erosion of "preexisting rocks", and excludes reworking of particles from non-welded or unconsolidated volcanic materials.

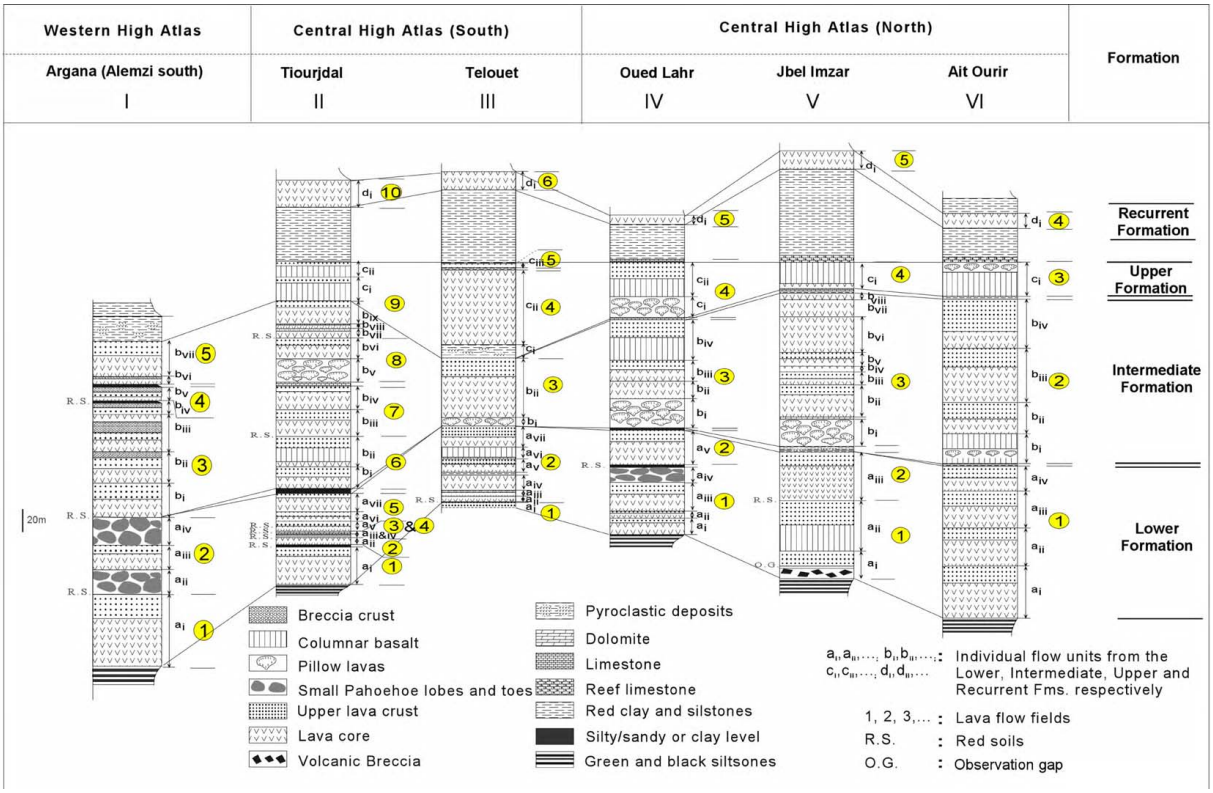

Figure 2. Lithostratigraphic columns across the CAMP volcanic succession of Morocco at the studied sections. See Figure 1 for the location of sections.

Detailed sections were investigated in six areas of the CAMP volcanic piles of Morocco (Figure 1), recording the morphology, internal structure and stratigraphy of the lava flows. The correlation between the studied sections has been performed following our field-work observations and the published petrographic and geochemical data [Bertrand, 1991, Bertrand et al., 1982, Deenen et al., 2010, Knight et al., 2004, Marzoli et al., 2004, 2019, Youbi et al., 2003]. For the first criterion, the correlation was made based on the epiclastic levels separating the different units, which may attest for significant time intervals between volcanic episodes. For the latter, we used the pioneering work of Bertrand et al. [1982] who recognized systematic geochemical changes in the stratigraphy of the Moroccan CAMP lava piles. Indeed, based on major and trace element analyses and on field-work observations, Bertrand et al. [1982] have subdivided the lava piles into four main formations (fms), the Lower, Intermediate, Upper and Recurrent fms (Figure 2). The Lower and Intermediate fms represent about 90% of the preserved lava volume, whereas the Upper and Recurrent fms hardly exceed 10%.

Individual eruptions were identified based on the presence of reddened flow surfaces (slightly weathered surfaces thermally metamorphosed by overlying flows), development of incipient or more or less evolved red and grey soils, or deposition of thin layers of fine epiclastic sediments between lava flows, representing time intervals separating the emplacement of each package of lava flow-units. Individual flow units are identified on the basis of their morphology and internal structure especially the presence of upper/lower crusts, changes in vesiculation, jointing style and volcanic textures. The identification of pahoehoe flow lobes in the field is based on the recognition of a three-partite internal structure, consisting of a basal lava crust, a lava core and an upper lava crust, and absence of a clinker envelope. The subdivision into a three-partite structure considers the variations of three groups of internal features: (i) the vesicula-

tion pattern, which is defined by distribution, mode, shape, size of vesicles and other degassing features (ii) the jointing style which refers to the arrangement and morphology of cooling joints; and (iii) the petrographic texture in terms of crystallinity and crystal size, properties that are controlled by a number of parameters, such as cooling rate, volatile content, and crystal nucleation rate.

3. Results

The six sections were investigated in detail from SW to NE across the volcanic pile cropping out in the northern and southern flanks of the High Atlas Basin (Figures 1, 2). Subaerial lava flows from the Moroccan CAMP can be grouped into two main categories: compound pahoehoe flows and simple flows. The former type is exclusively confined to the Lower and Intermediate fms while only simple flows occur in the Upper and Recurrent fms. According to Keszthelyi's (2002) classification, some transitional types between pahoehoe compound flows and aa flows, such as "rubbly pahoehoe flows", have also been observed in the Western High Atlas CAMP sequences of Morocco (e.g., Argana Basin; El Hachimi et al. 2011). Besides the subaerial flows, pillow lavas, displaying radial jointing and glassy rinds, subaquatic sheet flows and hyaloclastites are frequently found in the lower part of the Intermediate and Upper fms. In the following sections, we describe the characteristics of the volcanic lava piles for each formation at the studied areas.

3.1. *Lower formation*

The base of the Lower Formation (Fm) is usually sharp and overlies a 2 to 10 cm-thick pale grey to black silty-sandy soil or a slightly to strongly weathered surface at the top of a thick red clay-to-sand sedimentary sequence (Figure 3A) dated as Rhaetian by Panfili et al. [2019]. In the Tiourjdal section, the basalt–sediment contact is characterized by "injections" of basalt into the underlying sediment ("load casts"; Dal Corso et al. 2014, Marzoli et al. 2004). These load casts form as a result of the rapid deposition of basalt onto a water-saturated sediment and indicate that the underlying deposits were still soft or only slightly consolidated at the time of emplacement of the volcanic rock, further suggesting that the first lava flows were almost contemporaneous with the deposition of the Upper Triassic sediments. In this case, water would have played an important role by quickly cooling the basalt and reducing its thermal effect on the sediment. Furthermore, in the Oued Lahr section, the basalt–sediment contact is characterized by a volcanic breccia, typical of the base of pahoehoe-like lava flows [Self et al., 1997], which has acted as an insulator between basalt and sediment.

The Lower Fm is a 55 to 173 m-thick succession composed of 3 to 7 individual flows resulting from 1 to 5 eruptions (Figures 2, 3B). It makes up to c. 30–50% of the total preserved lava thickness in the Central and Western High Atlas. These basaltic lava flows show external and internal features typical of inflated pahoehoe flows such as a three-tiered structure with vesicle zonation, presence of tumuli, and grain size variations. They display morphological characteristics similar to those described for inflated pahoehoe flows in other CFB provinces [Aubele et al., 1988, El Hachimi et al., 2011, Kontak, 2008, Self et al., 1997, 1998, Thordarson and Self, 1998, Waichel et al., 2006].

Pahoehoe lava flows of the Lower Fm are of the compound type, 2 to 40 m thick, composed of several stacked lava lobes (Figure 3C, D). The lateral extent of the flows usually exceeds hundreds of meters. As described in Aubele et al. [1988], Thordarson and Self [1998], and Self et al. [1998], lava flows of the Lower Fm display a three-tiered structure with (i) a thin "basal lava crust" which is vesicular, often with pipe vesicles (Figure 3E), (ii) a dense "lava core" usually not vesiculated or presenting few cm-sized spherical or irregular vesicles, and (iii) an "upper lava crust" showing increased vesicularity towards the top and horizontal vesicle concentration zones. This "three-tiered structure" is a clear evidence of endogenous growth by inflation, suggesting a slow emplacement during sustained eruptive episodes.

In the Central High Atlas, epiclastic sediments intercalated in the volcanic sequence are clearly baked by the overlying lavas. An example can be observed at Oued Lahr, where lava flows contain injections of red sediment ("clastic dikes" and "sills" of baked red silt; Figure 3F). The clastic dikes rise from the base of the lavas without reaching the top of the flows and, in some cases, display upward flow structures and, thus, they cannot be interpreted as the filling of fractures from above. This magma/sediment mingling can be interpreted as a peperite (see Skilling et al. 2002 for

Plate 1

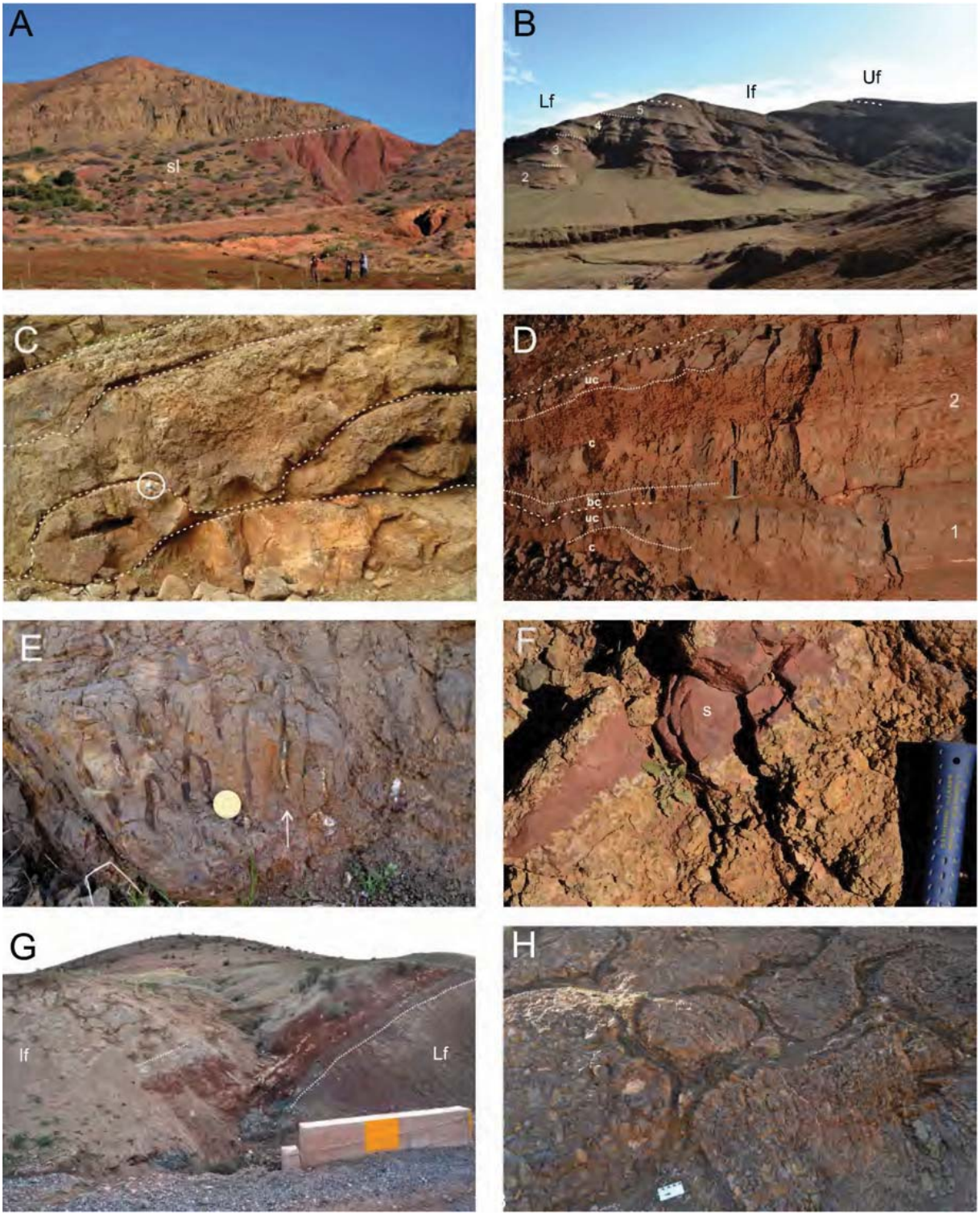

Figure 3. A-H (see captions below).

Plate 2

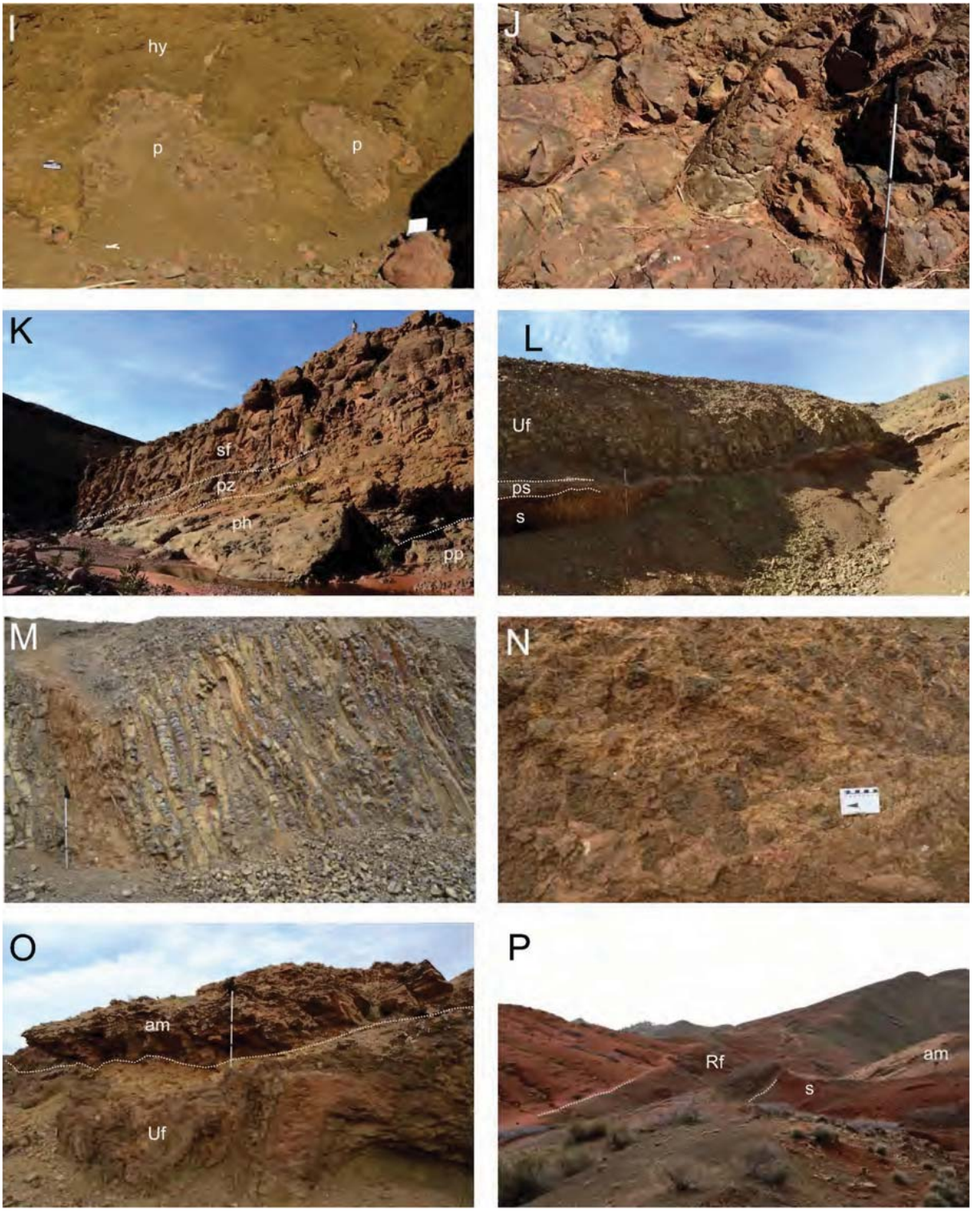

Figure 3. I-P (see captions below).

Figure 3. Field photographs illustrating some of the most characteristic aspects of the Moroccan CAMP volcanic sequences: (A) Contact (dotted white line) between the Lower Fm. lava pile and the underlying Rhaetian red silts at the Oued Lahr section. The top of the sediments is a pale grey layer. The central part of the lower half of the slope is slumped (sl). (B) General view looking SE of the Ait Ourir section. The contacts between the Lower (Lf), Intermediate (If), and Upper (Uf) formations are marked by dashed white lines. In the Lower Fm. successive lava flows (numbers and dotted white lines) are separated by reddened surfaces (the lowermost lava flow 1, is not visible in the photograph). (C) Aspect of a compound lava flow of the Lower Fm. at the Oued Lahr section, corresponding to a pile of superposed thin pahoehoe toes (highlighted by dashed white lines). Wrist watch for scale encircled. (D) Compound lava flow of the Lower Fm. lava sequence at the Oued Lahr section, composed of several superposed pahoehoe lobes (two of which – 1, 2 – are shown separated by dashed white lines) presenting chilled dense basal (bc) and upper (uc) crusts enveloping a variably vesiculated lava core (c) (contacts highlighted by dotted white lines). Hammer for scale. (E) Pipe vesicles perpendicular to the base of a subaerial pahoehoe lava flow from the Lower Fm. from the Ait Ourir section. Pipes start about 4–5 cm above the base and extend upwards some 25 cm. Coin as scale is 2.7 cm in diameter. (F) Red silt lens injected into the core of an inflated pahoehoe flow from the Lower Fm. at the Oued Lahr section. Note the peperitic interaction at the edge of the injected sediment, meaning that the lava core was still partially molten, although the sharp contacts of the feeder sediment dike (not shown) suggest that the base of the lava was already brittle when the sediment injection occurred. Hammer handle for scale. (G) Sedimentary sequence separating the Lower (Lf) and Intermediate (If) formations at the Sidi-Rahal section. The 3 m-thick sediments include, from base to top, grey, green and red mudstones, red sandstones, red mudstones, limestones, red sandstones, red and light-grey mudstones. The volcanic rocks are extremely weathered, but the densely packed pillows of the Intermediate Fm. above the sediments are clearly defined by their darker glassy rind. (H) Weathered densely packed pillow of the base of the subaquatic lava flow from the base of the Intermediate Fm. at the Ait Ourir section. The pillows present cm-thick glassy rinds, and the few spaces between them are filled by hyaloclastite. Ruler as scale is 8 cm-long. (I) The same lava flow of photo H passes upwards into hyaloclastites (hy) with dispersed large pillows (p). Note frequent invaginations of the glassy rind of the pillows. Field book at the left is 16 cm long. (J) Aspect of densely packed, well-preserved pillows, from the base of a partially subaquatic lava flow from the base of the Intermediate Fm. at the Oued Lahr section. The pillows can be seen in three dimensions with some of them exposed in longitudinal view and others in transversal section. Once removed the ~15° northwards tilt of the whole sequence, the pillows still dip 30°–45° to the north, thus suggesting a northwards prograding lava delta. Walking stick for scale is 1.3 m long. (K) General view of the same lava flow dipping ~15° to the north: the lava flow is composed of densely packed pillows (pp) at the base (shown in photo J), followed by isolated pillows in hyaloclastite (ph), a transition zone of mixed subaquatic-subaerial facies (pz), and the 8 m-thick upper, columnar-jointed, subaerial part of the lava flow (sf). The thickness of the subaquatic part of the flow (25–30 m) corresponds to the depth of the lake. The underlying Lf lavas are subaerial and the two units are separated by a thin discontinuous red clay layer. Dotted white lines mark the transition between different zones of the flow. Shephard and flock on top of the cliff give scale. L. Sediments (s) and paleosoil (ps) separating the Intermediate (If) and Upper (Uf) formations at the Ait Ourir section. The base of the Uf corresponds to a subaquatic sheet flow presenting well-developed columnar jointing (see also photo M). Walking stick for scale is 1.3 m long. (M) Subaquatic sheet flow from the base of the Upper Fm. at the Ait Ourir section displaying typical thin undulating columns. Walking stick for scale is 1.3 m long. (N) Outcrop of pillow breccia in a matrix of hyaloclastites from the top of the uppermost lava flow of the Upper Fm. (Ait Ourir section). Ruler for scale is 8 cm long. (O) Top of the Upper Fm. (Uf) at the Ait Ourir section, overlain by a 2 m-thick algal mat limestone (am). The upper part of the Uf sequence at this location corresponds to hyaloclastites with intrusive pillows and pillow breccias. Walking stick for scale is 1.3 m long; (P) South (left) dipping upper part of the Ait Ourir volcanic sequence composed of algal mat limestones (am), red silty mudstones (s), the 5 m-thick simple flow of the Recurrent Fm. (Rf), which is covered by several meters of red silty mudstones.

more details). These occurrences indicate the interaction between lava flows and unlithified wet sediments (clay to sand), suggesting that volcanism and sedimentation were coeval (see Skilling et al. 2002). Thus, peperites observed in the lava flows of the Lower Fm show that the underlying or intercalated red siltites were still soft or poorly consolidated when the lava flows were emplaced. Similar structures have been observed in the Argana basin (Western High Atlas; El Hachimi et al. 2011) and in the Algarve (Portugal) CAMP sequences [Martins et al., 2008]. They have also been described at the base of a large pahoehoe lobe in the Western Ghats of the Deccan Volcanic Province [Duraiswami et al., 2003], in the Neo-Proterozoic volcanic sequence of the Anti-Atlas (in lava flows and ignimbrites), and, even in carbonatitic tuffs in ocean island volcanoes (e.g. Santiago, in Cape Verde) (J. Madeira unpublished data). Thus, although their genesis is not yet fully understood, these sedimentary intrusions seem to be relatively common features.

Coalescence of lobes and toes is another relatively common feature often found at the top of some compound pahoehoe flows from the Oued Lahr and Argana sections. The smallest lobes are sometimes elongated lenses trending NE-SW. The glassy contacts between lobes are often thermally oxidized. P-type lobes are more frequent than S-type lobes.

Tumuli and breakout structures characteristic of the compound pahoehoe flow type have been observed at three of the studied localities: Tiourjdal section in the southern Central High Atlas, the Argana section in the western High Atlas and the Ait Ourir section in the northern Central High Atlas (Figure 1C). Tumuli are found within pahoehoe lava flow fields containing multiple lobes and flows. The flows are often up to 5 m thick, and show the classic internal three-tiered structure described above. In the Tiourjdal area, the upper crust of the lower lava flow is marked by a thick squeeze-up, which is 70 cm wide, oriented N50, and that can be followed horizontally over 20 m. Its length suggests that it may have been extruded through an axial cleft of a pressure ridge. The squeeze-up contains vesicles that increase in size inwards. It presents a chilled margin indicating the contact with the colder upper crust of the host lava flow. In the Argana basin, some pahoehoe lava flows display thick squeeze-ups breaking through the upper crust and sometimes forming small pahoehoe toes on top of the feeder lava flow (see El Hachimi et al. 2011 for details).

At the Ait Ourir section, fault planes offset the basal compound pahoehoe flows but are fossilized by the overlying flows, indicating the occurrence of syn-volcanic extensional tectonics.

3.2. *Intermediate formation*

The Lower and Intermediate fms are separated by silt-to-sand sediments of variable thicknesses, locally also including limestones (Figure 3G), or by 0.15 to 2 m-thick red paleosoils. The paleosoils are structureless (sometimes faintly bedded, suggesting a pedogenized sedimentary nature) and usually contain rounded volcanic clasts embedded in a clay to silty matrix. The Intermediate Fm is up to 130 m-thick, and is composed of 2 to 9 flows corresponding to up to 4 eruptions. Lava flows present typical pahoehoe features (cf. Cas and Wright 1987, Francis and Oppenheimer 2004, Macdonald 1967, 1972, Self et al. 1998, Wilmoth and Walker 1993). They are almost always compound in nature [Walker, 1971]. Pahoehoe lava flows display the three-tiered structure previously described. Each lava flow is defined by chilled tops and bottoms and the boundaries of the internal sub-divisions are clearly defined by marked changes in the vesiculation pattern, jointing style, and petrographic texture [Thordarson and Self, 1998]. Segregation structures, characteristic of the compound pahoehoe flows type, such as pipes vesicles, cylinder vesicles [Goff, 1996], and horizontal vesicular sheets [Thordarson and Self, 1998] are common. Sometimes, the pipe axes are inclined, thus recording the lava movement and are reliable markers of the flow direction (e.g., Walker 1987). Walker [1987] relates the pipe vesicles to the rise of bubbles through the lower part of cooling lava flow when it has acquired yield strength of the order of 50 $N{\cdot}m^2$, and a flow rate equivalent or smaller than the rate of bubble rise, a condition that is favoured by lava flowing on very low angle slopes. Vesicle cylinders are observed in the core of compound pahoehoe flows. They are almost always rootless and not connected with the pipe vesicles in the basal crust. Cylinders in thick lobes can be up to 0.50 m long. They are sometimes connected with vesicle sheets. Horizontal vesicular sheets occur near the interface between the upper crust and the core. The sheets thickness is 10 cm in average,

but can reach up to 30 cm. The vesicle sheets display irregular shapes and branching patterns, which suggests that they have filled joints that formed at the early stages of cooling. In the Tiourjdal section (southern Central High Atlas), compound pahoehoe flows are composed of coalescing well-defined toes producing irregular upper surfaces of the flow field.

The lower flows of the Intermediate Fm often present subaquatic facies represented by densely packed pillows (Figure 3H), pillows in a hyaloclastite matrix (Figure 3I), and subaquatic sheet flows. Pillow-lavas vary in diameter from 10 cm to 2.5 m. The internal structure of the basaltic pillows is characterized by two concentric layers: an outer cortex and the core. The cortex corresponds to a 0.1 to 14 cm thick glassy envelope. At the Oued Lahr section, the first lava flow of the Intermediate Fm entered an approximately 25–30 m-deep lake, as suggested by the thickness between the transition zone (separating the subaquatic and subaerial facies) and the base of the flow (see Ramalho et al. 2010, 2017 for examples of the use of this type of markers). It corresponds to a lava delta consisting of prograding foresets of pillow lavas and hyaloclastites passing upwards into an 8 m-thick subaerial pahoehoe flow (Figure 3J, K). Pillow lavas from this section present horizontal and vertical diameters ranging from 0.2 to 1.6 m and 0.18 to 1.18 m, respectively. At other locations, where the transition zone is not exposed or the sequence is entirely composed of subaquatic volcanics, only a minimum water depth can be determined.

In some areas of the Central High Atlas, the subaerial lava flows of the Intermediate Fm show well-developed columnar jointing. In one outcrop from the Tiourjdal section a 15 m-thick lava flow displays radial jointing in its lower half, indicating that the lava entered a 6–7 m deep body of water (river, lake?).

In the Tiourjdal section, the Intermediate Fm is marked by the presence of thin layers of lacustrine limestone (~1 m thick) interbedded within the volcanic sequence.

3.3. *Upper formation*

The Upper Fm sequence is 15 to 76 m thick, representing a volume of 5 to 8% of the preserved lava piles. It is separated from the uppermost flows of the Intermediate Fm by a thin level (0.5 to 1 m) of red to greyish siltstones, laminated limestones, or red-green mottled paleosoils (Figure 3L). The Upper Fm is composed of one or two lava flows representing one or two eruptions.

The subaerial lava flows of the Upper Fm usually display well-developed prismatic jointing, sometimes corresponding to laterally extensive simple flows, usually ranging in thickness from 5 to 30 m. The thickest simple flow (~40 m) is observed in the Telouet section. Simple flows are clearly separated from underlying flows by weathering surfaces or paleosoils several centimetres thick. They appear as dense and massive flows, but can be subdivided, as compound pahoehoe flows, into a three-tiered structure [Aubele et al., 1988, El Hachimi et al., 2011, Thordarson and Self, 1998] with a thin basal crust, a dense lava core and an upper crust, indicating thickening by inflation. The lower crust of the simple flows is 0.25 to 0.5 m thick, representing 2 to 3% of the total thickness of the flow. Although vesicles may be numerous, pipe vesicles were not observed. The lava core is the thickest part of the flow, up to 30 m in the Telouet section. It usually appears as a poorly vesiculated zone with respect to the upper crust. The upper crusts are 4–20 m thick and strongly vesiculated. Lobes, layering of vesicle-poor ("dense") and vesicle-rich ("vesicular") bands, tumuli and squeeze-up structures which are characteristic of the compound pahoehoe flows type have not been observed within the upper crust of these simple flows.

Subaquatic flows also occur at the base of the unit where they may reach 4 to 20 m in thickness. At the Ait Ourir section, the facies of subaquatic flows varies laterally or vertically from sheet flows, presenting thin, undulating columnar jointing (10 to 15 cm in diameter; Figure 3M), to pillow lavas intruded into hyaloclastite, or pillow breccias (Figure 3N).

In the Telouet section (Central High Atlas), the lowermost lava flow of the Upper Fm displays injections of brownish red siltstone forming irregular sedimentary bodies (4 cm–1 m long) randomly dispersed in the core of the lava flow, indicating peperitic interaction.

3.4. *Recurrent formation*

The Recurrent Fm is limited to the Central High Atlas lava piles and is absent in the Argana basin. It is separated from the Upper Fm by a sedimentary unit

which may reach 80 m such as in the south flank of the Central High Atlas. The sediments are composed of red silty-mudstones, locally overlying algal mat limestones (Figure 3O, P). The base of the Recurrent Fm lava flow frequently displays load casts into the underlying mudstones, indicating that the sediments were still soft.

The Recurrent Fm is the result of a single eruption and is composed of a 5–50 m thick simple lava flow. This lava flow has a dense and massive texture. Segregation structures characteristic of compound pahoehoe flows such as pipe vesicles, cylinder vesicles and vesicular sheet are absent.

This late unit represents a small volume eruption (<5% of the CAMP total). The Recurrent Fm is covered by Early Jurassic silt-to-clay and carbonated sediments and it is found only in the northern and southern flanks of Central High Atlas basins. A similar formation has been described from the Newark and Hartford basins in North America [Olsen et al., 2003], but was not found in Iberia.

4. Discussion: *emplacement mechanisms of the CAMP lava flows of Morocco*

Once considered to be composed by monotonous stacks of basaltic lava, continental flood basalt (CFB) provinces are now known to display considerable diversity in lava flow morphology. Whereas most initial studies of flood basalt morphology and emplacement focused on younger provinces such as the Miocene Columbia River Basalt (e.g., Self et al. 1996, Thordarson and Self 1998), subsequent investigations targeted older provinces such as the ca. 201 Ma Central Atlantic Magmatic Province (CAMP, e.g., El Hachimi et al. 2011, Kontak 2008, Martins et al. 2008), the ca. 132 Ma Paraná-Etendeka [Jerram et al., 999a,b, Rossetti et al., 2014, Waichel et al., 2006, 2012], and the ca. 66 Ma Deccan Volcanic Province (DVP, e.g., Bondre et al. 004a,b, Duraiswami et al. 2001, 2003, 2014, Keszthelyi et al. 1999, Sheth 2006, Sheth et al. 2011). The morphology of lava flow lobes in CFB provinces can help understanding the mechanisms involved in their emplacement as shown by Self et al. [1997].

The CAMP lava flows of Morocco show clear evidence of endogenous growth or inflation in the sense of Self et al. [1997, 1998]. The features indicating endogenous growth are: (i) the three-partite structural division of sheet lobes in a thin basal crust, a dense lava core, and a vesicular upper crust, which, when thick, tends to show layering of alternating massive and vesicular levels; (ii) the vertical distribution of vesicles and the presence of segregation structures such as spherical vesicles, pipe vesicles, vesicle cylinders and vesicle sheets, and (iii) the occurrence of tumuli and squeeze-ups. In this sense, they are similar to other inflated pahoehoe flows found in Hawaii [Hon et al., 1994], Columbia River Basalt Province [Thordarson and Self, 1998], in the Cenozoic volcanic Province of North Queensland in Australia [Whitehead and Stephenson, 1998], Deccan Traps [Bondre et al., 004a,b, Keszthelyi et al., 1999, Jay and Widdowson, 2008], Paraná-Etendeka CFB [Jerram et al., 999a,b, Waichel et al., 2006], the CAMP flows of the Fundy basin, Canada [Kontak, 2008], and the CAMP basins of Argana [El Hachimi et al., 2011], Berrechid and Doukkala, Morocco [Bensalah et al., 2011], and Algarve, Portugal [Martins et al., 2008]. The predominance of P-type lobes in compound flows can be related to breakouts emerged from larger inflated sheet flows [Hon et al., 1994, 2003]. According to Wilmoth and Walker [1993], these lobes can be found almost anywhere in the pahoehoe flow field, but are more common in areas with shallow slopes (<4°). Lava flows with subaquatic facies represent subaerial lavas that flowed into ponds or lakes occupying depressions on the pre-volcanic topography. Most of these depressions probably correspond to asymmetric graben structures, as suggested by the occurrence of syn-volcanic tectonism, common in Morocco. At odds with what is stated by Mattis [1977] and Lorenz [1988], the presence of subaquatic lava flows does not require a widespread subaquatic environment at the time of eruption. Indeed, the limited lateral continuity of pillow lavas and their almost constant stratigraphic position, the existence of lava flows with subaerial characteristics associated to sediments containing fossilized wood, clearly support a generally subaerial emplacement of CAMP basalts. These subaquatic volcanic sequences can also be used to determine the depth (or minimum depth) of these water bodies, based on the thickness of the subaquatic portion of the lava flow, and suggest that these lakes could be as deep as 20 m and, probably, were not temporary ponds.

The emplacement of the CAMP occurred in an

extensional tectonic setting, related to the break-up of the megacontinent Pangea and subsequent opening of the Central Atlantic Ocean [Sahabi et al., 2004, Labails et al., 2010, Marzoli et al., 2017]. The magmatic activity was syn-to slightly post-extensional, with lava flows emplaced in progressively subsiding grabens or sealing them [Hafid, 2006, Marzoli et al., 2019]. Thordarson and Self [1998] show that the emplacement of the Roza lavas (Colombia River Basalt Province) was produced by one long single eruption. In contrast to this, the morphologic, textural and stratigraphic features of the Moroccan CAMP volcanic pile favour an emplacement during several sustained eruptions. Significant time breaks within the volcanic sequence are marked by the presence of red oxidized surfaces, paleosoils between pahoehoe compound and simple flows produced by individual eruptions within each formation, or by the presence of epiclastic sedimentary sequences separating the four classical formations. These imply significant volcanic quiescence periods between the emplacement of successive simple lava flows or flow fields. According to Marzoli et al. [2019], Lower to Upper CAMP flows in Morocco were erupted in four pulses each lasting about 400 years [Font et al., 2011, Knight et al., 2004], with an eruption rate during the pulses of about 8 km^3/year. Such an eruption rate is over one order of magnitude higher than at Hawaii and similar to e.g., the Laki eruption in Iceland (15 km^3 in 9 months during the years 1783–1784), which had a considerable effect on the climate in the northern hemisphere [Thordarson and Self, 1993].

Based on the physical volcanology, the comparison of the CAMP basaltic succession in Morocco with the Deccan volcanic Province (India), Paraná (Brazil), Columbia River Basalt Province (USA) and other CFBs indicates that these Large Igneous Provinces (LIP) do not have a simple, "layer-cake stratigraphy", but present complex architectures. Such architectures are governed by the volume of individual eruption events, the location and abundance of volcanic centers, and the evolution of these centers through time [Jerram, 2002, Jerram and Widdowson, 2005, White et al., 2009]. The architecture of the Moroccan CAMP and of most, if not all, CFB provinces reveals that the production of compound pahoehoe flows was followed by flows with a simpler sheet-like geometry, indicating a fundamental temporal change in the emplacement process of lava flows. Accordingly, it appears that flood basalt volcanism starts by sustained eruptions with relatively low effusion rates [Jerram, 2002, Walker, 1971], and gradually accelerates to high effusion rates leading to high-volume but short-lived eruptions [Shaw and Swanson, 1970, Walker, 1971]. This worldwide similarity suggests that the magma genesis and/or magma ascension processes are essentially similar in all CFB provinces [Duraiswami et al., 2014, El Hachimi et al., 2011, Jerram, 2002, Jerram and Widdowson, 2005, Jerram et al., 999a,b, Martins et al., 2008, Planke et al., 2000, Rossetti et al., 2014, Waichel et al., 2012, White et al., 2009], although local conditions (such as regional topography, surface and underground water availability) may constrain the details of the internal architecture of each province [El Ghilani et al., 2017, Luchetti et al., 2014].

5. Summary and conclusions

The data presented here indicate that the CAMP volcanic pile of Morocco formed during four phases of geochemically distinct volcanic activity, represented by the Lower, Intermediate, Upper and Recurrent fms. Epiclastic sediments, intercalated or separating the Lower, Intermediate and Upper fms are rare and usually thin.

The studied sections display evidence for a variable number of eruptions in each formation (1 to 5 eruptions in the Lower Fm, 1 to 3 eruptions in the Intermediate Fm, 1 or 2 eruptions in the Upper Fm, and a single eruption in the Recurrent Fm). The products of the distinct eruptions can be separated by the presence of reddened top surfaces, development of incipient or more evolved soils, or deposition of thin layers of fine epiclastic sediments, representing time intervals separating the emplacement of each package of lava flows.

Except for the Recurrent Fm, each of the remaining formations shows thick successions of individual flows. The older formations (Lower and Intermediate fms) are composed of compound pahoehoe flows that display the entire range of pahoehoe morphology including inflated lobes, the three-partite structure of sheet lobes, vertical distribution of vesicles, presence of segregation structures and tumuli structures, while the younger formations (Upper and Recurrent fms) are constituted by simple flows forming extensive thick sheets capped by highly vesicular,

weathered crusts, or flow-top breccias, and exhibiting a three-tiered structure. Pillow lavas are common in the Intermediate fm. throughout Morocco, but are absent or rarer in the other units.

The architecture of most, if not all, CFB provinces reveals that the production of compound pahoehoe flows was followed by flows with a simpler sheet-like geometry indicating a fundamental temporal change in the emplacement of flows. Accordingly, the morphology of CAMP lava volcanic sequence of Morocco suggests an increase in effusion rate of eruptions from the first to the last pulse of volcanism.

Acknowledgements

Most of this work was carried out at the Department of Geology of the Faculty of Sciences-Semlalia, Cadi Ayyad University of Marrakech. We acknowledge the CNRST for funding the student-grant no. a 03/034-2005-2007. Financial support for this work was also provided by several research projects: (i) Moroccan PARS (SDU-30) to Fida Medina (ii) PICS, CNRS (France)-CNRST (Morocco) to Hervé Bertrand and Nasrrddine Youbi, (iii) CNRi (Italy)-CNRST (Morocco) to Giuliano Bellieni, Andrea Marzoli and Nasrrddine Youbi, and FCT (Portugal)-CNRST (Morocco) to José Madeira, João Mata, Línia Martins, and Nasrrddine Youbi, who also acknowledge project FCT/UID/GEO/50019/2019 - IDL, funded by FCT.

Guest editors S. Bourquin and R. Essamoud are gratefully acknowledged for their patience and support. The comments of two anonymous reviewers are also appreciated.

References

Aubele, J. C., Crumpler, L. S., and Elston, W. E. (1988). Vesicle zonation and vertical structure of basalt flows. *J. Volcanol. Geotherm. Res.*, 35(4):349–374.

Bensalah, M. K., Youbi, N., Mahmoudi, A., Bertrand, H., Mata, J., El Hachimi, H., Madeira, J., Martins, L., Marzoli, A., Bellon, H., Medina, F., Karroum, L. A., Karroum, M., and Ben Abbou, M. (2011). The Central Atlantic Magmatic Province (CAMP) volcanic sequences of Berrechid and Doukkala basins (Western Meseta, Morocco): volcanology and geochemistry. *Comun. Geol.*, 98:15–27.

Bertrand, H. (1991). The Mesozoic tholeiitic Province of Northwest Africa: a volcanotectonic record of the early opening of central Atlantic. In Kampunzu, A. B. and Lulab, R. T., editors, *Magmatism in Extensional Settings: The Phanerozoic African Plate*, pages 147–188. Springer, Berlin, Heidelberg.

Bertrand, H., Dostal, J., and Dupuy, C. (1982). Geochemistry of early Mesozoic tholeiites from Morocco. *Earth Planet. Sci. Lett.*, 58:225–239.

Bertrand, H., Fornari, M., Marzoli, A., Garcia-Duarte, R., and Sempere, T. (2014). The Central Atlantic Magmatic Province extends into Bolivia. *Lithos*, 188:33–43.

Blackburn, T. J., Olsen, P. E., Bowring, S. A., Mclean, N. M., Kent, D., Puffer, J., McHone, G., Rasbury, E. T., and Et-Touhami, M. (2013). Zircon U-Pb geochronology links the end-triassic extinction with the Central Atlantic Magmatic Province. *Science*, 340:941–945.

Bondre, N. R., Duraiswami, R. A., and Dole, G. (2004a). A brief comparison of lava flows from the Deccan volcanic province and the Columbia–Oregon Plateau flood basalts: implications for models of flood basalt emplacement, in: Sheth, H. C., Pande, K., editors, Magmatism in India through Time. Proc. Indian Acad. Sci. *Earth Planet. Sci.*, 113(4):809–817.

Bondre, N. R., Duraiswami, R. A., and Dole, G. (2004b). Morphology and emplacement of flows from the Deccan volcanic province, India. *Bull. Volcanol.*, 66(1):29–45.

Callegaro, S., Marzoli, A., Bertrand, H., Blichert, T. J., Reisberg, L., Cavazzini, G., Jourdan, F., Davies, J. H. F. L., Parisio, L., Bouchet, R., Paul, A., Schaltegger, U., and Chiaradia, M. (2017). Geochemical constraints provided by the freetown layered complex (Sierra Leone) on the origin of high-Ti tholeiitic CAMP magmas. *J. Petrol.*, 58(9):1811–1840.

Cas, R. A. F. and Wright, J. V. (1987). *Volcanic Successions Modern and Ancient.* Allen and Unwin, London. 528 p.

Dal Corso, J., Marzoli, A., Tateo, F., Jenkyns, H. C., Bertrand, H., Youbi, N., Mahmoudi, A., Font, E., Buratti, N., and Cirilli, S. (2014). The dawn of CAMP volcanism and its bearing on the end-Triassic carbon cycle disruption. *J. Geol. Soc.*, 171:153–164.

Davies, J. H. F. L., Marzoli, A., Bertrand, H., Youbi, N., Ernesto, M., and Schaltegger, U. (2017). End-Triassic mass extinction started by intrusive CAMP activity. *Nat. Commun.*, 8.

De Min, A., Piccirillo, E. M., Marzoli, A., Bellieni, G.,

Renne, P. R., Ernesto, M., and Marques, L. S. (2003). The Central Atlantic Magmatic Province (CAMP) in Brazil: petrology, geochemistry, 40Ar/39Ar ages, paleomagnetism and geodynamic implications. In Hames, W., McHone, G., Renne, P. R., and Ruppel, C., editors, *AGU- Geophysical Monograph 136, The Central Atlantic Magmatic Province*, volume 136, pages 91–128. American Geophysical Union Monograph.

Deckart, K., Bertrand, H., and Liegeois, J. P. (2005). Geochemistry and Sr, Nd, Pb isotopic composition of the Central Atlantic Magmatic Province (CAMP) in Guyana and Guinea. *Lithos*, 82:289–314.

Deenen, M. H. L., Ruhl, M., Bonis, N. R., Krijgsman, W., Kuerschner, W. N., Reitsma, M., and van Bergen, M. J. (2010). A new chronology for the end-Triassic mass extinction. *Earth Planet. Sci. Lett.*, 291:113–125.

Duraiswami, R. A., Bondre, N. R., Dole, G., Phadnis, V. M., and Kale, V. S. (2001). Tumuli and associated features from the western Deccan volcanic province, India. *Bull. Volcanol.*, 63:435–442.

Duraiswami, R. A., Dole, G., and Bondre, N. R. (2003). Slabby pahoehoe from the western Deccan Volcanic Province: evidence for incipient pahoehoe-a'a transitions. *J. Volcanol. Geotherm. Res.*, 121(3/4):195–217.

Duraiswami, R. A., Gadpallu, P., Shaikh, T. N., and Cardin, N. (2014). Pahoehoe-a'a transitions in the lava flow fields of the western Deccan Traps, India- implications for emplacement dynamics, flood basalt architecture and volcanic stratigraphy. *J. Asian Earth Sci.*, 84:146–166.

El Arabi, E. H., Bienvenid, J. D., Broutin, J., and Essamoud, R. (2006). Première caractérisation palynologique du Trias moyen dans le Haut Atlas; implications pour l'initiation du rifting téthysien au Maroc. *C. R. Geosci.*, 338(9):641–649.

El Ghilani, S., Youbi, N., Madeira, J., Chellai, E. H., Lopez-Galindo, A., Martins, L., and Mata, J. (2017). Environmental implication of subaqueous lava flows from a continental Large Igneous Province: examples from the Moroccan Central Atlantic Magmatic Province (CAMP). *J. Afr. Earth Sci.*, 127:211–221.

El Hachimi, H., Youbi, N., Madeira, J., Bensalah, M. K., Martins, L., Mata, J., Bertrand, H., Marzoli, A., Medina, F., Munhá, J., Bellieni, J., Mahmoudi, A., Ben Abbou, M., and Assafar, H. (2011). Morphology, internal architecture, and emplacement mechanisms of lava flows from the Central Atlantic Magmatic Province (CAMP) of Argana basin (Morocco). In Van Hinsbergen, D. J. J., Buiter, S. J. H., Torsvik, T. H., Gaina, C., and Webb, S. J., editors, *The Formation and Evolution of Africa: A Synopsis of 3.8 Ga of Earth History*, volume 357, pages 167–193. Geol. Soc. London Spec. Publ.

Fisher, R. V. (1961). Proposed classification of volcaniclastic sediments and rocks. *Geol. Soc. Am. Bull.*, 72:1409–1414.

Fisher, R. V. (1966). Rocks composed of volcanic fragments and their classification. *Earth-Sci. Rev.*, 1:287–298.

Fisher, R. V. and Schmincke, H.-U. (1984). *Pyroclastic Rocks*. Springer-Verlag, Berlin, Heidelberg.

Font, E., Youbi, N., Fernandes, S., El Hachimi, H., Kratinova, Z., and Hamim, Y. (2011). Revisiting the magnetostratigraphy of the Central Atlantic Magmatic Province from Morocco. *Earth Planet. Sci. Lett.*, 309:302–317.

Francis, P. and Oppenheimer, C. (2004). *Volcanoes*. Oxford University Press, New York.

Goff, F. (1996). Vesicle cylinders in vapor-differentiated basalt flows. *J. Volcanol. Geotherm. Res.*, 71(2/4):167–185.

Hafid, M. (2006). Styles structuraux du Haut Atlas de Cap Tafelney et de la partie septentrionale du Haut Atlas occidental: tecttonique salifère et relation entre l'Atlas et l'Atlantique. *Notes Mém. Serv. Geol.*, 465:1–174.

Hames, W. E., McHone, J. G., Renne, P., and Ruppel, C. (2003). The Central Atlantic Magmatic Province: insights from fragments of Pangea. *Am. Geophys. Union Monograph.*, 136:1–269.

Hon, K., Gansecki, C., and Kauahikaua, J. (2003). The Transition from A'a to Pahoehoe Crust on Flows Emplaced During the Pu'u 'Ō'ō-Kūpaianaha Eruption. In Heliker, C., Swanson, D. A., and Takahashi, T. J., editors, *The Puu'u 'Ō'ō-Kūpaianaha Eruption of Kīlauea Volcano, Hawai'i: The First 20 Years*, U.S.G.S. Professional Paper 1676, pages 89–103.

Hon, K., Kauahikaua, J., Denlinger, R., and Mackay, K. (1994). Emplacement and inflation of pahoehoe sheet flows: observations and measurements of active lava flows on Kilauea Volcano, Hawaii. *Geol. Soc. Am. Bull.*, 106(3):351–370.

Jay, A. E. and Widdowson, M. (2008). Stratigraphy, structure and volcanology of the SE Deccan

continental flood basalt province: implications for eruptive extent and volumes. *J. Geol. Soc. Lond.*, 165(1):177–188.

Jerram, D. A. (2002). Volcanology and facies architecture of flood basalts. In Menzies, M. A., Klemperer, S. L., Ebinger, C. J., and Baker, J., editors, *Volcanic Rifted Margins*, Geol. Soc. Am. Special Paper 362, pages 121–135.

Jerram, D. A., Mountney, N., Holzförster, F., and Stollhofen, H. (1999b). Internal stratigraphic relationships in the Etendeka Group in the Huab Basin, NW Namibia: understanding the onset of food volcanism. *J. Geodyn.*, 28(4/5):393–418.

Jerram, D. A., Mountney, N., and Stollhofen, H. (1999a). Facies architecture of the Etjo Sandstone Formation and its interaction with the Basal Etendeka food basalts of NW Namibia: implications for offshore analogues. In Cameron, N., Bate, R., and Clure, V., editors, *The Oil and Gas Habitats of the South Atlantic*, volume 153, pages 367–380. Geol. Soc. London Special Publication.

Jerram, D. A. and Widdowson, M. (2005). The anatomy of Continental Flood Basalt Provinces: geological constraints on the processes and products of flood volcanism. *Lithos*, 79(3/4):385–405.

Keszthelyi, L. (2002). Classification of the mafic lava flows from OPD Leg 183. In Frey, F. A., Coffin, M. F., Wallace, P. J., and Quality, P. G., editors, *Proc. ODP, Sci. Results*, volume 183, pages 1–28. Texas A&M University, Texas.

Keszthelyi, L., Self, S., and Thordarson, T. (1999). Application of recent studies on the emplacement of basaltic lava flows to the Deccan Traps. In Subbarao, K. V., editor, *Deccan Volcanic Province, Memoir 43*, pages 485–520. Geological Society of India, Bangalore, India.

Keszthelyi, L. and Thordarson, T. (2000). Rubbly pahoehoe: a previously undescribed but widespread lava type transitional between a'a and pahoehoe. In *Meeting of the Geological Society of America Abstracts with programme, 32, 7*.

Klitgord, K. D. and Schouten, H. (1987). Plate kinematics of the Central Atlantic. In Tucholke, B. E. and Vogt, P. R., editors, *The Geology of North America. Volume M, The Western Atlantic Region*, volume M(1), pages 351–378. Geol. Soc. America.

Knight, K. B., Nomade, S., Renne, P. R., Marzoli, A., Bertrand, H., and Youbi, N. (2004). The Central Atlantic magmatic province at the Triassic–Jurassic boundary: paleomagnetic and $^{40}Ar/^{30}Ar$ evidence from Morocco for brief, episodic volcanism. *Earth Planet. Sci. Lett.*, 228(1/2):143–160.

Kontak, D. J. (2008). On the edge of CAMP: geology and volcanology of the Jurassic North Mountain Basalt, Nova Scotia, in: Dostal, J., Greenough, J. D., Kontak, D. J., editors, Rift-related Magmatism. *Lithos*, 101(1/2):74–101.

Labails, C., Olivet, J. L., Aslanian, D., and Roest, W. R. (2010). An alternative early opening scenario for the Central Atlantic Ocean. *Earth Planet. Sci. Lett.*, 297:355–368.

Lorenz, J.-C. (1988). Synthesis of Late Paleozoic and Triassic redbed sedimentation in Morocco. In Jacobshagen, V. H., editor, *The Atlas System of Morocco: Studies on Its Geodynamic Evolution*, volume 15, pages 139–168. Springer-Verlag.

Luchetti, A. C. F., Nardy, A. J. R., Machado, F. B., Madeira, J., and Arnósio, J. M. (2014). New insights on the occurrence of peperites and sedimentary deposits within the silicic volcanic sequences of the Paraná Magmatic Province. *Braz. Solid Earth*, 5:121–130.

Macdonald, G. A. (1953). Pahoehoe, a'a, and block lava. *Am. J. Sci.*, 251:169–191.

Macdonald, G. A. (1967). Forms and structures of extrusive basaltic rocks. In Hess, H. H. and Poldervaart, A., editors, *Basalts: The Poldervaart Treatise on Rocks of Basaltic Composition*, volume 1, pages 1–61. Interscience, New York.

Macdonald, G. A. (1972). *Volcanoes*. Prentice Hall Inc., Englewood Cliffs. 510.

Manville, V., Németh, K., and Kano, K. (2009). Source to sink: a review of three decades of progress in the understanding of volcaniclastic processes, deposits, and hazards. *Sediment. Geol.*, 220:136–161.

Martins, L. T., Madeira, J., Youbi, N., Munhá, J., Mata, J., and Kerrich, R. (2008). Rift-related magmatism of the Central Atlantic Magmatic Province in Algarve, southern Portugal, in: Dostal, J., Greenough, J. D., Kontak, D. J., editors, Rift-related Magmatism. *Lithos*, 101(1/2):102–124.

Marzoli, A., Bertrand, H., Knight, K. B., Cirilli, S., Buratti, N., Vérati, C., Nomade, S., Renne, P. R., Youbi, N., Martini, R., Allenbach, K., Neuwerth, R., Rapaille, C., Zaninetti, L., and Bellieni, G. (2004). Synchrony of the Central Atlantic magmatic province and the Triassic–Jurassic boundary climatic and biotic crisis. *Geology*, 32(11):973–976.

Marzoli, A., Bertrand, H., Youbi, N., Callegaro, S., Merle, R., Reisberg, L., Chiaradia, M., Brownlee, S., Jourdan, F., Zanetti, A., Davies, J., Cuppone, T., Mahmoudi, A., Medina, F., Renne, P. R., Bellieni, G., Crivellari, S., El Hachimi, H., Bensalah, M. K., Meyzen, C. M., and Tegner, C. (2019). The Central Atlantic Magmatic Province (CAMP) in Morocco. *J. Petrol.*, 60(5):945–996.

Marzoli, A., Callegaro, S., Dal Corso, J., Davies, J. H. F. L., Chiaradia, M., Youbi, N., Bertrand, H., Reisberg, L., Merle, R., and Jourdan, F. (2018). The Central Atlantic Magmatic Province (CAMP): a review. In Tanner, L. H., editor, *The Late Triassic World. Topics in Geobiology*, volume 46, pages 91–125. Springer, Heidelberg.

Marzoli, A., Davies, J. H. F. L., Youbi, N., Merle, R., Dal Corso, J., Dunkley, D. J., Fioretti, A. M., Bellieni, G., Medina, F., Wotzlaw, J. F., McHone, G., Font, E., and Bensalah, M. K. (2017). Proterozoic to Mesozoic evolution of North-West Africa and Peri-Gondwana microplates: detrital zircon ages from Morocco and Canada. *Lithos*, 278–281:229–239.

Marzoli, A., Renne, P. E., Piccirillo, E. M., Ernesto, M., Bellieni, G., and De Min, A. (1999). Extensive 200-million-year-old continental flood basalts of Central Atlantic Magmatic Province. *Science*, 284(5414):616–618.

Mattis, A. F. (1977). Non-marine Triassic sedimentation, Central High Atlas Mountains, Morocco. *J. Sedim. Petrol.*, 47:107–119.

McHone, J. G. and Puffer, J. H. (2003). Flood basalt province of the Pangean Atlantic rift: regional extent and environmental significance. In Letourneau, P. M. and Olsen, P. E., editors, *The Great Rift Valleys of Pangea in Eastern North America, Aspects of Triassic–Jurassic Rift Basin Geoscience*, volume 1, pages 141–154. Columbia University Press.

Meddah, A., Bertrand, H., Seddiki, A., and Tabeliouna, M. (2017). The Triassic-Liassic volcanic sequence and rift evolution in the Saharan Atlas basins (Algeria). Eastward vanishing of the Central Atlantic magmatic province. *Geol. Acta*, 15(1):11–23.

Medina, F. (1995). Syn-and postrift evolution of the El Jadida- Agadir basin (Morocco): constraints for the rifting models of the Central Atlantic. *Can. J. Earth Sci.*, 32(9):1273–1291.

Medina, F. (2000). Structural styles of the Moroccan Triassic basins. Epicontinental Triassic International Symposium. *Zentralbl. Geol. Paläontol.*, Teil I(9/10):1167–1192.

Merle, R., Marzoli, A., Bertrand, H., Reisberg, L., Verati, C., Zimmermann, C., Chiaradia, M., Bellieni, G., and Ernesto, M. (2011). $^{40}Ar/^{39}Ar$ ages and Sr–Nd–Pb–Os geochemistry of CAMP tholeiites from the western Maranhão basin (NE Brazil). *Lithos*, 122(3/4):137–151.

Merle, R., Marzoli, A., Reisberg, L., Bertrand, H., Nemchin, A., Chiaradia, M., Callegaro, S., Jourdan, F., Bellieni, G., Kontak, D., Puffer, J., and McHone, J. G. (2014). Sr, Nd, Pb and Os isotope systematics of CAMP Tholeiites from Eastern North America (ENA): evidence of a subduction-enriched mantle source. *J. Petrol.*, 55(1):133–180.

Olsen, P. E., Kent, D. V., Et-Touhami, M., and Puffer, J. (2003). Cyclo-, Magneto-, and Bio-stratigraphic constraints on the duration of the CAMP event and its relationship to the Triassic–Jurassic boundary. In Hames, W. E., McHone, J. G., Renne, P. R., and Ruppel, C. R., editors, *The Central Atlantic Magmatic Province; Insights from Fragments of Pangea, Geophysical Monograph*, volume 136, pages 7–32. American Geophysical Union, Washington.

Panfili, G., Cirilli, S., Dal Corso, J., Bertrand, H., Medina, F., Youbi, N., and Marzoli, A. (2019). New palynological constraints show rapid emplacement of the Central Atlantic magmatic province during the end-Triassic mass extinction interval. *Glob. Planet. Change*, 172:60–68.

Planke, S., Symonds, P. A., Alvestad, E., and Skogseid, J. (2000). Seismic volcanostratigraphy of large-volume basaltic extrusive complexes on rifted margins. *J. Geophys. Res.*, 105(B8):19335–19351.

Ramalho, R., Helffrich, G., Schmidt, D. N., and Vance, D. (2010). Tracers of uplift and subsidence in the Cape Verde Archipelago. *J. Geol. Soc.*, 167(3):519–538.

Ramalho, R. S., Helffrich, G., Madeira, J., Cosca, M., Thomas, C., Quartau, R., Hipólito, A., Rovere, A., Hearty, P. J., and Ávila, S. P. (2017). The emergence and evolution of Santa Maria Island (Azores) - the conundrum of uplifting islands revisited. *GSA Bull.*, 129(3/4):372–391.

Rossetti, L. M., Lima, E. F., Waichel, B. L., Scherer, C. M., and Barreto, C. J. (2014). Stratigraphical framework of basaltic lavas in Torres syncline main valley, southern Parana-Etendeka Volcanic Province. *J. South Am. Earth Sci.*, 56:409–421.

Rowland, S. K. and Walker, G. P. L. (1987). Toothpaste lava: characteristics and origin of a lava structural type transitional between pahoehoe and a'a. *Bull. Volcanol.*, 49(4):631–641.

Ruellan, E. (1985). *Géologie des marges continentales passives: évolution de la marge atlantique du Maroc (Mazagan); étude par submersible seabeam et sismique réflexion. Comparaison avec la marge NW africaine et la marge homologue E américaine.* PhD thesis, Université de Bretagne Occidentale, Brest. 297 p.

Sahabi, M., Aslanian, D., and Olivet, J. L. (2004). Un nouveau point de départ pour l'histoire de l'Atlantique central. *C. R. Geosci.*, 336(12):1041–1052.

Salvan, H. M. (1984). Les formations évaporitiques du Trias marocain. Problèmes stratigraphiques, paléogéographiques et paléoclimatologiques. Quelques réflexions. *Rev. Geogr. Phys. Geol. Dyn.*, 25:187–203.

Self, S., Keszthelyi, L., and Thordarson, T. (1998). The importance of pahoehoe. *Annu. Rev. Earth Planet. Sci.*, 26:81–110.

Self, S., Thordarson, T., and Keszthelyi, L. (1997). Emplacement of continental flood basalt lava flows. In Mahoney, J. J. and Coffin, M. F., editors, *Large Igneous Provinces: Continental, Oceanic, and Planetary Flood Volcanism*, AGU Geophysical Monograph Series 100, pages 381–410.

Self, S., Thordarson, T., Keszthelyi, L., Walker, G. P. L., Hon, K., Murphy, M. T., Long, P., and Finnemore, S. (1996). A new model for the emplacement of Columbia River basalts as large, inflated pahoehoe lava flow fields. *Geophys. Res. Lett.*, 23:2689–2692.

Shaw, H. R. and Swanson, D. A. (1970). Eruption and flow rates of flood basalts. In Gilmour, E. H. and Stradling, D., editors, *Proceedings of the Second Columbia River Basalt Symposium*, pages 271–299. Eastern Washington State College Press, Cheney.

Sheth, H. C. (2006). The emplacement of pahoehoe lavas on Kilauea and in the Deccan Traps. *J. Earth Syst. Sci.*, 115:615–629.

Sheth, H. C., Ray, J. S., Senthil Kumar, P., Duraiswami, R. A., Chatterjee, R. N., and Gurav, T. (2011). Recycling of flowetop breccia crusts into molten interiors of flood basalt lava flows: field and geochemical evidence from the Deccan Traps. In Ray, J., Sen, G., and Ghosh, B., editors, *Topics in Igneous Petrology*, pages 161–180. Springer.

Skilling, I. P., White, J. D. L., and Mcphie, J. (2002). Peperite: a review of magma-sediment mingling. *J. Volcanol. Geotherm. Res.*, 114(1/2):1–17.

Tegner, C., Michelis, S. A. T., McDonald, I., Youbi, N., Callegaro, S., Lindström, S., and Marzoli, A. (2019). Mantle Dynamics of the Central Atlantic Magmatic Province (CAMP): Constraints from platinum group, gold and lithophile elements in flood basalts of Morocco. *J. Petrol.*, 60(8):1621–1652.

Thordarson, T. and Self, S. (1993). The Laki (Skaftár Fires) and Grímsvötn eruptions in 1783–1785. *Bull. Volcanol.*, 55:233–263.

Thordarson, T. and Self, S. (1998). The Roza Member, Columbia River Basalt Group: a gigantic pahoehoe lava flow field formed by endogenous processes? *J. Geophys. Res.*, 103(B11):27411–27445.

Van Houten, F. B. (1977). Triassic-Liassic deposits of Morocco and East North America; a comparison. *Am. A. Petrol. Geol. Bull.*, 61(1):79–99.

Verati, C., Rapaille, C., Féraud, G., Marzoli, A., Bertrand, H., and Youbi, N. (2007). $^{40}Ar/^{39}Ar$ ages and duration of the Central Atlantic Magmatic Province volcanism in Morocco and Portugal and its relation to the Triassic–Jurassic boundary. *Palaeogeogr. Palaeoclimatol. Palaeoecol.*, 244(1/4):308–325.

Waichel, B. L., Lima, E. F., Viana, A. R., Scherer, C. M., Bueno, G. V., and Dutra, G. (2012). Stratigraphy and volcanic facies architecture of the Torres Syncline, Southern Brazil, and its role in understanding the Parana-Etendeka Continental Flood Basalt Province. *J. Volcanol. Geotherm. Res.*, 215–216:74–82.

Waichel, P. L., Lima, E. F., Lubachesky, R., and Sommer, C. A. (2006). Pahoehoe flows from the central Paraná Continental Flood Basalts. *Bull. Volcanol.*, 68:599–610.

Walker, G. P. L. (1971). Compound and simple lava flows and flood basalts. *Bull. Volcanol.*, 35(3):579–590.

Walker, G. P. L. (1987). Pipe vesicles in Hawaiian basaltic lavas: their origin and potential as paleoslope indicators. *Geology*, 15:84–87.

White, J. D. L., Bryan, S. E., Ross, P. S., Self, S., and Thordarson, T. (2009). Physical volcanology of large igneous provinces: update and review. In Thordarson, T., Self, S., Larsen, G., Rowland, S., and Hoskuldsson, A., editors, *Studies in Volcanology: The Legacy of George Walker*, volume 2 of *Special*

Publ. of IAVCEI, pages 291–321. Geol. Soc., London.

White, J. D. L. and Houghton, B. F. (2006). Primary volcaniclastic rocks. *Geology*, 34:677–680.

Whitehead, P. W. and Stephenson, P. J. (1998). Lava rise ridges of the Toomba basalt flow, north Queensland, Australia. *J. Geophys. Res.*, 103(B11):27371–27382.

Wilmoth, R. A. and Walker, G. P. L. (1993). P-type and S-type pahoehoe: a study of vesicle distribution patterns in Hawaiian lava flows. *J. Volcanol. Geotherm. Res.*, 55(1/2):129–142.

Youbi, N., Martins, L. T., Munhá, J. M., Ibouh, H., Madeira, J., Ait Chayeb, H., and El Boukhari, A. (2003). The Late Triassic-Early Jurassic Volcanism of Morocco and Portugal in the framework of the Central Atlantic Magmatic province: an overview. In Hames, W. E., MacHone, J. G., Renne, P. R., and Ruppel, C., editors, *The Central Atlantic Magmatic Province: Insights from Fragments of Pangea*, Geophysical Monograph Series 136, pages 179–207. American Geophysical Union.

Comptes Rendus
Géoscience — Sciences de la Planète
2020, 352, nº 6-7, p. 475-493
https://doi.org/10.5802/crgeos.12

Some aspects of current State of Knowledge on Triassic series on both sides of the Central Atlantic Margin / *Quelques aspects de l'état des connaissances des séries triasiques de part et d'autre de la Marge Atlantique*

State of the art of Triassic palynostratigraphical knowledge of the Cantabrian Mountains (N Spain)

Manuel A. Juncal *, [a], **José B. Diez** [a], **Raúl De la Horra** [b], **José F. Barrenechea** [c, d], **Violeta Borruel-Abadía** [b, c] and **José López-Gómez** [c]

[a] Departamento de Xeociencias M. e O.T., Facultade de Ciencias do Mar, Universidade de Vigo, Campus As Lagoas - Marcosende, E-36310, Vigo, Spain

[b] Departamento de Geodinámica, Estratigrafía y Paleontología, Facultad de Geología, Universidad Complutense de Madrid, C/ José Antonio Nováis 12, E-28040, Madrid, Spain

[c] Instituto de Geociencias (UCM, CSIC), C/ Doctor Severo Ochoa 7, E-28040, Madrid, Spain

[d] Departamento de Mineralogía y Petrología, Facultad de Geología, Universidad Complutense de Madrid, C/ José Antonio Nováis 12, E-28040, Madrid, Spain

E-mails: majuncales@uvigo.es (M. A. Juncal), jbdiez@uvigo.es (J. B. Diez), rhorraba@ucm.es (R. De la Horra), barrene@ucm.es (J. F. Barrenechea), violeta.borruel@igeo.ucm-csic.es (V. Borruel-Abadía), jlopez@ucm.es (J. López-Gómez)

Abstract. The present-day Cantabrian Mountains (North Spain) represent the western continuation of the Pyrenean-Cantabrian Orogen, which arose from a Cenozoic collision between the Iberian and Eurasian plates. The early Alpine sedimentary record of the Cantabrian basin is represented by the latest Carboniferous-Permian and Triassic rocks, mostly of continental origin. A lack of palaeontological data has led, until recently, to erroneous interpretations of the stratigraphic position of this sedimentary record. Within the framework of the Triassic sedimentary record in northern Spain, the precise age of six samples was determined and they were grouped into four palynological assemblages according to their taxonomic composition. The study of these assemblages includes a review of all the Triassic assemblages published to date as regards the Cantabrian Mountains, thereby optimising our Triassic palynostratigraphical knowledge of this area enabling comparisons with other Triassic assemblages of Central and SW Europe.

Keywords. Palynology, Ladinian, Carnian, Norian, Rhaetian.

* Corresponding author.

1. Introduction

Today's Cantabrian Mountains (North Spain) run parallel to the Bay of Biscay and it is considered the western range of the Pyrenean-Cantabrian Orogen that arose when the Iberian and Eurasian plates collided during the Cenozoic [Barnolas and Pujalte, 2004, Gallastegui et al., 2002, Martín-González and Heredia, 011a,b, Pulgar et al., 1999]. The early Alpine sedimentary record of the Cantabrian basin mostly consists of Carboniferous, Permian and Triassic rocks. These rocks have been traditionally analysed in separate zones broadly related to the three main geographical provinces of this area: Asturias, Cantabria and Palencia (Figure 1).

Until recently, the Permian and Triassic sedimentary record of the Cantabrian Mountains was mainly based on works from the second half of the last century (e.g., De Jong 1971, García-Mondejar et al. 1986, Martínez-García 1981, Suárez-Rodríguez 1988). Recent syntheses have tried to describe the complex stratigraphic nomenclature that existed in this region [López-Gómez et al., 2002, Martínez-García, 1990, 991a,b, Robles, 2004, Robles and Pujalte, 2004], but the lack of precise palaeontological data and the complex tectonics in the Cantabrian Mountains ruled out any definition of a detailed stratigraphic succession. As a result, numerous lithostratigraphic nomenclatures have been used for the same units, and these units have even been wrongly laterally correlated because they were only valid locally (e.g., Suárez-Rodríguez [1988], for the Asturias province; Gand et al. [1997], Martínez-García [991a,b]; for the Cantabria and Palencia provinces). In spite of these confusing correlations, studies based on tectonosedimentary analysis made it possible to define the main fault lineaments and their post-Variscan activity [Alonso et al., 1996, Cadenas et al., 2018, Cámara, 2017, García-Espina, 1997, Julivert, 1971, Martín-González and Heredia, 011a,b, Merino-Tomé et al., 2009, Pulgar et al., 1999, Rodríguez-Fernández et al., 2002].

A recent multidisciplinary study by López-Gómez et al. [2019] has provided a new stratigraphic chart for the Permian and Triassic record of the Cantabrian Mountains, using new age attributions assigned to new lithostratigraphic units based on palaeontological data. The newly defined stratigraphic succession of these units was established for the different geographical provinces of the Cantabrian Mountains, and clearly shows lateral continuity between them. The 30 Mry long period since the early-middle Permian transition until the Middle Triassic is particularly striking because it lacks any sedimentary record. There are also other notable internal disruptions and unconformities between the lithostratigraphic units. Based on these characteristics, López-Gómez et al. [2019] have described six lithostratigraphic units (formations) from the latest Carboniferous to the Late Triassic (Figures 2, 3): the San Tirso, Acebal, Sotres, Cicera, Rueda and Transición formations. Figure 3 shows the location of samples collected along the four stratigraphic sections studied in this work.

Palynological data for the Triassic of the Cantabrian Mountains are scarce. Most of the palynological samples described prior to this work were located without stratigraphic precision and assigned to broad attributions, including general terms for facies such as "Buntsandstein" or "Keuper".

In the Triassic record, only three palynological samples have been described in previous works in the "Buntsandstein facies" (later named Cicera Formation (Fm), Figure 2). These samples were obtained near Verbios village (Palencia Province, sample 1349) and Tres Mares peak (Cantabrian Province, samples 1379 and 1410) [Sánchez-Moya et al., 2005, Sopeña et al., 2009] (Figure 4). The samples indicated a Ladinian age (Middle Triassic) and Carnian age (Late Triassic), respectively. In the "Keuper facies", Salvany [990a,b] identified a Norian assemblage near Aguilar de Campoo (Palencia province). In similar facies, two palynological samples were described near Reinosa (Cantabria province, Figure 4) and attributed an early-middle Norian age by Calvet et al. [1993]. Finally, in the same facies, two samples recovered in laminated gypsum near Poza de la Sal (southern Cantabria Province) were assigned to the late Carnian-early Norian by Barrón et al. [2001]. In the Transición Unit, defined by Suárez-Vega [1974] for the lithofacies of the transition between the Upper Triassic and Lower Jurassic, Martínez-García et al. [1998] established a late Rhaetian age near Huerces (Asturian Province). Later, in the same unit, Barrón et al. [2002, 2005, 2006] assigned different analysed samples to a Rhaetian age (Figure 4). Unfortunately, the biostratigraphic value of these assemblages is relative as they were not figured (or are only partially figured), thus preventing the verification of these taxo-

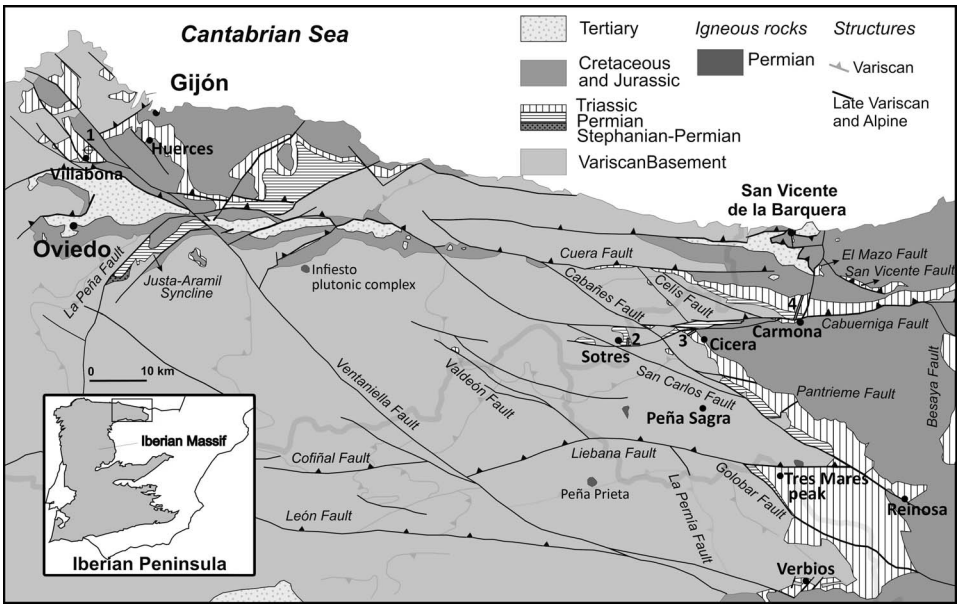

Figure 1. Simplified geological map of the central Cantabrian Mountains with the location of the studied sections and localities. Studied sections: 1 - Villabona, 2 - Sotres, 3 - Cicera, 4 - Carmona. See the sections in Figure 3. (Modified from López-Gómez et al. [2019]).

nomic classifications.

The focus of this work is the state of the art in Triassic palynological studies of the Cantabrian Mountains, along with descriptions of the four complete figured assemblages, briefly referred to previously in López-Gómez et al. [2019], using the new lithostratigraphic succession defined by these authors. These assemblages are also compared to similar ones described in different units in central and southern Europe.

2. Geological setting

The study area is located in the central part of the Cantabrian Mountains, N Spain, which includes the provinces of Cantabria, Asturias and Palencia (Figure 1). The area, located between the Astur-Galician and Basque-Cantabrian regions, flanks the middle of the Pyrenean-Cantabrian Orogen to the west and east, respectively [Martín-González and Heredia, 011a] (Figure 1). The two regions show a different evolution during the Mesozoic and Cenozoic. The western region, which presents a highly deformed Variscan basement, is almost devoid of Mesozoic sediments, and the Cenozoic synorogenic record is restricted to isolated depressions [Martín-González and Heredia, 011b]. In contrast, the eastern Basque-Cantabrian region is characterised by a thick and complete Middle Triassic to Cretaceous sedimentary record related to extensional basins [Espina, 1997, Pulgar et al., 1999].

The Uppermost Carboniferous-Lower Permian and Triassic rocks lie unconformably on the Palaeozoic basement. This basement, which represents a folded and thin-skinned belt, belongs to the foreland of the Variscan Orogen [Julivert, 1971, Rodríguez-Fernández and Heredia, 1987]. In the northern Palencia province, the latest Carboniferous sedimentary record was affected by the last emplacements of the end of the main Variscan deformation (e.g., Picos de Europa region), including foreland deposits towards the south [Merino-Tomé et al., 2009, Rodríguez-Fernández and Heredia, 1987, Rodríguez-Fernández et al., 2002]. During the early Permian, small-isolated basins developed due to collapse of the Variscan belt [Pérez-Estaún et al., 1991]. These basins were controlled by lineaments related to Variscan faults that remained active until the end of the early Permian [Rodríguez-Fernández et al., 2002], when this area was located near the equator [Ziegler, 1993].

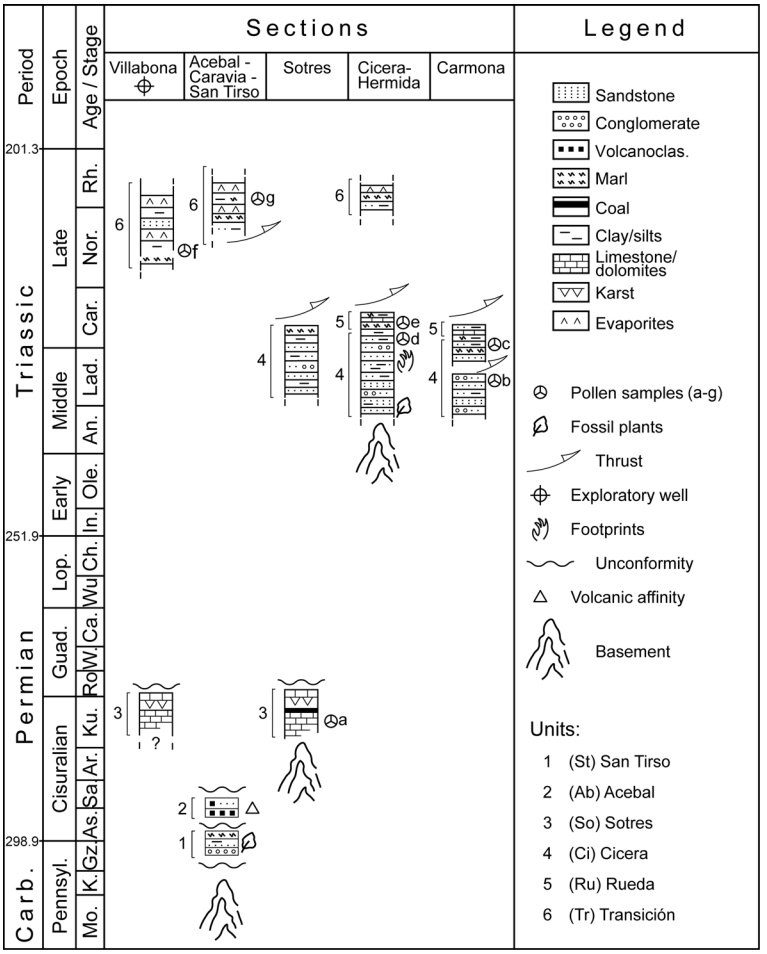

Figure 2. Stratigraphic location of the differentiated Permian and Triassic lithostratigraphic units (1 to 6) based on new palaeontological data in the Cantabrian Mountains. Palynological samples: (a) So1, (b) Ca1, (c) SP5, (d) Cic11, (e) Cic12, (f) VBO17, (g) Cueli (modified from López-Gómez et al. [2019]).

Substantial plate reorganisation started during the beginning of the Mesozoic with an extensional event related to the break-up of Pangea and opening of the Bay of Biscay [Ziegler, 1993, Ziegler and Stampfli, 2001]. This extensional phase expanded until the Late Triassic-Early Jurassic but was reactivated in the Late Jurassic-Early Cretaceous [Cadenas et al., 2018, Espina, 1997, Tugend et al., 2014]. The present-day relief of the Cantabrian Mountains is the consequence of an Eocene-early Oligocene crustal uplift episode [Fillon et al., 2016, Martín-González et al., 2012, 2014] that continued locally until the latest Miocene [Martín-González and Heredia, 011b].

2.1. *Triassic lithological units*

This work is based on the Triassic stratigraphical scheme recently proposed in the Cantabrian Mountains by López-Gómez et al. [2019]. In order to locate accurately the palynological assemblages studied here, a summary of the three Triassic formations defined in that scheme is outlined below (Figures 2, 3):

Cicera Fm. This unit near Cicera village was first described in López-Gómez et al. [2019] (Figure 1). It is mostly comprised of fine-medium grained red sandstones alternating in the middle-upper half with red dark lutites. The Cicera Fm rests unconformably

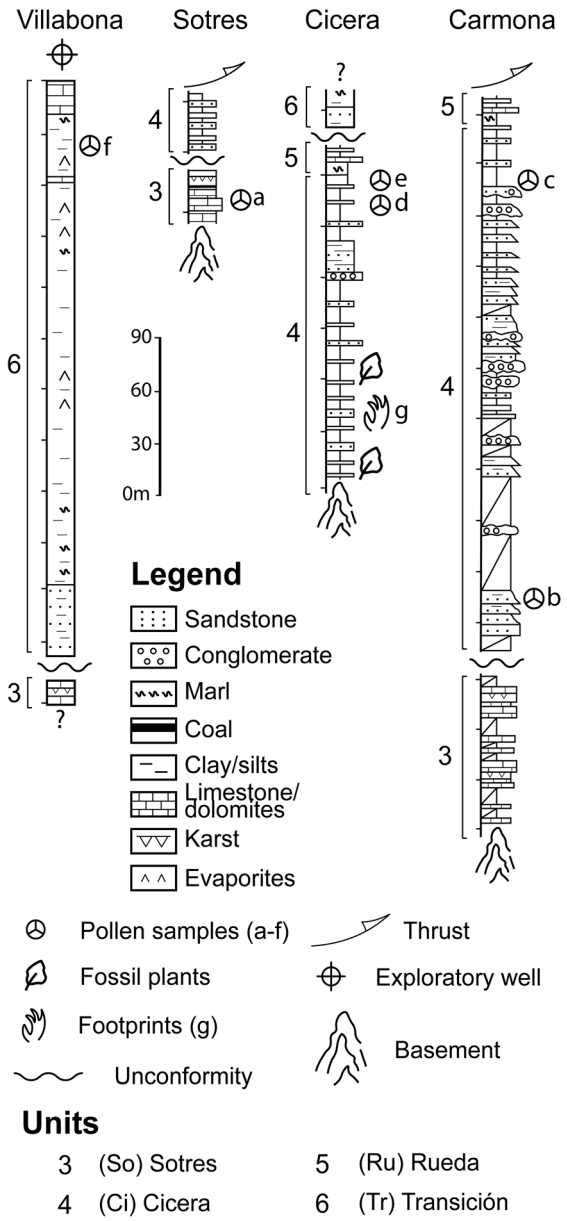

Figure 3. Field sections and borehole Villabona where the samples were obtained. For a more detailed lithological and sedimentological description see López-Gómez et al. [2019]. Samples: a. SO-1 [Juncal et al., 2016], b. Carmona 1, c. S. Pedro-5, d. Cic11, e. Cic12, f. VBO-17, g. Cic-x. Location of the samples (in m from the base of the sections): a - 23 m, b - 35 m, c - 411 m, d - 92.5 m, e - 93 m, f - 394 m, g - 18 m. Sample Cu-1, described in the text, was obtained from De la Horra et al. [2012] at Cueli village, near Villabona borehole, and in similar stratigraphical position to VBO-17 sample. Geographical location of the sections: Villabona: 43° 27′ 50″, 5° 50′ 18″; Sotres: 43° 14′ 09″, 4° 44′ 18″; Cicera: 43° 14′ 10″, 4° 34′ 12″; Carmona: 43° 16′ 50″, 4° 20′ 18″.

on various previous units, or directly on the basement. It represents the classic Triassic "Buntsandstein facies", as described by García-Mondejar et al. [1986] and Robles and Pujalte [2004] for La Cohilla

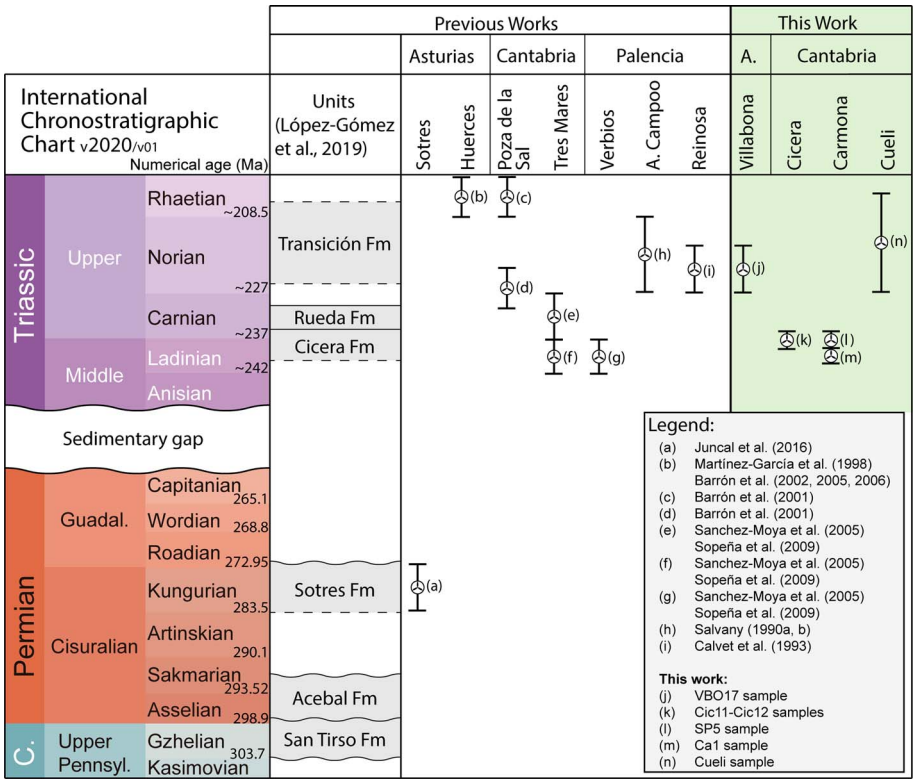

Figure 4. Age attributions of lithostratigraphic units based on palynological assemblages in the Cantabrian Mountains. Comparison with previous works.

section, north of the Peña Sagra peak, in southern Cantabria (Figure 1). It is interpreted as the development of mixed sandy and gravelly braided fluvial systems in the lower part of the unit, evolving into increased floodplain deposits in the middle part. This unit, however, has been erroneously described as the Caravia Fm in different areas, and considered Lower or upper Permian, depending on the study (e.g., Martínez-García 991a,b, Martínez-García et al. 2001, Wagner and Martínez-García 1982). Prior to the work of López-Gómez et al. [2019], this misinterpretation generated erroneous stratigraphic correlations.

Rueda Fm. This unit was first described in López-Gómez et al. [2019]. It lies conformably on the Cicera Fm and consists of yellowish-grey dolomites and green marls to form a total thickness of 3.5 m. The unit was interpreted by these authors as shallow-carbonate, marine inter-supratidal deposits.

Transición Fm. This unit was first described by Suárez-Vega [1974] and later also studied by Suárez-Rodríguez [1988] and Manjón et al. [1992] and related to the Upper Triassic–Lower Jurassic sedimentary record. It consists of red-green marls with intercalated red sandstones, and shows gypsum beds and limestones at the top. The unit was interpreted by these authors as deposited under shallow marine and supratidal conditions.

3. Material and method

The studied palynological samples are stratigraphically located in in three different sections (Sotres, Cicera and Carmona) and one borehole (near Villabona village) described in López-Gómez et al. [2019]. Detailed sedimentary data are shown in this latter work, but a sketch of these units is shown in Figures 2 and 3.

Table 1. List of species recorded from study area

Assemblages / Taxa List	Carmona	San Pedro	Cicera	Villabona
Alisporites grauvogeli Klaus 1964	■	■	■	
Alisporites opii Daugherty 1941			■	
Aratrisporites granulatus Klaus 1960	■		■	
Calamospora tener (Leschik) Mädler 1964		■		
Camerosporites secatus Leschik 1956	■	■	■	■
Chordasporites singulichorda Klaus 1960	■		■	
Classopollis torosus (Reissinger) Balme 1957				■
Classopollis zwolinskae (Lund) Traverse 2004				■
Duplicisporites granulatus (Leschik) Scheuring 1970	■	■	■	■
Enzonalasporites vigens Leschik 1955		■	■	
Illinites chitonoides Klaus 1964				
Lunatisporites noviaulensis (Leschik) de Jersey 1979		■		
Microcachryidites doubingeri Klaus 1964		■		
Microcachryidites fastidioides (Jansonius) Klaus 1964				
Ovalipollis cultus Scheuring 1970			■	
Ovalipollis ovalis (Krutzsch) Scheuring 1970		■		
Ovalipollis pseudoalatus (Thiergart) Schuurman 1976		■	■	■
Paracirculina quadruplicis Scheuring 1970				■
Patinasporites densus Leschik 1955				■
Ptasiodictyon mosellanum Wille 1970			■	
Praecirculina granifer (Leschik) Klaus 1960		■		
Quadraculina anellaeformis Malyavkina 1949				■
Rhaetipollis germanicus Schulz 1967				■
Triadispora crassa Klaus 1964		■	■	
Triadispora epigona Klaus 1964			■	
Triadispora falcata Klaus 1964		■	■	
Triadispora plicata Klaus 1964		■	■	
Triadispora staplinii (Jansonius) Klaus 1964		■	■	
Triadispora suspecta Klaus 1964	■			
Triadispora verrucata (Schulz) Scheuring 1970		■		
Vallasporites ignacii Leschik 1956			■	
Vitreisporites pallidus (Reissinger) Nilsson 1958		■		
Alisporites sp.		■		■
Calamospora sp.		■		
Chasmatosporites sp.	■			
Chordasporites sp.			■	
Cycadopites sp.				
Platysaccus sp.	■			
Trachysporites sp.				
Verrucosisporites sp.		■	■	

Samples Ca1 and SSP5 were collected at 35 m and 411 m respectively from the base of the Carmona Section (Figures 2 and 3). Cic11 and Cic12 were obtained at 92.5 m and 93 m in the upper part of Cicera section near Cicera village (Figures 2, 3). Sample VBO17 was obtained at 394 m from the Villabona borehole exploratory well (cuN-69B) in the Transición Fm via the MINERSA mining company (Villabona village, Asturias, Spain) and Sample Cu-1, described in the text, was obtained from De la Horra et al. [2012] at Cueli village, near the Villabona borehole, in a similar stratigraphic position to VBO17 sample.

Palynological samples were processed in the Palynology Laboratories of the Department of Geodinámica, Estratigrafía y Paleontología (Complutense University of Madrid) and the Geosciences Department (University of Vigo). In the former, laboratory-standard palynological procedures were used. To remove carbonate and silicate minerals, hydrochloric acid (HCl, 10%) and hydrofluoric acid (HF 40%) were first added and the samples then were stirred with 10% hydrochloric acid for 45 min to remove secondary compounds produced during the hydrofluoric acid attack. At the University of Vigo, a dispersing agent was added to facilitate filtering and sieving at 10 μm. The prepared slides were examined at this University's facilities using a Leica DM 2000 LED microscope and a Leica ICC50 W camera to take photos at ×1000 magnification.

4. Results

Six new palynological samples were obtained from the Triassic record of the Cantabrian Mountains (Figure 3), four in the Cicera Fm (Samples Ca1, SP5, Cic11 and Cic12) and two in the Transición Fm (samples VBO17 and Cu-1) (Figure 4). The Cueli Beach sample (Cu-1 sample), which belongs to the Transición Fm, is attributed to the Norian-middle Rhaetian interval due to the presence of *Classopollis* spp. and *Ovalipollis pseudoalatus* (Thiergart) Schuurman 1976. This latter sample is poorly preserved with no robust palynological assemblage, but we consider it is worthwhile to indicate its existence. The other five positive samples have been grouped into four assemblages due to their similar composition (Table 1, Figure 5). The palynological assemblages are figured separately in the supplementary data (Supplementary Figures S1, S2, S3 and S4).

5. Discussion

The scarcity of the Triassic palaeontological data in the Cantabrian Mountains and the misguided lithostratigraphy used in some previous works are among the main reasons for the revision offered in our study.

The present work shows the complete data partially presented in López-Gómez et al. [2019], which are essential to infer the age of the lithological units

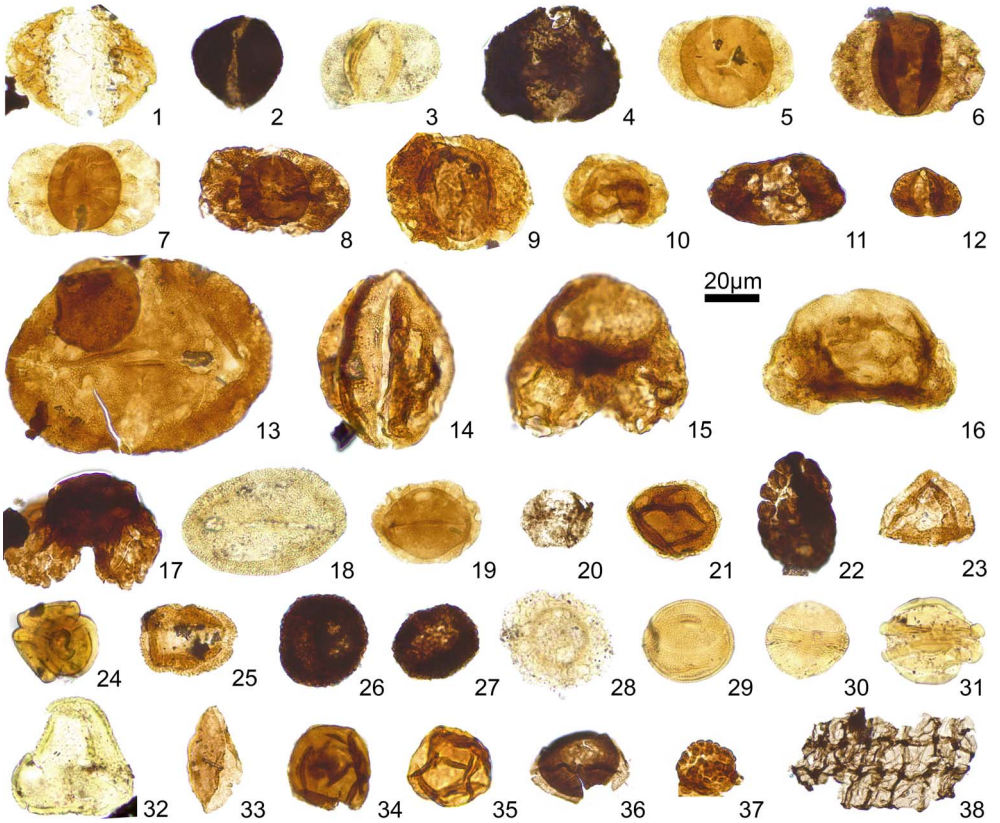

Figure 5. Representative palynomorphs of the different associations. Palynological assemblages are figured completely in supplementary data. (1) *Alisporites grauvogeli* Klaus 1964. (2) *Alisporites opii* Daugherty 1941. (3) *Alisporites* sp. (4) *Triadispora epigona* Klaus 1964. (5) *Triadispora plicata* Klaus 1964. (6) *Triadispora staplinii* (Jansonius) Klaus 1964. (7) *Triadispora crassa* Klaus 1964. (8) *Triadispora suspecta* Klaus 1964. (9) *Triadispora verrucata* (Schulz) Scheuring 1970. (10) *Lunatisporites noviaulensis* (Leschik) de Jersey 1979. (11) *Chordasporites singulichorda* Klaus 1960. (12) *Vitreisporites pallidus* (Reissinger) Nilsson 1958. (13) *Illinites chitonoides* Klaus 1964. (14) *Chasmatosporites* sp. (15) *Microcachryidites doubingeri* Klaus 1964. (16) *Microcachryidites fastidioides* (Jansonius) Klaus 1964. (17) *Platysaccus* sp. (18) *Ovalipollis pseudoalatus* (Thiergart) Schuurman 1976. (19) *Ovalipollis ovalis* (Krutzsch) Scheuring 1970. (20) *Ovalipollis cultus* Scheuring 1970. (21) *Praecirculina granifer* (Leschik) Klaus 1960. (22) *Camerosporites secatus* Leschik 1956. (23) *Duplicisporites granulatus* (Leschik) Scheuring 1970. (24) *Paracirculina quadruplicis* Scheuring 1970. (25) *Quadraeculina anellaeformis* Malyavkina 1949. (26) *Vallasporites ignacii* Leschik 1956. (27) *Enzonalasporites vigens* Leschik 1955. (28) *Patinasporites densus* Leschik 1955. (29) *Classopollis torosus* (Reissinger) Balme 1957. (30) *Classopollis zwolinskae* (Lund) Traverse 2004. (31) *Rhaetipollis germanicus* Schulz 1967. (32) *Trachysporites* sp. (33) *Cycadopites* sp. (34) *Calamospora tener* (Leschik) Mädler 1964. (35) *Calamospora* sp. 36. *Aratrisporites granulatus* Klaus 1960. (37) *Verrucosisporites* sp. (38) *Plaesiodictyon mosellanum* Wille 1970.

in this area. A complete list of figured elements is provided to correlate our new data with previous palynological records in nearby areas.

5.1. *Late Ladinian-early Carnian assemblages*

The palynological data of the Triassic rocks starts with the study of the Cicera Fm characterised by the presence of voltzian conifer types (including

the genera *Triadispora* and *Ovalipollis*) and the Circumpolles group (*Duplicisporites*, *Camerosporites*, *Paracirculina*). Cicera Fm could be separated into lower part with a Longobardian age (Carmona assemblage), and an upper part with a Longobardian-Cordevolian transition in age (San Pedro and Cicera assemblages).

The Carmona assemblage (Figure S1, Supplementary data) from the lower part of the Cicera Fm is Longobardian in age (late Ladinian), due to the presence of *Camerosporites secatus*, *Chordasporites singulichorda*, *Duplicisporites granulatus*, *Illinites chitonoides*, *Lunatisporites noviaulensis*, *Microcachryidites doubingeri*, *Ovalipollis pseudoalatus*, *Triadispora falcata, Triadispora staplinii*, and *Triadispora suspecta*. This composition is equivalent to the "second assemblage" in Adloff et al. [1987], the SC-1 assemblage from Sancerre-Couy core, Paris Basin [Juncal et al., 2018] and the palynological associations described from the Mâconnais Region in France [Adloff and Doubinger, 1979], in Jura, France [Adloff et al., 1984], the Largentière area, Ardèche, France [Doubinger and Adloff, 1977], the Monte San Giorgio, Southern Alps, Switzerland [Scheuring, 1978]. These assemblages correspond to the *Camerosporites secatus–Enzonalasporites vigens* phase [Van Der Eem, 1983], the *Heliosaccus dimorphus* Zone of Orłowska-Zwolińska [1983, 1985, 1988] emended by Herngreen [2005], the *Heliosaccus dimorphus* Zone [Kürschner and Herngreen, 2010] (Figure S5, Supplementary data). The bisaccate pollen grain *Lunatisporites noviaulensis* started to occur first in the Guadalupian (middle Permian) of WestEurope (e.g., Bercovici et al. 2009) and in the late Permian (Lopingian) in the southern Alps of Italy (Bulla section, western Dolomites, Italy; Spina et al. [2015]). The presence of this taxa in assemblage with other taxa such as *Illinites chitonoides*, *Microcachryidites doubingeri* and *Microcachryidites fastidioides* is characteristic of the Early-Middle Triassic and rarely appear in early Carnian assemblages (e.g., Doubinger and Adloff 1983, Doubinger and Bühmann 1981, Eshet 1990, Foster 1979, Galasso et al. 019a,b, Kürschner and Herngreen 2010, Orłowska-Zwolińska 1984, 1985). These taxa co-occur with the circumpolles species *Camerosporites secatus, Duplicisporites granulatus* and *Praecirculina granifer* which show significant diversification on the Ladinian – Carnian boundary (e.g., Brugman et al. 1994, Cirilli 2010, Kürschner and Herngreen 2010, Mietto et al. 2012, Roghi 2004, Roghi et al. 2010, Van Der Eem 1983, Visscher and Brugman 1981, Visscher and Krystyn 1978).

The San Pedro and Cicera assemblages (Figures S2 and S3, Supplementary data) are attributed to the Longobardian-Cordevolian transition (late Ladinian-early Carnian) due to the presence of Middle Triassic sporomorphs such as *Chordasporites singulichorda*, *Lunatisporites noviaulensis*, *Triadispora crassa*, *Triadispora epigona*, *Triadispora falcata*, *Triadispora plicata*, *Triadispora staplinii* and the late Ladinian-Carnian taxa such as *Camerosporites secatus*, *Duplicisporites granulatus*, *Ovalipollis pseudoalatus,* as well as the occurrence of the typical Carnian taxa *Triadispora verrucata* and *Vallasporites ignacii*. The taxonomic composition of the San Pedro and Cicera assemblages is equivalent to that of the SC-2 assemblage, described by Juncal et al. [2018], of the Sancerre-Couy core (Paris Basin), obtained from levels associated with anhydrite sabkha deposits with black silty clays. These levels correspond to the Ladinian-lower Carnian cycle, which is the lateral equivalent of the Lettenkhole Fm in the eastern part of the Paris Basin [Bourquin et al., 2002]. The occurrence of typical Carnian taxa such as *Vallasporites ignacii* in association with late Ladinian-Carnian sporomorphs is also reported in the lower part of the Koudiat El Halfa borehole in Central Tunisia [Mehdi et al., 2009] and in the early Carnian microflora from the Djerba Melita 1 Borehole in southeasstern Tunisia [Buratti et al., 2012].

The San Pedro and Cicera assemblages correspond to the *Triadispora verrucata* subzone of the *Camerosporites secatus* Zone Herngreen [2005], which is defined by the first appearance datum (FAD) of *Triadispora verrucata* and correlates with the *Conbaculatisporites longdonensis*, later *Porcellispora longdonensis*, Zone of Orłowska-Zwolińska [1983, 1985, 1988] and zones GTr 12–13 of Heunisch [1999] (Figure S5, Supplementary data). The *Camerosporites secatus* Zone Herngreen [2005] is defined by the FAD of *Camerosporites secatus*, which coincides with the early Carnian *Enzonalasporites vigens–Patinasporites densus* phase of Van Der Eem [1983] (Figure S5, Supplementary data), and it is associated with the first appearance of *Patinasporites densus, Triadispora verrucata*, and *Vallasporites ignacii* [Blendinger, 1988, Buratti and Cirilli, 2007, Cirilli, 2010, Fisher and

Dunay, 1984, Hochuli and Frank, 2000, Hochuli et al., 1989, Kürschner and Herngreen, 2010, Roghi, 2004, Roghi et al., 2010, Van Der Eem, 1983, Visscher and Brugman, 1981].

The composition of the Carmona assemblage, occurring in the lower levels of the Cicera Fm, almost exclusively comprises conifer pollen (e.g., *Chordasporites, Lunatisporites, Microcachryidites*), including numerous *Triadispora* specimens. In contrast, in the San Pedro and Cicera assemblages, the presence of water-transported spores, such as those of lycophytes (*Aratrisporites*), horsetails (*Calamospora*) and ferns (as *Verrucosisporites* and *Vitreisporites*), can be seen. Moreover, the appearance of the fresh-brackish water alga *Plaesiodictyon mosellanum* suggests proximity to a fluvio-deltaic source or coastal system as it tolerates hypersaline environments [Brugman et al., 1994, Hochuli et al., 1989, Kustatscher et al., 2012, Lindström et al., 017a, Paterson et al., 2017, Vigran et al., 2014]. This hypothesis is coherent with the sedimentological interpretations of the Cicera Fm, since the uppermost part of this unit shows a transition with the underlying Rueda Fm, interpreted as intersupratidal, shallow-marine mixed sediment [López-Gómez et al., 2019]. Furthermore, in the Cicera section, two footprint samples were obtained 74.5 m below Cic11 sample [López-Gómez et al., 2019] (Figure 3). In the latter work, the authors suggest that these footprints could correspond to *Lagerpetidae*, and they have been linked to biped animals, in accordance with their functional tridactyl II–IV pes, which is similar to numerous tridactyl footprints of dinosauroïd forms found in Anisian–Ladinian beds in SE France [Gand and Demathieu, 2005].

The Ladinian-early Carnian assemblage of the Cicera Fm is equivalent to the upper part of the "Buntsandstein facies" described by Sánchez-Moya et al. [2005] and Sopeña et al. [2009], who collected three palynological samples near the Verbios village (Palencia Province, sample 1349) and the Tres Mares peak (Cantabrian Province, samples 1379 and 1410). These authors attributed Samples 1349 and 1410 to the Ladinian (Middle Triassic), based on the presence of the genera *Duplicisporites* and *Triadispora*, the taxa *Ovalipollis pseudoalatus* and "the absence of *Echinitosporites iliacoides, Heliosaccus dimorphicus, Partitisporites quadruplices*", and the predominance of bisaccate pollen. Moreover, the presence of *Eucommiidites microgranulatus* is reported in sample 1410. According to Schulz and Heunisch [2005], the presence of this species indicates a Ladinian-early Carnian age [Sopeña et al., 2009]. These two samples were compared with the Ladinian assemblages from the Pyrenees [Fréchengues et al., 1993], the Catalan Coastal Range [Solé de Porta et al., 1987] and the Iberian Ranges [Doubinger et al., 1990, Sopeña et al., 1995]. The last sample obtained in the Tres Mares peak (Cantabrian Province, Sample 1379) was assigned to the Carnian (Late Triassic) due to the presence of *Vallasporites ignacii* and *Enzonalasporites* sp., and "the absence of *Kuglerina meieri, Craterisporites rotundos, Partitisporites* sp. and *Spiritisporites spirabilis*" [Sánchez-Moya et al., 2005]. Sopeña et al. [2009] removed *Vallasporites ignacii* and *Enzonalasporites* sp. from the list and attributed it to the late Ladinian-Carnian due to increased circumpolles and similarity with the upper Ladinian of the Castilian Branch of the Iberian Ranges [Sopeña et al., 1995] and the Carnian of the Miravet Fm, Prades area of the Catalan Coastal Range [Solé de Porta et al., 1987].

5.2. *Norian assemblages*

Between the early Carnian and Norian, an overall decline of 50% in palynofloral diversity has been described in NW Europe [Kürschner and Herngreen, 2010]. Thus, Norian flora in Europe generally show low taxonomic diversity and are dominated by conifers (accounting for 80–90% of the assemblages: Dalla-Vecchia [2000], Dalla-Vecchia and Selden [2013], Dobruskina [1993, 1994], Kustatscher et al. [2018], Pacyna [2014]). During the Norian, a significant change is recorded for the "Late Triassic palynofloras" that corresponds to the first appearance of *Classopollis* pollen [Visscher and Brugman, 1981], and this is broadly related to the diversity decline among terrestrial vertebrates and marine invertebrates [Tanner et al., 2004, Weems, 1992]. This gymnosperm pollen is produced by plants belonging to the extinct conifer family Cheirolepidiaceae [Francis, 1983, Jarzen and Nichols, 1996], which are similar to the extant family Cupressaceae and resemble modern juniper bushes [Riding et al., 2013], and it is dominant in assemblages obtained in the Transición Fm (Villabona assemblage).

The presence of the late Ladinian-Carnian genera *Duplicisporites, Enzonalasporites* and

Camerosporites is common in lower Norian successions [Cirilli, 2010], but has not been recorded in younger sediments [Kürschner and Herngreen, 2010]. The Norian successions were attributed by Herngreen [2005] to the *Granuloperculatipollis rudis* Zone (Figure S5, Supplementary data), based on the FAD of its marker species and the abundance of *Classopollis meyeriana* and *Classopollis zwolinskae*. This zone corresponds to zones 16–17 of Heunisch [1999], the middle-upper part of the *Corollina meyeriana* Zone of Orłowska-Zwolińska [1984] (Figure S5, Supplementary data). Moreover, although *Rhaetipollis germanicus* was considered a Rhaetian age taxon (e.g., Schulz and Heunisch 2005, Visscher and Brugman 1981), the FAD of *Rhaetipollis germanicus* is uncertain. Fisher [1979] described the appearance of this taxon in Norian palynological assemblages (Palynological Zone VIII, Canadian Artic Archipelago) and Smith [1982] suggested reconsidering the palynological dating involving this taxon after studying the early Norian ammonoid-dated strata in Svalbard. Kürschner and Herngreen [2010] also suggest that a late Norian appearance of this taxon cannot be excluded in central and northwestern Europe, due to the absence of continental deposits during this time that could be readily correlated with marine successions. Therefore, Norian and lower Rhaetian palynological assemblages are generally rather homogeneous [Kustatscher et al., 2018].

For all the aforementioned reasons, and due to the presence *Camerosporites secatus*, *Classopollis zwolinskae*, *Classopollis torosus*, *Duplicisporites granulatus*, and *Rhaetipollis Germanicus*, the Villabona assemblage (Figure S4, Supplementary data) of the Transición Fm is Lacian-Aulanian in age (early-middle Norian).

In "Keuper facies" such as those present in the Transición Fm, Salvany [990a,b] identified a scarce Norian assemblage in Aguilar de Campoo (Palencia province). This sample contains *Triadispora* sp., *Ovalipollis ovalis*, *Praecirculina granifer*, *Duplicisporites granulatus*, *Patinasporites densus*, *Camerosporites secatus*, *Classopollis* sp., *Granuloperculatispollis rudis* and unidentified bisaccates. These authors suggest a lower-middle Norian age, based on the abundance of *Classopollis* and the presence of *Granuloperculatispollis rudis*. The presence of *Triadispora* sp., *Classopollis* sp., *Duplicisporites granulatus* and *Camerosporites secatus* is coherent with this assignation. In similar facies, two palynological samples were described in the Reinosa area (Cantabria province) and attributed an early-middle Norian age by Calvet et al. [1993]. These samples include *Alisporites* sp., *Ovalipollis ovalis*, *Praecirculina granifer*, *Duplicisporites granulatus*, *Classopollis* sp. and *Granuloperculatispollis rudis*.

Furthermore, Barrón et al. [2001] described two assemblages in laminated gypsum deposits near Poza de la Sal (Cantabria Province). These samples would correspond to the Transición Fm. These authors suggested a late Carnian-early Norian age for one of the assemblages because of the presence of *Triadispora* spp. and *Camerosporites secatus* and the "absence of genus *Corollina*" (= *Classopollis*). They considered that the gypsum of Poza de la Sal was older than similar lithologies with Norian age proposed by Hernando et al. [1977] in Albendiego (Guadalajara, Spain) and Salvany [990a,b] for the grey gypsum of Aguilar de Campoo (Palencia, Spain) included in "Keuper facies". The second assemblage was attributed to the Rhaetian, based on the relative abundance of the genus *Corollina* (= *Classopollis*) and because "the first register (genus *Corollina*) was in Rhaetian age by Visscher and Brugman [1981], or in the upper part of Norian by Pedersen and Lund [1980]". Today, we know that the genus *Classopollis* appears in the early Norian (e.g., Kürschner and Herngreen 2010), hence the gypsum of Poza de la Sal described by Barrón et al. [2001] should be early Norian.

5.3. *Rhaetian assemblages*

In the Transición Fm, a palynological assemblage was also described near Huerces (Asturias Province) by Martínez-García et al. [1998] (Figure 4). These authors suggested a Rhaetian-late Rhaetian age owing to the presence of *Classopollis classoides*, and relative abundance of *Ovalipollis ovalis* and *Rhaetipollis germanicus*. Later, in the same unit, Barrón et al. [2002, 2005, 2006] proposed a Rhaetian age based on different analytical criteria. Barrón et al. [2002] considered the "relative abundance of *Corollina meyeriana* and *Corollina torosus*" and the presence of *Ovalipollis* cf. *pseudoalatus* and *Rhaetipollis germanicus* as indicative of a Rhaetian-late Rhaetian age at the Bárzana section in the Villaviciosa region (Asturias, Spain). Barrón et al. [2005] studied 49 successive samples

collected from the Vilorteo and Cantavieyo Diamond Drill Holes, La Camocha Mine area near Gijón (Asturias), and they distinguished three assemblages (PA1, PA2 and PA3) for the Late Triassic-Lower Jurassic time interval. The PA1 assemblage is related to the *Rhaetipollis germanicus* Zone [Orbell, 1973], the third phase of "Grès et Schiste à *Avicula contorta*", to "Argiles de Levallois" [Schuurman, 1977] and the Rhaetian assemblages to NW Europe [Batten and Koppelhus, 1996, Visscher and Brugman, 1981]. The PA2 and PA3 assemblages are associated with the *Heliosporites* Zone of Orbell [1973] and the assemblage of St. Audrie's Bay [Hounslow et al., 2004]. These preliminary palynological studies were finally expanded in Barrón et al. [2006] in a palynological, biostratigraphic, sedimentological and sequence stratigraphy study to characterise the Triassic-Jurassic boundary in Asturias (North Spain). The authors suggested that the PA1 assemblage, which corresponds to the lower part of both boreholes, could be assigned a Rhaetian age due to a similarity with the *Rhaetipollis germanicus* Zone and the presence of *Ovalipollis pseudoalatus* and *Tsugaepollenites pseudomassulae*. However, they could not assign the PA2 assemblage to the Rhaetian or Hettangian due to "the absence of representative palynomorphs of these ages", but the PA3 was interpreted as Hettangian, based on the presence of *Ischyosporites variegatus* and *Cerebropollenites thiergartii*.

Although unable to verify the described taxa due to the partial absence of figures, on the basis of our palynological comparison the presence of *Kraeuselisporites reissingeri*, *Tsugapollenites pseudomassulae* and the genus *Cerebropollenites* in PA3 would be indicative of late Rhaetian or Rhaetian–Hettangian transition. Although *Ischyosporites variegatus* and *Cerebropollenites thiergartii* are considered the best markers for the Triassic-Jurassic boundary, their lowest occurrences have been recorded several meters below the FAD of the ammonite *Psiloceras spelae* defining the base of the Hettangian in the GSSP stratotype Kuhjoch section (Karwendel Mountains, Austria) [Bonis et al., 2009, Cirilli et al., 2018, Hillebrandt et al., 2013, Kürschner and Herngreen, 2010]. However, the PA3 assemblage is equivalent to the one described in the Noto Fm and the Upper Streppenosa Mb (SE Sicily, Italy; Cirilli et al. [2018]) with a Rhaetian age, due to the abundance of *Classopollis* species (*Classopollis meyeriana* and minor *Classopollis torosus*) and other index species such as *Ischyosporites variegatus*, *Porcellispora longdonensis* and *Trachysporites fuscus*. The presence of *Ischyosporites variegatus* in association with *Classopollis* spp., *Porcellispora longdonensis* and *Kraeuselisporites reissingeri*, could indicate a latest Rhaetian age in the PA3 assemblage, as in the case of the upper part of the Upper Streppenosa Mb [Cirilli et al., 2018, Hillebrandt et al., 2013].

The presence of *Kraeuselisporites reissingeri* is reported together with *Carnisporites spiniger*, *Classopollis meyeriana*, *Convolutispora klukiforma*, *Ovalipollis pseudoalatus*, *Taurocusporites verrucatus* and the dinoflagellates *Dapcodinium priscum* and *Rhaetogonyalax rhaetica* in the SC-4 assemblage (late Raethian age) described by Juncal et al. [2018] in the Sancerre-Couy core (Paris Basin). The presence of *Kraeuselisporites reissingeri* and *Tsugapollenites pseudomassulae* is also described in the lower Malanotte Fm of the Triassic–Jurassic transition in the western Southern Alps (Northern Italy; Galli et al. [2007]) in an assemblage that contains *Classopollis torosus, Cerebropollenites macroverrucosus* and the dinoflagellate cysts *Dapcodinium priscum*. A similar microfloral composition is reported at the Rhaetian–Hettangian transition from the St Audrie's Bay section in United Kingdom [Bonis et al., 2010, Hesselbo et al., 2002, 2004, Hounslow et al., 2004, Lindström, 2016, Lindström et al., 017b, Orbell, 1973, Warrington, 1996] and in the intra- and infra-basaltic sediments from different localities at the base of the CAMP lava piles in Morocco [Panfili et al., 2019].

6. Conclusions

We present here a detailed study of four palynological assemblages obtained from three stratigraphical sections and one borehole from the Triassic sedimentary record of the Cantabrian Mountains, North Spain. These data have made it possible to (i) make an accurate correlation of the Triassic record of this area, (ii) integrate the different palynostratigraphic information that already existed but had not been well determined stratigraphically, and (iii) carry out a comparative analysis with other samples studied in Triassic sections from Centre and SW of Europe.

Four assemblages from the Triassic sedimentary record were examined. Three of these were obtained from the Cicera Fm of continental origin (Carmona, San Pedro and Cicera assemblages). A Longobardian age is suggested for the lower (Carmona assemblage) and a Ladinian-Carnian transition for the upper part of this formation (San Pedro and Cicera assemblages). The uppermost part of this formation shows a transition with the overlying Rueda Formation, of shallow marine origin. This transition is indicated by the presence of *Plaesiodictyon mosellanum*, a freshwater-shallow marine environment alga. These palynological assemblages are equivalent to the samples obtained near Verbios village (Palencia Province) and the Tres Mares peak (Cantabrian Province) in the upper part of the "Buntsandstein facies" by Sánchez-Moya et al. [2005].

The last palynological assemblage (Villabona assemblage) has a Lacian-Aulanian age and it was obtained in Transición Fm (mostly of shallow marine origin). This assemblage corresponds to the Norian assemblage obtained in "Keuper facies" in Aguilar de Campoo (Palencia province) by Salvany [990a,b] and to the early-middle Norian assemblage described in the Reinosa area (Cantabria province; Calvet et al. [1993]). Moreover, this assemblage is comparable with the assemblages obtained in laminated gypsum deposits near Poza de la Sal (Cantabrian Province) by Barrón et al. [2001] with an upper Carnian-early Norian age.

The palynological assemblages obtained in this work were compared with the microflora coming from the same paleolatitude (same paleoclimate belt), and they were also compared with the main Triassic palynostratigraphic subdivisions in Central and NW Europe.

Acknowledgements

The authors are grateful to the anonymous reviewer and Dr. Amalia Spina for helpful and constructive suggestions. This work was supported by projects PGC 2018-098272-B-100 and CGL2015-70970-P (Spanish Ministry of Economy) and GRC 2015/020 (Xunta de Galicia). The projects: "Sistemas Sedimentarios y Variabilidad Climática" (642853) of the CSIC, Basin Analysis (910429), and Palaeoclimatology and Global Change (910198) of the Universidad Complutense de Madrid have also contributed to this study. The authors thank Nemesio Heredia (IGME, Oviedo) and Fidel Martín-González (Universidad Rey Juan Carlos, Móstoles, Madrid) for field support, and Luis Villa Iglesias and José Antonio Marín Barcaíztegui (MINERSA GROUP) for their personal support, providing all the required borehole data for the Villabona Mine (Asturias) and facilitating access to the mine galleries for sampling. We also thank Aida Adsuar Vaquero, from the IGEO (CSIC-UCM), who helped in the preparation of the palynological samples.

Supplementary data

Supporting information for this article is available on the journal's website under https://doi.org/10.5802/crgeos.12or from the author.

References

Adloff, M. C., Appia, C., Doubinger, J., and Lienhardt, M. J. (1984). Zonations palynostratigraphiques dans les séries triasiques traversées par les sondages dans le Jura et le Bas-Dauphiné. *Geologie de la France*, 1–2:3–21.

Adloff, M. C., Courel, L., Giot, D., Lacombe, P., and Marteau, P. (1987). Le Trias. *Documents BRGM*, 136:27–30.

Adloff, M. C. and Doubinger, J. (1979). Étude palynologique dans le mésozoïque de base de la bordure ne du massif central français. In *7ème réunion annuelle des Sciences de la terre, Lyon, 1979*. Société géologique de France 1.

Alonso, J., Pulgar, J., García-Ramos, J., and Barba, P. (1996). Tertiary basins and Alpine tectonics in the Cantabrian Mountains (NW Spain). In Friend, P. and Dabrio, C. J., editors, *Tertiary basins of Spain: the stratigraphic record of crustal kinematics*, pages 214–227. Cambridge University Press.

Barnolas, A. and Pujalte, V. (2004). La Cordillera Pirenaica. In Vera, J. A., editor, *Geología de España*, pages 233–343. IGME-SGE, Madrid.

Barrón, E., Gómez, J. J., and Goy, A. (2001). Dataciones con palinomorfos en los materiales del tránsito Triásico–Jurásico de Poza de la Sal (Burgos). In *Publicaciones de Seminarios de Paleontología*, pages 46–55. Universidad de Zaragoza 5.1.

Barrón, E., Gómez, J. J., and Goy, A. (2002). Los materiales del tránsito Triásico-Jurásico en la región de

Villaviciosa (Asturias, España). *Geogaceta*, 31:197–200.

Barrón, E., Gómez, J. J., Goy, A., and Pieren, A. P. (2005). Asociaciones palinológicas del tránsito Rhaetiense–Hettangiense en Asturias (España). *Geo-Temas*, 8:133–136.

Barrón, E., Gómez, J. J., Goy, A., and Pieren, A. P. (2006). The Triassic–Jurassic boundary in Asturias (northern Spain): Palynological characterisation and facies. *Rev. Palaeobot. Palynol.*, 138:187–208.

Batten, D. J. and Koppelhus, E. B. (1996). Biostratigraphic significance of uppermost Triassic and Jurassic miospores in Northwest Europe. In Jansonius, J. and McGregor, D. C., editors, *Palynology: Principles and Applications*, pages 795–806. American Association of Stratigraphic Palynologist Foundation 2.

Bercovici, A., Diez, J. B., Broutin, J., Bourquin, S., Linol, B., Villanueva-Amadoz, U., López-Gómez, J., and Durand, M. (2009). A palaeoenvironmental analysis of Permian sediments in Minorca (Balearic Islands, Spain) with new palynological and megafloral data. *Rev. Palaeobot. Palynol.*, 158:14–28.

Blendinger, E. (1988). Palynostratigraphy of the late Ladinian and Carnian in the southeastern Dolomites. *Rev. Palaeobot. Palynol.*, 53:329–348.

Bonis, N. R., Kürschner, W. M., and Krystyn, L. (2009). A detailed palynological study of the Triassic–Jurassic transition in key sections of the Eiberg Basin (Northern Calcareous Alps, Austria). *Rev. Palaeobot. Palynol.*, 156:376–400.

Bonis, N. R., Ruhl, M., and Kürschner, W. M. (2010). Milankovitch-scale palynological turnover across the Triassic-Jurassic transition at St. Audrie's Bay, SW UK. *J. Geol. Soc.*, 167:877–888.

Bourquin, S., Robin, C., Guillocheau, F., and Gaulier, J. M. (2002). Three-dimensional accommodation analysis of the Keuper of the Paris Basin: discrimination between tectonics, eustasy, and sediment supply in the stratigraphic record. *Marine Petroleum Geol.*, 19:469–498.

Brugman, W. A., Van Bergen, P. R., and Kerp, J. H. E. (1994). A quantitative approach to Triassic palynology: the Lettenkeuper of the Germanic Basin as an example. In Traverse, A., editor, *Sedimentation of Organic Particles*, pages 409–429. Cambridge University Press.

Buratti, N. and Cirilli, S. (2007). Microfloristic provincialism in the Upper Triassic circumediterranean area and its palaeogeographic implication. *Geobios*, 40:133–142.

Buratti, N., Mehdi, D., Cirilli, S., Kamoun, F., and Mzoughi, M. (2012). A Carnian (Julian) microflora from the Djerba Melita 1 borehole (Gulf of Gabes, South-eastern Tunisia). *Micropaleontology*, 58(4):377–388.

Cadenas, P., Fernández-Viejo, G., Pulgar, J. A., Tugend, J., Manatschal, G., and Minshull, T. A. (2018). Constraints imposed by rift inheritance on the compressional reactivation of a hyperextended margin: mapping rift domains in the North Iberian margin and in the Cantabrian Mountains. *Tectonics*, 37(3):758–785.

Calvet, F., Solé de Porta, N., and Salvany, J. M. (1993). Cronoestratigrafía (Palinología) del Triásico Sudpirenaico y del Pirineo Vasco-Cantábrico. *Acta Geológica Hispánica*, 28:33–48.

Cámara, P. (2017). Salt and Strike-Slip Tectonics as Main Drivers in the Structural Evolution of the Basque-Cantabrian Basin, Spain. In Soto, J. I., Flinch, J. F., and Tari, G., editors, *Permo-Triassic Salt Provinces of Europe, North Africa and the Atlantic Margins. Tectonics and Hydrocarbon Potential*, pages 371–392. Elsevier.

Cirilli, S. (2010). Upper Triassic–lowermost Jurassic palynology and palynostratigraphy: a review. In Lucas, S. G., editor, *The Triassic Timescale*, Special Publications 334, pages 285–314. Geological Society, London.

Cirilli, S., Panfili, G., Buratti, N., and Frixa, A. (2018). Paleoenvironmental reconstruction by means of palynofacies and lithofacies analyses: An example from the Upper Triassic subsurface succession of the Hyblean Plateau Petroleum System (SE Sicily, Italy). *Rev. Palaeobot. Palynol.*, 253:70–87.

Dalla-Vecchia, F. M. (2000). Macrovegetali terrestri nel Mesozoico Italiano: un'ulteriore evidenza di frequenti emersioni. *Natura Nascosta*, 20:18–35.

Dalla-Vecchia, F. M. and Selden, P. A. (2013). A Triassic spider from Italy. *Acta Palaeontologica Polon.*, 58:325–330.

De Jong, J. D. (1971). Molasse and clastic-wedge sediments of the southern Cantabrian Mountains (NW Spain) as geomorphological and environmental indicators. *Geol. en Mijnb.*, 50(3):399–416.

De la Horra, R., Cárdenes, V., Pérez-Huerta, A., and

González-Acebrón, L. (2012). Primera descripción de niveles con glauconita en el "Tramo de Transición", de edad Retiense (Triásico Superior), en el área de Caravia, Asturias, España. *Geo-Temas*, 13:103–107.

Dobruskina, I. A. (1993). First data of the Seefeld conifer flora (Upper Triassic, Tyrol, Austria). In Lucas, S. G. and Morales, M., editors, *The Nonmarine Triassic*, volume 3 of *New Mexico Museum of Natural History and Science Bulletin*, pages 113–115.

Dobruskina, I. A. (1994). Triassic Floras of Eurasia. *Österr Akad Wissensch, Schriftenreihe Erdwiss Kommiss*, 10:1–422.

Doubinger, J. and Adloff, M. C. (1977). Études palynologiques clans le Trias de la bordure sud-est du Massif central français (bassin de Largentiere, Ardeche). *Sci. Geol. Strasbourg*, 30(1):59–74.

Doubinger, J. and Adloff, M. C. (1983). Triassic palynomorphs of the mediterranean area. C.N.R.S report, 26 p.

Doubinger, J. and Bühmann, D. (1981). Röt bei Borken und bei Schlüchtern (Hessen, Deutschland): Palynologie und Tonmineralogie. *Zeitschrift der Deutschen Geologischen Gesellschaft*, 132(1):421–449.

Doubinger, J., López-Gómez, J., and Arche, A. (1990). Pollen and spores from the Permian and Triassic of the southeastern Iberian ranges, Cueva de Hierro (Cuenca) to Chelva Manzanera (Valencia Teruel) region, Spain. *Rev. Palaeobot. Palynol.*, 66:25–45.

Eshet, Y. (1990). The palynostratigraphy of the Permian Triassic boundary in Israel: Two approaches to biostratigraphy. *Israel J. Earth Sci.*, 39:1–15.

Espina, R. (1997). *La estructura y evolución tectonoestratigráfica del borde occidental de la Cuenca Vasco-Cantábrica (Cordillera Cantábrica, NO de España)*. PhD thesis, Universidad de Oviedo. 230 p.

Fillon, C., Pedreira, D., van der Beek, P. A., Huismans, R. S., Barbero, L., and Pulgar, J. A. (2016). Alpine exhumation of the central Cantabrian Mountains, northwest Spain. *Tectonics*, 35:339–356.

Fisher, M. J. (1979). The Triassic palynofloral succession in the Canadian Arctic Archipelago. *American Association of Stratigraphic Palynologists Foundation Contribution*, 5:83–100.

Fisher, M. J. and Dunay, R. E. (1984). Palynology of the Petrified Forest Member of the Chinle Formation (Upper Triassic), Arizona, USA. *Pollen et Spores*, 26:241–284.

Foster, C. B. (1979). Permian plant microfossils of the Blair Atholl Coal Measures, Baralaba coal measures and basal Rewan Formation of Queensland. *Geol. Surv. Queensland Publications*, 372:1–244.

Francis, J. E. (1983). The dominant conifer of the Jurassic Purbeck Formation, England. *Palaeontology*, 26:277–94.

Fréchengues, M., Peybernés, B., Fournier-Vinas, C., and Lucas, C. (1993). Palynologic assemblages within the depositional sequences from the Middle to Late Triassic series of the Spanish and French Pyrenees. *Revista española de micropaleontología*, 25:91–105.

Galasso, F., Fernandes, P., Montesi, G., Marques, J., Spina, A., and Pereira, Z. (2019a). Thermal history and basin evolution of the Moatize-Minjova Coal Basin (N'Condédzi sub-basin, Mozambique) constrained by organic maturation levels. *J. Afr. Earth Sci.*, 153:219–238.

Galasso, F., Pereira, Z., Fernandes, P., Spina, A., and Marques, J. (2019b). First record of Permo-Triassic palynomorphs of the N'Condédzi subbasin, Moatize-Minjova Coal Basin, Karoo Supergroup, Mozambique. *Rev. Micropaleontologie*, 64:100357.

Gallastegui, J., Pulgar, J. A., and Gallart, J. (2002). Initiation of an active margin at the North Iberian continent ocean transition. *Tectonics*, 21:1501–1514.

Galli, M., Jadoul, F., Bernasconi, S. M., Cirilli, S., and Weissert, H. (2007). Stratigraphy and paleoenvironmental analysis of the Triassic-Jurassic transition in Western southern Alps (Northern Italy). *Palaeogeogr. Palaeoclimatol. Palaeoecol.*, 244:52–70.

Gand, G. and Demathieu, G. (2005). Les pistes dinosauröidesdu Trias moyen francais: intérpretation et réevaluation de la nomenclature. *Geobios*, 38:725–749.

Gand, G., Kerp, H., Parsons, C., and Martínez-García, E. (1997). Palaeoenvironmental and stratigraphic aspects of the discovery of animal traces and plant remains in Spanish Permian red beds (Peña Sagra, Cantabrian Mountains, Spain). *Geobios*, 30:295–318.

García-Espina, R. (1997). *La estructura y evolución tectonoestratigráfica del borde occidental de la Cuenca Vasco-Cantábrica (Cordillera Cantábrica, NO de España)*. PhD thesis, Universidad de Oviedo. 230 p., unpublished.

García-Mondejar, J., Pujalte, V., and Robles, S. (1986). Características sedimentológicas, secuenciales y tectonoestratigráficas del Triásico de Cantabria y norte de Palencia. *Cuadernos de Geología Ibérica*, 10:151–172.

Hernando, S., Doubinger, J., and Adloff, M. C. (1977). Datos cronoestratigráficos del Triásico superior de la región de Ayllón-Atienza. *Cuadernos de Geología Ibérica*, 4:399–410.

Herngreen, G. F. W. (2005). Triassic sporomorphs of nw europe: taxonomy, morphology and ranges of marker species with remarks on botanical relationship and ecology and comparison with ranges in the alpine triassic. Kenniscentrum Biogeology (UU/TNO)—TNO report, NITG 04–176-C, Ned Inst Toegepaste Geowet TNO, Utrecht.

Hesselbo, S., Robinson, S. A., and Surlyk, F. (2004). Sea-level change and facies development across potential Triassic–Jurassic boundary horizons, SW Britain. *J. Geol. Soc. London*, 161:365–379.

Hesselbo, S. P., Robinson, S. A., Surlyk, F., and Piasecki, S. (2002). Terrestrial and marine extinction at the Triassic–Jurassic boundary synchronized with major carbon-cycle perturbation: a link to initiation of massive volcanism? *Geology*, 30:251–254.

Heunisch, C. (1999). Die Bedeutung der Palynologie für Biostratigraphie und Fazies in der Germanischen Trias. In Hauschke, N. and Wilde, V., editors, *Trias, Eine ganz andere Welt, Mitteleuropa im frühen Erdmittelalter*, pages 207–220. Pfeil Verlag, München.

Hillebrandt, A. V., Krystyn, L., Kürschner, W. M., Bonis, N. R., Ruhl, M., Richoz, S., Schobben, M. A. N., Urlichs, M., Bown, P. R., Kment, K., McRoberts, C. A., Simms, M., and Tomãsových, A. (2013). The Global Stratotype Sections and Point (GSSP) for the base of the Jurassic Systemat Kuhjoch (Karwendel Mountains, northern Calcareous Alps, Tyrol, Austria). *Episodes*, 36:162–198.

Hochuli, P. A., Colin, J. P., and Vigran, J. (1989). Triassic biostratigraphy of the Barents Sea area. In Collins, J. D., editor, *Correlation in Hydrocarbon Exploration*, pages 131–153. Norwegian Petroleum Society, Graham and Trotman Ltd, Oslo.

Hochuli, P. A. and Frank, S. M. (2000). Palynology (dinoflagellate cysts, spore-pollen) and stratigraphy of the lower Carnian Raibl Group in the eastern Swiss Alps. *Eclogae Geologicae Helvetiae*, 93:429–443.

Hounslow, M. H., Posen, P. E., and Warrington, G. (2004). Magnetostratigraphy and biostratigraphy of the Upper Triassic and Lowermost Jurassic succession, St. Audrie's Bay, UK. *Palaeogeogr. Palaeoclimatol. Palaeoecol.*, 213:331–358.

Jarzen, D. M. and Nichols, D. J. (1996). Chapter 9. Pollen. In Jansonius, J. and McGregor, D. C., editors, *Palynology: Principles and Applications*, volume 1, pages 261–291. American Association of Stratigraphic Palynologist Foundation.

Julivert, M. (1971). Decollement tectonics in the Hercynian Cordillera of Northwest Spain. *Am. J. Sci.*, 270(1):1–29.

Juncal, M., Bourquin, S., Beccaletto, L., and Diez, J. B. (2018). New sedimentological and palynological data from the Permian and Triassic series of the Sancerre-Couy core, Paris Basin, France. *Geobios*, 51(6):517–535.

Juncal, M., Diez, J. B., Broutin, J., and Martínez-García, E. (2016). Palynoflora from the Permian Sotres Formation (Picos de Europa, Asturias, northern Spain). *Spanish J. Palaeontology*, 31(1):85–94.

Kürschner, W. and Herngreen, G. F. W. (2010). Triassic palynology of central and northwestern Europe: a review of palynofloral diversity patterns and biostratigraphic subdivisions. In Lucas, S. G., editor, *The Triassic Timescale*, Special Publications, 334, pages 263–283. Geol. Soc. London.

Kustatscher, E., Ash, S., Karasev, E., Pott, C., Vajda, V., Yu, J., and McLoughlin, S. (2018). Flora of the Late Triassic. In Tanner, L. H., editor, *The Late Triassic World*, volume 46 of *Topics in Geobiology*, pages 545–622.

Kustatscher, E., Heunisch, C., and van Konijnenburg-van Cittert, J. H. A. (2012). Taphonomical implications of the Ladinian megaflora and palynoflora of Thale (Germany). *PALAIOS*, 27:753–764.

Lindström, S. (2016). Palynofloral patterns of terrestrial ecosystem change during the end-Triassic event – a review. *Geol. Mag.*, 153(2):223–251.

Lindström, S., Erlström, M., Piasecki, S., Nielsen, H. L., and Mathiesen, A. (2017a). Palynology and terrestrial ecosystem change of the Middle Triassic to Lowermost Jurassic succession of the eastern Danish Basin. *Rev. Palaeobot. Palynol.*, 244:65–95.

Lindström, S., van de Schootbrugge, B., Hansen, K. H., Pedersen, G. K., Alsen, P., Thibault, N., Dybkjær, K., Bjerrum, C. J., and Nielsen, L. H. (2017b).

A new correlation of Triassic–Jurassic boundary successions in NW Europe, Nevada and Peru, and the Central Atlantic Magmatic Province: A timeline for the end-Triassic mass extinction. *Palaeogeogr. Palaeoclimatol. Palaeoecol.*, 478:80–102.

López-Gómez, J., Arche, A., and Pérez-López, A. (2002). Permian and Triassic. In Gibbons, W. and Moreno, T., editors, *Geology of Spain*, pages 195–212. The Geol. Soc. London.

López-Gómez, J., Martín-González, F., Heredia, N., De la Horra, R., Barrenechea, J. F., Cadenas, P., Juncal, M., Diez, J. B., Borruel-Abadía, V., Pedreira, D., García Sansegundo, J., Farias, P., Galé, C., Lago, L., Ubide, T., Fernández-Viejo, G., and Gand, G. (2019). New lithostratigraphy for the Cantabrian Mountains: A common tectono-stratigraphic evolution for the onset of the Alpine cycle in the W Pyrenean realm, N Spain. *Earth-Sci. Rev.*, 188:249–271.

Manjón, M., Gutiérrez-Claverol, M., and Martínez-García, E. (1992). La sucesión posthercínica preliásica del área de Villabona, Asturias (Asturias, N España). *Actas III Congreso Geológico de España*, 2:107–111.

Martín-González, F., Barbero, L., Capote, R., Heredia, N., and Gallastegui, G. (2012). Interaction of two successive Alpine deformation fronts: constraints from low-temperature thermochronology and structural mapping (NW Iberian Peninsula). *Int. J. Earth Sci.*, 101:1331–1342.

Martín-González, F., Freudenthal, M., Heredia, N., Martín-Suárez, E., and Rodríguez-Fernández, R. (2014). Palaeontological age and correlations of the Tertiary deposits of the NW Iberian Peninsula: the tectonic evolution of a broken foreland basin. *Geological J.*, 49(1):15–27.

Martín-González, F. and Heredia, N. (2011a). Geometry, structures and evolution of the western termination of the Alpine-Pyrenean Orogen reliefs (NW Iberian Peninsula). *J. Iberian Geol.*, 37(2):103–120.

Martín-González, F. and Heredia, N. (2011b). Complex tectonic and tectonostratigraphic evolution of an Alpine foreland basin: The western Duero Basin and the related Tertiary depressions of the NW Iberian Peninsula. *Tectonophysics*, 502:75–89.

Martínez-García, E. (1981). El Paleozoico de la Zona Cantábrica oriental. *Trabajos de Geología*, 11:95–127.

Martínez-García, E. (1990). Stephanian and Permian basins. In Dallmeyer, R. D. and Martínez-García, E., editors, *Pre-Mesozoic Geology of Iberia*, pages 39–54. Springer-Verlag, Berlin.

Martínez-García, E. (1991a). Orogénesis y sedimentación a finales del Paleozoico en el NE del Macizo Ibérico (Asturias, Cantabria, Palencia). In *Volumen Homenaje a J. Ramírez del Pozo*, pages 167–174. Asociación de Geólogos y Geofísicos Españoles del Petróleo.

Martínez-García, E. (1991b). Hercynian syn-orogenic and post-orogenic successions in the Cambrian and Palentian zones (NW Spain). Comparison with other western European occurrences. *Giornale di Geologia*, 53(1):208–228.

Martínez-García, E., Coquel, R., Gutiérrez Claverol, M., and Quiroga, J. L. (1998). Edad del "tramo de transición" entre el Pérmico y el Jurásico en el área de Gijón (Asturias NW de España). *Geogaceta*, 24:215–218.

Martínez-García, E., Wagner, R. H., Gand, G., Villa, E., and Alegre-Mateo, M. T. (2001). Permian of the Cantabrian Mountains (Asturias and Cantabria, NW Spain) and its tectonic significance. In *XV Annual Field Meeting of the Association des Géologues du Permien (AGP), Oviedo, Spain*, pages 1–64.

Mehdi, D., Cirilli, S., Buratti, N., Kamoun, F., and Trigui, A. (2009). Palynological characterisation of the lower Carnian of the Kea5 borehole (Koudiat El Halfa Dome; Central Atlas, Tunisia). *Geobios*, 42:63–71.

Merino-Tomé, O., Bahamonde, J. R., Colmenero, J. R., Heredia, N., Villa, E., and Farias, P. (2009). Emplacement of the Cuera and Picos de Europa imbricate system at the core of the Ibero-Armorican arc (Cantabrian Zone, N Spain): new precisions concerning the timing of arc closure. *Geol. Soc. Am. Bull.*, 121:729–751.

Mietto, P., Manfrin, S., Preto, N., Rigo, M., Roghi, G., Furin, S., Gianolla, P., Posenato, R., Muttoni, G., Nicora, A., Buratti, N., Cirilli, S., Spötl, C., Bowring, S. A., and Ramezani, J. (2012). The Global Boundary Stratotype Section and Point (GSSP) of the Carnian Stage (Late Triassic) at Prati di Stuores/Stuores Wiesen Section (Southern Alps, NE Italy). *Episodes*, 35(3):414–430.

Orbell, G. (1973). Palynology of the British Rhaeto-Liassic. *Bull. Geol. Surv. Great Britain*, 44:1–44.

Orłowska-Zwolińska, T. (1983). Palynostratigraphy of the upper part of Triassic Epicontinental sedi-

ments in Poland. *Prace Instytutu Geologicznego, Wydawnictwa Geologiczne*, 104:1–89.

Orłowska-Zwolińska, T. (1984). Palynostratigraphy of the Buntsandstein in sections of western Poland. *Acta Palaeontologica Polon.*, 29(3–4):161–194.

Orłowska-Zwolińska, T. (1985). Palynological zones of the Polish epicontinental Triassic. *Bull. Polish Acad. Sci., Earth Sciences*, 33(3–4):107–117.

Orłowska-Zwolińska, T. (1988). Palynostratigraphy of Triassic deposits in the vicinity of Brzeg (SE part of the Fore-Sudetic Monocline). *Kwartalnik Geologiczny*, 32(2):349–366.

Pacyna, G. (2014). Plant remains from the Polish Triassic. Present knowledge and future prospects. *Acta Palaeobotanica*, 54:3–33.

Panfili, G., Cirilli, S., Dal Corso, J., Bertrand, H., Medina, F., Youbi, N., and Marzoli, A. (2019). New biostratigraphic constraints show rapid emplacement of the Central Atlantic Magmatic Province (CAMP) during the end-Triassic mass extinction interval. *Global Planetary Change*, 172:60–68.

Paterson, N. W., Mangerud, G., and Mørk, A. (2017). Late Triassic (early Carnian) palynology of shallow stratigraphical core 7830/5-U-1, offshore Kong Karls Land, Norwegian Arctic. *Palynology*, 41(2):230–254.

Pedersen, K. R. and Lund, J. J. (1980). Palynology of the plant-bearing Rhaetian to Hettangian kap Steward Formation, Scoresby sund, East Greenland. *Rev. Palaeobot. Palynol.*, 31:1–69.

Pérez-Estaún, A., Martínez-Catalán, J. R., and Bastida, F. (1991). Crustal thickenning and deformation sequence in the footwall to the suture of the Variscan belt of northwest Spain. *Tectonophysics*, 191:243–253.

Pulgar, J. A., Alonso, J. L., Espina, R. G., and Marín, J. A. (1999). La deformación alpina en el basamento varisco de la Zona Cantábrica. *Trabajos de Geología*, 21:283–294.

Riding, J. R., Leng, M. J., Kender, S., Hesselbo, S. P., and Feist-Burkhardt, S. (2013). Isotopic and palynological evidence for a new Early Jurassic environmental perturbation. *Paleogeogr. Paleoclimatol. Paleoecol.*, 374:16–27.

Robles, S. (2004). El Pérmico de la Cuenca Vasco-Cantábrica. In Vera, J. A., editor, *Geología de España, SGE-IGME*, pages 269–271.

Robles, S. and Pujalte, V. (2004). El Triásico de la Cordillera Cantábrica. In Vera, J. A., editor, *Geología de España, SGE-IGME*, pages 274–276.

Rodríguez-Fernández, L. R., Fernández, L. P., and Heredia, N. (2002). Carboniferous of the Pisuerga-Carrión Unit. In García-López, S. and Bastida, F., editors, *Paleozoic conodonts from Northern Spain*, volume 1 of *Cuadernos del Museo Geominero*, pages 93–104.

Rodríguez-Fernández, L. R. and Heredia, N. (1987). La estratigrafía del Carbonífero y la estructura de la Unidad del Pisuerga-Carrión. *Cadernos Laboratorio Xeolóxico Laxe*, 12:207–229.

Roghi, G. (2004). Palynological investigations in the Carnian of the Cave del Predil area (Julian Alps, NE Italy). *Rev. Palaeobot. Palynol.*, 132:1–35.

Roghi, G., Gianolla, P., Minarelli, L., Pilati, C., and Preto, N. (2010). Palynological correlation of Carnian humid pulses throughout western Tethys. *Palaeogeogr. Palaeoclimatol. Palaeoecol.*, 290:89–106.

Salvany, J. M. (1990a). El Keuper del Diapiro de Poza de la Sal (Burgos). In Ortí, F. and Salvany, J. M., editors, *Formaciones evaporíticas de la Cuenca del Ebro y cadenas periféricas y de la zona de Levante. Nuevas aportaciones y guía de superficie*, pages 21–28. ENRESA-GPPG, Barcelona, España.

Salvany, J. M. (1990b). Parada 18: Diapiro de Poza de la Sal (Keuper). In Ortí, F. and Salvany, J. M., editors, *Formaciones evaporíticas de la Cuenca del Ebro y cadenas periféricas, y de la zona de Levante. Nuevas aportaciones y guía de superficie*, pages 196–198. ENRESA-GPPG, Barcelona, España.

Sánchez-Moya, Y., Barrón, E., and Sopeña, A. (2005). Nuevos datos sobre la edad del Buntsandstein de la Cordillera Cantábrica. XV Congreso Nacional de Sedimentología y IV Coloquio de Estratigrafía y Paleontografía del Pérmico y Triásico de España. *Geo-Temas*, 8:251–253.

Scheuring, B. (1978). Mikrofloren aus den Meridelkalken des Monte San Giorgio (Kanton Tessin). *Abhandlungen der Schweizerischen Paläontologischen Gesellschaft*, 100:1–205.

Schulz, E. K. and Heunisch, C. (2005). Palynostratigraphische Gliederungsmöglichkeiten des deutschen Keupers. In Beutler, G., Hauschke, N., Nitsch, E., and Vath, U., editors, *Stratigraphie von Deutschland IV*, volume 253 of *Courier Forschungs Institut Senckenberg*, pages 43–49.

Schuurman, W. M. L. (1977). Aspects of Late Triassic Palynology. 2. Palynology of the "Grès et

Schiste à *Avicula contorta*" and "Argiles de Levallois" (Rhaetian) of northeastern France and southern Luxemburg. *Rev. Palaeobot. Palynol.*, 23:159–253.

Smith, D. G. (1982). Stratigraphic significance of a palynoflora from ammonoid-bearing early Norian strata in Svalbard. *Newsletters on Stratigraphy*, 11:154–161.

Solé de Porta, N., Calvet, F., and Torrentó, L. (1987). Análisis palinológico del Triásico de los Catalánides (NE España). *Cuadernos Geología Ibérica*, 11:237–254.

Sopeña, A., Doubinger, J., Ramos, A., and Pérez-Arlucea, M. (1995). Palynologie du Permien et du Trias dans le centre de la Péninsule Ibérique. *Sci. Geol. Bull. Strasbourg*, 48:119–157.

Sopeña, A., Sánchez-Moya, Y., and Barrón, E. (2009). New palynological and isotopic data for the Triassic of the western Cantabrian Mountains (Spain). *J. Iberian Geol.*, 35(1):35–45.

Spina, A., Cirilli, S., Utting, J., and Jansonius, J. (2015). Palynology of the Permian and Triassic of the Tesero and Bulla sections (Western Dolomites, Italy) and consideration about the enigmatic species *Reduviasporonites chalastus*. *Rev. Palaeobot. Palynol.*, 218:3–14.

Suárez-Rodríguez, A. (1988). Estructura del área de Villaviciosa-Libardón (Asturias, Cordillera Cantábrica). *Trabajos de Geología*, 17:87–98.

Suárez-Vega, L. C. (1974). Estratigrafía del Jurásico de Asturias. *Cuadernos de Geología Ibérica*, 3:1–368.

Tanner, L. H., Lucas, S. G., and Chapman, M. G. (2004). Assessing the record and causes of Late Triassic extinctions. *Earth-Sci. Rev.*, 65:103–139.

Tugend, J., Manatschal, G., Kusznir, N. J., Masini, E., Mohn, G., and Thinon, I. (2014). Formation and deformation of hyperextended rift systems: Insights from rift domain mapping in the Bay of Biscay-Pyrenees. *Tectonics*, 33:1239–1276.

Van Der Eem, J. G. L. A. (1983). Aspects of Middle and Late Triassic Palynology: 6. Palynological investigations in the Ladinian and Lower Karnian of the western Dolomites, Italy. *Rev. Palaeobot. Palynol.*, 39:189–300.

Vigran, J. O., Mangerud, G., Mørk, A., Worsley, D., and Hochuli, P. A. (2014). *Palynology and geology of the Triassic succession of Svalbard and the Barents Sea*, volume 14 of *Special Publication*. Geol. Surv. Norway.

Visscher, H. and Brugman, W. (1981). Ranges of selected palynomorphs in the Alpine Triassic of Europe. *Rev. Palaeobot. Palynol.*, 34:115–128.

Visscher, H. and Krystyn, L. (1978). Aspects of Late Triassic palynology. 4. A palynological assemblage from ammonoid-controlled late Karnian (Tuvalian) sediments of Sicily. *Rev. Palaeobot. Palynol.*, 26:93–112.

Wagner, R. H. and Martínez-García, E. (1982). Description of an Early Permian flora from Asturias and comments on similar occurrences in the Iberian Península. *Trabajos de Geología*, 12:273–287.

Warrington, G. (1996). Palaeozoic spores and pollen (Chapter 18E) Permian. In Jansonius, J. and McGregor, D. C., editors, *Palynology: Principles and Applications, Volume 3*, pages 607–619. American Association of Stratigraphical Palynologists Foundation, Dallas, TX.

Weems, R. E. (1992). The "terminal Triassic catastrophic extinction event" in perspective: a review of Carboniferous through Early Jurassic terrestrial vertebrate extinction patterns. *Palaeogeogr. Palaeoclimatol. Palaeoecol.*, 94:1–29.

Ziegler, P. A. (1993). Late Paleozoic-Early Mesozoic plate reorganization: evolution and demise of the Variscan fold belt. In Ramer, J. F. and Neubauer, F., editors, *Pre-Mesozoic Geology in the Alps*, pages 203–216. Springer Verlag, Berlin.

Ziegler, P. A. and Stampfli, G. M. (2001). Late Paleozoic-Early Mesozoic plate boundary reorganization: collapse of the Variscan orogen and opening of the Neotethys. *Natura Bresciana*, 27:17–34.

Comptes Rendus
Géoscience — Sciences de la Planète
2020, 352, nº 6-7, p. 495-513
https://doi.org/10.5802/crgeos.34

Some aspects of current State of Knowledge on Triassic series on both sides of the Central Atlantic Margin / *Quelques aspects de l'état des connaissances des séries triasiques de part et d'autre de la Marge Atlantique*

Overview of the Late Triassic (Carnian) actinopterygian fauna from the Argana Basin (Morocco)

Bouziane Khalloufi[*, a, b] **and Nour-Eddine Jalil**[c, d]

[a] Palaeontological Research and Education Centre, Mahasarakham University, Khamrieng, Kantarawichai district, Maha Sarakham 44150, Thailand

[b] Laboratoire Informatique et Systématique UMR 7205, Université Pierre et Marie Curie (UPMC-Paris 6), Muséum national d'Histoire naturelle, Paris, France

[c] Centre de Recherche en Paléontologie – Paris (MNHN, CNRS, Sorbonne Université), CP 38, 57 rue Cuvier, CP 38, 75231 Paris CEDEX 5, France

[d] Muséum d'Histoire naturelle de Marrakech, Dept. de Géologie (FSSM), Université Cadi Ayyad, Maroc

E-mails: khalloufi.bouziane@hotmail.fr (B. Khalloufi), nour-eddine.jalil@mnhn.fr (N.-E. Jalil)

Abstract. The continental outcrops of the Argana Basin (High Atlas of Morocco) have provided the richest tetrapod assemblage and the only known actinopterygian fauna of the Triassic of North Africa. Unlike the tetrapod remains, widely distributed throughout the basin, the actinopterygians are rare and come from a single locality. They are dated as the Late Triassic (Carnian) and have been attributed to six forms. Here, this ichthyofauna is reviewed for the first time since its original description. Two forms, endemic to the basin, are recognized as valid species and their generic attributions confirmed: the redfieldiiform *Mauritanichthys rugosus*, related to the genus *Lasalichthys* from the Late Triassic of North America, and the "perleidiform" *Dipteronotus gibbosus*, congeneric with Middle Triassic species of Europe. The other actinopterygian taxa are known by insufficiently preserved remains and need a complete material to be confidently identified. Two specimens previously referred to the redfieldiiform *Ischnolepis* are considered as Redfieldiiformes indet. and probably correspond to a new taxon. The three last forms, previously referred to the "perleidiforms" *Procheirichthys* and *Perleidus*, and to the redfieldiiform *Atopocephala*, are considered as Actinopterygii indet.

Keywords. Actinopterygii, Redfieldiiformes, "Perleidiforms", High Atlas, Argana Corridor.

Available online 8th January 2021

* Corresponding author.

1. Introduction

In North Africa, the Argana Basin, or Argana Corridor, provides exceptional exposures of Permian to Upper Triassic continental fluvial-dominated sediments deposited in a rift basin. These sediments crop out in the western High Atlas of Morocco between the cities of Imi n'Tanout in the north and Amskroud in the south and extend over a length of 80 km for a maximum width of approximately 25 km (Figure 1A,B). Exposures consist of red-beds mainly formed by conglomerates, sandstones and siltstones, and have been divided into eight lithostratigraphical units or members (named T1 to T8, Figure 1C) belonging to three formations: the Permian Ikakern Fm (T1 and T2), and the Triassic Timezgadiouine (T3 to T5) and Bigoudine Fms (T6 to T8, Brown, 1980, Khaldoune et al., 2017, Tixeront, 1973, Tourani et al., 2000). Fossil remains have been reported from the lithostratigraphical units T2, T3, T4, T5 and T6 and dozens of localities have been identified by Dutuit [1976] and successive researchers. Fossils consist of charophytes, ostracods and abundant and diversified vertebrates represented both by isolated or articulated bone remains and ichnofossils [Dutuit, 1976, Jalil, 1999, Jalil and Janvier, 2005, Jalil and Peyer, 2007, Khaldoune et al., 2017, Klein et al., 2010, Lagnaoui et al., 2012, Medina et al., 2001, Tourani et al., 2010, Zouheir et al., 2020]. They offer the most important Permian-Triassic vertebrate fauna of North Africa. Tetrapods are represented by more than 15 species belonging to amphibians (nectrideans, metoposaurids, almasaurids), sauropsids (pareiasaurs, captorhinids, azendohsaurids, phytosaurs, aetosaurs, and rauisuchians), and dicynodont synapsids (see Khaldoune et al. [2017] for a taxonomic list). Other sarcopterygian remains are identified as a ceratodontid lungfish and possibly a coelacanth [Martin, 1979a,b, 1981]. Actinopterygians are Late Triassic (Carnian) in age and, except isolated scales, are all from the so-called locality XI of Dutuit [1976], at the base of the unit T5 [Dutuit, 1976, Khaldoune et al., 2017, Khalloufi et al., 2017, Martin, 1979a, 1980b,a, 1982].

The locality XI (Figure 1B) consists of three fossiliferous layers with different faunal associations. The basal most layer yielded postcranial remains of a dicynodont, the intermediate provided dicynodonts, rauisuchian reptiles and metoposaurid temnospondyls, and the upper most level, formed by a reddish to brownish sandstone, delivered temnospondyls, lungfishes and the actinopterygian remains [Dutuit, 1976]. The actinopterygian material has been studied by Martin [1979a, 1980b,a, 1982], who identified two main groups, Redfieldiiformes (represented by *Mauritanichthys rugosus* Martin, 1980b and by fragments attributed to the genera *Atopocephala* and *Ischnolepis*) and "perleidiforms" (represented by *Dipteronotus gibbosus* Martin, 1980a and the genera *Perleidus* and *Procheirichthys*). This is the only occurrence of these groups in North Africa. No review of the Argana Basin actinopterygians has been realized since their original description. The aim of this paper is to provide an updated overview of this fauna with comments on anatomy and phylogenetical affinities.

2. Materials and methods

The actinopterygian material from the Argana Basin consists of about 30 specimens, housed in the palaeontological collection of the Muséum national d'Histoire naturelle, Paris, France. They are in anatomical connection but incomplete for most of them. Apart few exceptions, the specimens are badly preserved, as they are often fragmented and crushed with sometimes displaced or missing bones. In order to highlight the contrast between bones and sediment, the specimens were observed under UV light, in addition to white light. Observations were made with a stereomicroscope and photographs were taken with a Nikon D800 camera. UV light observations were realized thanks to two Fluotest Forte UV quartz lamps emitting at 180 W (λ excitation centered around 365 nm). The close-up view of the scale (Figure 3G) was captured using a digital microscope Hirox RH2000. Silicone molds have been made for a few specimens preserved as natural casts (negative bone imprint). Photographs of the holotype of *Dipteronotus cyphus* (GSM18188 and GSM18189), housed at the British Geological Survey, were obtained from GB3D Type Fossils (http://www.3d-fossils.ac.uk). Photographs of specimens of *Dipteronotus aculeatus* (Triassic, France) from the Grauvogel collection were obtained from the Staatliches Museum für Naturkunde Stuttgart. Bone nomenclature follows the terminology of Schultze [2008] and Wiley [2008], based on homologies between sarcopterygian

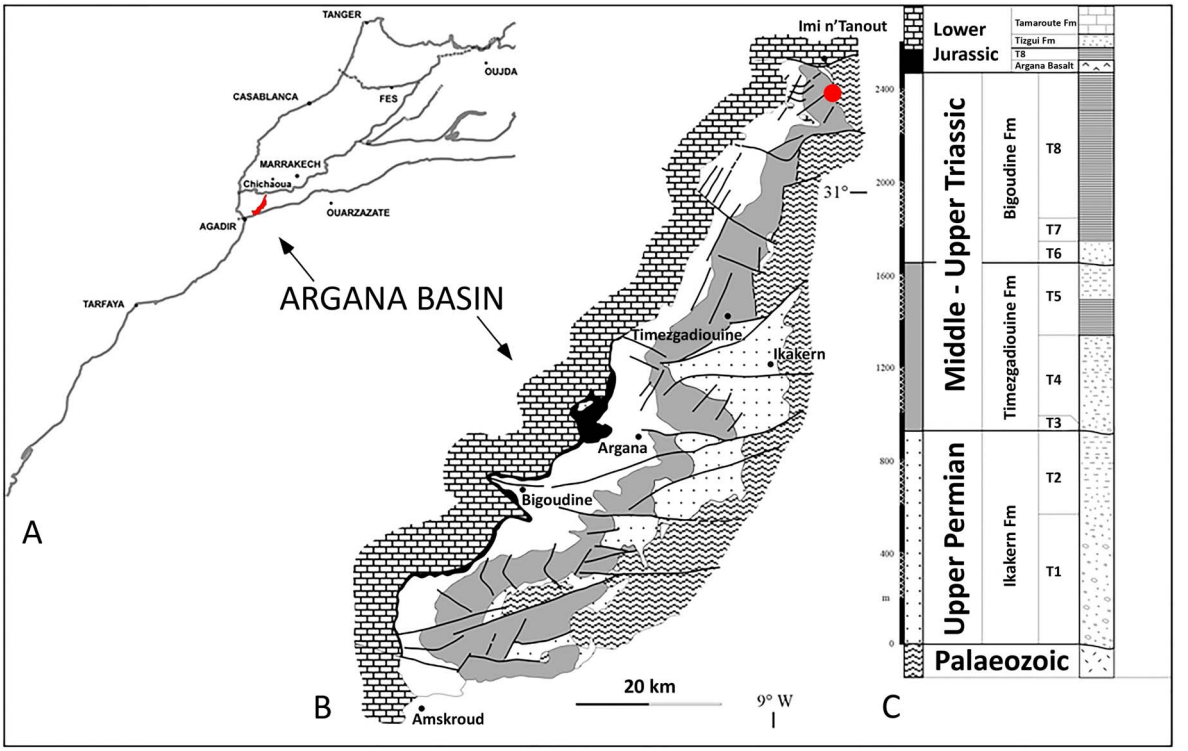

Figure 1. Location and stratigraphy of the Argana Basin. (A) Geographical map of Morocco, showing the location of the Argana Basin, in red. (B) Simplified geological map of the Argana Basin (modified from Tixeront, 1973, 1974). The locality XI is indicated by a red dot. (C) Stratigraphical section of the Argana Basin (modified from Tourani et al., 2000).

and actinopterygian skull bones, and that of Mickle [2015] for snout bones, which mainly corresponds herein to the use of "parietal" and "postparietal" instead of "frontal" and "parietal", respectively.

Institutional abbreviation. MNHN.F, Muséum national d'Histoire naturelle, Paris, France, Palaeontological collection.

3. Palaeontological systematics

Actinopterygii Cope, 1887
Redfieldiiformes Berg, 1940

Redfieldiiformes are a clade of actinopterygians formed by at least 17 genera, known from the Lopingian to Early Jurassic, mostly in non-marine environments of Australia, Africa (Morocco, South Africa, Zambia and possibly Madagascar), Asia (South Korea), South America (Argentina), North America (USA) and putatively Europe (England, Germany, Ireland, Poland and Switzerland, see Gibson, 2018, Gouiric-Cavalli et al., 2017, Hutchinson, 1973a, Kim et al., 2020, Lombardo, 2013, Schaeffer, 1984, Schaeffer and Mc Donald, 1978, Sytchevskaya et al., 2009). Their general features include an elongated body covered with ganoid scales, the dorsal and anal fins located posteriorly, and a hemi-heterocercal caudal fin. The prominent snout, which can be ornamented with ridges and/or tubercles, is formed by nasals, premaxillo-antorbitals, a rostral and usually a postrostral. The nasal is usually excluded from the orbital rim by the supraorbital, and the single pair of nostrils are surrounded by the nasal, supraorbital, premaxillo-antorbital and rostral. Other features of the skull concern the presence of a large and rectangular dermopterotic, a rectangular or crescent-shaped dermosphenotic, a hatchet-shaped preopercle, and a single (rarely two) plate-like branchiostegal ray [Gibson, 2018, Hutchinson, 1973a, Schaeffer, 1984]. Extensive studies and cladistic analyses

have been performed by Hutchinson [1973a, 1978], Schaeffer [1967, 1984] and Schaeffer and Mc Donald [1978], and the monophyly of the group is currently not questioned. Its phylogenetical position among actinopterygians remains unclear and Xu [2020] suggested to consider it as stem-Neopterygii related to Pholidopleuriformes. In Africa, redfieldiiforms have been reported in the Lopingian Madumabisa shales in Zambia (*Ischnolepis*, Haughton, 1934, Hutchinson, 1973a), but they are mostly known from the Anisian of the Upper Beaufort series in South Africa (*Atopocephala*, *Daedalichthys*, *Denwoodichthys* and *Helichthys*, Brough, 1931, 1934, Hutchinson, 1973a, Sytchevskaya et al., 2009) and from the Carnian of the Argana Basin in Morocco (*Mauritanichthys*, cf. *Ischnolepis* and cf. *Atopocephala*, Martin [1979a, 1980b, 1982], see Discussions below for the last two).

Mauritanichthys rugosus Martin [1980b] (Figure 2A–D)

Holotype. MNHN.F.ALM 312, specimen with missing posterior part and incomplete skull.

Referred material. MNHN.F.ALM 313, 314, 315, incomplete bodies.

Description. The specimens ALM 312 and ALM 313, the most complete, reach 11–12 cm in length, corresponding to an estimated standard length of 15 cm. The body is fusiform, covered with ganoid scales, and was apparently five to six times longer than deep. The pectoral fin is in ventral position. The pelvic fin is located midway between the pectoral and anal fins. The dorsal and anal fins are incompletely known and, although no specimen shows the posterior extremity of the body, they were probably located very posteriorly, owing to the dorsal and ventral outlines of the body. The caudal skeleton is unknown.

The skull is incompletely preserved in all specimens and then can only be partly reconstructed. The snout region, very damaged, is ornamented with tubercles. The postrostral separates the nasals, at least in their posterior portion. More anteriorly, tubercle marks on the sediment correspond to the position of the rostral. The skull roof, mainly observed on the holotype, is ornamented with tubercles and ridges. It is formed by a large pair of parietals ("frontals" sensu Martin, 1979a, 1980b, 1982) and a pair of wider than long trapezoidal postparietals ("parietals" sensu Martin, 1979a, 1980b, 1982). The dermopterotic is rectangular, lying ventrally along the postparietal and the posterior part of the parietal. The dermosphenotic is also rectangular, longer than deep, and forms a large part of the dorsal edge of the orbit. The reconstruction proposed by Martin [1979a, 1980b, 1982]) for the other bones of the skull roof and the orbital region cannot be confirmed herein.

The morphology of the opercular series and jaws are mostly known from the specimen ALM 314 (Figure 2C,D). The subopercle (Sop, Figure 2D) and the opercle (Op., Figure 2D) are both deeper than long, anteriorly inclined and almost comparable in size. Their surface is slightly ornamented with horizontal to radial ridges. The anterodorsal part of the opercle is damaged and the presence of an antopercle cannot be assessed. The preopercle (Pop, Figure 2D) is hatchet-shaped, with two limbs forming a right angle. Its dorsal limb, incompletely preserved, is massive and anteriorly in contact with the jugal (i.e., the infraorbital edging posteroventrally the orbit). It is surrounded ventrally by the maxilla and dorsally by the dermohyal and the dermopterotic (this last contact is visible on the specimen ALM 313).

The dermohyal (Dh, Figure 2D) is only known by its triangular ventral tip, alongside the anterior border of the opercle and the posterodorsal margin of the preopercle. A large circular branchiostegal ray (B.r, Figure 2D) lies close to the subopercle and the mandible.

The maxilla (Mx, Figure 2D) is anteriorly tapered and posteriorly expanded, without any posteroventral process. It is ornamented with longitudinal ridges. Its anterior part extends to the snout and bears small and sharp teeth. The posterior part bears a dorsal expansion, in close contact with the anteroventral margin of the preopercle and the jugal. The lower jaw is formed by a deep angular (Ang, Figure 2D), with faint ornamentation, and by an elongated dentary (De, Figure 2D) marked by strong longitudinal ridges. The oral border of the dentary is not apparent and no teeth can be observed.

The infraorbital series is incompletely preserved. The jugal (Ju, Figure 2D) is tear-shaped, with a large and rounded posterior part. Its surface is ornamented with radial ridges.

The cleithrum is only known by incomplete remains. The supracleithrum (Scl, Figure 2D) is very deep and it extends along the opercle and a large

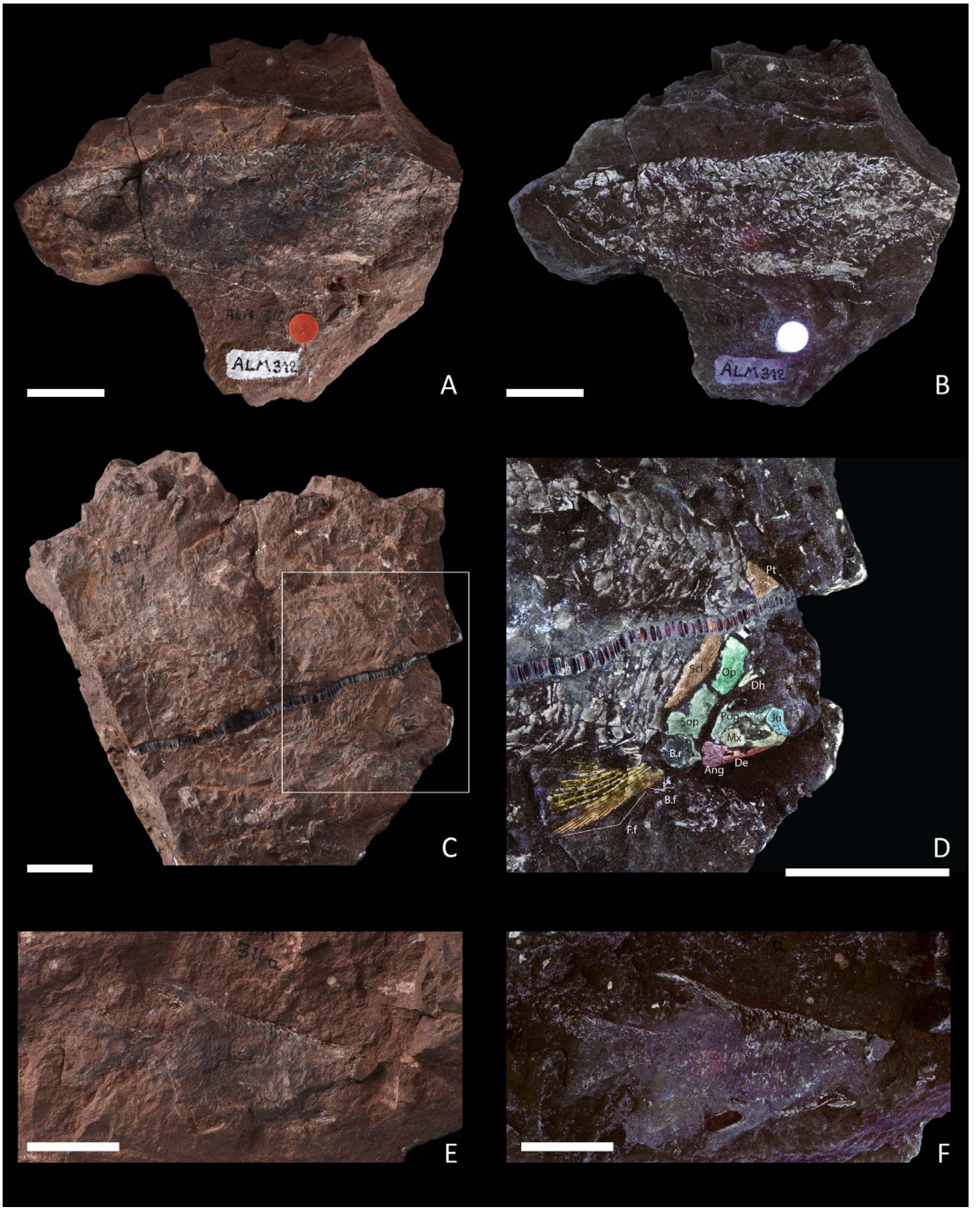

Figure 2. (A–D). *Mauritanichthys rugosus* Martin [1980b]. (A,B) MNHN.F.ALM 312, holotype, under white (A) and UV (B) lights. (C) MNHN.F.ALM 314, under white light, (D) MNHN.F.ALM 314, close up of the skull, with labeled and colored bones, under UV light. (E,F) Redfieldiiformes indet., formerly referred to cf. *Ischnolepis* [Martin, 1979a, 1982]). MNHN.F.ALM 311a, under white (E) and UV (F) lights. Abbreviations: Ang, angular; B.f, basal fulcra; B.r, branchiostegal ray; De, dentary; Dh, dermohyal; F.f, fringing fulcra; Ju, jugal; Mx, maxilla; Op, opercle; Pop, preopercle; Pt, post-temporal; Scl, supracleithrum; Sop, subopercle. Scale bars: 20 mm.

part of the subopercle. It is ornamented with well-marked longitudinal ridges. The post-temporal (Pt, Figure 2D) is triangular, longer than deep although its anterior part is not entirely preserved. It is ornamented with rugae. The pectoral fin comprises at least 10–12 rays, which are unsegmented proximally, their distal part being not well preserved. The fin is preceded by two basal fulcra (B.f, Figure 2D) and the first two rays support a dozen of fringing fulcra (F.f, Figure 2D). The pelvic fin is represented by remains corresponding to 7 to 8 rays, preceded by scutes.

Only a few rays of the dorsal fin are preserved. The anal fin comprises at least 20 rays, including segmented and distally branched ones.

The body is covered with ganoid scales arranged in at least 35 rows from the pectoral girdle region to middle of the anal fin. As suggested by Martin [1979a, 1980b, 1982]), more than 40 rows should be present. The most anterior flank scales are deeper than long, while they are rhomboid in the rest of the body. All scales have a unornamented surface and a smooth posterior border.

Discussion. *Mauritanichthys rugosus* can be referred to Redfieldiiformes based on the presence of a single plate-like branchiostegal ray, hatchet-shaped preopercle, large and rectangular dermopterotic, rectangular dermosphenotic, skull bones and snout ornamented with tubercles and ridges. Redfieldiiformes usually possess a well-developed dermosphenotic, which can be narrow and crescent-shaped (as in *Atopocephala*, *Schizurichthys*, *Ischnolepis*, *Brookvalia*, *Phlyctaenichthys*, *Calaichthys* and *Denwoodichthys*, most of them formerly included in the Brookvaliidae and Schizurichthyidae, sensu Hutchinson, 1973a) or as developed as the dermopterotic. This latter condition, considered as derived according to Schaeffer [1984], is present in *Mauritanichthys* and in the South African genera *Daedalichthys* and *Helichthys*, the Autralian *Geitonichthys* and *Molybdichthys*, and the North American *Cionichthys*, *Lasalichthys*, *Dictyopyge* and *Redfieldius* [Gibson, 2018, Hutchinson, 1973a, 1978, Schaeffer, 1967, 1984, Schaeffer and Mc Donald, 1978]). Among these, *Molybdichthys*, *Cionichthys* and *Lasalichthys* share with *Mauritanichthys* a pectoral girdle ornamented with parallel ridges, and unornamented scales with smooth posterior border (except *Cionichthys greeni* which possesses posteriorly denticulated scales, see Schaeffer, 1967). *Mauritanichthys* differs from all these genera by the exclusive combination of the following features: the opercle and subopercle deeper than long, the marked anterior contact of the preopercle with the jugal, the anteriormost flank scales significantly deeper than long, and the contact between the preopercle and the dermopterotic.

Martin [1980b] closely linked *Mauritanichthys* to *Lasalichthys*, noting that the latter differs by the postrostral less reduced in size, the triangular shape of postparietal and the absence of preopercle/dermopterotic contact. He insisted to maintain the validity of *Mauritanichthys* and *Lasalichthys* by considering the postrostral size variability as a generic diagnostic feature. As a result, he avoided putting also in synonymy *Lasalichthys* and *Synorichthys*, which also mainly differ by the postrostral condition, reduced in *Lasalichthys* and absent in *Synorichthys*. On the contrary, Gibson [2018] considered the absence or presence of a reduced postrostral as intrageneric variability and placed *Synorichthys* into synonymy with *Lasalichthys*. From the three features used by Martin [1980b] to distinguish *Mauritanichthys* from *Lasalichthys*, the postrostral dimension cannot be herein confidently described in *Mauritanichthys* (see above) and the contact between the preopercle and the dermopterotic is possibly present in specimens referred to *Lasalichthys* (see Gibson [2018]: Figure 6). Thus, the differences between *Mauritanichthys* and *Lasalichthys* seem to be restricted to the shape of the postparietal (trapezoidal in the former and triangular in the latter) together with the aforementioned combination of features which includes the opercle and subopercle deeper than long, the marked anterior contact of the preopercle with the jugal and the anteriormost flank scales significantly deeper than long. These elements are considered sufficient to maintain the validity of the genus *Mauritanichthys*.

Redfieldiiformes indet. (Figure 2E, F)
1979a, 1982 cf. *Ischnolepis*, Martin

Referred material. MNHN.F.ALM 310, 311, subcomplete specimens.

Discussion. Martin [1979a, 1982] doubtfully related two specimens from the Argana Basin to *Ischnolepis*,

mainly on the basis of the cranial bones. The only described species of the genus is *Ischnolepis bancrofti* Haughton [1934], known by a few specimens originating from an imprecise locality in Lunsemfwa Valley, Madumabisa shales, in Zambia. The age of the locality was debated but it is most likely to be Lopingian (see Discussion in Barbolini et al. 2016a,b, Haughton 1934, Hutchinson 1973a, Jubb and Gardiner 1975, Murray 2000), which makes *Ischnolepis* the only known Palaeozoic redfieldiiform.

Although subcomplete, both Argana specimens are poorly preserved and only the general body proportions, fin morphology, and the shape and ornamentation patterns of a few bones can be confidently reconstructed. Based on the descriptions, reconstructions and photographs in Haughton [1934] and Hutchinson [1973a], *I. bancrofti* shares with the two Argana specimens a well-developed pelvic fin, long-based anal fin, oblique opercular series with a small opercle, cleithrum ornamented with ridges, and anteriorly placed orbit. However, none of these features is exclusive to these two taxa, which significantly differ on the general proportions of the body and fins. The body of *I. brancrofti* is 3.5–4 times longer than deep, and the head is about one fifth of the body length, while the Moroccan specimens have a body less elongated, only 2.5 times longer than deep, and their head length is about one quarter to one third the body length. Another difference concerns the relative position of the unpaired fins. In *I. bancrofti*, the dorsal fin front is nearly opposite to the anal fin front, which is considered by Xu [2020] as a derived feature supporting the clade formed by the Pholidopleuriformes and Redfieldiiformes. On the contrary, the Argana specimens show a dorsal fin front located well anteriorly to the anal fin front, almost reaching the level of the pelvic fin front, a conformation also encountered in the redfieldiiforms *Brookvallia spinosa* and *Phlyctaenichthys* [Hutchinson, 1973a, Wade, 1935]. The anal fin of the Argana specimens clearly shows fringing fulcra while the presence of these latter cannot be confirmed in *I. bancrofti*. A small portion of the cleithrum of ALM 311 (Figure 2E,F) shows an ornamentation with longitudinal grooves, which corresponds to the description of *Ischnolepis* by Haughton [1934], while Hutchinson [1973a] described the cleithrum of *Ischnolepis* as covered by fine grooves with rows of tiny tubercles.

The skull morphology of the two Argana specimens fits well with the Redfieldiiformes diagnosis, with a hatchet-shaped preopercle and a probable crescent-shaped dermosphenotic. Nevertheless, the body and fin proportions are different from those of all known redfieldiiforms, including *Mauritanichys* from the Argana Basin, and *Ischnolepis*. These two specimens, which probably correspond to the same species, are considered as Reldfiediiformes indet.

4. “Perleidiforms”

“Perleidiforms” are a paraphyletic assemblage constituted by Triassic to Early Jurassic stem-neopterygian families. They are known in marine and continental environments, in an almost cosmopolitan distribution, with occurrences in Africa, North and South America, Europe (including Greenland), China and Australia [Bürgin, 1992, Hutchinson, 1973a, López-Arbarello and Zavattieri, 2008, Sun et al., 2009]. Together with the Peltopleuriformes, they were previously referred to the grade “subholosteans”, mainly characterized by a hemiheterocercal caudal fin with epaxial rays, flank scales deeper than long, vertical or almost vertical preopercle (usually still in contact with the maxilla), and an equal ratio between radials and lepidotrichia. “Perleidiforms” differ from peltopleuriforms by a larger and wedge-shaped preopercle, a supraorbital sensory canal entering in the postparietals, different squamation pattern (with thick and subrectangular to rhomboid scales, deeper than long only in the anterior trunk region), and tooth morphology, with peg-like marginal teeth and crushing inner ones [Lombardo and Brambillasca, 2005, Schaeffer, 1956, Sun et al., 2012, 2013, Tintori and Lombardo, 1996]. They show a great morphological diversity, with elongated to deep-bodied forms (e.g., Bürgin, 1992, Lombardo and Tintori, 2004). In the Argana Basin, Martin [1979a, 1980a, 1982] described a new species of *Dipteronotus*, *D. gibbosus*, and referred with caution five specimens to the genera *Perleidus* and *Procheirichthys*. Recently, Xu [2020] investigated the phylogenetical relationships of several neopterygian taxa and proposed to use the clades Platysiagiformes (Platygiasidae), Polzbergiiformes (Polzbergiidae and Cleithrolepididae) and Louwoichthyiformes (Pseudobeaconiidae, including *Dipteronotus*, and Louwoichthyidae) to include

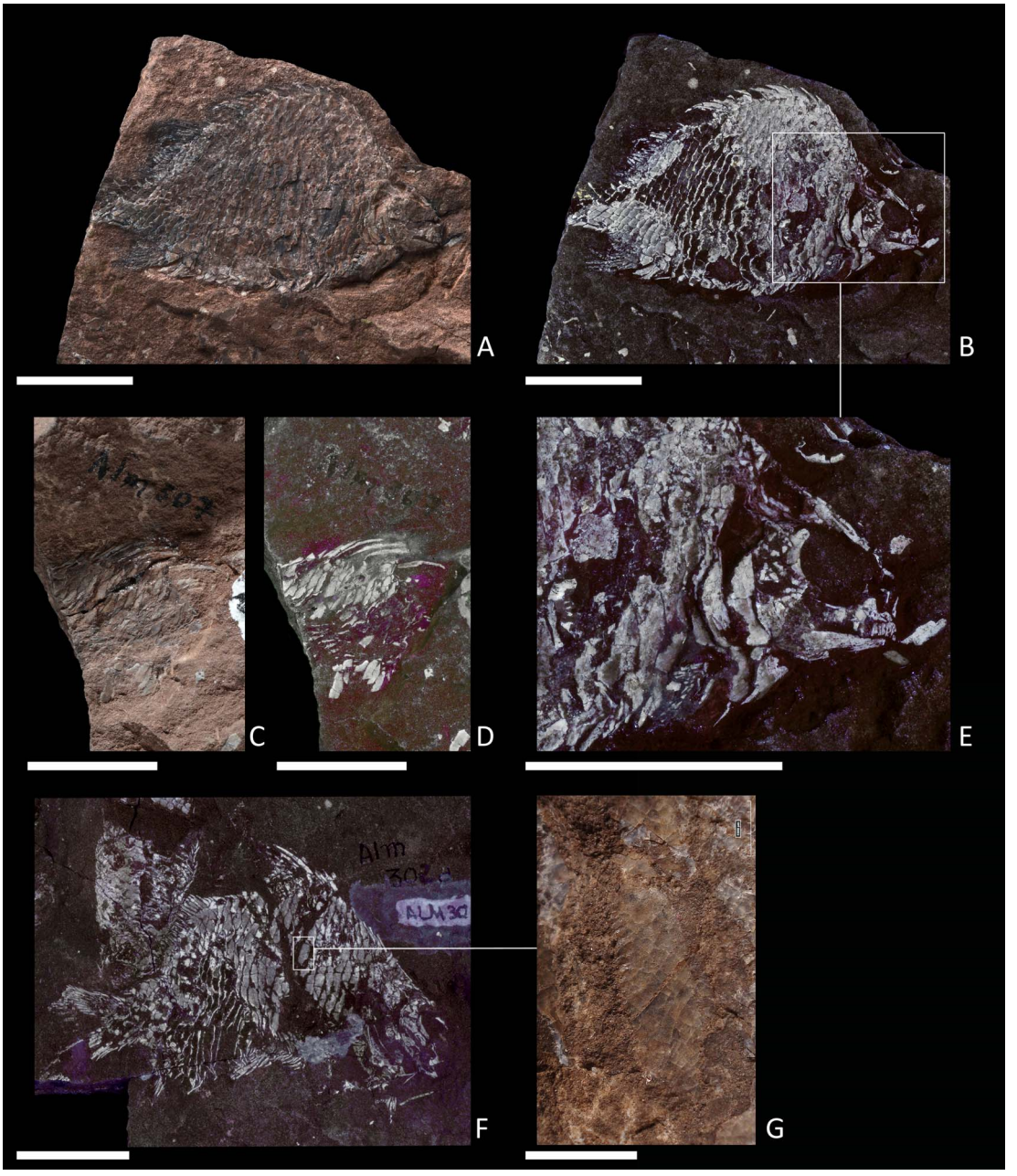

Figure 3. *Dipteronotus gibbosus* Martin, 1980a. (A,B) MNHN.F.ALM 301b, holotype, under white (A) and UV (B) lights. (C,D) MNHN.F.ALM 307, under white (C) and UV (D) lights. (E) Close-up of the skull of MNHN.F.ALM 301b, under UV light. (F) MNHN.F.ALM 302a, under UV light. (G) MNHN.F.ALM 302a, close-up view of one scale, under white light. Scale bars: 20 mm (A–F), 2 mm (G).

several "perleidiform" genera. Although based on a cladistic analysis, this nomenclature is not followed herein because of doubts on the position of *Dipteronotus* (see Discussion).

Dipteronotus gibbosus Martin [1980a] (Figure 3)

Holotype. MNHN.F.ALM 301a,b, subcomplete specimen, part and counterpart.

Referred material. MNHN.F.ALM 302a,b, subcomplete specimen, part and counterpart; MNHN.F.ALM 303 (not seen), 307, 308, 309 (with doubt), incomplete bodies. The specimens ALM 306 and 322, doubtfully referred by Martin [1979a, 1982]) to the species, are not retained herein.

Description. The body is deep, ca. 1.7 times longer than deep on the holotype ALM301a,b, which measures 6 cm in standard length for a total depth of 3.6 cm (3.4 cm excluding the elongated dorsal spine-like ridge scales). The head is slightly deeper than long and its length is little less than a quarter of the standard length. The dorsal and anal fins are posteriorly located, the dorsal fin being longer with a front located more anteriorly than the anal. The body is covered by ganoid scales and its dorsal outline shows a marked hump located immediately behind the skull. This hump is extended on the anterior half of the body and is curved or with a marked angle, depending on specimens (Figure 3A–D,F, see Discussion). It is covered by elongated spine-like ridge scales ("first dorsal fin" sensu Gall et al., 1974, Martin, 1979a, 1980a, 1982, see Discussion in Tintori, 1990).

The skull roof is incompletely preserved. The parietal ("frontal" sensu Martin, 1979a, 1980a, 1982) covers most of the orbit. It is visible in section and is ornamented with tubercles. Imprints of the postparietal ("parietal" sensu Martin, 1979a, 1980a, 1982), dermopterotic and extrascapular are present, but without any accurate delimitations between bones. As noted by Martin [1979a, 1982], the rostral region of the skull is markedly anteroventrally curved. The orbit is large. The preopercle is only known by its ventral part, the dorsal part being either not preserved or fragmented in the available material. It is almost vertical, according to the position of the orbit and the opercle, and to the course of the slightly curved preopercle sensory canal (visible on ALM 302a, Figure 3F). Its ventral part is posteriorly bordered by the subopercle and anteroventrally by the maxilla. The opercle is ovoid. The subopercle is deeper than long, roughly twice deeper than the opercle; its anterior margin is concave.

The maxilla has a well-developed posterior part, with dorsal and ventral expansions, and a straight and thinner anterior part. As reported by Martin [1982], a premaxilla could be present, but with no clear evidence. Teeth are limited to the anteriormost half of the upper jaw. They are peg-like, long, slender and tightly packed. The mandible is massive with well-marked posterior part and symphysis. It does not bear teeth on the holotype but the specimen ALM 309, putatively attributed to *D. gibbosus*, shows dentary teeth which are acute and tightly packed.

The cleithrum and supracleithrum are unornamented. The cleithrum shape can be described from its imprint on ALM 301a. It is arched, with a slightly posterior protrusion between the dorsal and ventral branches. The supracleithrum and post-temporal are damaged. The pectoral fin contains at least 8–10 rays, with fringing fulcra on the leading rays (as observed on ALM 302a, Figure 3F). The pelvic fin possesses at least 5 rays.

Scales are arranged in 32 or 33 anteriorly inclined rows. No ornamentation can be observed on their surface, but the posterior margin, when preserved, shows a dentate edge (Figure 3G). Scales of the flank are deeper than long, and those located around the dorsal and anal fins are smaller and more irregularly distributed. Scales at the level of the caudal peduncle are almost rhomboid. The dorsal and ventral body midlines are covered by a series of spine-like ridge scales, which are elongated along the dorsal hump. On the holotype, the dorsal hump is curved and covered by ten moderately elongated spine-like ridge scales, posteriorly oriented (Figure 3A,B). On the specimens ALM 302a,b, 307 and 308 the hump outline shows a more marked angle and the spine-like ridge scales are slenderer (Figure 3C,D,F). These variations in size and shape could be related to ontogeny or sexual dimorphism (see Discussion). Ventrally, the spine-like ridge scales located in front of the anal fin are also well developed, without reaching the size of the dorsal ones. No distinction is made herein between ridge scales and scutes.

The dorsal fin is extended from the 23rd to the 29–30th rows of scales, and reaches the level of the caudal peduncle. Three fulcra of increasing size and at least 17–18 rays are present. However, the distinction between basal fulcra, ridge scales and even first rays is uneasy, especially when the rays are unsegmented or when only the proximal segment is preserved. No fringing fulcra can be observed, possibly because of a lack of preservation of the distal part of the first rays.

The anal fin contains at least 15 rays, formed by an unsegmented proximal part, shorter than those of

the dorsal fin rays and by a segmented and branched distal part. However, the branching pattern cannot be accurately described. The posterior part of the fin is not preserved. As for the dorsal fin, no fringing fulcra is observed, possibly due to the poor preservation of the distal portion of the leading rays.

The caudal fin is deeply forked and hemiheterocercal in configuration, with a short axial body lobe. The fin contains about 24 rays, including 4 or 5 in epaxial position. The rays are segmented but no pattern of branching can be described since their distal extremity is not preserved. The upper lobe of the fin is preceded by one or two scutes and two to three basal fulcra, whereas the lower lobe is preceded by three or four scutes and two basal fulcra, but the distinction between first rays and basal fulcra is unclear. No fringing fulcra is observed.

Discussion. The genus *Dipteronotus* comprises three Middle Triassic (Anisian–Ladinian) European species, *D. cyphus*, *D. aculeatus* and *D. olgiatii* [Egerton, 1854, Gall et al., 1974, Jörg, 1969, Milner et al., 1990, Tintori, 1990, Tintori et al., 2016]. The main generic feature is the presence of a dorsal hump covered with elongated spine-like ridge scales, with a well-marked angle immediately posteriorly to the last elongated ridge scale. A fourth European species, "*Dipteronotus*" *ornatus* Bürgin, 1992, was described from the Middle Triassic of Monte San Giorgio, but shows a hump with reduced ridge scales. This species was removed from *Dipteronotus* by Lombardo and Tintori [2004] and included in the genus *Stoppania* by Lombardo et al. [2008].

Based on the presence of a dorsal hump covered by elongated spine-like ridge scales, Martin [1979a, 1980a, 1982] attributed the Argana specimens to the genus *Dipteronotus*, and erected the species *D. gibbosus*. However, noting that the Moroccan species differs by its curved dorsal hump and the head proportions, he emended the diagnosis of *Dipteronotus* of Gall et al. [1974] by replacing "dorsal outline of the body showing a marked angle" by "showing a curve or a marked angle" and "head height comprised at least 3 times in the body height" by "at least 2.5 times". Tintori [1990] rejected this emendation, and consequently the attribution of the Moroccan form to *Dipteronotus*, considering the sharp angle of the hump behind the last elongated spine-like ridge scale as "the most striking character of *Dipteronotus* itself". He suggested close relationship of the Moroccan form with *Pseudobeaconia*.

As in *Dipteronotus aculeatus*, the body shape of *D. gibbosus* shows a significant intraspecific variability, possibly related to ontogeny (Jörg, 1969: Figures 1–2; Gall et al., 1974: 138–139, pl. IIIc; Martin 1979a, 1982). Gall et al. [1974] discussed these variations and pointed out the presence of a marked angle on the hump of *D. aculeatus* in deeper specimens, when the hump outline is more curved in a slenderer specimen, presumably juvenile. In *D. gibbosus*, Martin (1979a: 98–99; 1982: 359) described one or two possible young specimens (ALM 306 and 322) but their identifications are doubtful and they are not considered herein. However, two specimens (ALM 302a,b and 307) show a dorsal hump with a more marked angle than in the holotype. ALM 302a,b (Figure 3F) is deformed and ALM 307 (Figure 3C,D) is very incomplete, but they clearly show a marked angle immediately posteriorly to the last elongated spine-like ridge scale. When compared to the holotype, these two specimens also show more elongated spine-like ridge scales, closer in shape to those of the European *Dipteronotus* species. Another specimen from the Argana Basin, ALM 308, possesses comparable spine-like ridge scales but the dorsal hump outline cannot be retraced. In these respects, the dorsal ridge scales and the dorsal hump of *D. gibbosus* do not significantly differ from those of the other species of the genus; *D. gibbosus* is thus maintained in *Dipteronotus*. The holotype ALM 301a,b, with a smooth curved hump, probably corresponds to a subadult specimen or shows sexual dimorphism.

D. gibbosus differs from *D. cyphus*, *D. aculeatus* and *D. olgiatii* by meristic features, body proportions, and by the subopercle significantly deeper than the opercle (instead of being of about same size in *D. olgiatii*, the situation is confused in the other species, see Gall et al., 1974, Lombardo and Tintori, 2004, Tintori, 1990, Woodward, 1910). In all *Dipteronotus* species, the scale surface is smooth, and the posterior border is serrate in *D. cyphus*, *D. gibbosus* and *D. aculeatus* (Figure 3G; Gall et al., 1974:133, Woodward, 1910) while it shows a single spine-like process in *D. olgiatii* [Tintori, 1990]. The head height to body height ratio is variable among species, but also among individuals. Gall et al. [1974] diagnosed *Dipteronotus* (*D. aculeatus* and *D. cyphus*) with a body height at least 3 times the head height, and

they noticed intraspecific variability in *D. aculeatus*. The holotype of *D. gibbosus* shows a body height about 2.5 times the head height, which led Martin [1979a, 1980a, 1982]) to modify the generic diagnosis (see above). This ratio slightly differs in ALM 302a,b (Figure 3F). In *D. olgiatii*, the body height is less than 2.2 times the head height, but the original description is based on a single specimen. This ratio is too variable to be reliably used as diagnostic for the genus.

The genus *Dipteronotus* was usually considered as a Perleididae or a Cleithrolepididae (see Bürgin, 1992, López-Arbarello and Zavattieri, 2008, Milner et al., 1990, Sun et al., 2012, Tintori, 1990, Tintori et al., 2016, Wade, 1935). Recently, Xu [2020] related it to Pseudobeaconiidae, a family erected by López-Arbarello and Zavattieri (2008, see also López-Arbarello et al., 2010) to include *Pseudobeaconia* and *Mendocinichthys*, both from the Late Triassic of Argentina. A similar view was proposed by Hutchinson (1973b: 18–19), who suggested to link "*Praesemionotus*" (=*Dipteronotus*) *aculeatus*, *Pseudobeaconia* and "*Mendocinia*" (=*Mendocinichthys*). All these taxa share the presence of a series of dorsal spine-like ridge scales between the skull and the dorsal fin. However, *Pseudobeaconia* and *Mendocinichthys* only show reduced dorsal spine-like ridge scales and possess no dorsal hump. Moreover, among the diagnosis of the family [López-Arbarello and Zavattieri, 2008], the elongated body is 2–3.5 times longer than deep, the dorsal and anal fins are equal or almost equal in size, and the scales are ornamented with marginal concentric ridges of ganoine and possess a smooth border. *Dipteronotus* differs by the deeper shape of its body, the dorsal fin longer than the anal fin, and the absence of scale ornamentation, except for the posterior border, which is not smooth. The inclusion of *Dipteronotus* into Pseudobeaconiidae, which would require deep changes on the diagnosis of the family, is not followed herein.

Dipteronotus gibbosus shows superficial resemblances with the deep-bodied "perleidiforms" *Stoppania*, *Felberia*, *Cleithrolepidina, Cleithrolepis* and *Hydropessum*. It differs from these taxa by the dorsal elongated spine-like ridge scales. It also differs from *Stoppania* and *Felberia* by the absence of ornamented scales, from *Cleithrolepidina* and *Cleithrolepis* by its deeper dentary and the tooth morphology and from *Hydropessum* by the lack of ornamentation of the opercular series and pectoral girdle [Hutchinson, 1973a, Lombardo and Tintori, 2004]. *D. gibbosus* shares with *Stoppania ornata* and *Felberia* the reduced scales at the basis of the dorsal and anal fins. This feature is unknown (absent or undescribed) in the European species of *Dipteronotus*.

From this comparison, the Moroccan form strongly differs and cannot be related to pseudobeaconiids and to the deep-bodied "perleidiforms" *Stoppania*, *Felberia*, *Cleithrolepidina, Cleithrolepis* and *Hydropessum*. It shares the synapomorphies of *Dipteronotus*, including a hump showing a marked angle and covered by elongated spine-like ridge scales; consequently, it constitutes a valid species of this genus.

Actinopterygii indet. The three following taxa cannot be confidently referred or related to any actinopterygian clade.

Actinopterygii indet. sp. 1 (Figure 4A,B)
1979a, 1982 cf. *Procheirichthys*, Martin

Referred material. ALM 317, 318, 320, articulated post-cranial bodies; ALM 319a,b, post-cranial body with incomplete skull and pectoral girdle, part and counterpart (missing from MNHN.F collection).

Discussion. Martin [1979a, 1982] included these four specimens in *Procheirichthys*, a monotypic genus known by a single specimen of *P. ferox* from the Anisian of Hawkesbury Sandstone, Brookvale, Australia [Hutchinson, 1973a, Wade, 1935]. The Argana specimens share with *Procheirichthys* the dorsal and anal fins of limited extent, located in the last third part of the body and preceded by basal and fringing fulcra, and the caudal skeleton with epaxial rays. Based on the descriptions of Wade [1935], Hutchinson [1973a], Martin [1979a, 1982]) and Frickhinger [1995], they also share a somewhat similar squamation, with smooth scales of moderate size, and an anal fin with the most proximal ray segment longer than the following ones. Except the size, the Argana specimens being considerably smaller (7 cm) than *P. ferox* (16.3 cm), the differences between these two forms are weak. The anal fin of the Argana specimens possesses more rays and is more posteriorly extended. Due to the almost total absence of skull,

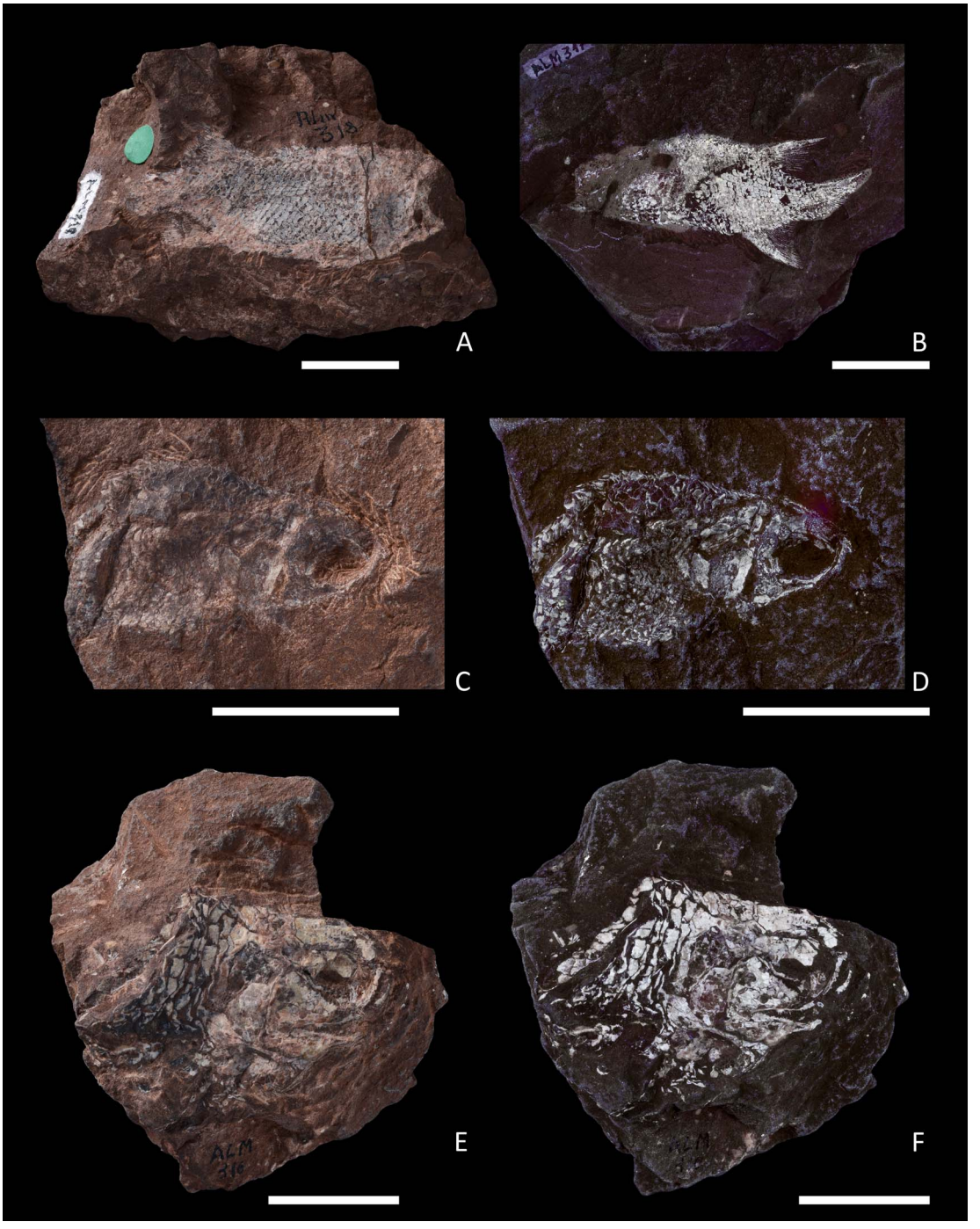

Figure 4. (A,B) Actinopterygii indet. sp. 1, formerly referred to cf. *Procheirichthys* [Martin, 1979a, 1982]. (A) MNHN.F.ALM 318, under white light. (B) MNHN.F.ALM 317, under UV light. (C,D) Actinopterygii indet. sp. 2, formerly referred to cf. *Atopocephala* [Martin, 1979a, 1982], MNHN.F.ALM 321, under white (C) and UV (D) lights. (E,F) Actinopterygii indet. sp. 3, formerly referred to cf. *Perleidus* [Martin, 1979a, 1982], MNHN.F.ALM 316, under white (E) and UV (F) lights. Scale bars: 20 mm.

the precise proportions of the Argana specimens are unknown but they seem slightly less deep than *Procheirichthys*, and the unpaired fins are located slightly more posteriorly.

The only known cranial features were described by Martin [1979a, 1982] from a specimen not studied herein (ALM 319a,b, missing from the MNHN.F collection) in which the skull material is limited to the opercular series, a small portion of the maxilla and the branchiostegal rays. Post-cranial features like the moderately elongated body and the dorsal and anal fins posteriorly located and in almost opposite position are also encountered, to some degree, in different Triassic actinopterygians, such as the pseudobeaconiid *Mendocinichthys*, the "perleidiforms" *Fuyuanperleidus* and *Manlietta*, and various redfieldiiforms. These taxa differ from the Argana specimens by meristic features of the fins and scale rows. *Mendocinichthys* also differ by the presence of small spine-like ridge scales between the skull and dorsal fin and *Fuyuanperleidus* by the very deep series of flank scales [López-Arbarello and Zavattieri, 2008, Sun et al., 2012]. According to the skull description of ALM 319a,b by Martin [1979a, 1982], *Manlietta* also differs by the opercular series proportions [Hutchinson, 1973a] and redfieldiiforms by the presence of one or two plate-like branchiostegal rays. These Argana specimens are herein considered as Actinopterygii indet.

Actinopterygii indet. sp. 2 (Figure 4C, D)
1979a, 1982 cf. *Atopocephala*, Martin

Referred material. MNHN.F.ALM 321, subcomplete specimen.

Discussion. This single small specimen was referred with caution to the redfieldiiform *Atopocephala* by Martin [1979a, 1982]. It is subcomplete but preserved folded up on itself. Except squamation and part of the pectoral girdle, few post-cranial features can be observed. The skull is incomplete and well exposed.

The genus *Atopocephala* comprises the single species *A. watsoni* Brough, 1934, described on the basis of a unique specimen from the Anisian of Karoo Series, at Bekkerskraal, South Africa [Hutchinson, 1973a, López-Arbarello, 2004]. As noticed by Martin [1979a, 1982], the skull of ALM 321 shows several similarities with *Atopocephala*, the most important of which are the well-developed parietal ("frontal" sensu Martin [1979a, 1982]) and the strong opercle (in Martin [1982], "strong preopercle" in Martin [1979a]). To these can be added the curved upper jaws, large and anteriorly placed orbit, ornamentation of cranial dermal bones with tubercles, maxilla close to the ventral border of the orbit, and presence of longitudinal ridges on the pectoral girdle. However, none of these features or their combination is specific to *Atopocephala*. Differences between ALM 321 and *Atopocephala* concern the subopercle, significantly larger than the opercle in the former while the opercle is the largest in the latter. As highlighted by Martin [1979a, 1982], *Atopocephala* differs also by the less developed opercular series and pectoral girdle. The backwardly directed spines on the opercle and subopercle, distinctive of *Atopocephala*, cannot be confidently confirmed on ALM 321, in which the posterior part of the opercular series is damaged. Martin [1979a, 1982] interpreted tenuous imprints on the pectoral girdle as possible subopercle spines but this view is not shared herein.

One of the most striking features of ALM 321 is the upwardly curved upper jaw, a morphology reminiscent of the condition observed in *Atopocephala* and, to a certain extent, in various short snouted redfieldiiforms such as *Dictyopyge*, *Helichthys*, *Geitonichthys*, and *Molybdichthys* [Hutchinson, 1973a, Schaeffer, 1984]. In ALM 321, the presence of a premaxilla is unclear, but the anterior part of the upper jaw is flanked or extended by a bone ornamented with denticles. Identified as the antorbital by Martin [1979a, 1982], it constitutes an important part of the snout and possibly a portion of the anterior edge of orbit. It is evocative in shape and position of the "antorbital", "premaxilla" or "premaxillo-antorbital" of various redfieldiiforms, in which teeth–bearing bone and bone ornamentated with denticles can be confused. However, the preservation of ALM 321 is not sufficient to confidently relate it to Redfieldiiformes; this specimen is herein considered as Actinopterygii indet.

Actinopterygii indet. sp. 3 (Figure 4E, F)
1979a, 1982 cf. *Perleidus*, Martin

Referred material. ALM 316, skull with partial pectoral girdle and squamation.

Discussion. This single specimen consists of a skull with several missing areas, associated to an incomplete pectoral girdle and the very first scale rows. Martin [1979a, 1982] related it to *Perleidus* on the basis of the proportion of the skull and the deepness of the cleithral scales. He emphasized features shared with "*Perleidus*" *madagascariensis* and "*Perleidus piveteaui*", from the Early Triassic of Madagascar, such as the infraorbital inserting between the suborbital ("preopercle" in Martin, 1979a) and the maxilla, the square postparietal, and the proportion of the mandible. Lombardo [1995] questioned this identification owing to the limited preservation of the Moroccan specimen. The two Malagasy "*Perleidus*" species were recently reviewed, synonymized, included in the genus *Teffichthys* and excluded from Perleididae by Marramà et al. [2017]. ALM 316 differs from *Teffichthys* and perleidids in particular by the shape of the preopercle, hatchet-shaped and in contact with the anterodorsal edge of the maxilla in the Moroccan specimen while it is deeper and usually in contact only with the posterodorsal edge of the maxilla in the two other taxa (note that the preopercle shape shows a sizeable intraspecific variability in *Teffichthys*, see Marramà et al., 2017: Figure 4). The first scales beyond the two or three first rows are moderately deeper than long in ALM 316 instead of being several times deeper than long as it is in perleidids and several specimens of *Teffichthys*. Another important difference is the shape of the jaw, which is curved upward anteriorly in ALM 316; oral margins of the maxilla and dentary are straight in *Teffichthys* and perleidids.

Such curved jaws are reminiscent of the Argana specimen ALM 321, related with caution to the redfieldiiform *Atopocephala* by Martin ([1979a, 1982] but considered herein as an indeterminate actinopterygian), and also of various redfieldiiforms. The "nasal" (sensu Martin, 1979a, 1982) of ALM 316 is also evocative of the "antorbital" of ALM 321 (sensu Martin, 1979a, 1982) by its position, edging anteriorly the orbit, and its ornamentation, with strong denticles. However, in ALM 316, a small bone edging anteroventrally the orbit and bearing what appears to be the tripartite canal should correspond to the antorbital. Portions of sensory canals present on the parietal and the preopercle of ALM 316 show a double row of pores, which is an uncommon feature among actinopterygians, but known in the redfieldiiform *Lasalichthys* [Gibson, 2018, Schaeffer, 1984]. Other features of Redfieldiiformes, like the single branchiostegal ray and the skull roof ornamented with ridge and/or tubercles, are not directly observed in ALM 316. Martin [1979a] identified numerous branchiostegal rays but they are too poorly preserved to be confirmed as such. Except the "nasal" ornamented with denticles, the skull roof bones of ALM 316 are apparently smooth but minute imprints on the sediment suggest that the hidden face is possibly ornamented with tubercles.

The morphology of the preopercle and the flank scales tends to exclude ALM 316 from Perleididae but also from "perleidiforms" and *Teffichthys*, while features shared with ALM 321 are reminiscent of redfieldiiforms. This specimen is treated as Actinopterygii indet.

5. Conclusion

In North Africa, extended Permian and Triassic fossiliferous continental exposures have been reported in Algeria (Permian, Triassic, Tiguentourine and Zarzaïtine Series, see Attar et al., 1981, Dahoumane et al., 2016, Jalil, 1999), Niger (Permian, Moradi Formation, see Steyer et al., 2006) and Morocco (Permian, Triassic, Argana Basin, see Jalil, 1999, Khaldoune et al., 2017), but only the Argana Basin has yielded a significant actinopterygian fauna. Except ichnofossils, a few occurrences of microfossils (charophytes and ostracods) in the T4 member [Medina et al., 2001], and unpublished plant remains in the Ikakern Formation (Dutuit, 1976, Feys and Greber, 1963, Jalil, 1999, Koning, 1957; N.J. pers. obs.), most of the body fossils from the Argana Basin are macrovertebrate bone remains. The age of the different units, with the exception of the T4 member, was estimated from vertebrates and throughout comparison with closely related faunal assemblages. The tetrapod fauna from the T5 member (aetosaurs, metoposaurids, almasaurids, stahleckeriid dicynodonts, rauisuchians and phytosaurs, see Buffa et al., 2019, Butler et al., 2019, Jalil and Peyer, 2007, Khaldoune et al., 2017, Olivier et al., 2019) strongly suggests a Late Triassic (Carnian) age. In particular, this fauna is very close to the Late Triassic assemblages of the North American Chinle Formation and Newark Supergroup, and from Krasiejów and Woźniki, in Poland [Khaldoune et al., 2017]. The contribution of the actinopterygians in

dating and biogeography purposes is limited. From the six forms previously described in the basin, only two taxa are reliably identified, *Mauritanichthys rugosus* Martin [1980b] and *Dipteronotus gibbosus* Martin [1980a]. *Mauritanichthys*, endemic to the Argana Basin, shows affinities with the subcontemporaneous *Lasalichthys* from the Chinle Formation and the Newark Supergroup. *Dipteronotus gibbosus* is the youngest representative of a genus otherwise known by several European species ranging from Anisian to Ladinian, in marine, brackish or deltaic environments [Bürgin, 1992, Gall and Grauvogel-Stamm, 2005, Tintori, 1990, Tintori et al., 2016]. Other actinopterygian taxa from the Argana Basin probably correspond to new forms, but are represented by poorly preserved material and their phylogenetical affinities remain unclear, except saying that they are neither Holostei nor Teleosteomorpha. The absence of these two clades in the Argana Basin agrees with their relative abundance during the Triassic, low in continental localities comparatively to marine environments [Cavin, 2017, Romano et al., 2016]. Further study on this ichthyofauna requires more detailed investigation for specimens preserved in volume (e.g., by the use of micro-computed tomography scanning), or the collect of new material.

The actinopterygian remains are rare in the Argana Basin, in comparison to tetrapods. All the actinopterygian material was collected from a hard sandstone level of the locality XI, using dynamite, during a single fieldwork in 1966 [Dutuit, 1976]. Recent fieldworks and prospecting throughout the Permian-Triassic outcrops of the Argana Basin led to the discovery of new localities and several tetrapod bones (e.g., pareiasaurs, rhynchosaurians, moradisaurin captorhinids, metoposaurids, phytosaurs; see Khaldoune et al., 2017), but no new actinopterygian remains have been found. This peculiar distribution pattern can partly be explained by the deposition conditions along the basin. Isolated remains are common but the localities providing well preserved material are rare, and most tetrapod localities are related to in-situ massive mortality or post-mortem accumulation [Dutuit, 1976]. Taphonomic and detailed sedimentological studies for the locality XI and for the basin, like those performed for the metoposaurid locality XIII [Tourani and Benaouiss, 2009] will better guide future prospecting for actinopterygian remains.

Acknowledgments

Authors are grateful to Rachid Essamoud (Geology Department, Faculty of Sciences Ben M'sik, Hassan II University of Casablanca) and Sylvie Bourquin (UMR 6118, Rennes University) for their invitation to contribute to this special volume, to Gaël Clément and Alan Pradel (UMR 7207, MNHN, Paris) for access to the collections under their care, to Erin Maxwell (Staatliches Museum für Naturkunde, Stuttgart) and Léa Grauvogel-Stamm for photographs of *Dipteronotus aculeatus*, to Dario de Franceschi and Didier Merle (UMR 7207, MNHN, Paris) for technical support, to Philippe Loubry (UMR 7207, MNHN, Paris) for the photographs and to Fatima Khaldoune (OCP Group, Khouribga) for useful discussions. This manuscript was improved thanks to the comments of Sebastian Voigt and an anonymous reviewer. BK was partly funded by the Fondation Ars Cuttoli, Paul Appell.

References

Attar, A., Fabre, J., Janvier, P., and Lehman, J. P. (1981). Les Vertébrés de la formation de Tiguentourine (Permo-Carbonifère, bassin d'Illizi, Algérie). *Bull. M.N.H.N., Paris, 4e sér.*, 3(section C, no. 4), 301–309.

Barbolini, N., Bamford, N. K., and Tolan, S. (2016a). Permo-Triassic palynology and palaeobotany of Zambia: a review. *Palaeontol. Afr.*, 50, 18–30.

Barbolini, N., Smith, R. M. H., Tabor, N. J., Sidor, C. A., and Angielczyk, K. D. (2016b). Resolving the age of Madumabisa fossil vertebrates: palynological evidence from the mid-Zambezi Basin of Zambia. *Palaeogeogr. Palaeoclimatol. Palaeoecol.*, 457, 117–128.

Berg, L. S. (1940). Classification of fishes, both recent and fossil. *Trav. Inst. Zool., Académie des Sciences de l'URSS*, 5, 1–517.

Brough, J. (1931). On the fossil fishes from the Karroo System, and some general considerations on the bony fishes of the Triassic period. *Proc. Zool. Soc. Lond.*, 101(1), 235–296.

Brough, J. (1934). On the structure of certain catopterid fishes. *Proc. Zool. Soc. Lond.*, pages 559–571.

Brown, R. H. (1980). Triassic rocks of Argana valley, southern Morocco, and their regional structural implications. *Bull. Am. Assoc. Pet. Geol.*, 64, 988–1003.

Buffa, V., Jalil, N.-E., and Steyer, J.-S. (2019). Redescription of *Arganasaurus (Metoposaurus) azerouali* (Dutuit) comb. nov. from the Upper Triassic of the Argana Basin (Morocco), and the first phylogenetic analysis of the Metoposauridae (Amphibia, Temnospondyli). *Pap. Palaeontol.*, 5, 699–717.

Bürgin, T. (1992). Basal Ray-finned Fishes (Osteichthyes; Actinopterygii) from the Middle Triassic of Monte San Giorgio (Canton Tessin, Switzerland) – Systematic Palaeontology with Notes on Functional Morphology and Palaeoecology. *Schweizerische Palaontologische Abhandlungen (Mémoires suisses de Paléontologie, Memorie svizzere di Paleontologia)*, 114, 1–164.

Butler, R. J., Jones, A. S., Buffetaut, E., Mandl, G. W., Scheyer, T. M., and Schultz, O. (2019). Description and phylogenetic placement of a new marine species of phytosaur (Archosauriformes: Phytosauria) from the Late Triassic of Austria. *Zool. J. Linnean Soc.*, 187, 198–228.

Cavin, L. (2017). *Freshwater Fishes - 250 Million Years of Evolutionary History*. ISTE Press, Elsevier, London, Oxford, UK.

Cope, E. D. (1887). Geology and palaeontology - Zittel's manuel of palaeontology. *Am. Naturalist*, 21, 1014–1019.

Dahoumane, A., Nedjari, A., Aït-Ouali, R., Taquet, P., Vacant, R., and Steyer, J.-S. (2016). A new Mastodonsauroid Temnospondyl from the Triassic of Algeria: implications for the biostratigraphy and palaeoenvironments of the Zarzaïtine Series, Northern Sahara. *C. R. Palevol.*, 15, 918–926.

Dutuit, J.-M. (1976). Introduction à l'étude paléontologique du Trias continental marocain. *Mem. M.N.H.N., nouvelle série (C), Sciences de la Terre*, 36, 1–253.

Egerton, P. M. d. G. (1854). On a fossil fish from the Upper Beds of the New Red Sandstone at Bromsgrove, Palichthyologic notes, No. 6. *Quart. J. Geol. Soc. Lond.*, 10, 367–371.

Feys, R. and Greber, C. (1963). Le Stéphanien et l'Autunien du Souss dans les Ida ou Zal (Haut-Atlas occidental – Maroc). *Notes et Mem. Serv. Geol. Maroc*, 22, 19–35.

Frickhinger, K. A. (1995). *Fossil Atlas Fishes*. Mergus, Melle, Germany.

Gall, J. C., Grauvogel, L., and Lehman, J. P. (1974). Faune du Buntsandstein. V. - Les poissons fossiles de la collection Grauvogel-Gall. *Ann. Paléontol. (Vertébrés)*, 60, 129–147.

Gall, J.-C. and Grauvogel-Stamm, L. (2005). The early Middle Triassic 'Grès à Voltzia' Formation of eastern France: a model of environmental refugium. *C. R. Palevol.*, 4, 637–652.

Gibson, S. Z. (2018). A new species of *Lasalichthys* (Actinopterygii, Redfieldiiformes) from the Upper Triassic Dockum Group of Howard County, Texas, with revisions to the genera *Lasalichthys* and *Synorichthys*. *J. Vert. Paleontol.*, 38, article no. e1513009.

Gouiric-Cavalli, S., Zavattieri, A. M., Gutierrez, P. R., Cariglino, B., and Balarino, L. (2017). Increasing the fish diversity of the Triassic faunas of Gondwana: a new redfieldiiform (Actinopterygii) from the Middle Triassic of Argentina and its palaeobiogeographical implications. *Pap. Palaeontol.*, 3, 559–581.

Haughton, S. H. (1934). 3. On some Karroo fishes from Central Africa. *Ann. South Afr. Mus.*, 31, 97–104.

Hutchinson, P. (1973a). A revision of the redfieldiiform and perleidiform from the Triassic of Bekker's Kraal (South Africa) and Brookvale (New South Wales). *Bull. Br. Mus. (Nat. Hist.), Geol.*, 22, 233–354.

Hutchinson, P. (1973b). *Pseudobeaconia*, a perleidiform fish from the Triassic Santa Clara Formation, Argentina. *Breviora*, 398, 1–24.

Hutchinson, P. (1978). The anatomy and phylogenetic position of *Helichthys*, a redfieldiiform fish from the Triassic of South Africa. *Paleontology*, 21(4), 881–891.

Jalil, N.-E. (1999). Continental Permian and Triassic vertebrate localities from Algeria and Morocco and their stratigraphical correlations. *J. Afr. Earth Sci.*, 29, 219–226.

Jalil, N.-E. and Janvier, P. (2005). Les pareiasaures (Amniota, Parareptilia) du Permien supérieur du Bassin d'Argana, Maroc. *Geodiversitas*, 27, 35–132.

Jalil, N.-E. and Peyer, K. (2007). A new rauisuchian (Archosauria, Suchia) from the Upper Triassic of the Argana Basin, Morocco. *Palaeontology*, 50, 417–430.

Jörg, E. (1969). Eine Fischfauna aus dem Oberen Buntsandstein (Unter-Trias) von Karlsruhe-Durlach (Nordbaden). *Beiträge zur naturkundlichen Forschung in Südwestdeutsch-*

land, 28, 87–102.

Jubb, R. A. and Gardiner, B. G. (1975). A preliminary catalogue of identifiable fossil fish material from Southern Africa. *Ann. South Afr. Mus.*, 67, 381–440.

Khaldoune, F., Germain, D., Jalil, N.-E., and Steyer, J.-S. (2017). Les vertébrés du Permien et du Trias du Maroc (Bassin d'Argana, Haut Atlas occidental) : fenêtre ouverte sur l'évolution autour de la grande crise fini-paléozoïque. In Zouhri, S., editor, *Paléontologie des vertébrés du Maroc : état des connaissances*, Mem. Soc. geol. France, nouvelle série, 180, pages 103–166. La Société Géologique de France, Paris.

Khalloufi, B., Brito, P. M. M., Cavin, L., and Dutheil, D. B. (2017). Revue des ichthyofaunes mésozoïques et cénozoïques marocaines. In Zouhri, S., editor, *Paléontologie des vertébrés du Maroc: état des connaissances*, Mem. Soc. geol. France, nouvelle série, 180, pages 167–248. La Société Géologique de France, Paris.

Kim, S.-H., Lee, Y.-N., Park, J.-Y., Lee, S., and Lee, H.-J. (2020). The first record of redfieldiiform fish (Actinopterygii) from the Upper Triassic of Korea: implications for paleobiology and paleobiogeography of Redfieldiiformes. *Gondwana Res.*, 80, 275–284.

Klein, H., Voigt, S., Hminna, A., Saber, H., Schneider, J., and Hmich, D. (2010). Early triassic archosaur-dominated footprint assemblage from the Argana basin (Western High Atlas, Morocco). *Ichnos*, 17, 215–227.

Koning, G. d. (1957). *Géologie des Ida-ou-Zal (Maroc). Stratigraphie, pétrographie et tectonique de la partie SW du bloc occidental du Massif ancien du Haut Atlas.* PhD thesis, Leide University, Leide. 209 p.

Lagnaoui, A., Klein, H., Voigt, S., Hminna, A., Saber, H., Schneider, J. W., and Werneburg, R. (2012). Late Triassic Tetrapod-Dominated Ichnoassemblages from the Argana Basin (Western High Atlas, Morocco). *Ichnos*, 19, 238–253.

Lombardo, C. (1995). *Perleidus altolepis* (Actinopterygii, Perleidiformes) from the Kalkschieferzone of Ca' Del Frate (N. Italy). *Geobios M.S.*, 19, 211–213.

Lombardo, C. (2013). A new basal actinopterygian fish from the Late Ladinian of Monte San Giorgio (Canton Ticino, Switzerland). *Swiss J. Geosci.*, 106, 219–230.

Lombardo, C. and Brambillasca, F. (2005). A new perleidiform (Actinopterygii, Osteichthyes) from the Late Triassic of Northern Italy. *Bollettino della Società Paleontologica Italiana*, 44, 25–34.

Lombardo, C., Rusconi, M., and Tintori, A. (2008). New perleidiform from the Lower Ladinian (Middle Triassic) of the northern Grigna (Northern Italy). *Rivista Italiana di Paleontologia e Stratigrafia*, 114, 263–272.

Lombardo, C. and Tintori, A. (2004). New perleidiforms from the Triassic of the Southern Alps and the revision of *Serrolepis* from the Triassic of Württemberg (Germany). In Arratia, G. and Tintori, A., editors, *Mesozoic Fishes 3 – Systematics, Paleoenvironments and Biodiversity*, pages 179–196. Verlag Dr. Friedrich Pfeil, München, Germany.

López-Arbarello, A. (2004). The record of Mesozoic fishes from Gondwana (excluding India and Madagascar). In Arratia, G. and Tintori, A., editors, *Mesozoic Fishes 3 – Systematics, Paleoenvironments and Biodiversity*, pages 597–624. Verlag Dr. Friedrich Pfeil, München, Germany.

López-Arbarello, A., Rauhut, O., and Cerdeño, E. (2010). The Triassic fish faunas of the Cuyana Basin, Western Argentina. *Palaeontology*, 53, 249–276.

López-Arbarello, A. and Zavattieri, A. M. (2008). Systematic revision of *Pseudobeaconia* Bordas, 1944, and *Mendocinichthys* Whitley, 1953 (Actinopterygii: 'Perleidiformes') from the Triassic of Argentina. *Palaeontology*, 51, 1025–1052.

Marramà, G., Lombardo, C., Tintori, A., and Carnevale, G. (2017). Redescription of '*Perleidus*' (Osteichthyes, Actinopterygii) from the Early Triassic of northwestern Madagascar. *Rivista Italiana di tle Paleontologia e Stratigrafia*, 123, 219–242.

Martin, M. (1979a). Actinoptérygiens, Dipneustes et Crossoptérygiens du Trias Continental supérieur marocain. Thèse de 3e cycle, Université Paris VII, Paris. 121 p.

Martin, M. (1979b). *Arganodus atlantis* et *Ceratodus arganensis*, deux nouveaux Dipneustes du Trias supérieur continental marocain. *C. R. Acad. Sci. Paris D*, 289, 89–92.

Martin, M. (1980a). *Dipteronotus gibbosus* (Actinopterygii, Chondrostei), nouveau colobodontidé du Trias supérieur continental maro-

cain. *Geobios*, 13, 445–449.

Martin, M. (1980b). *Mauritanichthys rugosus* n. gen. et n. sp., Redfieldiidae (Actinopterygi, Chondrostei) du Trias supérieur continental marocain. *Geobios*, 13, 437–440.

Martin, M. (1981). Les Dipneustes et Actinistiens du Trias supérieur continental marocain. *Stuttgarter Beiträge zur Naturkunde, B (Geologie und Paläontologie)*, 69, 1–29.

Martin, M. (1982). Les actinoptérygiens (Perleidiformes et Redfieldiiformes) du Trias supérieur continental du couloir d'Argana (Atlas occidental, Maroc). *Neues Jahrbuch für Geologie und Paläontologie, Abhandlungen*, 162, 352–372.

Medina, F., Vachard, D., Colin, J.-P., Ouarhache, D., and Ahmamou, M. F. (2001). Charophytes et ostracodes du niveau carbonaté de Taourirt Imzilen (Membre d'Aglegal, Trias d'Argana); implications stratigraphiques. *Bulletin de l'Institut Scientifique, Rabat, section Sciences de la Terre*, 23, 21–26.

Mickle, K. E. (2015). Identification of the Bones of the Snout in Fossil Lower Actinopterygians -A New Nomenclature Scheme Based on Characters. *Copeia*, 103, 838–857.

Milner, A. R., Gardiner, B. G., Fraser, N. C., and Taylor, M. A. (1990). Vertebrates from the Middle Triassic Otter Sandstone Formation of Devon. *Palaeontology*, 33, 873–892.

Murray, A. M. (2000). The Palaeozoic, Mesozoic and Early Cenozoic fishes of Africa. *Fishes Fisheries*, 1, 111–145.

Olivier, C., Battail, B., Bourquin, S., Rossignol, C., Steyer, J. S., and Jalil, N.-E. (2019). New dicynodonts (Therapsida, Anomodontia) from near the Permo-Triassic boundary of Laos: implications for dicynodont survivorship across the Permo-Triassic mass extinction and the paleobiogeography of Southeast Asian blocks. *J. Vert. Paleontol.*, 39, e1584745.

Romano, C., Koot, M. B., Kogan, I., Brayard, A., Minikh, A. V., Brinkmann, W., Bucher, H., and Kriwet, J. (2016). Permian–Triassic Osteichthyes (bony fishes): diversity dynamics and body size evolution. *Biol. Rev.*, 91, 106–147.

Schaeffer, B. (1956). Evolution of the Subholostean fishes. *Evolution*, 10, 201–212.

Schaeffer, B. (1967). Late Triassic fishes from the Western United States. *Bull. Amer. Museum Natural History, New York*, 135, 285–342.

Schaeffer, B. (1984). On the relationships of the Triassic-Liassic redfieldiiform fishes. *Am. Mus. Novitates*, 2795, 1–18.

Schaeffer, B. and Mc Donald, N. (1978). Redfieldiid fishes from the Triassic-Liassic Newark Supergroup of eastern North America. *Bull. Am. Mus. Nat. Hist., New York*, 159, 129–174.

Schultze, H. P. (2008). Nomenclature and homologization of cranial bones in actinopterygians. In Arratia, G., Schultze, H. P., and Wilson, M. V. H., editors, *Mesozoic Fishes 4 – Homology and Phylogeny*, pages 23–48. Verlag Dr. Friedrich Pfeil, München, Germany.

Steyer, J. S., Damiani, R., Sidor, C. A., O'Keefe, F. R., Larsson, H. C. E., Maga, A., and Ide, O. (2006). The vertebrate fauna of the Upper Permian of Niger. IV. *Nigerpeton ricqlesi* (Temnospondyli: Cochleosauridae), and the Edopoid Colonization of Gondwana. *J. Vert. Paleontol.*, 26, 18–28.

Sun, Z., Lombardo, C., Tintori, A., Jiang, D., Hao, W., Sun, Y., and Lin, H. (2012). *Fuyuanperleidus dengi* Geng et al., 2012 (Osteichthyes, Actinopterygii) from the Middle Triassic of Yunnan Province, South China. *Rivista Italiana di Paleontologia e Stratigrafia*, 118, 359–373.

Sun, Z., Tintori, A., Jiang, D., Lombardo, C., Rusconi, M., Hao, W., and Sun, Y. (2009). A New Perleidiform (Actinopterygii, Osteichthyes) from the Middle Anisian (Middle Triassic) of Yunnan, South China. *Acta Geol. Sin.*, 8, 460–470.

Sun, Z., Tintori, A., Jiang, D., and Motani, R. (2013). A new perleidid from the Spathian (Olenekian, Early Triassic) of Chaohu, Anhui Province, China. *Rivista Italiana di Paleontologia e Stratigrafia*, 119, 275–285.

Sytchevskaya, E. K., Anderson, H. M., and Anderson, J. M. (2009). Late Triassic fishes of South Africa. In Shishkin, M. A. and Tverdokhlebov, V. P., editors, *Researches on paleontology and biostratigraphy of ancient continental deposits (Memories of Professor Vitalii G. Ochev)*, pages 197–215. Nauchnaya Kniga, Saratov.

Tintori, A. (1990). *Dipteronotus olgiatii* n. sp. (Actinopterygii, Perleidiformes) from the Kalkschieferzone of Ca' Del Frate (N. Italy) (Preliminary note). *Atti Ticinensi di Scienze della Terra*, 33, 191–197.

Tintori, A. and Lombardo, C. (1996). *Gabanellia agilis* gen. n. sp. n., (Actinopterygii, Perleidiformes) from

the Calcare di Zorzino of Lombardy (North Italy). *Rivista Italiana di Paleontologia e Stratigrafia*, 102, 227–236.

Tintori, A., Lombardo, C., and Kustatscher, E. (2016). The Pelsonian (Anisian, Middle Triassic) fish assemblage from Monte Prà della Vacca/Kühwiesenkopf (Braies Dolomites, Italy). *Neues Jahrbuch für Geologie und Paläontologie, Abhandlungen*, 282, 181–200.

Tixeront, M. (1973). Lithostratigraphie et minéralisations cuprifères et uranifères stratiformes, syngénétiques et familières des formations détritiques permo-triasiques du couloir d'Argana, Haut-Atlas occidental (Maroc). *Notes et Mem. Serv. Geol. Maroc*, 249, 147–177.

Tixeront, M. (1974). Carte géologique et minéralisations du Couloir d'Argana. *Notes et Mem. Serv. Geol. Maroc*, 205.

Tourani, A. and Benaouiss, N. (2009). Depositional and climatic settings of the Upper Triassic temnospondyl-bearing strata of the Irohalene mudstone in Argana Basin (Western High Atlas, Morocco). In *1er Congrès International sur la Paléontologie des Vertébrés du Nord de l'Afrique, Marrakesh, Morocco*. Abstract book, 34.

Tourani, A., Benaouiss, N., Gand, G., Bourquin, S., Jalil, N.-E., Broutin, J., Battail, B., Germain, D., Khaldoune, F., Sebban, S., Steyer, J.-S., and Vacant, R. (2010). Evidence of an Early Triassic age (Olenekian) in Argana Basin (High Atlas, Morocco) based on new chirotherioid traces. *C. R. Palevol.*, 9, 201–208.

Tourani, A., Lund, J. J., Benaouiss, N., and Gaupp, R. (2000). Stratigraphy of Triassic syn-rift deposition in Western Morocco. In Bachmann, G. H. and Lerche, I., editors, *Epicontinental Triassic, Volume 2 - International Symposium Halle, 21.-23, September 1998*, pages 1193–1215. Schweizerbart Science Publishers, Stuttgart, Germany.

Wade, T. T. (1935). *The Triassic fishes of Brookvale, New South Wales*. British Museum (Natural History), London, England.

Wiley, E. O. (2008). Homology, identity and transformation. In Arratia, G., Schultze, H. P., and Wilson, M., editors, *Mesozoic Fishes 4 - Homology and phylogeny*, pages 9–21. Verlag Dr. Friedrich Pfeil, München, Germany.

Woodward, A. S. (1910). On *Dipteronotus cyphus*, Egerton. A ganoid fish from the Lower Keuper of Bromsgrove, Worcestershire. *Proc. Geol. Assoc.*, 21, 322–323.

Xu, G.-H. (2020). A new stem-neopterygian fish from the Middle Triassic (Anisian) of Yunnan, China, with a reassessment of the relationships of early neopterygian clades. *Zool. J. Linnean Soc.*, zlaa053, 1–20.

Zouheir, T., Hminna, A., Klein, H., Lagnaoui, A., Saber, H., and Schneider, J. W. (2020). Unusual archosaur trackway and associated tetrapod ichnofauna from Irohalene member (Timezgadiouine formation, Late Triassic, Carnian) of the Argana Basin, Western High Atlas, Morocco. *Hist. Biol.*, 32, 589–601.

Comptes Rendus
Géoscience — Sciences de la Planète
2020, 352, nº 6-7, p. 515-538
https://doi.org/10.5802/crgeos.33

Some aspects of current State of Knowledge on Triassic series on both sides of the Central Atlantic Margin / *Quelques aspects de l'état des connaissances des séries triasiques de part et d'autre de la Marge Atlantique*

Paleobotanical and palynological evidence for the age of the Matzitzi Formation, Mexico

Uxue Villanueva-Amadoz*, [a], Marycruz Gerwert Navarro [a, b], Manuel A. Juncal [c] and José B. Diez [c]

[a] ERNO, Instituto de Geología, UNAM, L.D. Colosio y Madrid S/N, Campus Unison. C.P. 83000 Hermosillo, Sonora, Mexico

[b] Posgrado en Ciencias de la Tierra, ERNO, Instituto de Geología, UNAM, L.D. Colosio y Madrid S/N, Campus Unison. C.P. 83000 Hermosillo, Sonora, Mexico

[c] Departamento de Xeociencias Mariñas e Ordenación do Territorio, Universidade de Vigo, 36200 Vigo, Spain

E-mails: uxue@geologia.unam.mx (U. Villanueva-Amadoz), marygn22@gmail.com (M. G. Navarro), majuncales@gmail.com (M. A. Juncal), jbdiez@uvigo.es (J. B. Diez)

Abstract. This study addresses some of the stratigraphical problems of the Matzitzi Formation of Puebla and Oaxaca States in Mexico. The age assignment for this unit is controversial although most researchers today accept a Leonardian age (Kungurian, 279.3–272.3 Ma) based on the presence of the gigantopterid *Lonesomia mexicana* Weber. However, after re-examination of the holotype and two paratypes, the absence of diagnostic taxonomic characters prevents the assignment of this fossil type species to the gigantopterid group. Excluding the presence of gigantopterids in this formation, the macroflora seems to be Permian in age. Samples were collected for palynological analysis to determine the age of the formation. Studied palynological assemblages seem to be reworked and are represented by 18 fossil taxa assigned to the following genera: *Calamospora*, *Deltoidospora*, *Densosporites*, *Granulatisporites*, *Laevigatosporites*, *Latipulvinites*, *Lophotriletes*, *Platysaccus*, *Punctatosporites*, *Raistrickia*, *Schopfipollenites*, *Thymospora*, *Triquitrites*, *Verrucosisporites*, and *Vesicaspora*. Described palynomorphs are likely Late Pennsylvanian according to the presence of *Latipulvinites kosankii* and *Thymospora thiessenii*. The biostratigraphic and geochronologic age disparities should be solved in the future.

Keywords. Paleobotany, Palynology, Matzitzi Formation, *Lonesomia mexicana*, Mexico.

1. Introduction

The Paleozoic Matzitzi Formation is the most important continental unit from Mexico due to its diverse and abundant fossil flora, and because it is a key to understanding the terminal stages of Pangea amalgamation in southern Mexico [Ortega-Gutiérrez, 1992].

Southern Mexico was subjected to large-scale thrusting, reactivation of preexisting structures, metamorphism and magmatism that occurred at different depths during burial and exhumation

* Corresponding author.

throughout the late Paleozoic and early Mesozoic [Elías-Herrera et al., 2007]. The Matzitzi Formation was affected by the Caltepec fault, a dextral transpressional fault, which is one of the best examples of this main structure with multiple reactivation episodes in Mexico [Ortega-Gutiérrez et al., 2018]. It represents the tectonic contact between the Acatlán crystalline Complex (Cambrian-Ordovician boundary to the latest Devonian) and Mesoproterozoic Oaxacan Complex, delimiting the Mixteco and Zapoteco terranes [Elías-Herrera et al., 2007, Ortega-Gutiérrez et al., 2018]. Whether accretion of the Acatlán and Oaxacan complexes took place during the Devonian or the Cretaceous is still a matter of debate [Elías-Herrera et al., 2007, García-Duarte, 1999, González-Hervert et al., 1984, Ramírez-Espinosa, 1984, Sedlock et al., 1993, Yañez et al., 1991].

The Matzitzi Formation is a post-collisional unit, overlying the amalgamation of the metamorphic Acatlán and Oaxacan complexes, and is also an important lithostratigraphic unit for understanding the western end termination of Pangea amalgamation [Elías-Herrera et al., 2007, 2011, García-Duarte, 1999, Hernández-Láscares, 2000].

The age of the Matzitzi Formation has been variously estimated as Pennsylvanian-Permian based on floral content [Magallón-Puebla, 1991, Silva-Pineda, 1970, Weber, 1997, Weber et al., 1987] to Permian, Triassic and Jurassic based on geological data [Bedoya et al., 2020, Burckhardt, 1930, Calderón-García, 1956, Elías-Herrera et al., 2011, Erben, 1956, Hernández-Láscares, 2000, Mülleried, 1933a,b, 1934]. On the basis of its rich macrofossil plant assemblage, this deposit has been considered as Pennsylvanian [Hernández-Láscares, 2000, Silva-Pineda, 1970] or Permian [Magallón-Puebla, 1991, Velasco-Hernández and Lucero-Arellano, 1996, Weber, 1997, Weber et al., 1987]. However, the Matzitzi Formation is now widely accepted as Leonardian (Kungurian, latest early Permian) [Weber, 1997, Weber and Cevallos-Ferriz, 1994], on the basis of the presence of the gigantopterid *Lonesomia mexicana*. Gigantoperids are believed to have first appeared in North American in the Leonardian (Kungurian, latest early Permian) and this age assignment was based mainly by correlation to their appearance in Texas [Weber, 1997]. Gigantopterids are a poorly defined group of uncertain botanical affinity characterized by their distinctive megaphyll leaves with marked reticular venation [Glasspool et al., 2004], Permian-Triassic in age [Wang, 2010]. According to Weber [1997] Leonardian age was also supported by *Sigillaria ichthyolepis-brardii* group, *Pterophyllum*, *Rhipidopsis* or *Ginkgoites* sp., cf. *Sphenophyllum* ex gr. *thonii*, *Sphenophyllum* sp., *Taeniopteris* cf. *multinervis*, which extend since the Late Carboniferous to the early Permian and *Fascipteris* known in China since the Permian. However, these fossil genera have a wider stratigraphic range.

Assigning a Permian age to the Matzitzi Formation based on the presence of gigantopterids is problematic for two reasons: (1) lack of defining traits, (2) vague stratigraphic range. First, many paleobotanists exclude fossils attributed to gigantopterids from Mexico because of the absence of defining characters (Booi et al., 2009, DiMichele et al., 2011b, among others). Many works on gigantopterids indicate that the venation pattern is an important trait to include a fossil plant within this group [Booi et al., 2009, Koidzumi, 1936, Liu and Yao, 2002, Mamay, 1988, Ricardi-Branco, 2008, Seyfullah et al., 2014]. Weber [1997] created a new genus of gigantopterids, *Lonesomia*, because it was difficult to observe its venation pattern, possibly due to trichomes obscuring the surface. Today the only published gigantopterid from the Matzitzi Formation are three samples of *Lonesomia mexicana* (holotype and two paratypes), which corresponds to a new genus and species within this group by Weber [1997]. Second, the stratigraphic range of gigantopterids in North America is unclear, but it may extend into the middle Permian in the United States of America [DiMichele et al., 2011b]. Moreover, we do not know whether gigantoperid-bearing beds in the United States [DiMichele et al., 2000, 2001, 2004a, 2011b] are synchronous with the Matzitzi Formation.

Palynology is an important biostratigraphic tool for continental deposits. There are no formally published palynological studies from the Matzitzi Formation. There is only one palynological report corresponding to the Matzitzi Formation from an abstract that indicates a Pennsylvanian age in the Río Hondo section [Di Pasquo and Hernández-Láscares, 2013].

To provide a better estimate of the deposition age of this formation, in this study we re-examine the holotype and paratypes of *Lonesomia mexicana* Weber and discuss the macroflora content and palynological assemblages from the Matzitzi Formation

of Puebla and Oaxaca States in Mexico.

2. Geological setting

The Matzitzi Formation crops out in the southern part of Puebla State (Figure 1). The Oaxacan and Acatlán Complexes appear unconformably underlying this unit or in fault contact with the Matzitzi Formation in the Los Reyes Metzontla area, being the crystalline basement of the region [Centeno-García et al., 2009]. The latter is unconformably overlain in Caltepec-Metzontla area by Mesozoic red beds (conglomerates and quartz-feldspathic sandstones) [Centeno-García et al., 2009] informally named as Red Conglomerate Unit [González-Hervert et al., 1984], Caltepec red conglomerate [Hernández-Láscares, 2000] and Metzontla Formation [García-Duarte, 1999] (Figure 2).

Aguilera and Ordoñez [1896] were the first to informally describe the Matzitzi Formation, based on studies of localities between Los Reyes Metzontla and San Luis Atolotitlán. Flores [1909] also studied this formation and collected some fossil plants that were the basis for a comprehensive work of the fossil plants from this formation [Silva-Pineda, 1970]. This formation was informally described in a fieldwork guide by Calderón-García [1956] as a 600 m thick sequence of sandstones intercalated by dark shales with abundant fossil plants and occasionally containing conglomerate and coal seams. Later Centeno-García et al. [2009] described the formation as a clastic succession mainly dominated by sandstones intercalated by shales, carbonaceous mudstone, conglomeratic sandstone, and conglomerate (Figure 3A). They also reported coarse massive conglomerate strata near the locality of Los Reyes Metzontla containing metamorphic clasts from the Oaxacan Complex. This continental deposit has been interpreted as an anastomosing fluvial system with six facies associations described along the road connecting Los Reyes Metzontla and Coatepec localities [Centeno-García et al., 2009]. Described facies by these authors include: (1) alluvial and fluvial channel fill (probably debris flows), (2) probably transverse bedforms, conglomeratic bars and channel fill, (3) sandy channel fill, longitudinal bedforms and/or sandy point bars, with scarce paleosols, (4) mostly sandy channel fill eroded by small currents (scour hollows) which may be the result of crevasse splays in some cases, (5) floodplains and/or crevasse splays, and (6) small swamps associated with the river system or floodplains.

The felsic Atolotitlán Tuff of volcanic-arc origin, exposed in San Luis Atolotitlán, is believed to correspond to the Matzitzi Formation [Centeno-García et al., 2009, Elías-Herrera et al., 2011] (Figure 2). This volcanic unit has been dated by U-Pb method (240 ± 3 Ma) as Middle Triassic [Bedoya, 2018, Elías-Herrera et al., 2011] (Figure 2).

It is important to note that a comprehensive stratotype for the Matzitzi Formation has not been established due to incomplete depositional sequence and tectonically separated deposition from this unit has not been correlated yet. The lack of continuous exposures together with the presence of thrusting and faulting makes it difficult to define a single continuous section of even a composite stratotype, due to difficulty to correlate among sections. The Matzitzi Formation has been dated by its relative stratigraphic position between younger and older deposits (Figure 3A) as formally described by Elías-Herrera et al. [2005, 2011]. This deposit lies in different fault blocks, so the outcrops in many cases appear isolated as it is very difficult to correlate strata. Also, modern vegetation obscures bedrock in the studied area. For this reason, it is difficult to locate the stratigraphic levels of the palynological samples from the nearby areas of Los Reyes Metzontla and San Luis Atolotitlán localities (labelled as MATZ samples) within the synthetic stratigraphic column. Only the Río Hondo section presents a stratigraphic continuity, with some minor faulting, and the palynological samples labelled as MATZ RH could be stratigraphically located (Figure 3B). This latter deposit consists of sandstones and siltstones and shales with floral remains (Figure 3B).

The Matzitzi Formation has been much studied for its rich well-preserved macrofloras [Carrillo and Martínez-Hernández, 1981, Flores-Barragan et al., 2019a,b, Silva-Pineda, 1970, Silva-Pineda et al., 2003, Velasco-Hernández and Lucero-Arellano, 1996, Velasco-de León et al., 2015, Weber, 1997, Weber and Cevallos-Ferriz, 1994, Weber et al., 1989]. Most of the macroflora determinations correspond to professional and Master dissertations [Flores-Barragan, 2018, Galván-Mendoza, 2000, Hernández-Láscares, 2000, Magallón-Puebla, 1991, Rincón-Pérez, 2010, Valdés-Vergara, 2017]. Based on these studies the

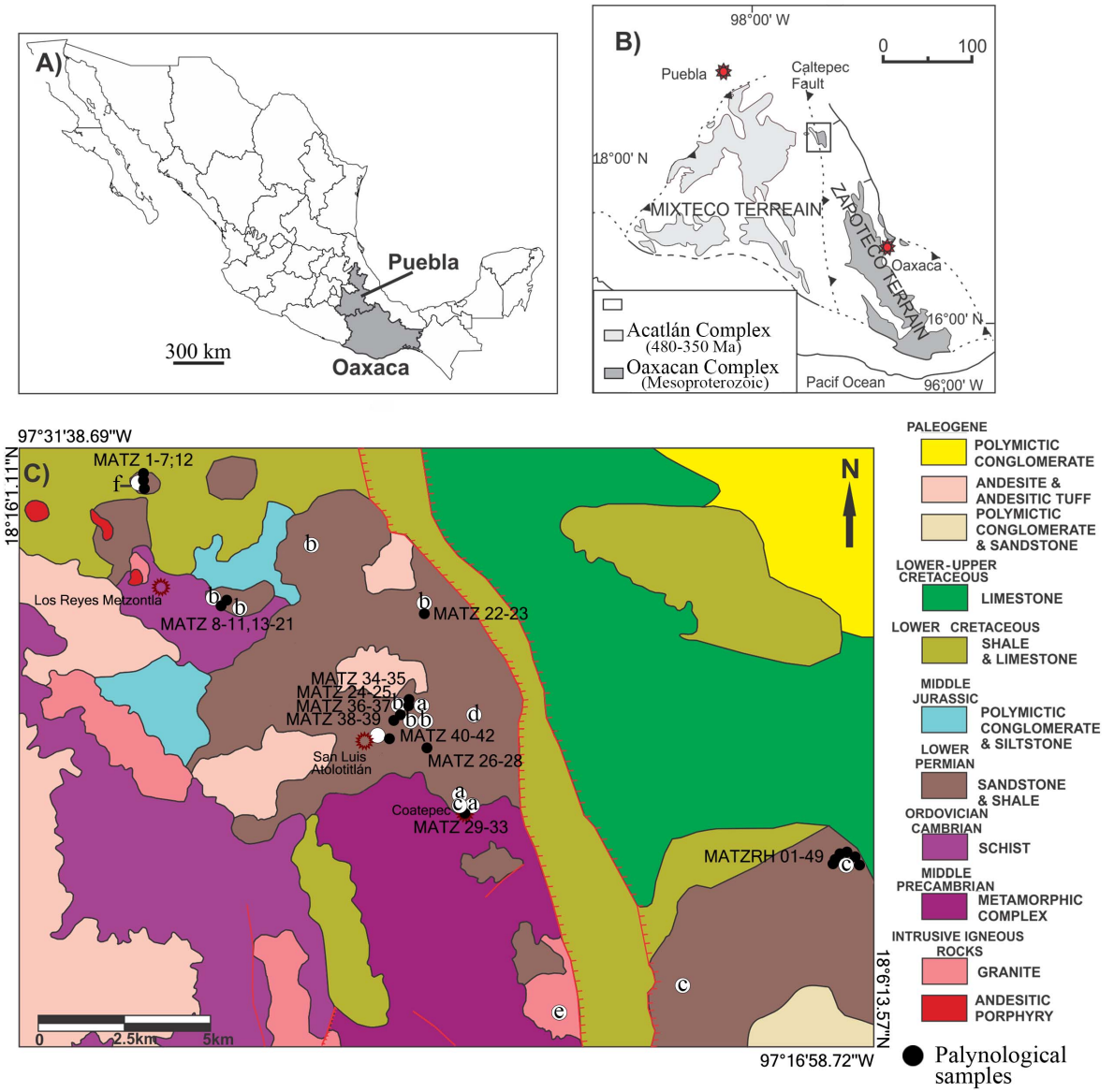

Figure 1. Geographic location, geological setting, and sample location of the studied area. (A) Geographic location of the study area in Mexico. (B) Regional geological setting of the studied area (modified from Elías-Herrera et al., 2005). (C) Detailed geological setting of the studied area. Black circles indicate collected palynological samples (MATZ samples from the nearby areas of Los Reyes Metzontla and San Luis Atolotitlán localities; MATZ RH samples from the Río Hondo section). The location of previously studied biostratigraphic and geochronologic data are indicated by white circles and a letter: fossil plants (a: locations of Weber, 1997; b: Magallón-Puebla, 1991; c: Valdés-Vergara, 2017; Flores-Barragan, 2018); geochronological isotope dating (d: Atolotitlán tuff, Elías-Herrera et al., 2011; e: Cozahuico Granite, Elías-Herrera et al., 2005; f: Bedoya, 2018). *Lonesomia* bearing strata are indicated by the letter a within a white circle, northeast of San Luis Atolotitlán locality.

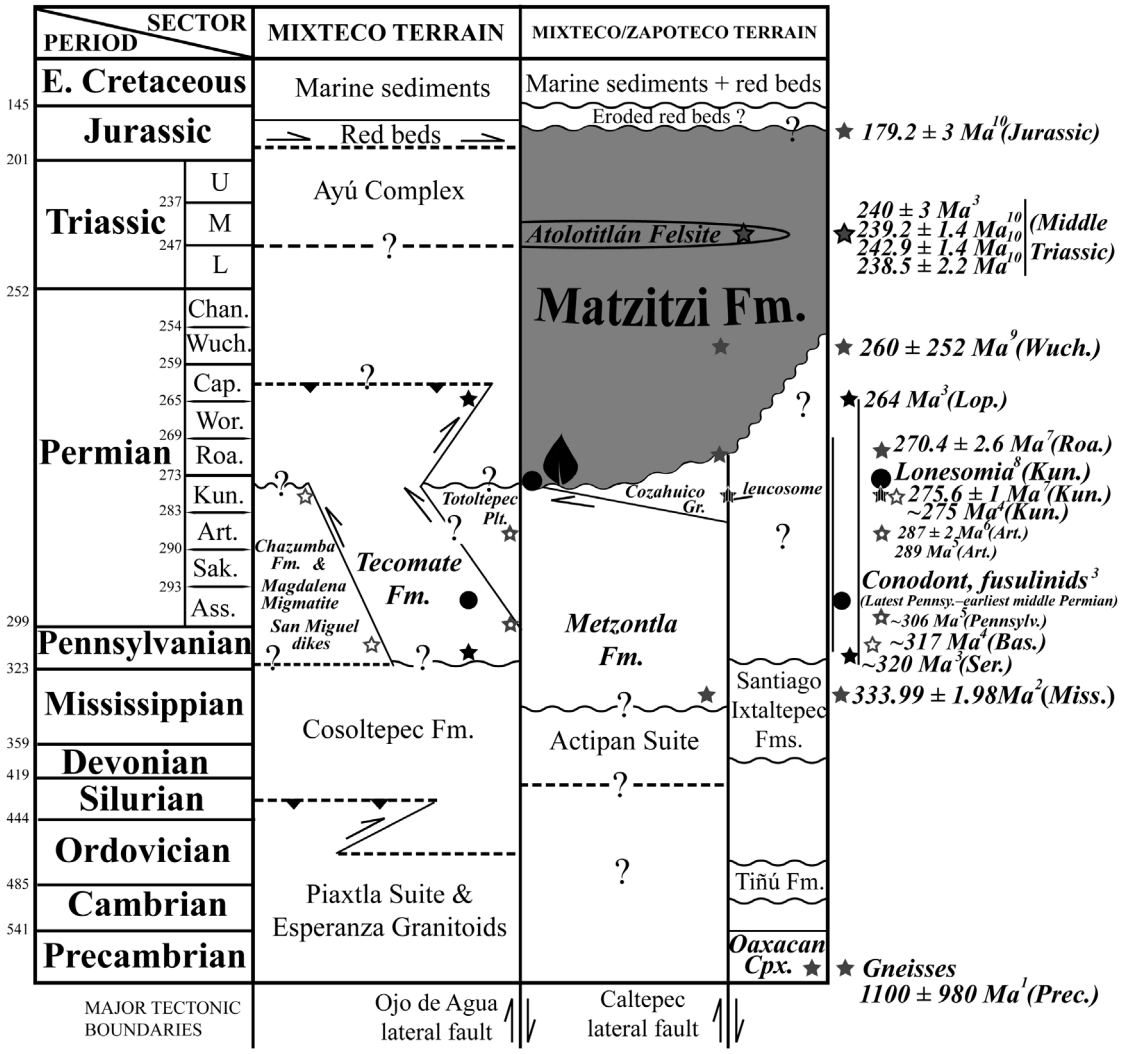

Figure 2. Correlation chart with stratigraphic units present in the studied area and adjacent States. Biostratigraphic and chronostratigraphic data are included. [1]Oaxacan Complex: 1100 ± 980 Ma (Precambrian) [Solari et al., 2003]; [2]Metzontla Formation: 333.99 ± 1.98 Ma (Mississippian) [Elías-Herrera et al., 2011]; [3]Tecomate Formation: Latest Pennsylvanian–earliest Middle Permian (conodont,fusulinids), ~320–264 Ma [Keppie et al., 2004]; [4]Chazumba Suite: ~317–275 Ma [Talavera-Mendoza et al., 2005]; [5]Totoltepec Pluton: ~306–289 Ma [Kirsch et al., 2012]; [6]Totoltepec Pluton: 287 ± 2 Ma (Artinskian) [Yañez et al., 1991]; [7]Anatectic leucosome (275.6 ± 1 Ma); Cozahuico Granite: 270.4 ± 2.6 Ma (Roadian); Matzitzi Formation: 240 ± 3 Ma (Atolotitlán Felsite, Middle Triassic) [Elías-Herrera et al., 2007, 2011]; [8]Matzitzi Formation: Kungurian (Leonardian) on the basis of the presence of the gigantopterid *Lonesomia mexicana* [Weber, 1997]; [9]relative position of the Matzitzi Formation: 260 ± 252 Ma (Wuchiapingian) [Elías-Herrera et al., 2019]; [10]Matzitzi Formation: 238.5 ± 2.2, 239.2 ± 1.4, 242.9 ± 1.4 Ma (Atolotitlán Felsite, Middle Triassic), 179.2 ± 1.98 Ma (Jurassic) [Bedoya et al., 2020]. Cpx.: Complex; Fm.: Formation; Gr.: Granite; Plt.: Pluton; Ass.: Asselian; Sak.: Sakmarian; Art.: Artinskian; Kun.: Kungurian; Roa.: Roadian; Wor.: Wordian; Cap.: Capitanian; Wuch.: Wuchiapingian; Chan.: Changhsingian; L: Lower; M: Middle; U: Upper; E: Early; Prec.: Precambrian; Miss.: Mississippian; Ser.: Serpukhovian; Bas.: Bashkirian; Pennsylv.: Pennsylvanian; Lop.: Lopingian.

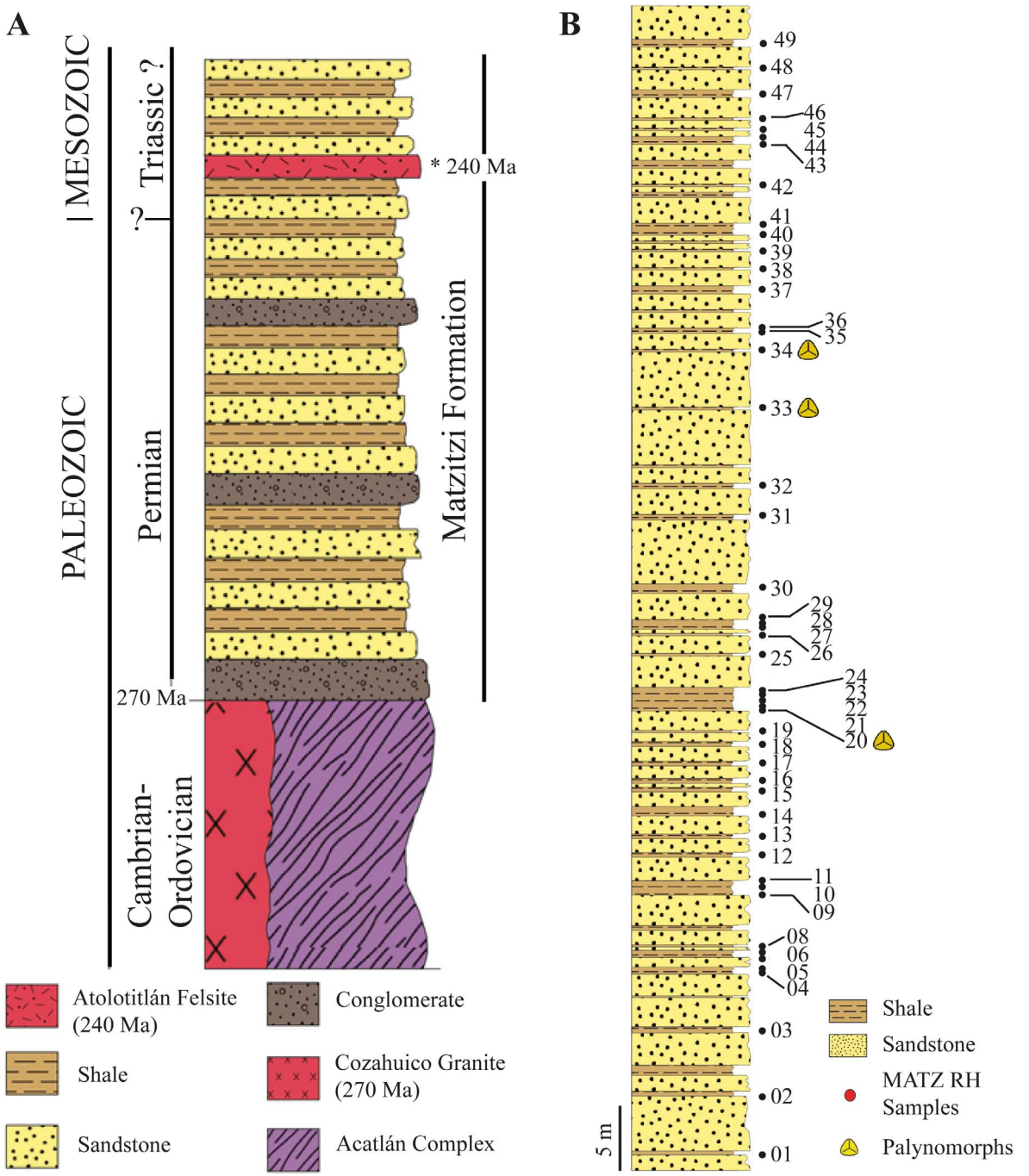

Figure 3. Stratigraphy of the Matzitzi Formation. (A) Synthetic stratigraphic column of the Matzitzi Formation based on Elías-Herrera et al. [2005, 2011]. (B) Stratigraphic column for the Río Hondo Section indicating the stratigraphic position of the 49 collected samples.

macroflora is represented by calamitaleans, lepidodendraleans, gigantopterids, ginkgoales, glossopterids and fossil genera including: *Annularia*, *Asolanus*, *Bjuvia*, *Comia*, *Fascipteris*, indeterminate Cycadophyte, *Holcospermum*, *Lesleya*, *Macrotaeniopteris*, *Mexiglossa*, *Neuropteris*, *Pecopteris*, *Plumsteadia*, *Pseudoctenis*, cf. *Psygmophyllum*, *Pterophyllum*, *Schizoneura*, *Sphenophyllum*, *Sphenopteris*, *Taeniopteris*, *Trigonocarpus*, and *Velascoa*.

3. Material and methods

For macroflora studies, images taken by a Nikon D5600 camera were later processed with Photoshop CS6. The re-examined holotype (IGM-PB-1027-1059) and two paratypes (IGM-PB-1027-1058, IGM-PB-1027-1060) of *Lonesomia mexicana* deposited in the National Paleontological Collection at the Instituto de Geología of the Universidad Nacional Autónoma de México (UNAM) were re-studied and re-photographed under a fluorescence stereo microscope (Zeiss AX10 Zoom V16) and were analyzed using Zen Pro software. These three specimens belong to the locality 1027 described by Weber [1997] as Escurridero in the Barranca Xoconoxtitla about 0.5 km northeast of San Luis Atolotitlán in the Puebla State (18° 11′ 36″ N, 97° 24′ 46″ W).

Ninety-one palynological samples were collected from two main areas: nearby Los Reyes Metzontla and San Luis Atolotitlán localities (42 samples) labelled as MATZ located in the state of Puebla and also from the Río Hondo area located in the Mexican Federal Highway 135D connecting Tehuacán and Oaxaca (49 samples) labelled as MATZ RH (Figures 1, 2). None of the palynological sampling localities corresponds to formerly reported macroflora sites except for the Río Hondo section. We also sampled a *Lonesomia mexicana* holotype-containing a piece of rock but lacking palynomorphs. We used standard palynological methods [Batten, 1999, Erdtman, 1960] for palynomorph extraction, using HCl and HF acid digestions followed by Schulze's solution. For palynomorph concentration, we used a 5-micron nylon mesh. Four slides for each stratigraphic level were prepared using Loctite© 349.

We classified and photographed palynomorphs under light microscopy (Olympus BH2, Axio Imager A2m, and Leica DM 2000 LED-equipped by Nikon Coolpix 990, AxioCam Icc5 and Leica ICC50 W cameras respectively). The sample and slide numbers are followed by England Finder© coordinates. All figured specimens are housed at the Paleontology Collection of the Estación Regional del Noroeste (ERNO-UX0016 to ERNO-UX0027), Instituto de Geología, UNAM, in Hermosillo, Sonora, Mexico.

4. Results

4.1. *Macroflora*

The abundant and well-preserved fossil flora from the Matzitzi Formation appears as impression and compression forms. These fossils are autochthonous, parautochthonous, and allochthonous in terms of transportation. Most of the previously studied plant-bearing localities correspond to facies associated with floodplain and/or crevasse splay deposits in anastomosing river system [Centeno-García et al., 2009]. Pieces of evidence supporting the autochthonous nature of fossil plants are the in situ *Calamites* trunks near San Luis Atolotitlán municipality [Carrillo and Martínez-Hernández, 1981] and numerous paleosols associated to these fossiliferous strata from San Francisco Xochiltepec locality [Weber, 2007]. Many paleosols from the Matzitzi Formation and in situ undetermined stumps (possibly of Filicophyta affinity) are also present [Centeno-García et al., 2009, Weber and Cevallos-Ferriz, 1994]. However, most of the flora assemblages are associated to planar or cross-bedding stratification [Centeno-García et al., 2009] corresponding to parautochthonous material. The well-preserved material, the large leaves in connection with the axis, and their disposition parallel to the stratification are an indication of short transport before burial. Lepidodendraleans and calamitalean in most cases are possibly allochthonous (except for in situ autochthonous specimens), and in few cases parautochthonous, as they appear fragmentary associated to channel deposits.

In the Río Hondo section, the plant-bearing strata are scarce and they also present parautochthonous and allochthonous material. Most of the fossil flora from this section is parautochthonous; however, lepidodendraleans and calamitalean appear fragmentary in most cases associated with channel deposits that possibly are parautochthonous–allochthonous (parautochthonous in the case of *Stigmaria*).

We re-examined the holotype and two paratypes of the fossil plant *Lonesomia mexicana* Weber 1997 to determine its affinity to the gigantopterid group. They are poorly preserved as impressions. It is noteworthy that cuticles are not preserved within the flora remains contained in the Matzitzi Formation. As described by Weber [1997] these specimens are characterized by having: "*leaf simple, symmetrical, sessile or with very short petiole, blade elliptic to lanceolate, lamina leathery, arched between midrib and margin, base rounded, tip rounded or retuse, margin entire, lamina reaching about 5 cm in width and over 20 cm in length (length/width ratio about 5). Petiole to 5 mm in width. Midrib straight, to 3 mm wide at lamina base, narrowing to the tip. Venation of at least three orders, secondaries intersected at the midrib at 75°–80°, tertiaries intersected on these at about 45°*".

Only the primary and secondary veins are distinguished in the paratypes (IGM-PB-1027-1058 and IGM-PB-1027-1060) (Figure 4). The tertiary veins only can be observed in the holotype (IGM-PB-1027-1059), and they are not clearly defined (Figure 5A–C). Zen Pro software was used to determine the intersection angles between venation orders in the holotype (Figure 5C). The measured angles differ slightly with Weber's description: secondary veins extend from the midrib at an angle of around 62°–65° (Weber reported 75°–80°) and an angle of 29°–34° at the intersection of the secondaries at the midrib and tertiaries (Weber reported around 45°). The use of a fluorescence stereo zoom microscope (Zeiss Discovery V8) did not help determine third-order or higher venation patterns, which are only visible in a small area of the holotype leaf (Figure 5D). For this reason, until more specimens are found, it will be risky to classify *Lonesomia mexicana* as a gigantopterid.

4.2. *Microflora*

From 91 collected palynological samples of the Matzitzi Formation, only five samples produced scarce and poorly preserved palynomorphs with a total of 18 fossil taxa identified (Figures 6, 7, Tables 1 and 2). Three samples (MATZ 27, MATZ RH 33, and MATZ RH 34) produced less than 10 palynomorphs per stratigraphic level, and only two (MATZ 1 and MATZ RH 20) have more abundance with less than 50 palynomorphs for each stratigraphic level.

Most of the studied palynomorphs from San Luis Atolotitlán, Los Reyes Metzontla (MATZ), and Río Hondo areas (MATZ RH) have a wide stratigraphic range and almost all identified genera indicate a Late Carboniferous–early Permian age. The palynological assemblages correspond to wetland microflora genera as *Calamospora* (Equisetales including calamitaceans, Sphenophyllales and Noeggerathiales), *Deltoidospora*, *Granulatisporites*, *Lophotriletes*, *Triquitrites* and *Raistrickia* (herbaceous fern spores), *Laevigatosporites* (Sphenophyllales and Marattiales), *Punctatosporites* and *Thymospora* (Marattiales), *Schopfipollenites* (Medullosales) and *Vesicaspora* (Peltaspermales). All of the identified spores are typical of Late Pennsylvanian palynofloras elsewhere, but the presence of *Thymospora thiessenii* and *Latipulvinites kosankii* could restrict the age of MATZ RH 20 stratigraphic level of Río Hondo deposit to the Middle-Late Pennsylvanian [e.g. Peppers, 1964, 1985, Ravn, 1979, 1986]. On the one hand, *Latipulvinites kosankii* Peppers 1964 (Figure 6G) is restricted to the Pennsylvanian of Illinois, Kentucky, Texas, and England [Peppers, 1964, Stone, 1969, Ravn, 1979, Turner, 1991]. On the other hand, *Thymospora thiessenii* (Kosanke) Wilson and Venkatachala, 1963 (Figure 6J) known from the Bolsovian–Westphalian boundary (Westphalian C-D) in Europe and the United States of America to the Stephanian C, that is to say, Middle-Late Pennsylvanian [Clendening, 1972, Hower et al., 1983, Jerzykiewicz, 1987, Kosanke, 1984, Lesnikowska and Willard, 1997, Peppers, 1985, Playford and Dino, 2005, Vozárová, 1998, Waters et al., 2011]. This latter fossil species has also been reported from MATZ 27 stratigraphic level from the San Luis Atolotitlán area.

Even though most of the taxa extend into the early Permian, they are gradually supplanted by Permian forms, such as taeniates, which are completely absent in these assemblages. The lack of Permian pollen and spores does not determine that they were not present during the deposition of the Matzitzi Formation because they may not have been preserved or restricted to other paleoenvironmental conditions. So, we could confidently conclude that the palynological assemblages at the Río Hondo section (MATZ RH 20) and MATZ 27 are likely Pennsylvanian, possibly earliest Permian.

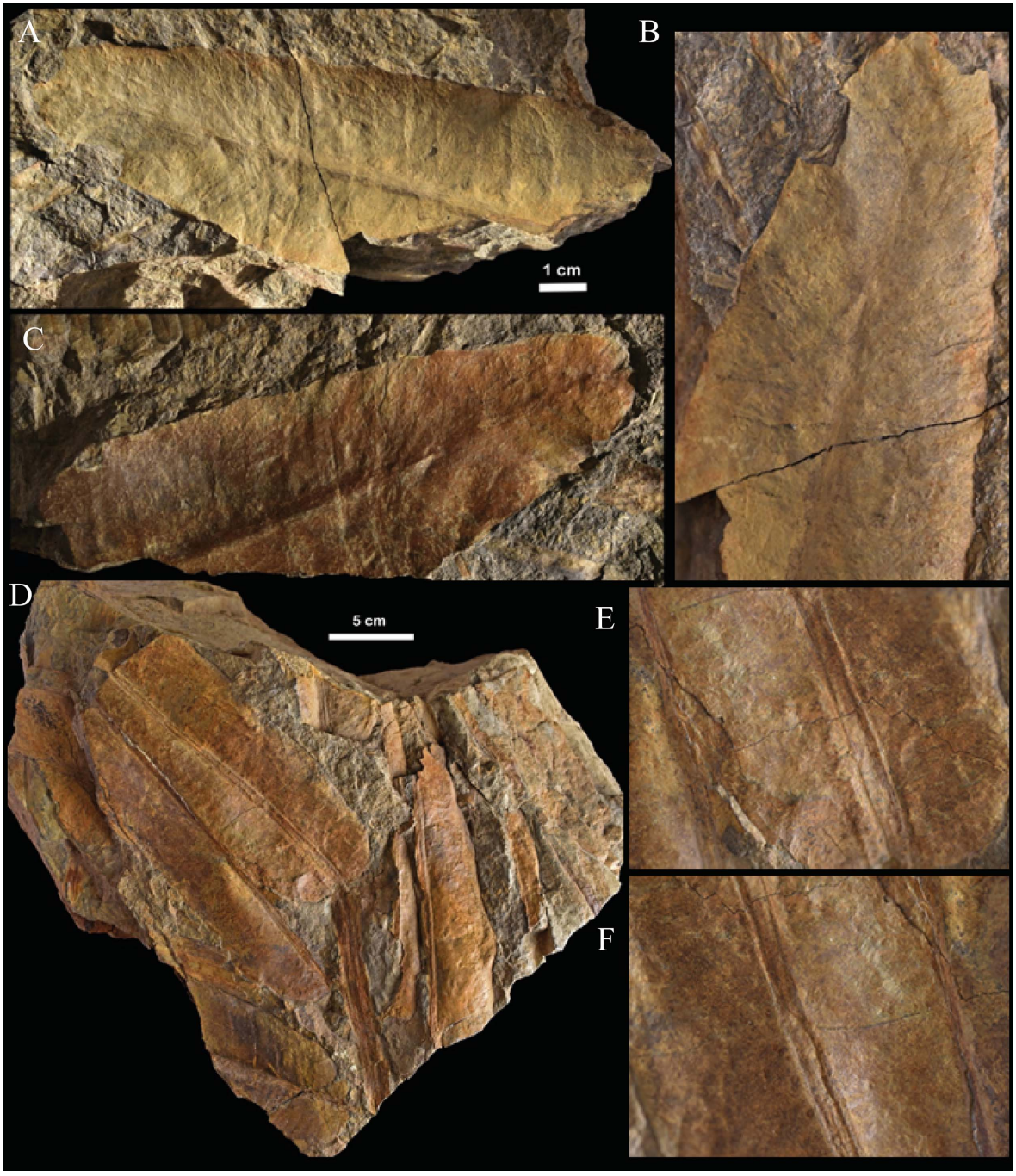

Figure 4. *Lonesomia mexicana* paratypes IGM-PB-1027-1058 and IGM-PB-1027-1060 (A–C). (A) Part and counterpart of the paratype IGM-PB-1027-1060. (B) Detail of the paratype IGM-PB-1027-1060 lacking preserved venation above the second order. (D) Paratype IGM-PB-1027-1058. (E,F) A detail of the leaf belonging to the paratype IGM-PB-1027-1058 which lacks venation above the second order.

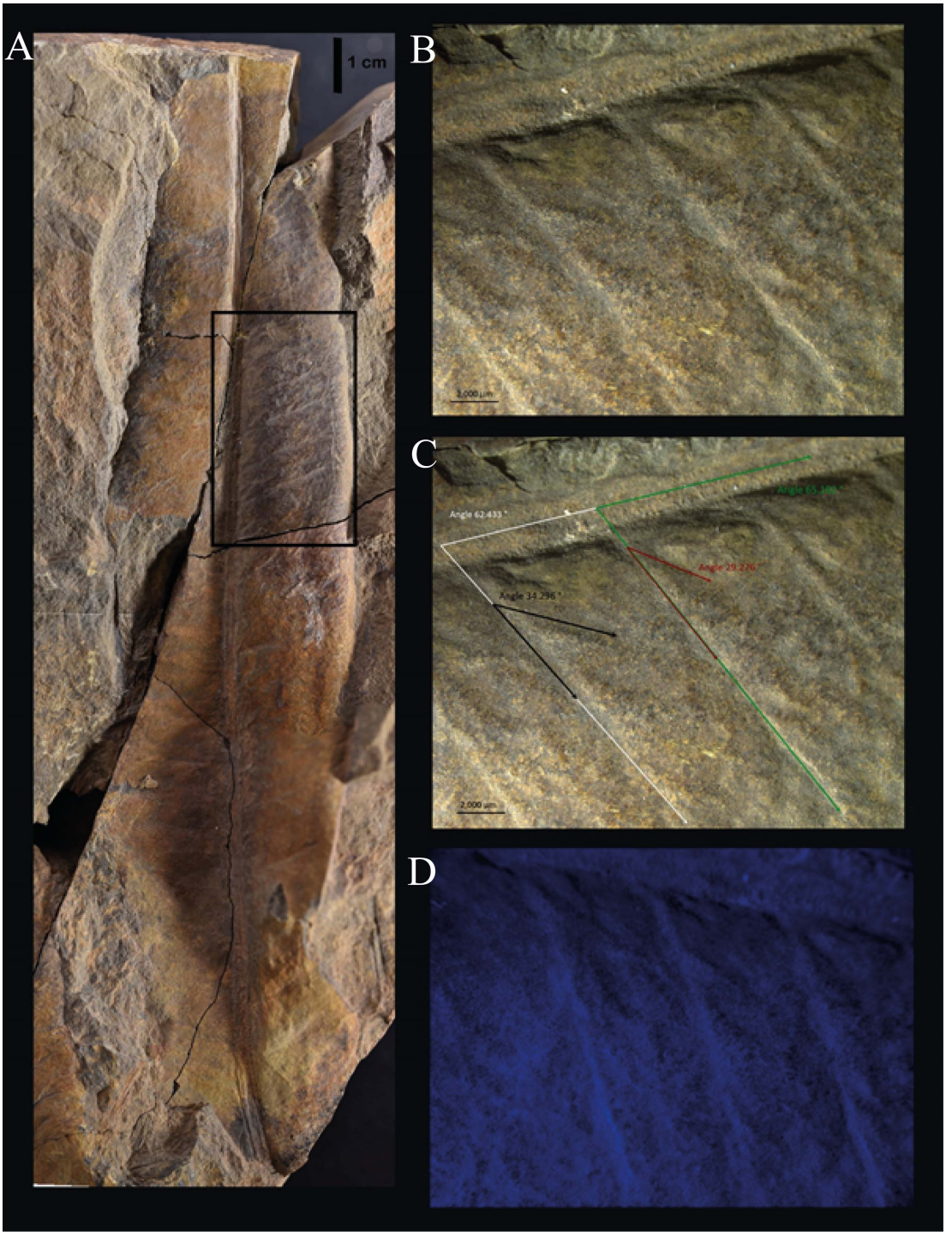

Figure 5. (A) *Lonesomia mexicana* IGM-PB-1027-1059 holotype. (B) Detail of an area of the leaf (indicated by a black square) used for the character description under white light. (C) Image taken using the Zen Pro programme indicating the second and third order venation angles. (D) Image under ultraviolet light that demonstrates the difficulty for determining third order venation pattern.

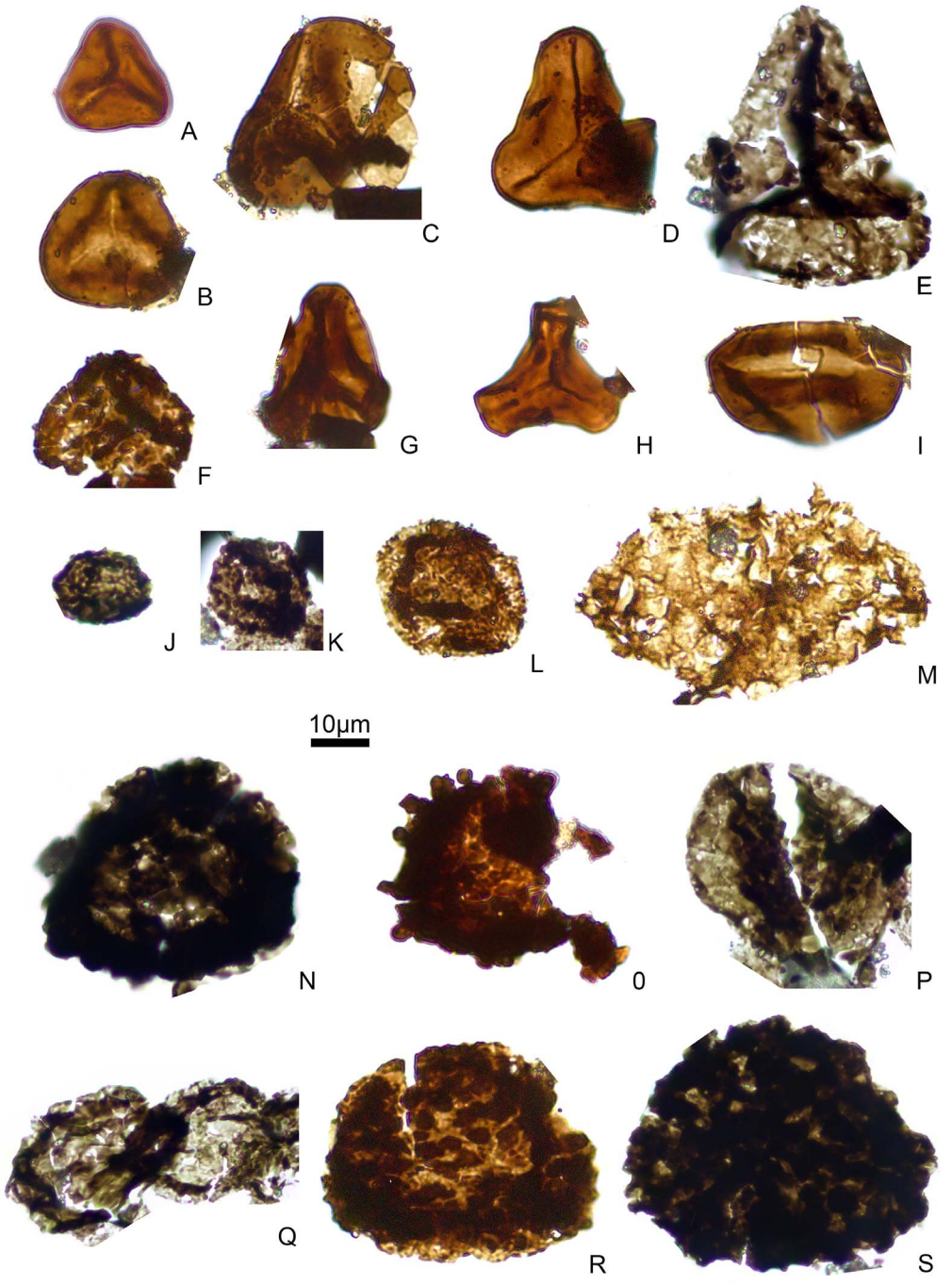

Figure 6. Palynomorphs from the Matzitzi Formation from San Francisco Xochiltepec, Santiago Coatepec, San Luis Atolotitlán, Los Reyes Metzontla and Río Hondo areas, Mexico. (A) *Deltoidospora gracilis* (Imgrund) Ravn, 1986, EF: MATZ 1_4_4_U322. (B) *Deltoidospora levis* (Kosanke) Ravn, 1986 EF: MATZ 1_2_4_S520. (C) *Deltoidospora priddyi* (Berry) McGregor, 1973, EF: MATZ 1_3_4 D464. (D) *Deltoidospora adnata* (Kosanke) McLean, 1993, EF: MATZ 1_3_4 U301. (E) *Deltoidospora sphaerotriangula* (Loose) Ravn, 1986, EF: MATZ RH 20_2_4_T431. (F) *Granulatisporites* sp., EF: MATZ RH 34_3_4_V321.

Figure 6 (cont.). (G) *Latipulvinites kosankii* Peppers, 1964, EF: MATZ 1_4_4_C432. (H) *Triquitrites* sp., EF: MATZ 1_4_4_S310. (I) *Laevigatosporites medius* Kosanke, 1950, EF: MATZ 1_2_4_X681. (J) *Thymospora thiessenii* (Kosanke) Wilson and Venkatachala, 1963, EF: MATZ RH 20_2_4_S384. (K) *Punctatosporites minutus* (Ibrahim) Alpern and Doubinger, 1973, EF: MATZ RH 20_2_4_X430. (L) *Punctatosporites punctatus* Ibrahim, 1933, EF: MATZ RH 34_2_4_Q474. (M) *Laevigatosporites minor* Loose, 1934, EF: MATZ RH 20_2_4_P551. (N) *Densosporites* sp., EF: MATZ RH 20_4_4_R324 (O) *Raistrickia saetosa* (Loose) Schopf et al., 1944, EF: MATZ RH 34_4_4_O574. (P) *Vesicaspora* cf. *wilsonii* (Schemel) Wilson and Venkatachala, 1963, EF: MATZ RH 20_4_4_M394. (Q) *Platysaccus* sp., EF: MATZ RH 20_2_4_P352. (R) *Verrucosisporites* sp. Type 1, EF: MATZ RH 20_3_4_C490. (S) *Verrucosisporites* sp. Type 2, EF: MATZ RH 20_1_4_Q290. EF: England Finder® coordinates. Scale bar: 10 μm.

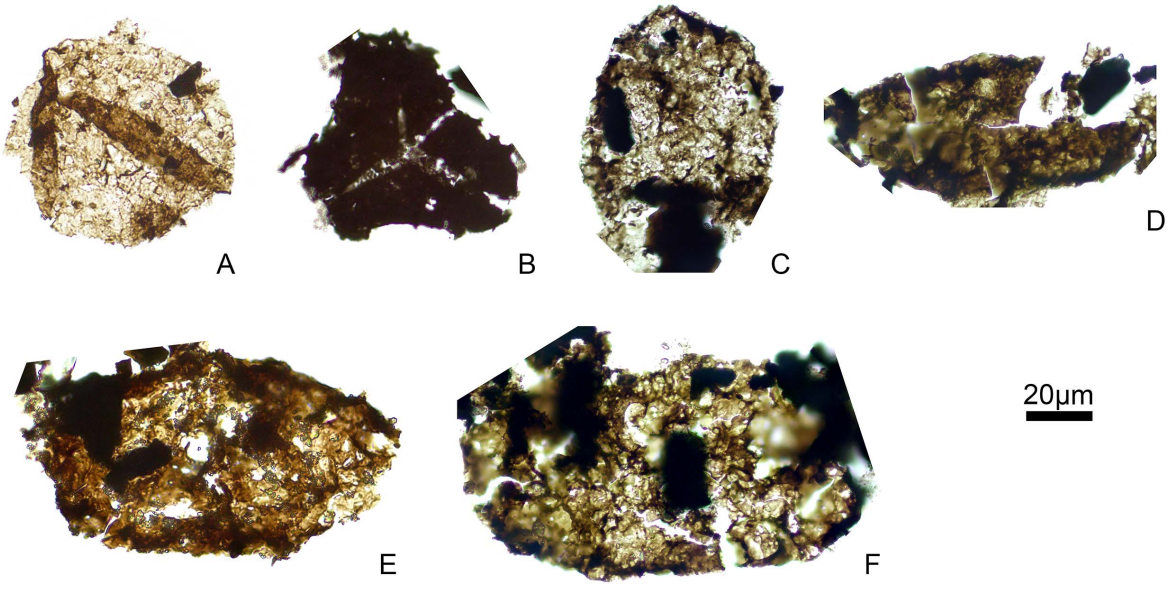

Figure 7. Palynomorphs from the Matzitzi Formation from San Francisco Xochiltepec, Santiago Coatepec, San Luis Atolotitlán, Los Reyes Metzontla, and Río Hondo areas, Mexico. (A) *Calamospora* sp., EF: MATZ RH 20_1_4_N353. (B) *Lophotriletes* sp., EF: MATZ 27_1_4_Y560. (C) *Schopfipollenites ellipsoides* (Ibrahim) Potonié and Kremp, 1954, EF: MATZ RH 20_2_4_Y380. (D) *Laevigatosporites vulgaris* (Ibrahim) Ibrahim, 1933, EF: MATZ RH 20_4_4_O340. (E) *Laevigatosporites maximus* (Loose) Potonié and Kremp, 1956, EF: MATZ RH 33_2_4 S522. (F) *Laevigatosporites maximus* (Loose) Potonié and Kremp, 1956, EF: MATZ RH 20_2_4_W312. EF: England Finder® coordinates. Scale bar: 20 μm.

5. Discussion

The palynomorphs seem to be reworked, especially given the poor condition of the preservation and the very low amount of grains, contrary to the parautochthonous fossil plants. Hence, it is impossible to correlate micro and macroflora. As stated by Silva-Pineda [1970] and Weber [1997] it seems that the Matzitzi Formation contains typical Late Pennsylvanian and early Permian macroflora.

In Euramerican areas, based on macroflora and palynological studies, it has been observed that the initial flora adapted to humid conditions in the tropics during the Late Mississippian (Namurian) was replaced by the Pennsylvanian wetland flora dominated by lycopsids, ferns, and primitive seed plants [DiMichele et al., 2006, Pfefferkorn et al., 2000]. During the Late Pennsylvanian, when aridity increased but alternated with wetter periods, floras rich in conifers, peltasperms, and other seed plants began

Table 1. Observed pollen and spores from studied palynomorph-containing samples

Genera/Levels	MATZ 1	MATZ 27	MATZ RH 20	MATZ RH 33	MATZ RH 34
Calamospora sp.			1		
Deltoidospora gracilis	1				
Deltoidospora levis	3				
Deltoidospora priddyi	7				
Deltoidospora adnata	16	1			
Deltoidospora sphaerotriangula			2		
Deltoidospora sp.		2	2		
Densosporites sp.			1		
Granulatisporites sp.			1		1
Laevigatosporites medius	7	1	1		3
Laevigatosporites minor			2		
Laevigatosporites maximus			1	1	
Laevigatosporites vulgaris			1		
Latipulvinites kosankii			2		1
Lophotriletes sp.		1		1	
Platysaccus sp.			1		
Punctatosporites minutus		4	2		
Punctatosporites punctatus					4
Raistrickia saetosa					1
Schopfipollenites ellipsoides			1		
Thymospora thiessenii		1	1		
Triquitrites sp.	3				
Verrucosisporites sp. Type 1			2		1
Verrucosisporites sp. Type 2			1		1
Vesicaspora cf. *wilsonii*			1		
Total	37	10	23	2	12

to appear while the species that dominated the Pennsylvanian wetlands declined [DiMichele et al., 2004b]. In the Euramerican Province, the transition from the Pennsylvanian to the Permian encompassed a gradual global environmental change from ever-wet during the Pennsylvanian to a drier Permian [e.g. DiMichele et al., 2004a, 2008, Michel et al., 2015, Tabor and Poulsen, 2008]. During this change, considerable tectonic activity in the tropics is recorded. These phenomena, may have combined to affect both local and regional microclimates and depositional environments [DiMichele et al., 2004a]. A replacement of hygrophytic by mesophytic and mesoxerophytic flora that tolerate seasonally dry climate is observed. Also, xeric floras can be found intercalated with vegetation typical of very wet conditions, even at the scale of individual outcrops [Broutin et al., 1990, DiMichele and Aronson, 1992, DiMichele et al., 2004b, 2019, Kerp and Fichter, 1985]. It seems that climatic conditions maintained along wetland corridors since Middle Pennsylvanian to Artinskian, possibly fringing the channels surrounded by plants adapted to a drier condition under a seasonal climate as reported for the Appalachians, New Mexico, Texas and Utah [DiMichele et al., 2011a]. It is also significant that the transition from wetter-to-drier climates during Pennsylvanian–Cisuralian range is different depending on the paleogeographic location; being earlier in New Mexico (Middle Pennsylvanian), and later in Texas–Appalachians (Late Pennsylvanian) and Utah (Permian) [DiMichele et al., 2011a] so it is worth expecting a diachronic disappearance of typically Carboniferous flora adapted to wetlands in drier conditions in Euramerica.

In the Euramerican Province (including Mexico and the U.S.A.), the more common small spores

Table 2. Collected samples and their coordinates. Outlined in grey colour indicate palynomorph-containing stratigraphic levels

Samples	Coordinates	Samples	Coordinates
	MATZ		MATZ RH
MATZ 1	18° 15′ 11.8″ N, 97° 29′ 42.6″ W	MATZ RH 1	18° 09′ 09.3″ N, 97° 18′ 2.8″ W
MATZ 2	18° 15′ 11.6″ N, 97° 29′ 42.7″ W	MATZ RH 2	18° 09′ 09.4″ N, 97° 18′ 3.0″ W
MATZ 3	18° 15′ 11.3″ N, 97° 29′ 42.5″ W	MATZ RH 3	18° 09′ 09.5″ N, 97° 18′ 3.2″ W
MATZ 4	18° 15′ 11.3″ N, 97° 29′ 42.5″ W	MATZ RH 4	18° 09′ 09.7″ N, 97° 18′ 4.0″ W
MATZ 5	18° 15′ 11.3″ N, 97° 29′ 42.5″ W	MATZ RH 5	18° 09′ 09.7″ N, 97° 18′ 4.0″ W
MATZ 6	18° 15′ 11.3″ N, 97° 29′ 42.6″ W	MATZ RH 6	18° 09′ 09.8″ N, 97° 18′ 4.3″ W
MATZ 7	18° 15′ 11.3″ N, 97° 29′ 42.6″ W	MATZ RH 7	18° 09′ 09.8″ N, 97° 18′ 4.3″ W
MATZ 8	18° 13′ 20.4″ N, 97° 28′ 22.5″ W	MATZ RH 8	18° 09′ 09.8″ N, 97° 18′ 4.3″ W
MATZ 9	18° 13′ 21.0″ N, 97° 28′ 22.3″ W	MATZ RH 9	18° 09′ 10.1″ N, 97° 18′ 4.9″ W
MATZ 10	18° 13′ 21.0″ N, 97° 28′ 22.3″ W	MATZ RH 10	18° 09′ 10.1″ N, 97° 18′ 4.9″ W
MATZ 11	18° 13′ 21.0″ N, 97° 28′ 22.3″ W	MATZ RH 11	18° 09′ 10.4″ N, 97° 18′ 5.2″ W
MATZ 12	18° 15′ 11.3″ N, 97° 29′ 42.6″ W	MATZ RH 12	18° 09′ 10.9″ N, 97° 18′ 5.8″ W
MATZ 13	18° 13′ 16.1″ N, 97° 28′ 13.1″ W	MATZ RH 13	18° 09′ 11.0″ N, 97° 18′ 6.1″ W
MATZ 14	18° 13′ 16.1″ N, 97° 28′ 13.1″ W	MATZ RH 14	18° 09′ 11.2″ N, 97° 18′ 6.3″ W
MATZ 15	18° 13′ 16.1″ N, 97° 28′ 13.1″ W	MATZ RH 15	18° 09′ 11.5″ N, 97° 18′ 6.8″ W
MATZ 16	18° 13′ 16.1″ N, 97° 28′ 13.1″ W	MATZ RH 16	18° 09′ 11.5″ N, 97° 18′ 6.8″ W
MATZ 17	18° 13′ 16.0″ N, 97° 28′ 12.6″ W	MATZ RH 17	18° 09′ 11.7″ N, 97° 18′ 7.3″ W
MATZ 18	18° 13′ 16.0″ N, 97° 28′ 12.6″ W	MATZ RH 18	18° 09′ 12.1″ N, 97° 18′ 8.2″ W
MATZ 19	18° 13′ 24.1″ N, 97° 28′ 09.4″ W	MATZ RH 19	18° 09′ 12.4″ N, 97° 18′ 8.8″ W
MATZ 20	18° 13′ 24.1″ N, 97° 28′ 09.4″ W	MATZ RH 20	18° 09′ 12.6″ N, 97° 18′ 9.2″ W
MATZ 21	18° 13′ 24.1″ N, 97° 28′ 09.4″ W	MATZ RH 21	18° 09′ 12.6″ N, 97° 18′ 9.2″ W
MATZ 22	18° 13′ 04.3″ N, 97° 24′ 53.4″ W	MATZ RH 22	18° 09′ 12.6″ N, 97° 18′ 9.2″ W
MATZ 23	18° 13′ 04.3″ N, 97° 24′ 53.4″ W	MATZ RH 23	18° 09′ 12.6″ N, 97° 18′ 9.2″ W
MATZ 24	18° 11′ 39.0″ N, 97° 25′ 00.2″ W	MATZ RH 24	18° 09′ 12.6″ N, 97° 18′ 9.2″ W
MATZ 25	18° 11′ 39.0″ N, 97° 25′ 00.2″ W	MATZ RH 25	18° 09′ 12.8″ N, 97° 18′ 9.6″ W
MATZ 26	18° 11′ 07.8″ N, 97° 24′ 38.9″ W	MATZ RH 26	18° 09′ 12.9″ N, 97° 18′ 9.9″ W
MATZ 27	18° 11′ 07.8″ N, 97° 24′ 38.9″ W	MATZ RH 27	18° 09′ 13.1″ N, 97° 18′ 10.1″ W
MATZ 28	18° 11′ 07.8″ N, 97° 24′ 38.9″ W	MATZ RH 28	18° 09′ 13.1″ N, 97° 18′ 10.1″ W
MATZ 29	18° 09′ 59.5″ N, 97° 23′ 53.6″ W	MATZ RH 29	18° 09′ 13.1″ N, 97° 18′ 10.1″ W
MATZ 30	18° 09′ 59.5″ N, 97° 23′ 53.6″ W	MATZ RH 30	18° 09′ 13.4″ N, 97° 18′ 10.7″ W
MATZ 31	18° 09′ 59.5″ N, 97° 23′ 53.6″ W	MATZ RH 31	18° 09′ 13.8″ N, 97° 18′ 11.9″ W
MATZ 32	18° 09′ 59.5″ N, 97° 23′ 53.6″ W	MATZ RH 32	18° 09′ 14.0″ N, 97° 18′ 12.3″ W
MATZ 33	18° 09′ 59.5″ N, 97° 23′ 53.6″ W	MATZ RH 33	18° 09′ 14.3″ N, 97° 18′ 13.6″ W
MATZ 34	18° 11′ 41.7″ N, 97° 24′ 59.2″ W	MATZ RH 34	18° 09′ 14.3″ N, 97° 18′ 14.3″ W
MATZ 35	18° 11′ 41.7″ N, 97° 24′ 59.2″ W	MATZ RH 35	18° 09′ 14.0″ N, 97° 18′ 14.6″ W
MATZ 36	18° 11′ 36.2″ N, 97° 25′ 03.1″ W	MATZ RH 36	18° 09′ 14.0″ N, 97° 18′ 14.6″ W
MATZ 37	18° 11′ 36.2″ N, 97° 25′ 03.1″ W	MATZ RH 37	18° 09′ 13.6″ N, 97° 18′ 15.0″ W
MATZ 38	18° 11′ 33.1″ N, 97° 25′ 08.6″ W	MATZ RH 38	18° 09′ 13.7″ N, 97° 18′ 15.4″ W
MATZ 39	18° 11′ 33.1″ N, 97° 25′ 08.6″ W	MATZ RH 39	18° 09′ 13.4″ N, 97° 18′ 16.1″ W
MATZ 40	18° 11′ 14.5″ N, 97° 25′ 18.2″ W	MATZ RH 40	18° 09′ 13.4″ N, 97° 18′ 16.3″ W
MATZ 41	18° 11′ 14.5″ N, 97° 25′ 18.2″ W	MATZ RH 41	18° 09′ 13.2″ N, 97° 18′ 16.5″ W
MATZ 42	18° 11′ 14.5″ N, 97° 25′ 18.2″ W	MATZ RH 42	18° 09′ 12.7″ N, 97° 18′ 17.5″ W

(continued on next page)

Table 2. (continued)

Samples	Coordinates
MATZ RH	
MATZ RH 43	18° 09′ 11.9″ N, 97° 18′ 18.6″ W
MATZ RH 44	18° 09′ 11.9″ N, 97° 18′ 18.6″ W
MATZ RH 45	18° 09′ 11.7″ N, 97° 18′ 18.8″ W
MATZ RH 46	18° 09′ 11.5″ N, 97° 18′ 18.9″ W
MATZ RH 47	18° 09′ 10.6″ N, 97° 18′ 19.4″ W
MATZ RH 48	18° 09′ 09.9″ N, 97° 18′ 19.8″ W
MATZ RH 49	18° 09′ 09.3″ N, 97° 18′ 20.0″ W

found in Late Pennsylvanian coals include Marattialean spores (*Thymospora* spp., *Punctatisporites minutus*, *Punctatosporites* spp., *Cyclogranisporites* spp., *Laevigatosporites minimus*, *Laevigatosporites medius*, *Laevigatosporites ovatus*), as well as such herbaceous fern taxa as *Lophotriletes*, *Raistrickia*, *Triquitrites* and *Deltoidospora* [DiMichele et al., 2018, Eble et al., 2013]. *Verrucosisporites* also occur, but much less frequently [Eble et al., 2013]. These taxa are typical of the uppermost Pennsylvanian coal from the Bursum Formation, New Mexico, including significant amounts of *Vesicaspora* [DiMichele et al., 2016] and coal of similar age described from north-central Texas [Looy and Hotton, 2014].

There is also evidence of calamitaleans, reported from macrofossil remains [DiMichele et al., 2016] in the Bursum Formation (Carrizo Arroyo, New Mexico, U.S.A.). Therefore, Marattialeans and calamitaleans were the most important wetland plant groups throughout western Pangea during the Late Pennsylvanian and well into the early Permian, reflecting their tolerance of soil moisture fluctuation and also their dispersal capacities [DiMichele et al., 2016].

In the eastern part of Euramerican Province (Western Europe), palynological assemblages display a broadly similar pattern [e.g. Clayton et al., 1977, Juncal et al., 2019]. The wetland microflora (marattialean spores and herbaceous fern taxa) and pollen of *Calamites* and *Cordaites* are dominant.

The only two studies [Rincón-Pérez, 2010, Valdés-Vergara, 2017] based on macrofloral content from the Río Hondo section, representing the most complete and continuous stratigraphic section for the Matzitzi Formation, show different abundance data due to methodological procedure: the first author without considering their stratigraphic level and the second author indicating it. The main flora representatives in this locality seem to be Filicophyta, Lycophyta and Spermatophyta and less abundant is Equisetophyta (calamitalean). The macroflora composition changes depending on its stratigraphic range [Valdés-Vergara, 2017] due to differences in the depositional environment. Both studies agree that Marattiales (*Pecopteris* spp.) and lepidodendrales (*Sigillaria*) are well-represented in the macroflora assemblage. Based on macroflora remains from the Río Hondo section [Rincón-Pérez, 2010, Valdés-Vergara, 2017] an early Permian age is suggested for the Matzitzi Formation. Four key taxa ranging from late Carboniferous to early Permian age have been described. *Sigillaria brardii-ichthyolepis* group is present in the Río Hondo section [Valdés-Vergara, 2017, Weber, 1997], which is also common in the Matzitzi Formation [Weber, 1997], and it ranges from the Late Pennsylvanian [Remy and Remy, 1977] to early Permian in USA [Blake and Gillespie, 2011]. *Taeniopteris multinervis* is known from the Late Pennsylvanian-early Permian in the USA [Remy and Remy, 1975] and medullosalean seed *Trigonocarpus* extend from Late Mississippian to early Permian [Cleal and Thomas, 2019]. *Holcospermum* is a common element from the Carboniferous but some reports have described it from the early Permian in Germany [Barthel, 2016] and Kansas [McKinley, 1966]. Moreover, the fossil genus *Comia* is known since the Permian [Mamay et al., 2009, Weber, 1997] and it occurs in North America (Texas and Oklahoma) in the early Permian (Artinskian, Cisuralian) [Mamay et al., 2009], restricting the age of the Matzitzi Formation in this locality to a probable age not older than the Artinskian. In consequence,

the macroflora from the Río Hondo section would likely correspond to the Artinskian–Kungurian. This would support the idea of reworked palynomorphs. Reports of *Pseudoctenis* from the Matzitzi Formation at Río Hondo and Camino sites [Valdés-Vergara, 2017] remain inconclusive due to the poor preservation of described specimens and lack of cuticle information. *Pseudoctenis* is known since the late Permian [Blomenkemper et al., 2018, Schweitzer, 1986] and it is an important component during the Mesozoic, especially in the uppermost Triassic and Jurassic [Taylor et al., 2009]. This fossil genus has been described from early and middle Permian deposits in India [Maheshwari and Bajpai, 2001], however, it has not been figured. If confirmed the occurrence of *Pseudoctenis* in the Matzitzi Formation, this fossil genus would extend its stratigraphic range up to the lower Permian.

Other fossil flora genera from the Matzitzi Formation known since the early Permian from other localities are *Fascipteris* [Magallón-Puebla, 1991] and *Bjuvia* [Velasco-de León et al., 2015]. Magallón-Puebla [1991], also noted that although a new species of *Pecopteris* might be present in this formation, it should have more Permian than Carboniferous affinities. Likewise, using the macroflora, a Permian age seems more likely for the Matzitzi Formation.

The fossil plants exhibit fragmentary preservation, breakup during collection, and obscured plant characters, that make much of the material unidentifiable. This is the case of *Lonesomia mexicana* that does not allow the identification of the venation pattern above the second order. In the long run, the identification of plant fossils of the Matzitzi Formation is greatly reduced due to the poor preservation of key diagnostic characters, their fragmented nature, and in some cases their very low abundance in the fossil record. This is especially problematic for specimens with glossopterid affinity. For example, a specimen initially described as *Glossopteris* was finally identified as *Sphenophyllum* ex gr. *thonii* [Weber, 1997]. There are also examples of misidentified specimens such as *Fascipteris* sp. cf. *F. hallei* [Magallón-Puebla, 1991] which was initially described as *Neuropteris jugosa* by Silva-Pineda [1970] and *Schizoneura gondwanensis* [Flores-Barragan, 2018] that was initially described as *Annularia* sp. by Velasco-de León et al. [2015]. These complications indicate that more studies are required for a comprehensive determination of the macroflora remains from the Matzitzi Formation, including consideration of their stratigraphic level and locality.

The available geochronological data for the Matzitzi Formation differs from our results (Figure 2). On the one hand, the Oaxacan Complex exposed southeast of San Luis Atolotitlán consists of quartz-feldspathic and garnet gneisses in granulite facies that are Grenvillian in age (1.1–0.98 Ga) [Keppie and Ortega-Gutiérrez, 1999, Solari et al., 2003]. On the other hand, the Acatlán Complex appears as highly deformed and metamorphosed green schists to the west of Los Reyes Metzontla and southeast of La Compañía (Puebla) whose age is poorly understood [Keppie et al., 2004]. The youngest units belonging to the Acatlán Complex (in chronological order: Tecomate Formation, Totoltepec stock, and San Miguel intrusions) are less deformed and metamorphosed compared to the oldest units of this complex [Yañez et al., 1991]. The Tecomate Formation has been considered the Latest Pennsylvanian–earliest middle Permian in age based on U–Pb SHRIMP dating (~320–264 Ma) and conodont and fusulinid content [Keppie et al., 2004]. One of the youngest units of the Acatlán Complex is the Chazumba Suite: the maximum depositional age of the Magdalena Formation is ~317 Ma, and the maximum depositional age of the overlying Chazumba Formation is ~275 Ma [Talavera-Mendoza et al., 2005]. The youngest unit of the Acatlán Complex, the San Miguel intrusive has interpreted with two distinct emplacement ages based on Rb–Sb dating indicating two thermal events in the Late Triassic–Early Jurassic (Rhaetian–Hettangian; 207 ± 9 Ma) and Middle Jurassic (Aalenian; 173 ± 0.3 Ma) [Ruiz-Castellanos, 1979]. The Magdalena migmatite also corresponding to one of the youngest units of the Acatlán Complex, is concordant with this Middle Jurassic age (Aalenian–Bajocian; 170 ± 2 Ma) by U–Pb method [Powell et al., 1999]. The amalgamation of the Acatlán and Oaxacan complexes apparently took place in the early Permian represented by the foliated Totoltepec pluton (287 ± 2 Ma; ~306–289 Ma) dated by U–Pb method in zircons [Kirsch et al., 2012, Yañez et al., 1991] and the anatectic leucosome (275.6 ± 1 Ma) and the syntectonic milonitized intrusive Cozahuico Granite (Kungurian–Roadian, 270.4 ± 2.6 Ma) dated by SHRIMP method [Elías-Herrera et al., 2007]. The

Cozahuico Granite has been interpreted as one of the oldest and deepest tectono-magmatic-metamorphic activity in the fault zone related to the oblique collision between Oaxacan and Acatlán complexes [Elías-Herrera and Ortega-Gutiérrez, 2002, Elías-Herrera et al., 2007]. In an abstract, Elías-Herrera et al. [2019] indicates an age not older than the Lopingian (260–252 Ma) for the Matzitzi Formation based on its relative stratigraphic position over deposits affected by the Caltepense Orogeny. However, it is unclear whether deposition of the Matzitzi Formation and this latter orogeny is contemporaneous or post-depositional. The Atolotitlán Tuff corresponding to this formation is reported as Middle Triassic (240 ± 3 Ma: Elías-Herrera et al., 2011; 239.2 ± 1.4/242.9 ± 1.4/238.5 ± 2.2 Ma: Bedoya, 2018). However, the geochronology of the Caltepense Orogeny and the Atolotitlán Tuff awaits formal publication. Moreover, the age of the Matzitzi Formation is a vexing matter by the Middle Jurassic maximum depositional age (177 Ma) for a sampled sandstone [Bedoya, 2018].

In summary, based on its relative stratigraphic position, the non-metamorphosed Matzitzi Formation has been placed overlying the metamorphosed units such as the Cozahuico Granite and the Acatlán Complex. Geochronological data indicate that the depositional age of the Matzitzi Formation should be not older than 270 Ma (earliest Roadian, middle Permian) corresponding to the underlying Cozahuico Granite and not older than Latest Pennsylvanian–earliest middle Permian (Tecomate Formation, Acatlán Complex), leading some geologists to think that the Matzitzi Formation is younger than the Roadian. Nevertheless, the Tecomate Formation has not been reported in direct contact with the Matzitzi Formation. Moreover, the macroflora remains indicate an Artinskian–Kungurian maximum age (e.g. Río Hondo section), so the deposition of the Matzitzi Formation was possibly contemporaneous, at least in part, to the Caltepense Orogeny and the emplacement of the Cozahuico Granite. The Atolotitlán Tuff corresponding to the Matzitzi Formation has been reported as Middle Triassic, and this formation also contains Jurassic deposits. Besides, the depositional setting and controls of deposition of the Matzitzi Formation and its geologic contacts with other metamorphosed rocks are still poorly understood. There is a great need for work to do to understand the geological contact between different geological units and also to disentangle the geological setting and evolution of the area.

Three important aspects should be clarified. First, the possibility that the Matzitzi Formation may include different chronostratigraphic units from the early Permian (or from the early middle Permian in the case of palynomorph reworking) to at least Middle Triassic or even younger (Jurassic) that may all record the same sedimentary environment must be considered. Also, a more comprehensive stratigraphic and sedimentologic work should be done. To achieve it, a re-examination of the already studied fossil flora controlling its stratigraphic level and geographical location is required. Besides, it is important to understand the evolution from Late Carboniferous wet conditions to drier conditions during the early Permian in Mexico. It has been proved a diachronous climatic change in the USA depending the locality so it is not worth expecting a diachronous appearance of certain macroflora and microflora key taxa. Second, it is important to control the correlation of the strata of the Matzitzi Formation, and third, a more comprehensive study of the geologic contact with underlying metamorphosed rocks is needed.

6. Conclusion

A more comprehensive study of the Matzitzi Formation is necessary to define its stratotype; not yet formally defined. Also, the biostratigraphic and geochronologic age disparities need to be resolved to improve stratigraphic correlation among disparate outcrops of the Matzitzi Formation. From those outcrops, it seems that the most continuous and complete stratigraphic section of this formation corresponds to the Río Hondo section. The fundamental problem of the Matzitzi Formation is that it may represent more than a single package of rocks with a similar depositional environment. The palynological assemblages presented in this study indicate most likely Late Pennsylvanian in the Río Hondo section. However, palynomorphs were possibly reworked and re-deposited in rock along with the Permian parautochthonous macroflora from this formation. If palynomorphs are reworked, their source would correspond to the erosion of Middle-Upper Pennsylvanian continental deposits. The re-study of

the holotype and paratypes of the gigantopterid fossil plant species *Lonesomia mexicana*, a key specimen for Kungurian age assignment, showed the lack of diagnostic characters to place them within the gigantopterids. Although these fossil plant specimens have a huge lamina, they do not have the reticulate venation that characterizes gigantopterids. The paratypes only showed primary and secondary veins whilst the holotype also presents a tertiary vein in a small area of the lamina due to the poor preservation of these specimens. Macroflora described from the early Permian Matzitzi Formation suggests wetland corridors possibly fringing the channels associated with anastomosing river systems related to a gradual global environmental change from ever-wet during the Late Pennsylvanian to a drier early Permian. This study suggests that maybe the deposition of the Matzitzi Formation possibly was contemporaneous, at least in part, to the Caltepense Orogeny and the emplacement of the Cozahuico Granite.

Acknowledgements

We are grateful to CONACyT for financial support by Project 220368 and Marycruz Gerwert also thanks to the CONACyT for scholarship and PAEP grant for Graduate Studies Program by UNAM. Drs Manuel Juncal and J.B. Diez were supported by projects PGC 2018-098272-B-100 and CGL2015-70970-P (Spanish Ministry of Economy) and GRC 2015/020 (Xunta de Galicia).

The authors appreciate the help of Mariano Elias during fieldwork, and we are also grateful for stratigraphic and sedimentological advice given by Elena Centeno. For paleobotanical work, we thank Jesús Alvarado Ortega and Violeta Amparo Romero Mayén for their assistance in the Paleontology Collection of the Instituto de Geología of UNAM. We thank Sergio R.S. Cevallos Ferriz for permitting us the use of the UV Fluorescence Microscope and Enoch Ortiz for his advice and support for photography acquisition under UV Fluorescence Microscope. We are grateful to Erik Ramirez for his partial graphic design in some figures. We thank Alberto Búrquez Montijo for English language editing. Two anonymous reviewers and the editor provided helpful comments on earlier drafts of the manuscript.

References

Aguilera, J. G. and Ordoñez, E. (1896). Bosquejo geológico de México. *Bol. Inst. Geol. Mex.*, 4–6:1–262.

Alpern, B. and Doubinger, J. (1973). *Microfossiles organiques du Paléozoïque. 6, Les spores : les miospores monolètes du paléozoïque.* Centre National de la Recherche Scientifique, Paris, France.

Barthel, M. (2016). The Lower Permian (Rotliegend) flora of the Döhlen Formation. *Geol. Saxonica*, 61(2):105–238.

Batten, D. J. (1999). Small palynomorphs. In Jones, T. P. and Rowe, N. P., editors, *Fossil Plants and Spores: Modern Techniques*, pages 15–19. Geological Society, London, UK.

Bedoya, A. (2018). Análisis de procedencia y termocronología detrítica de las Formaciones Matzitzi y Tianguistengo: Implicaciones tectónicas en la evolución Paleozoica–Mesozoica del sur de México. Master Thesis, Centro de Geociencias UNAM, Juriquilla, Mexico, 221 p.

Bedoya, A., Anaya-Guarneros, J. A., Abdullin, F., Martini, M., and Solari, L. (2020). Provenance analysis of the Matzitzi and Agua de Mezquite formations, southern Mexico: Different fluvial successions formed during late Paleozoic and post-Middle Jurassic time along the southernmost North America Pacific margin. *J. South Am. Earth Sci.* in press.

Blake, B. M. and Gillespie, W. H. (2011). The Enigmatic Dunkard Macroflora. In Harper, J. A., editor, *Geology of the Pennsylvanian–Permian in the Dunkard Basin: Guidebook*, 76th Annual Field Conference of Pennsylvania Geologists, Washington, pages 103–143. Field Conference of Pennsylvania Geologists, Washington.

Blomenkemper, P., Kerp, H., Hamad, A. A., DiMichele, W. A., and Bomfleur, B. (2018). A hidden cradle of plant evolution in Permian tropical lowlands. *Science*, 362:1414–1416.

Booi, M., Van Waveren, I. M., and Van Konijnenburg-Van Cittert, J. H. (2009). The Jambi gigantopterids and their place in gigantopterid classification. *Bot. J. Linn. Soc.*, 161(3):302–328.

Broutin, J., Doubinger, J., El Hamet, M. O., and Lang, J. (1990). Palynologie comparée du Permien nigérien (Afrique occidentale) et péritéthysien. Implications stratigraphiques et phytogéographiques. *Rev. Palaeobot. Palynol.*, 66:243–261.

Burckhardt, C. (1930). Étude synthetique sur le Mesozoique mexicain. *Mem. S. Paleont. Suisse*, 49–50:1–280.

Calderón-García, A. (1956). Bosquejo geológico de la región de San Juan Raya, Puebla. In García-Rojas, A., editor, *XX Congreso Geológico Internacional, Libreto guía Excursión A-11*, pages 9–27. Instituto de Geología UNAM, Ciudad de México, Mexico.

Carrillo, M. and Martínez-Hernández, E. (1981). Evidencias de Facies Continentales en la Formación Matzitzi, Estado de Puebla. *Rev. Inst. Geol. UNAM*, 5:117–118.

Centeno-García, E., Mendoza-Rosales, C. C., and Silva-Romo, G. (2009). Sedimentología de la Formación Matzitzi (Paleozoico superior) y significado de sus componentes volcánicos, región de Los Reyes Metzontla-San Luis Atolotitlán, Estado de Puebla. *Rev. Mex. Cienc. Geol.*, 26(1):18–36.

Clayton, G., Coquel, R., Doubinger, J., Gueinn, K. J., Loboziak, S., Owens, B., and Streel, M. (1977). Carboniferous miospores of western Europe: illustration and zonation. *Meded. Rijks Geol. Dienst*, 29:1–71.

Cleal, C. J. and Thomas, B. (2019). *Introduction to Plant Fossils*. Cambridge University Press, New York.

Clendening, J. A. (1972). Stratigraphic placement of the Dunkard according to palynological assemblages. *Castanea*, 37(4):258–287.

Di Pasquo, M. M. and Hernández-Láscares, D. (2013). Primeros registros palinológicos de las formaciones Matzitzi y Zapotitlán, regiones de Coatepec y Teotitlán, Estados de Oaxaca y Puebla, México. In Reynoso, V. H., editor, *VIII Congreso Latinoamericano de Paleontología y XIII Congreso Nacional de Paleontología (Guanajuato 2013), Abstracts, Guanajuato, Mexico*, page 45. Universidad de Guanajuato, Guanajuato (Mexico).

DiMichele, W. A. and Aronson, R. B. (1992). The Pennsylvanian-Permian vegetational transition: a terrestrial analogue to the onshore-offshore hypothesis. *Evolution*, 46:807–824.

DiMichele, W. A., Cecil, C. B., Chaney, D. S., Elrich, S. D., Lucas, S. G., Lupia, R., Nelson, W. J., and Tabor, N. J. (2011a). Pennsylvanian-Permian vegetational changes in tropical Euramerica. In Harper, J. A., editor, *Geology of the Pennsylvanian-Permian in the Dunkard basin: Guidebook. 76th Annual Field Conference of Pennsylvania Geologists, Washington, PA*, pages 60–102. Field Conference of Pennsylvania Geologists, Washington.

DiMichele, W. A., Chaney, D. S., Dixon, W. H., Nelson, W., and Hook, R. W. (2000). An Early Permian coastal flora from the central basin platform of Gaines County, West Texas. *Palaios*, 15(6):524–534.

DiMichele, W. A., Hook, R. W., Kerp, H., Hotton, C. L., Looy, C. V., and Chaney, D. S. (2018). Lower Permian flora of the Sanzenbacher Ranch, Clay County, Texas. In Krings, M., Harper, C. J., Cuneo, N. R., and Rothwell, G. W., editors, *Transformative Paleobotany*, pages 95–126. Academic Press, London (United Kingdom).

DiMichele, W. A., Hook, R. W., Nelson, W. J., and Chaney, D. S. (2004a). An unusual Middle Permian flora from the Blaine Formation (Pease River Group: Leonardian-Guadalupian Series) of King County, West Texas. *J. Paleontol.*, 78(4):765–782.

DiMichele, W. A., Hotton, C. L., Looy, C. V., and Hook, R. W. (2019). Paleoecological and paleoenvironmental interpretation of three successive macrofloras and palynofloras from the Kola Switch locality, Lower Permian (Archer City Formation, Bowie Group) of Clay County, Texas, USA. *Paläontol. Z.*, 93:423–451.

DiMichele, W. A., Kerp, H., and Chaney, D. S. (2004b). Tropical floras of the Late Pennsylvanian-Early Permian transition: Carrizo Arroyo in context. *Bull. N. M. Mus. Nat. Hist. Sci.*, 25:105–109.

DiMichele, W. A., Kerp, H., Tabor, N. J., and Looy, C. V. (2008). The so-called "Paleophytic–Mesophytic" transition in equatorial Pangea—Multiple biomes and vegetational tracking of climate change through geological time. *Palaeogeogr. Palaeoclimatol. Palaeoecol.*, 268:152–163.

DiMichele, W. A., Looy, C. V., and Chaney, D. S. (2011b). A new genus of gigantopterid from the Middle Permian of the United States and China and its relevance to the gigantopterid concept. *Int. J. Plant Sci.*, 172(1):107–119.

DiMichele, W. A., Mamay, S. H., Chaney, D. S., Hook, R. W., and Nelson, W. J. (2001). An Early Permian flora with Late Permian and Mesozoic affinities from North-central Texas. *J. Paleontol.*, 75(2):449–460.

DiMichele, W. A., Schneider, J. W., Lucas, S. G., Eble, C. F., Falcon-Lang, H. J., Looy, C. V., Nelson, W. J., Elrick, S. D., and Chaney, D. (2016). Megaflora

and palynoflora associated with a Late Pennsylvanian coal bed (Bursum formation, Carrizo Arroyo, New Mexico, USA) and paleoenvironmental significance. *New Mexico Geol. Soc. Annual Field Conf. Guidebook*, 67:351–368.

DiMichele, W. A., Tabor, N. J., Chaney, D. S., and Nelson, W. J. (2006). From wetlands to wet spots: environmental tracking and the fate of Carboniferous elements in Early Permian tropical floras. *Geol. Soc. Am. Spec. Pap.*, 399:223–248.

Eble, C. F., Grady, W. C., and Blake, B. M. (2013). Dunkard Group coal beds: Palynology, coal petrography and geochemistry. *Int. J. Coal Geol.*, 119:32–40.

Elías-Herrera, M., Macías-Romo, C., Sánchez-Zavala, J. L., Jaramillo-Méndez, C., Ortega-Gutiérrez, F., and Solari, L. (2019). Evento orogénico Cisuraliano-Guadalupiano ("Orogenia Caltepense") relacionado a la consolidación de pangea occidental: Nuevas evidencias tectonoestratigráficas y geocronológicas en el sur de México. *Bol. Inst. Geol. UNAM*, 122:6–7.

Elías-Herrera, M. and Ortega-Gutiérrez, F. (2002). Caltepec fault zone: an early Permian dextral transpressional boundary between the Proterozoic Oaxacan and Paleozoic Acatlán complexes, southern Mexico, and regional tectonic implications. *Tectonics*, 21(3):1013.

Elías-Herrera, M., Ortega-Gutiérrez, F., Macías-Romo, C., Sánchez-Zavala, J. L., and Solari, L. A. (2011). Colisión oblicua del Cisuraliano-Guadalupiano entre bloques continentales en el sur de México. Evidencias estratigráfico-estructurales y geocronológicas. In Ortega, F., Ferrusquía, I., Molina-Garza, R. S., and Centeno-García, E., editors, *Simposio en Honor del Dr. Zoltan de Cserna, Abstracts, Instituto de Geología UNAM, Ciudad de México, Mexico*, pages 159–164.

Elías-Herrera, M., Ortega-Gutiérrez, F., Sánchez-Zavala, J. L., Macías-Romo, C., Ortega-Rivera, A., and Iriondo, A. (2005). La falla de Caltepec: raíces expuestas de una frontera tectónica de larga vida entre dos terrenos continentales del sur de México. *Bol. Soc. Geol. Mex.*, 42(1):83–109.

Elías-Herrera, M., Ortega-Gutiérrez, F., Sánchez-Zavala, J. L., Macías-Romo, C., Ortega-Rivera, A., and Iriondo, A. (2007). The Caltepec fault zone: exposed roots of a long-lived tectonic boundary between two continental terranes of southern México. *Geol. Soc. Am. Spec. Pap.*, 422:317–342.

Erben, H. K. (1956). El Jurásico Medio y Calloviano de México. In García-Rojas, A., editor, *XX Congreso Geológico Internacional, Instituto de Geología UNAM, Ciudad de México, Mexico*, pages 1–140. Instituto de Geología UNAM, Ciudad de México (Mexico).

Erdtman, G. (1960). The acetolisis method. *Svensk Botanisk Tidskrift*, 54(4):561–564.

Flores, T. (1909). Datos para la geología del Estado de Oaxaca. *Bol. Soc. Geol. Mex.*, 5:107–128.

Flores-Barragan, M. A. (2018). Las Ginkgophytas de la Formación Matzitzi, implicaciones taxonómicas y ecológicas. Master Thesis, Facultad de Estudios Superiores Iztacala, Universidad Nacional Autónoma de México, Ciudad de México, Mexico, 83 p.

Flores-Barragan, M. A., Velasco-de León, M. P., Lozano-Carmona, D. E., and Ortega-Chavez, E. (2019a). Avance en el conocimiento de la paleoflora de la Formación Matzitzi y sus implicaciones temporales. *Bol. Inst. Geol. UNAM*, 122:21–22.

Flores-Barragan, M. A., Velasco-de León, M. P., Valdés-Vergara, N. A., and Fernández Barajas, M. R. (2019b). Avance en el conocimiento de la paleoflora de la Formación Matzitzi, implicaciones ecológicas y temporales (Localidad Carretera). *Paleontol. Mex. Spc. Num.*, 5:132.

Galván-Mendoza, E. (2000). Contribución al Conocimiento Paleoecológico de la Tafoflora Matzitzi, Paleozoico Tardío, sur del estado de Puebla. Master Thesis, Facultad de Ciencias UNAM, Ciudad de México, Mexico, 77 p.

García-Duarte, R. (1999). Evidencias de la naturaleza estructural y relaciones estratigráficas de la Formación Matzitzi en el sur de Puebla, México. Bachelor Thesis, Centro de Estudios Superiores del Estado de Sonora, Hermosillo, Mexico, 90 p.

Glasspool, I. J., Hilton, J., Collinson, M. E., Wang, S. J., and Li, C. S. (2004). Foliar physiognomy in Cathaysian gigantopterids and the potential to track Palaeozoic climates using an extinct plant group. *Palaeogeogr. Palaeoclimatol. Palaeoecol.*, 205:69–110.

González-Hervert, M. G. G., Martínez, P. R. G., Martínez, J. A. G., and Rojas-Rosas, R. (1984). Características estratigráficas y estructurales del límite de los terrenos Mixteco y Oaxaca, en la región de Los Reyes Metzontla, Pue. *Bol. Soc. Geol. Mex.*, 45(1/2):21–33.

Hernández-Láscares, D. (2000). Contribución al

conocimiento de la estratigrafía de la Formación Matzitzi, área Los Reyes Metzontla-Santiago Coatepec, extremo suroriental del estado de Puebla. Master Thesis, Colegio de Ciencias y Humanidades UNAM, Ciudad de México, Mexico, 117 p.

Hower, J. C., Fiene, F. L., Wild, G. D., and Helfrich, C. T. (1983). Coal metamorphism in the upper portion of the Pennsylvanian Sturgis Formation in western Kentucky. *Geol. Soc. Am. Bull.*, 94(12):1475–1481.

Ibrahim, A. C. (1933). *Sporenformen des Aegirhorizonts des Ruhr-Reviers*. PhD thesis, University of Berlin, Wurzburg, Germany. 47 p.

Jerzykiewicz, J. (1987). Latest Carboniferous (Stephanian) and Early Permian (Autunian) palynological assemblages from the intrasudetic basin, southwestern Poland. *Palynology*, 11(1):117–131.

Juncal, M. A., Lloret, J., Diez, J. B., López-Gómez, J., Ronchi, A., de la Horra, R., Barrenechea, J. F., and Arche, A. (2019). New Upper Carboniferous palynofloras from southern Pyrenees (NE Spain): Implications for palynological zonation of Western Europe. *Palaeogeogr. Palaeoclimatol. Palaeoecol.*, 516:307–321.

Keppie, J. D. and Ortega-Gutiérrez, F. (1999). Middle American Precambrian basement: A missing piece of reconstructed 1-Ga Origen. *Geol. Soc. Am. Spec. Pap.*, 336:199–210.

Keppie, J. D., Sandberg, C. A., Miller, B. V., Nance, R. D., and Poole, F. G. (2004). Implications of latest Pennsylvanian to Middle Permian paleontological and U–Pb SHRIMP data from the Tecomate Formation to re-dating tectonothermal events in the Acatlán Complex, southern Mexico. *Int. Geol. Rev.*, 46(8):745–753.

Kerp, H. and Fichter, J. (1985). Die Makrofloren des saarpfälzischen Rotliegenden (? Ober-Karbon-Unter-Perm; SW-Deutschland). *Mainzer Geowis. Mitteil.*, 14:159–286.

Kirsch, M., Keppie, J. D., Murphy, J. B., and Solari, L. (2012). Permian–Carboniferous arc magmatism and basin evolution along the western margin of Pangea: Geochemical and geochronological evidence from the eastern Acatlán Complex, southern Mexico. *Geol. Soc. Am. Bull.*, 124(9–10):1607–1628.

Koidzumi, G. (1936). Gigantopteris. *Acta Phytotax. Geobot.*, 5:130–144.

Kosanke, R. M. (1950). Pennsylvanian spores of Illinois and their use in correlation. *Illinois State Geol. Surv. Bull.*, 74:1–128.

Kosanke, R. M. (1984). Palynology of selected coal beds in the proposed Pennsylvanian System stratotype in West Virginia (No. USGS-PP-1318). *U.S. Geol. Surv. Prof. Pap.*, 1318:1–44.

Lesnikowska, A. D. and Willard, D. A. (1997). Two new species of *Scolecopteris* (Marattiales), sources of *Torispora securis* Balme and *Thymospora thiessenii* (Kosanke) Wilson et Venkatachala. *Rev. Palaeobot. Palyno.*, 95(1–4):211–225.

Liu, L. and Yao, Z. (2002). Comparison in leaf architecture between Chinese and American species of *Gigantopteridium*. *Acta Palaeontol. Sin.*, 41(3):322–333.

Loose, F. (1934). Sporenformen aus dem Floz Bismarck des Ruhrgebeites. *Arbeiten aus dem Institut Palaeobotanik und Petrographie der Brennsteine*, 4:128–164.

Looy, C. V. and Hotton, C. L. (2014). Spatiotemporal relationships among late Pennsylvanian plant assemblages: Palynological evidence from the Markley formation, West Texas, USA. *Rev. Palaeobot. Palyno.*, 211:10–27.

Magallón-Puebla, S. A. (1991). Estudio sistemático y biométrico de helechos del tipo Pecopteris (Marattiales; Pteridophyta) de la Formación Matzitzi (Permo-Carbonífero), estado de Puebla. Undergraduate Thesis, Facultad de Ciencias, Universidad Nacional Autónoma de México, Ciudad de México, Mexico, 110 p.

Maheshwari, H. and Bajpai, U. (2001). Phytostratigraphical succession in the *Glossopteris* flora of India. *Revista UNG Geociências*, VI(6):22–34.

Mamay, S. H. (1988). *Gigantonoclea* from the Lower Permian of Texas. *Phytologia*, 64:330–332.

Mamay, S. H., Chaney, D. S., and DiMichele, W. A. (2009). *Comia*, a seed plant possibly of peltaspermous affinity: A brief review of the genus and description of two new species from the Early Permian (Artinskian) of Texas, *C. greggii* sp. nov. and *C. craddockii* sp. nov. *Int. J. Plant Sci.*, 170(2):267–282.

McGregor, D. C. (1973). Lower and Middle Devonian spores of Eastern Gaspé, Canada. I. *Systematics. Palaeontographica Abt. B*, 142:1–77.

McKinley, K. (1966). The Mill Creek flora, Roca Shale, Wabaunsee County, Kansas. Ms Thesis, Kansas State University, 54 p.

McLean, D. (1993). *A palynostratigraphic classification of the Westphalian of the southern North*

Sea carboniferous basin. PhD thesis, University of Sheffield, Sheffield, Great Britain. 251 p.

Michel, L. A., Tabor, N. J., Montañez, I. P., Schmitz, M. D., and Davydov, V. I. (2015). Chronostratigraphy and Paleoclimatology of the Lodève Basin, France: Evidence for a pan-tropical aridification event across the Carboniferous-Permian boundary. *Palaeogeogr. Palaeoclimatol. Palaeoecol.*, 430:118–131.

Mülleried, F. (1933a). Estudios Paleontológicos y estratigráficos en la región de Tehuacán, Pue., Primera Parte. *An. Inst. Biol. UNAM*, 4(1):33–46.

Mülleried, F. K. G. (1933b). Estudios Paleontológicos y estratigráficos en la región de Tehuacán, Pue., Segunda Parte. *An. Inst. Biol. UNAM*, 4(2):79–93.

Mülleried, F. K. G. (1934). Estudios Paleontológicos y Estratigráficos de Tehuacán Pue., Conclusión. *An. Inst. Biol. UNAM*, 5(1):75–80.

Ortega-Gutiérrez, F. (1992). Tectonostratigraphic analysis and significance of the Paleozoic Acatlán Complex of southern Mexico. In Ortega-Gutiérrez, F., Centeno-García, E., Morán-Zenteno, D. J., and Gómez-Caballero, A., editors, *First Circum - Pacific and Circum-Atlantic Terrane Conference, Terrane geology of southern Mexico. Guidebook of field trip B*, pages 54–60. Instituto de Geología UNAM, Guanajuato, Mexico.

Ortega-Gutiérrez, F., Elías-Herrera, M., Morán-Zenteno, D. J., Solari, L., Weber, B., and Luna-Gutiérrez, L. (2018). The pre-Mesozoic metamorphic basement of Mexico, 1.5 billion years of crustal evolution. *Earth Sci. Rev.*, 183:2–37.

Peppers, R. A. (1964). Spores in strata of Late Pennsylvanian cyclothems in the Illinois Basin. *Ill. State Geol. Survey Bull.*, 90:1–72.

Peppers, R. A. (1985). Comparison of miospore assemblages in the Pennsylvanian System of the Illinois basin with those in the Upper Carboniferous of Western Europe. In Sutherland, P. K. and Manger, W. L., editors, *Biostratigraphy. Proc. Ninth International Congress for Carboniferous Stratigraphy and Geology, Southern Illinois University Press 2, Carbondale, United States*, pages 483–502.

Pfefferkorn, H. W., Gastaldo, R. A., and DiMichele, W. A. (2000). Ecological stability during the Late Paleozoic cold interval. *Paleontol. Soc. Spec. Pap.*, 6:63–78.

Playford, G. and Dino, R. (2005). Carboniferous and Permian palynostratigraphy. In Koutsoukos, E. A. M., editor, *Applied Stratigraphy*, pages 101–121. Springer, Dordrecht, Netherlands. Chapter 5.

Potonié, R. and Kremp, G. O. W. (1954). Die Gattungen der palaozoischen Sporae dispersae und ihre Stratigraphie. *Geol. Jb.*, 69:111–194.

Potonié, R. and Kremp, G. O. W. (1956). Die sporae dispersae des Ruhrkarbons. Teil II. *Palaeontographica Abt. B*, 99:85–191.

Powell, J. T., Nance, R. D., Keppie, J. D., and Ortega-Gutiérrez, F. (1999). Tectonic significance of the Magdalena Migmatite, Acatlán Complex, Mexico. *Geol. Soc. Am. Abstracts with Programs*, 31(7):A–294.

Ramírez-Espinosa, J. R. (1984). La acreción de los terrenos Mixteco y Oaxaca durante el Cretácico inferior. Sierra Madre del sur de México. *Bol. Soc. Geol. Mex.*, 45(1–2):7–19.

Ravn, R. L. (1979). An introduction to the stratigraphic palynology of the Cherokee Group (Pennsylvnian) coals of Iowa. *Iowa Geol. Surv. Tech. Pap.*, 6:1–117.

Ravn, R. L. (1986). Palynostratigraphy of the Lower and Middle Pennsylvanian coal of Iowa. *Iowa Geol. Surv. Tech. Pap.*, 7:1–245.

Remy, W. and Remy, R. (1975). Beiträge zur Kenntnis des Morpho-Genus *Taeniopteris* Brongniart. *Argumenta Palaeobot.*, 4:31–37.

Remy, W. and Remy, R. (1977). *Die Floren des Erdaltertums*. Glückauf Verlag, Essen, Germany.

Ricardi-Branco, F. (2008). Venezuelan paleoflora of the Pennsylvanian-Early Permian: Paleobiogeographical relationships to central and western equatorial Pangea. *Gondwana Res.*, 14(3):297–305.

Rincón-Pérez, A. (2010). Listado paleoflorístico de las plantas fósiles del Pérmico, pertenecientes a la Formación Matzitzi, ubicadas entre los kms. 90 a 95 de la carretera Cuacnopalan-Oaxaca. Bachelor Thesis, Instituto de Geología, Universidad Nacional Autónoma de México, Ciudad de México, Mexico, 213 p.

Ruiz-Castellanos, M. (1979). *Rubidium-strontium geochronology of the Oaxaca and Acatlán metamorphic areas of southern Mexico*. PhD thesis, University of Texas, Dallas, United States. 178 p.

Schopf, J. M., Wilson, L. R., and Bentall, R. (1944). An annotated synopsis of Paleozoic fossil spores and the definition of generic groups. *Illinois State Geol. Surv. Rep. Investigations*, 91:1–73.

Schweitzer, H. J. (1986). The land flora of the English

and German Zechstein sequences. In Harwood, G. M. and Smith, D. B., editors, *The English Zechstein and Related Topics*, volume 22 of *Geological Society Special Publication*, pages 31–54. The Geological Society, London.

Sedlock, R. L., Ortega-Gutiérrez, F., and Speed, R. C. (1993). Tectonostratigraphic terranes and tectonic evolution of Mexico. *Boulder, Geol. Soc. Am. Spec. Pap.*, 278:1–153.

Seyfullah, L. J., Glasspool, I. J., and Hilton, J. (2014). Hooked: habits of the Chinese Permian gigantopterid *Gigantonoclea*. *J. Asian Earth Sci.*, 83:80–90.

Silva-Pineda, A. (1970). Plantas del Pensilvánico de la región de Tehuacán. *Paleontol. Mex.*, 29:1–108.

Silva-Pineda, A., Buitrón-Sánchez, B., Arellano-Gil, J., Vachard, D., and Ramírez, J. (2003). Permian continental and Marine Biota of South-central Mexico: a synthesis. *Am. Assoc. Petr. Geol. Mem.*, 79:462–475.

Solari, L. A., Keppie, J. D., Ortega-Gutierrez, F., Cameron, K. L., Lopez, R., and Hames, W. E. (2003). 990 and 1100 Ma Grenvillian tectonothermal events in the northern Oaxacan Complex, southern Mexico; roots of an orogeny. *Tectonophysics*, 365(1–4):257–282.

Stone, J. F. (1969). Palynology of the Eddleman Coal (Pennsylvanian) of North-central Texas. In *The University of Texas at Austin, Bureau of Economic Geology, Report of Investigations 64, Austin, United States*, page 55. The University of Texas, Austin (United States of America).

Tabor, N. J. and Poulsen, C. J. (2008). Palaeoclimate across the Late Pennsylvanian–Early Permian tropical palaeolatitudes: a review of climate indicators, their distribution, and relation to palaeophysiographic climate factors. *Palaeogeogr. Palaeoclimatol. Palaeoecol.*, 268:293–310.

Talavera-Mendoza, O., Ruiz, J., Gehrels, G. E., Meza-Figueroa, D., Vega-Granillo, R., and Campa-Uranga, M. F. (2005). U–Pb geochronology of the Acatlán Complex and implications for the Paleozoic paleogeography and tectonic evolution of southern Mexico. *Earth Planet. Sci. Lett.*, 235:682–699.

Taylor, E. L., Taylor, T. N., and Krings, M. (2009). *Paleobotany: The Biology and Evolution of Fossil Plants*. Academic Press.

Turner, N. (1991). The occurrence of *Elaterites triferens* Wilson 1943 in miospore assemblages from Coal Measures of Westphalian D age, North Staffordshire, England. *Palynology*, 15(1):35–46.

Valdés-Vergara, N. A. (2017). Contribución al conocimiento de la flora fósil de la Formación Matzitzi. Bachelor Thesis, Facultad de Estudios Superiores Iztacala, Universidad Nacional Autónoma de México, Ciudad de México, Mexico, 56 p.

Velasco-de León, M. P., Flores-Barragan, M. A., and Lozano-Carmona, D. E. (2015). An analysis of a new foliar architecture of the Permian period in Mexico and its ecological interactions. *Am. J. Plant Sci.*, 6(05):612–619.

Velasco-Hernández, M. and Lucero-Arellano, M. R. (1996). Una localidad nueva de la Formación Matzitzi en el Río Calapa, límite estatal de Oaxaca y Puebla, México. *Rev. Cienc. Geol. Mex.*, 13(1):123–127.

Vozárová, A. (1998). Late Carboniferous to Early Permian time interval in the western Carpathians: Northern Tethys margin. *Geodiversitas*, 20(4):621–641.

Wang, X. (2010). *The Dawn Angiosperms*. Springer, Heidelberg, Germany.

Waters, C. N., Somerville, I. D., Stephenson, M. H., Cleal, C. J., and Long, S. L. (2011). Biostratigraphy. In Waters, C. N., Somerville, I. D., Jones, N. S., Cleal, C. J., Collinson, J. D., Waters, R. A., Besly, B. M., Dean, M. T., Stephenson, M. H., Davies, J. R., Freshney, E. C., Jackson, D. I., Mitchell, W. I., Powell, J. H., Barclay, W. J., Browne, M. A. E., Leveridge, B. E., Long, S. L., and McLean, D., editors, *A Revised Correlation of Carboniferous Rocks in the British Isles. London*, volume 26 of *The Geological Society London Special Report*, pages 11–22. Geological Society of London, Bath (United Kingdom).

Weber, R. (1997). How old is the Triassic flora of Sonora and Tamaulipas, and news on Leonardian floras in Puebla and Hidalgo, México. *Rev. Mex. Cienc. Geol.*, 14(2):225–243.

Weber, R. (2007). Virutas Paleobotánicas Pérmico de México.

Weber, R., Centeno-García, E., and Magallón-Puebla, S. A. (1987). La Formación Matzitzi tiene edad permocarbonífera. In Alcayde, M., editor, *II Simposio sobre la Geología Regional de México, Instituto de Geología UNAM, Ciudad de México, Mexico*, pages 57–59.

Weber, R. and Cevallos-Ferriz, S. R. S. (1994). Perfil

actual y perspectivas de la paleobotánica en México. *Bol. Soc. Bot. Mex.*, 55:141–148.

Weber, R., Magallón-Puebla, S. A., and Sour-Tovar, S. (1989). La flora paleozoica de Puebla. *ICYT*, 11:19–26.

Wilson, L. R. and Venkatachala, B. S. (1963). Thymospora, a new name for Verrucososporites. *Oklahoma Geol. Notes*, 23:75–79.

Yañez, P., Ruiz, J., Patchett, P. J., Ortega-Gutiérrez, and Gehrels, G. E. (1991). Isotopic studies of the Acatlán Complex, southern Mexico: implications for Paleozoic North American tectonics. *Geol. Soc. Am. Bull.*, 10:817–828.

Comptes Rendus

Géoscience

Objet de la revue

Les *Comptes Rendus Géoscience* sont une revue électronique évaluée par les pairs de niveau international, qui couvre l'ensemble des domaines des sciences de la Terre et du développement durable. Ils publient des articles originaux de recherche, des articles de revue, des mises en perspective historiques, des textes à visée pédagogique ou encore des actes de colloque, sans limite de longueur, en anglais ou en français. Les *Comptes Rendus Géoscience* sont diffusés selon une politique vertueuse de libre accès diamant, gratuit pour les auteurs (pas de frais de publication) comme pour les lecteurs (libre accès immédiat et pérenne).

Directeur de la publication : Étienne Ghys

Rédacteurs en chef : Éric Calais, Michel Campillo, François Chabaux, Ghislain de Marsily

Comité éditorial : Jean-Claude André, Pierre Auger, Mustapha Besbes, Sylvie Bourquin, Yves Bréchet, Marie-Lise Chanin, Philippe Davy, Henri Décamps, Sylvie Derenne, Michel Faure, François Forget, Claude Jaupart, Jean Jouzel, Eric Karsenti, Amaëlle Landais, Sandra Lavorel, Yvon Le Maho, Mickaele Le Ravalec, Hervé Le Treut, Benoit Noetinger, Carole Petit, Valérie Plagnes, Pierre Ribstein, Didier Roux, Bruno Scaillet, Marie-Hélène Tusseau-Vuillemin, Élisabeth Vergès

Secrétaire éditoriale : Adenise Lopes

À propos de la revue

Toutes les informations concernant la revue, y compris le texte des articles publiés qui est en accès libre intégral, figurent sur le site https://comptes-rendus.academie-sciences.fr/geoscience/.

Informations à l'attention des auteurs

Pour toute question relative à la soumission des articles, les auteurs peuvent consulter le site https://comptes-rendus.academie-sciences.fr/geoscience/.

Contact

Académie des sciences
23, quai de Conti, 75006 Paris, France
Tél. : (+33) (0)1 44 41 43 72
CR-Geoscience@academie-sciences.fr

Les articles de cette revue sont mis à disposition sous la licence Creative Commons Attribution 4.0 International (CC-BY 4.0) https://creativecommons.org/licenses/by/4.0/deed.fr

Comptes Rendus
de l'Académie des sciences

Géoscience
Sciences de la Planète

Volume 352, nº 6-7, 2020

Quelques aspects de l'état des connaissances des séries triasiques de part et d'autre de la Marge Atlantique **Special issue / *Numéro thématique***

Some aspects of current State of Knowledge on Triassic series on both sides of the Central Atlantic Margin / *Quelques aspects de l'état des connaissances des séries triasiques de part et d'autre de la Marge Atlantique*

Sylvie Bourquin, Rachid Essamoud
Some aspects of current State of Knowledge on Triassic series on both sides of the Central Atlantic Margin 415-416

Abdelkrim Afenzar, Rachid Essamoud
Sedimentological and sequence stratigraphy analyses of the syn-rift Triassic series of the Mohammedia–Benslimane–ElGara–Berrechid basin (Moroccan Meseta) 417-441

Manuel García-Ávila, Ramon Mercedes-Martín, Manuel A. Juncal, José B. Diez
New palynological data in Muschelkalk facies of the Catalan Coastal Ranges (NE of the Iberian Peninsula) 443-454

Hind El Hachimi, Nasrrddine Youbi, José Madeira, Andrea Marzoli, João Mata, Hervé Bertrand, Mohamed Khalil Bensalah, Moulay Ahmed Boumehdi, Miguel Doblas, Fida Medina, Mohamed Ben Abbou, Línia Martins
Physical volcanology and emplacement mechanism of the Central Atlantic Magmatic Province (CAMP) lava flows from the Central High Atlas, Morocco 455-474

Manuel A. Juncal, José B. Diez, Raúl De la Horra, José F. Barrenechea, Violeta Borruel-Abadía, José López-Gómez
State of the art of Triassic palynostratigraphical knowledge of the Cantabrian Mountains (N Spain) 475-493

Bouziane Khalloufi, Nour-Eddine Jalil
Overview of the Late Triassic (Carnian) actinopterygian fauna from the Argana Basin (Morocco) 495-513

Uxue Villanueva-Amadoz, Marycruz Gerwert Navarro, Manuel A. Juncal, José B. Diez
Paleobotanical and palynological evidence for the age of the Matzitzi Formation, Mexico 515-538

1778-7025 (electronic)

Académie des sciences — Paris

COMPTES RENDUS
DE L'ACADÉMIE DES SCIENCES
Géoscience
Volume 352, nº 6-7, 2020